Investigation of natural processes leading to nitrate enrichment in aquifers of semi-arid regions

Zur Erlangung des akademischen Grades eines
Doktors der Naturwissenschaften
an der Fakultät für Bauingenieur-, Geo- und Umweltwissenschaften
der Universität Karlsruhe
genehmigte
DISSERTATION

von

Susanne Stadler
aus Göttingen

Karlsruhe 2005

Tag der mündlichen Prüfung:	16.12.2005
Referent:	Prof. Dr. H. Hötzl
Korreferent:	Dr. habil. T. Himmelsbach

ABSTRACT

Enrichment of nitrate in groundwater is a worldwide phenomenon, mostly resulting from anthropogenic activities in densely populated areas. Groundwater in the semi-arid, mostly uninhabited Kalahari region of Botswana, however, exhibits nitrate concentrations that exceed the WHO guideline value of 50 mg/l by far. As high nitrate concentrations in water pose a serious health risk they put additional pressure on the scarce water resources of the country. In the present study an integrative approach was applied to identify nitrate enrichment processes and the fate of nitrate in the Ntane Sandstone Aquifer in Botswana, using combined methods from hydrochemistry, geochemistry and isotope hydrology. Natural processes in the unsaturated zone have been identified to be the source of the nitrate found in the groundwater. Despite the inhomogeneous distribution of nitrate concentrations in the aquifer very uniform ^{15}N- and ^{18}O-NO_3^- signatures were found in the groundwater. These ^{15}N- and ^{18}O-NO_3^- signatures agree well with the typical range for naturally occurring soil nitrate, while nitrogen input from the aquifer lithology, from uprising groundwater or from inflow of nitrate-rich water from perched aquifers is negligible. Results show no evidence for influence of the current cattle grazing activity on nitrate concentrations in the groundwater. Hydrochemical and isotopic data from groundwater investigations of the Ntane Sandstone Aquifer suggest a close link between nitrate concentrations and groundwater residence times. At least two groundwater components were identified that were formed independently at different times and contain different nitrate concentrations: The Ca-HCO_3 type is clearly correlated with elevated nitrate concentrations while the Na-HCO_3 type shows low nitrate concentrations. According to their different ^{14}C contents, the Ca-HCO_3 water type suggests modern groundwater (40 to 80 %-mod.), whereas the Na-HCO_3 type implies groundwater ages of several thousand years (less than 20 %-mod.). A connection of nitrate concentrations to recharge conditions was found: High nitrate concentrations were recharged under drier conditions while lower nitrate concentrations appear to be recharged under much wetter conditions. It is suggested that the differences are related to climatic change, as observed residence time differences lie within the ranges of past wetter phases, and that high nitrate concentrations are connected to present semi-arid conditions. The heterogeneous concentration distribution appears to be little influenced by reactive processes within the aquifer. Results of this study can provide the base for the general understanding of the fate of nitrate at other locations of semi-arid conditions.

ZUSAMMENFASSUNG

Erhöhte Nitratgehalte im Grundwasser sind ein global auftretendes Phänomen, das meist durch anthropogene Einflüsse in dicht besiedelten Gebieten ausgelöst wird. Grundwasser in der semi-ariden, unbesiedelten Kalahari in Botswana zeigt jedoch Nitratkonzentrationen, die deutlich über dem Grenzwert der Weltgesundheitsorganisation von 50 mg/l liegen. Hohe Nitratgehalte im Grundwasser stellen ein Gesundheitsrisiko dar und belasten die ohnehin schon geringen Wasserressourcen des Landes. Zur Identifizierung der Nitratquellen im Ntane Sandstein Aquifer in Botswana wurde in dieser Studie ein integrativer Ansatz verwendet, der Methoden der Grundwasserchemie, Geochemie und Isotopenhydrologie kombiniert. Natürliche Prozesse wurden als Quelle des Nitrats im Grundwasser ausgewiesen. Trotz heterogener Verteilung der Nitratkonzentrationen im Aquifer wurden sehr einheitliche ^{15}N- und ^{18}O-NO_3^--Signale im Grundwasser nachgewiesen. Diese ^{15}N- und ^{18}O-NO_3^--Signale liegen im für Nitrate aus dem Bodenkreislauf typischen Bereich, während Nitrateinträge aus der Aquiferlithologie und durch aufsteigendes Grundwasser aus tieferliegenden Aquiferen, sowie aus Zuflüssen aus hängenden Aquiferen im Untersuchungsgebiet vernachlässigbar klein sind. Hydrochemische und isotopenhydrologische Untersuchungen an Grundwasserproben zeigen eine Verbindung von Nitratkonzentrationen und Grundwasserverweilzeiten auf. Mindestens zwei Grundwasserkomponenten unterschiedlicher Bildungsbedingungen und verschiedener Nitratgehalte wurden ausgewiesen: Der Ca-HCO_3-Typ ist deutlich mit erhöhten Nitratgehalten assoziiert, während der Na-HCO_3-Grundwassertyp niedrige Nitratkonzentrationen aufweist. Gemäß seiner ^{14}C-Gehalte deutet der Ca-HCO_3-Typ auf ein modernes Grundwasser hin (40 bis 80 %-mod.), während der Na-HCO_3-Typ auf Verweilzeiten von mehreren tausend Jahren hindeutet (Paläowasser mit unter 20 %-mod.). Eine Verbindung zwischen Nitratgehalten und Neubildungsbedingungen wurde aufgezeigt: Hohe Nitratgehalte wurden unter trockeneren Bedingungen neugebildet, wobei niedrige Nitratgehalte unter feuchteren Bedingungen gebildet wurden. Diese Unterschiede resultieren vermutlich aus klimatischen Änderungen, da die beobachteten Grundwasserverweilzeiten im Aquifer innerhalb der Zeiträume größerer klimatischer Änderungen zu Feuchtphasen hin liegen, während hohe Nitratgehalte auf die Bindung an heutige semi-aride Bedingungen hindeuten. Die heterogene Nitratverteilung scheint nur wenig durch reaktive Prozesse beeinflusst zu sein. Die Ergebnisse dieser Studie können als Grund-

lage zum allgemeinen Verständnis der Nitratdynamik in semi-ariden Gebieten dienen.

PREFACE

This PhD thesis was realized at the Department of Applied Geology (AGK) of Karlsruhe University, Germany (Faculty of Civil Engineering, Geosciences and Environmental Sciences) in cooperation with the Federal Institute for Geosciences and Natural Resources (BGR), Hannover, Germany. It was kindly supervised by Prof. Dr. H. Hötzl (AGK) and Dr. habil. T. Himmelsbach (AGK/BGR).

The presented study forms part of the bilateral research project 'Investigation of the Processes leading to Nitrate Enrichment in the Ntane Sandstone Aquifer Serowe/Orapa' between BGR and the Department of Geological Survey (DGS), Botswana. This project was carried out in the framework of a regional research cooperation ('Nitrate in Groundwater in Semi-Arid Regions of Southern Africa') with the Council for Scientific and Industrial Research (CSIR), Republic of South Africa, and the Ministry of Agriculture, Water and Rural Development (MAWRD), Namibia. Project funding was supplied by BGR.

CONTENTS

LIST OF FIGURES

LIST OF TABLES

SYMBOLS AND ABBREVIATIONS

Symbols

L	length unit	
M	mass unit	
T	time unit	
$^{14}a_c$	activity of radiocarbon (^{14}C)	[%-mod.]
D_d	dispersion coefficient	[L^2/T]
D_m	molecular diffusion coefficient	[L^2/T]
Eh	redox potential	[mV]
g	acceleration of gravity (9.81 m/s^2)	[L/T^2]
i	hydraulic gradient	[-]
K	permeability coefficient	[L^2]
k_f	hydraulic conductivity	[L/T]
n_e	effective porosity	[-]
p	pressure	[Pa]
r	correlation coefficient	[-]
s	storage coefficient	[-]
v_a	transport velocity	[L/T]
v_f	flow (Darcy) velocity	[L/T]
$\tilde{x}$	median	[M, L, T]
α	isotope fractionation factor as defined in Eq. 6.9	[-]
δ	stable isotope ratio as defined in Eq. 6.8	[‰]
ΔNe	Ne content in excess air	[L^3/M]
ε	isotope enrichment factor as defined in Eq. 6.10	[-]
η	viscosity	[M/(L·T)]
ρ	density	[M/L^3]

Abbreviations

AAS	atomic-absorption spectroscopy
AGK	Department of Applied Geology (Institut für Angewandte Geologie), Karlsruhe University, Germany
amsl	above mean sea level

BGR	Federal Institute for Geosciences and Natural Resources (Bundesanstalt für Geowissenschaften und Rohstoffe), Hannover, Germany
BP	before present
CE	closed system equilibration
CSIR	Council for Scientific and Industrial Research, Republic of South Africa
Debswana	Debswana Diamond Co., Botswana
DGS	Department of Geological Survey, Botswana
DIC	dissolved inorganic carbon
DIN	DIN German Institute for Standardization (Deutsches Institut für Normung e.V.)
DO	dissolved oxygen
DOC	dissolved organic carbon
DWA	Department of Water Affairs, Botswana
Eq.	Equation
Fig.	Figure
Fm.	formation
GGA	Leibniz Institute for Applied Geosciences (Institut für Geowissenschaftliche Gemeinschaftsaufgaben), Hannover, Germany
ka	kilo years (1000 a)
LGM	Last Glacial Maximum
LM	Letlhakane Mine
MWL	meteoric water line
NPOC	non-purgeable organic carbon
OM	Orapa Mine
pptv	parts per trillion (volume)
PE	partial re-equilibrium
SHE	standard hydrogen electrode
SI	saturation index
SOM	soil organic matter
STP	standard temperature: 0°C, and pressure: 1.023 atm (cm^3 STP/g of dry air per g of water)
Tab.	Table
TD	total dissolution
TDIC	total dissolved inorganic carbon
TOC	total organic carbon

TU	tritium units
UFZ	UFZ-Centre for Environmental Research Leipzig-Halle, Germany (UFZ-Umweltforschungszentrum Leipzig-Halle)
WF	wellfield
wt.-%	percent by weight
WHO	World Health Organization
WTW	Wissenschaftlich-Technische Werkstätten, Weilheim, Germany
XRF	X-ray fluorescence spectroscopy
%-mod.	percent modern carbon

1 INTRODUCTION

1.1 Background and scope

Nitrate is one of the major pollutants of drinking water worldwide (Widory et al., 2004, Postma et al., 1991). The exposure of humans to high doses of nitrate in drinking water causes severe health effects, e.g. methemoglobinemia. Though generally associated with anthropogenic activities in densely populated areas (e.g. Wakida and Lerner, 2005, Razowska-Jaworek and Sadurski, 2004, Canter, 1997, Rohmann and Sontheimer, 1985), in recent years elevated nitrate concentrations have also been recorded in groundwater of mostly uninhabited regions around the world - especially in semi-arid settings (e.g. Walvoord et al., 2003, Aranibar et al., 2003, Edmunds and Gaye, 1997, Barnes et al., 1992). Elevated nitrate concentrations are equally known from groundwaters of the Kalahari of Botswana, where the WHO-guideline value (WHO, 1998) of 50 mg/l is exceeded by far (Mokokwe, 1999). In these groundwaters, natural nitrate accumulation processes seemed to play an important role. As enrichment processes were not fully understood (SGAB, 1988) and did not appear to stem from human impact, the current study was launched investigating natural nitrate enrichment processes in the Ntane Sandstone Aquifer in Central Botswana. The aim was to identify the (major) nitrate input factors and the fate of nitrate in the groundwater. Understanding the associated processes and their implications on groundwater management was especially important, as the investigated region experiences extreme water scarcity and heavily depends on the Ntane Sandstone Aquifer for water supply. The present study was conducted in close cooperation with a further PhD study within the same project (Schwiede, in prep.) which investigated nitrogen in soil in the same area.

As the Kalahari region offers much potential for nitrogen input from different compartments into the subsurface (Fig. 1-1), it was necessary to validate and investigate the different sources. Dominant input from outside the aquifer was suspected through atmospheric deposition (dry and wet fall) or from accumulation processes related to soil and biomass. The latter could be natural vegetation, as the predominant species in the study area are known for their N-fixing potential (especially acacia trees and shrubs). In addition, point sources such as termite mounds occur in the area that allow an accumulation of nitro-

gen in symbiosis with fungi cultures. Additional nitrogen may be supplied by cattle that, though extensive, cause (over)grazing and leave nitrogen from manure especially in Kraals (cattle posts). Besides this, potential nitrate sources lie within the aquifer: Influence from potentially nitrate-rich uprising groundwater from the lower lying aquifer (Mosolotsane Fm.) or other allochthonous processes could not be ruled out.

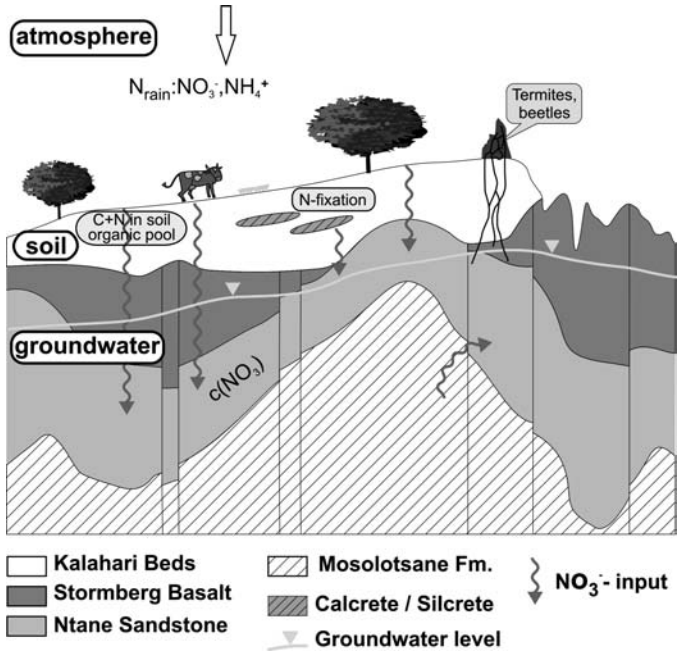

Fig. 1-1: Potential sources and pathways of nitrate in the study area.

However, the potential sink capacity of the aquifer also had to be considered, e.g. the presence of reaction partners for nitrate reduction in the aquifer. Moreover, lithology was suspected to provide nitrogen, e.g. calcretes and silcretes of the uppermost formation of the investigated area that may act as nitrogen source or hydraulic barrier. Coupled with the site-specific climatic aspects, all these features may enhance nitrate enrichment in the subsurface. The prevailing climatic aspects in the study area are typical for semi-arid

regions and comprise processes such as downward flushing during major rainfall events, while accumulating salts in dry phases, and the transport by surface flow and preferential flow of seepage water in macropores (root channels, animal burrows).

During this study, a combined approach of hydrochemical, isotope hydrological and geochemical methods was used to trace the fate and sources of nitrate. A short outline of this thesis is given in the following:

- Chapter 1 introduces the scope and outline of the project.
- Chapter 2 provides a literature review which summarizes the fate of nitrate in semi-arid regions, including sources and sinks.
- Chapter 3 gives a detailed insight into the specific features of the study area, including climate, paleoclimate, soils and vegetation. It as well provides information on the geological setting and the hydrogeology of the investigated aquifer.
- Chapter 4 summarizes the methods applied for the investigation of geochemistry, hydrochemistry and isotope hydrology.
- Chapter 5 explains the hydrogeochemical setting of the study. The results of nitrogen analyses of rocks are presented, followed by a lateral and vertical hydrochemical characterization of the aquifer. The origin of the groundwater types occurring in the Serowe-Orapa groundwater system is discussed.
- Chapter 6 provides an evaluation of the flow regime inferred from hydraulic head elevations, flow modeling and isotope hydrology. Groundwater residence times and recharge sources are established by a wide range of environmental tracers.
- Chapter 7 synthesizes all chapters, draws conclusions on the sources and sinks of nitrate in the Ntane Sandstone Aquifer, and analyzes the migratory pattern of nitrate influenced by the groundwater flow development. This chapter is superseded by an outlook in chapter 8 which suggests further research strategies.

2 FATE OF NITRATE IN THE SUBSURFACE

2.1 Nitrate and health

The extraordinary enrichment of nitrate in groundwater is a worldwide phenomenon, mostly due to anthropogenic activities. Often, nitrate contamination is a result of malfunctioning sanitary systems, fertilizer use, sewage and erosion of natural deposits (chapter 2.3). Negative health effects induced by nitrate in drinking water have been described in numerous general (European Parliament, 2000, Terblanche, 1991, Packham, 1991, WHO, 1985a, 1985b etc.) as well as regional studies (Europe: Razowska-Jaworek and Sadurski, 2004, Southern Africa: Hesseling, 1991, Super et al., 1981, Comly, 1945).

Nitrate itself has a low primary toxicity (Rohmann and Sontheimer, 1985), but when reduction to nitrite (NO_2^-) occurs, it becomes an oxidizing agent that converts the blood's hemoglobin (Hb) into methemoglobin (metHb) (secondary toxicity) (Eq. 2.1, DVWK, 1996). This so formed complex inhibits oxygen transport in the blood. The Hb of young infants is more susceptible to metHb formation than that of older children and adults (WHO, 1985b). Infants develop a condition called methemoglobinemia, leading to cyanosis (‘blue baby disease’) and mortality at higher doses (WHO, 1998, Addiscott et al., 1991). In Southern Africa the risk of infant mortality has increased as an immediate result of the AIDS epidemic which requires bottle-feeding of the infants with nitrate-rich water (Colvin, 1999). In animals, negative health effects due to nitrate have also been observed. Elevated nitrate concentrations lead to deficient growth and decreased reproduction in cattle (Davison et al., 1964), an important key sector in Botswana's economy. In Southern Africa, cases have been reported where cattle died after short time exposure to high doses of nitrate (Tredoux, 1993, 1985).

(2.1) $4Hb(Fe^{2+})\text{-}O_2 + 4\ NO_2^- + 2\ H_2O \rightarrow 4\ MetHb(Fe^{3+})\text{-}OH + 4\ NO_3^- + O_2$

(2.2) $R_2N\text{-}H + HNO_2 \rightarrow R_2N\text{-}N{=}O + H_2O$

Beside a first and secondary toxicity, a tertiary toxicity of nitrate is also discussed in the form of an endogenic synthesis of cancerogenic nitrosamines (R_2N-NO) from secondary amines (R_2N-H) (Eq. 2.2), quarternary ammonia

compounds or alkyl amides with NO_2^- as reaction partners (Petri, 1976). Statistical evidence could not yet be established sufficiently to relate elevated nitrate concentrations in drinking water to cancer cases (Addiscott et al., 1991), but several studies suggest that a link might well be possible (WHO, 1996b, Speijers et al., 1989), although not confirmed due to the inadequacy of the available data sets (WHO, 1985b). More detailed information on this issue can be found in Tredoux (2004) and Tredoux et al. (1993).

In many countries groundwater is used as drinking water, as it is generally bacteriologically acceptable, possesses constant temperatures and in many cases can be used without treatment (Rohmann and Sontheimer, 1985). The United States population takes 50 % of its drinking water supply from groundwater (Lichtenberg and Shapiro, 1997). For Germany groundwater is the most important drinking water supply, providing 64 % of the public water supply (BGW, 2004). In Botswana, 65 % of the scarce water resources stem from groundwater (Keipeile, 2004). Due to the growing population in the country's bigger villages and cities and Botswana's climatic conditions especially in regions near the Kalahari Desert, more groundwater has to be abstracted (Arntzen and Veendendaal, 1986).

To be used for drinking this water has to follow quality standards. Due to its toxicity the WHO has set an international guideline value for nitrate (Tab. 2-1) and for nitrite. In case of their co-occurrence the WHO require the sum of the ratios of the concentrations of each to its guideline value should not exceed 1 (Eq. 2.3):

$$\frac{c_{nitrite}}{gv_{nitrite}} + \frac{c_{nitrate}}{gv_{nitrate}} \leq 1 \qquad (2.3)$$

c: concentration
gv: guideline value

Nitrate in groundwater increased in the past years as a result of industrial and agricultural practices. The WHO e.g. noted a substantial increase of nitrate in water in Europe over the past 30 to 40 years (WHO, 2004), making nitrate an issue of environmental concern.

Tab. 2-1: Guideline values for nitrate in drinking water.

Organization	Concentration (mg/l) as NO_3^-	Concentration (mg/l) as NO_3-N	Reference
WHO (international)	50.0	11.3*	WHO, 1998
EPA (USA) (maximum contaminant level)	44.3*	10	US EPA, 2002
Botswana Bureau of Standards (BOS) Class II Guideline Value	45.0	10.2*	BOS, 2000
Orapa Potable Water Standard (Botswana)	100.0	22.6*	Debswana, 2004
CSIR Report 628 Crisis limit (South Africa)	100.0	22.6*	Debswana, 2004
Rural Water Supply Manual DWA Botswana	45.0	10.2*	Debswana, 2004
Germany	50.0	11.3*	TrinkwV, 2001
Livestock standards	**Concentration (mg/l) as NO_3^-**	**Concentration (mg/l) as NO_3-N**	**Reference**
Botswana	-	-	(no standard)
South Africa	400.0	90.4	Baard, 1992
Namibia	486.9*	110	DWA Namibia, 1977

*derived units (1 mg/l NO_3-N = 4.43 mg/l NO_3)

In Botswana the drinking water standards were set for the first time in 2000 by the Botswana Bureau of Standards (BOS, 2000), including a standard for nitrate (Tab. 2-1). An overview of the Southern African and international limits and guidelines for nitrate in drinking water can be found in Tab. 2-1.

2.2 Nitrogen in soil and subsoil

Nearly all nitrogen found in the soil originates from the atmosphere, which is made of 78.1 % of nitrogen. More than 95 % of nitrogen compounds in the soil are located in the topsoil, 90 – 95 % of which are bound in organic compounds in the A-horizon (DVWK, 1996). Despite its role as an essential nutrient for plants, nitrogen occurs in soils mostly in form of organic compounds that are not bioavailable to vegetation. Nitrogen compounds can be transformed by several mechanisms that include fixation, ammonification, assimilation, nitrification and denitrification. A schematic soil nitrogen cycle is shown in Fig. 2-1. The main processes of nitrogen transformation are shortly described in the following. A more detailed description can found in e.g. Scheffer and Schachtschnabel (2002), Canter (1997), or Burt et al. (1993).

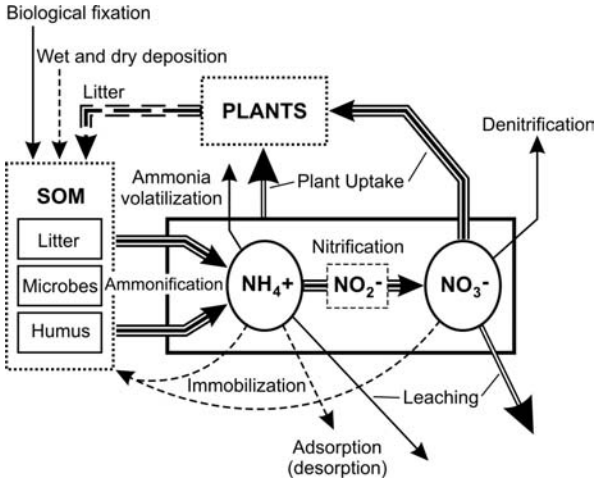

Fig. 2-1: Soil nitrogen cycle (after Porporato et al., 2003). The relative dimensions of the arrows describe the relative importance of the processes.

Fixation of nitrogen signifies the incorporation of inert, gaseous N_2 into a chemical compound useable for plants and animals. Fixation processes can occur through lightning, or can be industrial (e.g. in fertilizer production) or biological, of which biological fixation is the most important process (Canter, 1997). Fixation from N_2 to organic nitrogen is mainly performed by specialized microorganisms and their association with plants (US EPA, 1994). Bacteria associated with leguminous plants are able to fix atmospheric N_2 (and N_2O) by nodulation of the root system. This is described as an important process in many semi-arid areas (Cook and Herczeg, 2000). Still, many legume members which dominate moist, nutrient-poor savannas in Africa, have been found not to fix nitrogen (Grobbelaar and Rösch, 1981). Evidence for further fixation potential of atmospheric nitrogen has been found in cyanobacterial crusts in semi-arid ecosystems such as the Kalahari in their ability to fix atmospheric nitrogen (Shushu, 2000).

Nitrogen can, however, only be taken up by plants in form of ammonium (NH_4^+) and nitrate (NO_3^-) which can be mineralized from soil organic matter (SOM) decomposition by microorganisms. The rate of mineralization depends on external factors such as pH, temperature and soil moisture content. The first step of the mineralization process is ammonification, which can be described as follows:

(2.4) Organic nitrogen + microorganisms $\rightarrow NH_3/NH_4^+$

Another important process in the nitrogen cycle is the nitrification process, which occurs in the presence of oxygen. Nitrification is the biological two-step oxidation of ammonium ions (US EPA, 1994) via nitrite formation, catalyzed by the chemoautotrophic bacteria Nitrosomas and Nitrobacter:

(2.5) $$NH_4^+ + O_2 \xrightarrow{Nitrosomas} NO_2^- + O_2 \xrightarrow{Nitrobacter} NO_3^-$$

Those transformations proceed rapidly to the NO_3^--form. The resulting nitrate from this process is either used for plant growth or may be lost to denitrification. The subsequent assimilation (or synthesis) describes biochemical mechanisms in which ammonium or nitrate compounds are used to produce plant protein or other nitrogen-compounds (Canter, 1997):

(2.6) $NO_3^- + CO_2$ + green plants + sunlight → protein
or
(2.7) $NH_3/NH_4 + CO_2$ + green plants + sunlight → protein

Nitrogen sinks are, respectively loss from soil generally occurs through (i) plant uptake with subsequent harvesting of the plant, (ii) leaching, (iii) volatilization of gaseous N-compounds, (iv) (wind) erosion (DVWK, 1996) and (v) denitrification. In desert environments leaching is assumed to be negligible as N-sink by some authors (e.g. Peterjohn and Schlesinger, 1990, Boring et al., 1988). However, recent studies suggest that substantial quantities of nitrogen have leached and accumulated beneath the (active) soil zone over large time scales in desert ecosystems (Walvoord et al., 2003). Denitrification is likely to be insignificant in semi-arid to arid climate, as oxidizing conditions prevail as a result of the aerated conditions of the (e.g. sandy) soil. However, Tindall et al. (1995) observed a rapid denitrification when sandy soils have a vegetation cover. A description of the denitrification processes can be found in chapter 2.5.

Aside from pure biochemical aspects, nutrient cycling is closely related to hydrology, because water movement is the main transport mechanism for nutrients in and out of the soil system. The amount of water entering the soil is mainly driven by the regional precipitation pattern. Water output and thus the water budget of the soil is also influenced by the evapotranspiration at the given site. The relative importance of evapotranspiration depends on the climatic conditions at the site, the vegetation and on the soil hydraulic conditions. Beside its dependence on the total water budget – nitrate is easily lost by leaching due to its high solubility - the nitrogen cycle in the soil has a strong and complex interaction with soil moisture. Thus the dynamics of nitrate transport and transformation in unsaturated soils can already be affected by small, localized variations in the soil moisture (Porporato et al., 2003, Feral et al., 2002, Tindall et al., 1995). For high nitrification rates a balance of aeration and humid conditions for microbial biomass is crucial (Porporato et al., 2003). High soil moisture creates anoxic conditions that inhibit bacteria from the oxidation necessary for decomposition of organic matter. Under low moisture conditions decomposition is reduced due to a lack of substrate supply resulting from reduced water content: The sediment matrix dries, causing a thinning of the water film around matrix pores. This in turn increases diffusion path length (increased tortuosity). The rate of substrate diffusion to mi-

crobial cells is lowered and results in reduced microbial activity (Fenchel et al., 1998). Another limitation of decomposition is caused by low matrix potentials due to low water contents that reduce hydration and enzyme activity (Porporato et al., 2003). Under favourable conditions decomposition and nitrification can, however, occur rapidly. When e.g. hot dry areas receive sudden rainfall, a flush of nitrate production may be triggered (D'Odorico et al., 2003).

As seen from above, leaching is the main process for nitrate to be transported from the soil into the groundwater under semi-arid conditions. More detailed information on soil nitrogen cycling under semi-arid conditions can be found in Schwiede (in prep.).

2.3 Nitrogen of geogenic origin

Nitrogen-bearing rocks are globally distributed. Although often neglected in nutrient cycling in the past, geologic sources have been reported in recent studies to comprise a large potential pool of nitrogen (e.g. Holloway and Dahlgren, 2002, Lowe and Wallace, 2001, Holloway et al. 1998). This pool is estimated to contain about 20 % of the global nitrogen inventory (Schlesinger, 1997). Primarily sedimentary and low-grade metasedimentary rocks exhibit elevated nitrogen concentrations. In general, nitrogen concentrations in rocks range from trace levels in granites (less than 200 mg/kg) to concentrations greater than 1000 mg/kg in whole rock samples of some sediments and metasediments (Holloway and Dahlgren, 2002). Up to 32,000 mg/kg N was reported from NH_4^+-rich end members of muscovite and feldspar. Often, the amount of nitrogen in rock is not quantified as a result of the lack of comprehension of nitrogen into routine analytical procedures.

The main source of nitrogen in rocks is organic matter that is deposited in sediments. Alternatively nitrogen can stem from thermal waters as a mixture of sedimentary, mantle and meteoric origin. Nitrogen can be incorporated into rocks as organic matter (e.g. in carbonaceous shale), or as ammonium (NH_4^+) fixed in silicate minerals (Dahlgren and Holloway, 2002). The nitrogen that is contained in organic matter is converted to ammonium during diagenesis, which in turn can substitute for potassium (K^+) in silicate minerals. Ammonium end-member silicate minerals include buddingtonite, tobelite, ammonium muscovite and ammonium biotite (Lowe and Wallace, 2001).

Another important way of accumulating nitrogen is through atmospheric deposition, including wet and dry fall. This occurs especially in arid and semi-arid regions. Deposition, combined with the absence of sufficient precipitation prevent a leaching of accumulated (nitrogen-) salts from the soil. Atmospheric deposition of 43 mg NO_3-N and 1 mg NH_4-N per 100 g loess per month were found in the Negev desert of Israel (Offer et al., 1992). In the Atacama desert of Chile, caliche type deposits stemming from atmospheric deposition reach 15,000 to 163,000 mg N/kg (Ericksen, 1981). In the Mojawe desert of California 12,800 to 73,300 mg N/kg were measured (Ericksen et al., 1988). Among identified nitrate minerals in evaporites were nitratine, nitre, darapskite and humberstonite. Nitrogen salts are highly soluble. The solubility product (K_{sp}) of e.g. $NaNO_3$ at 25°C is 2.91. Normally the high solubility of nitrogen salts leads to a rapid leaching, but a lack or very limited amount of recharge potentiates a (temporal) salt accumulation.

Several authors have recognized that bedrock nitrogen might possibly affect soil and water quality (e.g. Lowe and Wallace, 2001, Holloway and Dahlgren, 2002) and that nitrate that is released through weathering may contribute to nitrogen (over-)saturation of an ecosystem (see also chapter 2.2). Lowe and Wallace (2001) consider natural geogenic nitrogen as an explanation in stream water in Utah. There, wastewater was suspected to be the cause of nitrate contamination. Despite an introduction of septic tank soil-absorption systems for wastewater disposal, the installation of those systems did not affect nitrate concentrations, and the authors did not detect seasonal concentration changes. These processes may be more pronounced in surface waters than in deeper groundwaters as the weathering rate of rocks and thus the release of nitrogen is higher under surface conditions. However, in some cases distinguishing between anthropogenic and geogenic origin of nitrate in groundwater is challenging and needs to be looked at on a case-by-case basis (Holloway and Dahlgren, 2002).

Apart from contributions from the primary rock, an influence of secondary factors might have to be considered. These secondary factors include weathering products and site or regional-specific environmental factors such as density of vegetation, unsaturated zone properties and climate (Tredoux and Kirchner, 1985). Especially in semi-arid to arid regions these factors are closely interrelated with soil processes (chapter 2.2).

2.4 Nitrate in groundwater of semi-arid regions

Nitrate is a common species in aquifers around the world. However, the amount and sources of nitrate in groundwater vary between different regions. In Europe, background concentrations of NO_3^- in groundwater generally range below 2 mg NO_3-N (equals 8.8 mg/l NO_3) beneath grasslands (Foster et al., 1982). Yet, concentrations often exceed established drinking water standards and are generally termed pollution (chapter 2.1). Numerous studies have focussed on this matter and have investigated the reasons for elevated nitrate concentrations. In moderate climate regions increased nitrate concentrations are almost exclusively of anthropogenic origin, mainly caused by agricultural activities and sewage problems (e.g. Razoskowa-Jaworek and Sadurski, 2004, Canter, 1997). Also in developing countries human impact starts to pose a problem for water quality which includes an increase in nitrate concentrations. In some semi-arid and arid regions, however, elevated nitrate concentrations have been recorded that are difficult to explain by anthropogenic pollution (as discussed later in this chapter). Firstly, the impact of anthropogenic pollution on nitrate concentrations in groundwater is discussed in this chapter. A selection of regional studies is presented, as anthropogenic causes of nitrate enrichment in groundwater range over a wide spectrum (Tab. 2-2), followed by examples of natural nitrate enrichment studies.

As seen from Tab. 2-2, the studies mainly describe the influence from unsewered sanitation, septic leaching and animal waste (e.g. Tredoux et al, 2001, Foster, 1985). In addition, a large number of studies on the influence of agricultural practices have been produced (e.g Hadas et al., 1999, Edmunds and Gaye, 1997). Other studies describe wastewater influence from mines, where ore-dressing processes associated with large water volumes mobilize natural components from rocks, resulting in high nitrate waters, or the use of explosives such as ammonia-nitrate (Matthes, 2002, Rosenthal et al., 1988). Also, changes of land-use and their effect on nitrogen in groundwater are investigated by a number of authors (e.g. Faillat and Rambaud, 1991).

Tab. 2-2: Overview of selected case studies investigating anthropogenic sources of nitrate enrichment in groundwater of semi-arid regions.

Type of contamination	**Description of the source of nitrate**	**Region**	**Author(s), year**
sanitation	Leaching from on-site sanitation	Botswana	Jacks et al., 1999
sanitation	Localized and diffuse influences from unsewered sanitiation	USA	Williams et al., 1998
sanitation	Septic leaching and animal waste	Botswana	Lagerstedt et al., 1994, 1992
sanitation	Unsewered sanitiation	Australia	Foster, 1985
sanitation	Leaching from excreta in villages	India	Jacks and Sharma, 1983
sanitation, sewage	Pollution due to on-site sanitation, sewage sludge application to land, wastewater irrigation and fertilizer application	Southern Africa	Tredoux et al., 2001
sanitation, sewage	Sewage effluents advecting and dispersing through macropores	Tanzania	Nkotagu, 1996
sewage	Pollution derived from animal waste	Namibia	Heaton, 1984
agriculture, sewage, sanitation	Diffuse pollution by agricultural fertilizer residues, point pollution by human wastewater, livestock faeces and mineralization of organic debris	Morocco	Lafthoui et al., 2003
agriculture	Intensification of agricultural practices and excessive use of nitrogen fertilizers	Morocco	Saadi and Maslouhi, 2003
agriculture	Application of nitrogen-rich fertililizer	Mexico	Pacheco et al., 2001

- continued-

Tab. 2-2 (continued): Overview of selected case studies investigating anthropogenic sources of nitrate enrichment in groundwater of semi-arid regions.

Type of contamination	**Description of the source of nitrate**	**Region**	**Author(s), year**
agriculture	Intensification of agricultural practices	Israel	Hadas et al., 1999
agriculture	Influence by agricultural practices	Senegal	Edmunds and Gaye, 1997
landfill	Local minor impact of landfills	South Africa	Blight, 1995
mining	Wastewater and blasting influence from mines on groundwater quality	Botswana	Matthes, 2002
mining	Mechanical ore-dressing processes associated with large water volumes mobilizes natural components from rocks	Israel	Rosenthal et al., 1988
land-use change	Implications from deforestation	Niger	Favreau, 2002, 2003
land-use change	Nitrate release from soil induced by land-use change, and pollution by latrines	Niger	Girard and Hillaire-Marcel, 1997
land-use change	Changes in land-use and their effect on nitrogen in groundwater	Côte d'Ivoire	Faillat and Rambaud, 1991

In the following, a selection of case studies on non-anthropogenic nitrate enrichment phenomena in semi-arid and arid regions is discussed. Most studies suggest that nitrate enrichment in groundwater of semi-arid regions is mainly caused by an initial build-up of a nitrate pool on the surface or in the unsaturated zone which is subsequently mobilized, eventually causing increased nitrate concentrations in the groundwater (e.g. Verhagen, 1995, Barnes et al., 1992, Lawrence, 1983). In some studies, nitrate has a geogenic origin and is released due to changed environmental conditions, e.g. weathering (e.g. Lowe and Wallace, 2001) (chapter 2.3).

Processes leading to a build-up of nitrogen in the subsurface include N-fixation (as discussed in chapter 2.2), and dry and wet deposition as NH_4^+ and NO_3^-. In addition to a direct input of N into the groundwater by wet deposition, its coupling with high evapotranspiration rates can inhibit direct leaching of nitrate into the groundwater and can thus enhance subsurface nitrogen accumulation. These conditions are typical for semi-arid to arid regions. In the case of very shallow groundwater levels, evapotranspiration from the saturated zone can occur, leading to elevated concentrations of substances in the groundwater, as water (vapor) leaves the system (Verhagen, 1995). Another enrichment process is described by Aranibar et al. (2003) in their studies in the Kalahari of Botswana. The authors stress the importance of cyanobacterial soil crusts in arid and semi-arid environments in their ability to fix atmospheric N_2. Estimates of N_2-fixation by soil crusts vary widely, but appear to be of importance in the Kalahari Desert (Skarpe and Henriksson, 1986). Indications for N-fixation in soils by bacteria have also been found in Australian studies (Barnes et al., 1992). In their study area nitrate enrichment is even more pronounced through a scarcity of denitrifiying bacteria and thus an enhanced flushing of nitrate through the unsaturated zone. This is facilitated by recharge pulses from extreme rainfall events. Also, N-fixing bacteria in termite mounds are described as point sources that eventually produce NH_4^+ which is bacterially oxidized to NO_3^- and leached by capillary action (AGSO, 1993, Sheard, 1982). Finally, an influence of fire is stated (Sanchez and Lazzari, 1999, Carreira and Neill, 1995, Barnes et al., 1992). Fires in arid areas are common practice and are of influence as they facilitate recharge and nitrate accession to the water table mainly by ash distribution and by altered macropore structures.

As already implied from chapters 2.2 and 2.3, processes such as water transport in the unsaturated zone play a more significant role regarding transport of dissolved species in semi-arid to arid regions than in more temperate regions. The balance between low precipitation rates and high evaporation rates determines if (and to what extent) groundwater recharge can occur, by which nitrate can be transported into the groundwater. In the absence of groundwater recharge nitrate can be accumulated in the unsaturated zone and surface, otherwise it is leached. The occurrence of recharge is controlled by site specific factors relating to unsaturated zone properties and to climatic factors. Already small, localized changes in precipitation can cause a build-up or decrease of nitrate (Austin et al., 2004). Finally, the absence of active drainage systems

can facilitate nitrate accumulation, as it is then retained and not removed from the system. These effects can be of short-term nature.

Long-term climatic effects, too, appear to have an influence on nitrate in the unsaturated and saturated zone of semi-arid regions, as shown in the following examples. Heaton et al. (1983) revealed nitrate concentrations of greater than 100 mg/l in paleowaters in the Western Kalahari. The elevated nitrate concentrations in groundwater are attributed to leaching of soil nitrogen. The authors emphazise the possibility of involvement of a change of environmental conditions during recharge on the nitrate concentrations, induced by climatic changes from wetter to semi-arid conditions. Similar observations were made by Edmunds and Gaye (1997). These authors observed more than 50 mg/l of nitrate in groundwater in the Sahel, Senegal, and confirm that a significant nitrate build-up occurs in the soil zone under the present semi-arid conditions. The accumulated nitrate may be leached and then increase nitrate in shallow groundwaters. They suggest fixation of nitrogen by leguminous plants as the enrichment process, with higher fixation rates during humid periods. Spatially varying nitrate concentrations in the unsaturated zone are explained by changing input over time, especially as a result of differences in humidity and induced or natural vegetation cover.

Rosenthal et al. (1987) found that nitrate in the Negev (Israel) is the result of a change of environmental conditions during the Pleistocene. At that time humid periods flushed previously deposited soluable salts, but with progressing desertification reaccumulation in the sediments of the unsaturated zone occurred. This study suggests that other deserts with similar environmental conditions, like the Negev, do not have nitrate-bearing surface crusts due to the very low, but not completely absent precipitation, and might as well be prone to nitrate accumulation below the ground. The Negev, e.g., receives a precipitation of 60 mm/a, while the Atacama of Chile only receives 2-5 mm/a. Pleistocenic climatic influences and impacts of an ‘easily overlooked potential [geologic] source’ on groundwater and soil nitrogen distribution are also described in Marrett et al. (1990) (chapter 2.3). (Paleo)climatic indications were also stated in Edmunds and Gaye (1997). In total, naturally high nitrate appears to be common in many arid and semi-arid regions and is suspected to be a tracer of past environmental conditions (Edmunds and Gaye, 1997).

2.5 Nitrate reduction in groundwater

For nitrate removal from groundwater, the only in-situ means is reduction. Unlike other substances nitrate does not form insoluble minerals that could precipitate, nor does it adsorb significantly under aquifer conditions (e.g. Appelo and Postma, 1996). The only larger known accumulations of nitrate minerals occur as e.g. nitre minerals in (semi)arid regions and are results of playa lakes (e.g. Garrett, 1985) or atmospheric deposition (e.g. Ericksen, 1981). Those minerals are, however, highly soluble (chapter 2.3).

Nitrate reduction in the subsurface is almost exclusively bacterially catalyzed (Rödelsperger et al., 1984). The following types of nitrate reduction can be distinguished (Rohmann and Sontheimer, 1985, Korom, 1992):

a) Assimilatory nitrate reduction (nitrate assimilation)

NO_3^- is reduced to NH_4^+ via the intermediate products NO_2^- and hydroxylamine (NH_2OH), which in turn is assimilated in the synthesis of amino acids (Payne, 1981) (Eq. 2.8). The formed NO_3^- is thus fully transformed into organic matter, at the same time reducing CO_2.

(2.8) $2\ NO_3^- + 4\ H_2O + 4\ CO_2 + 2\ H^+ \rightarrow 7\ O_2 + 2\ C_2H_5O_2N$

This reduction is of higher importance in the soil zone than in groundwater.

b) Nitrate ammonification (dissimilatory nitrate reduction to ammonium DNRA)

Organic carbon is oxidized and releases energy (dissimilatory NH_4^+-formation). As in nitrate assimilation the intermediate products in this reaction are also NO_2^-- and possibly hydroxylamine (NH_2OH).

(2.9) $2\ C_n(H_2O)_n + n\ NO_3^- \rightarrow 2\ n\ HCO_3^- + n\ H_2O + n\ NH_4^+$

This process only takes place under strictly anaerobic conditions and very low redox potentials. The reaction is only assumed to happen in aquifer zones where denitrification (see (c)) is no longer possible (e.g. Buresh and Patrick, 1978). In the literature it is generally seen as a subordinate process in aquifers

(e.g. Appelo and Postma, 1996, Smith et al., 1991). Other authors (e.g. Korom, 1992) see the need of further investigation of its role, as DNRA takes place under similar conditions as denitrification. As opposed to the nitrogen loss in denitrification this process conserves a system's nitrogen (Korom, 1992).

c) Denitrification

Denitrification describes the bacterially catalyzed process where NO_3^- is reduced to N_2O or N_2. The bacteria are facultative aerobes that oxidize organic substances (heterotrophic-chemoorganotrophic bacteria) to gaseous N-compounds or anorganic substances, e.g. S-compounds or H (autotrophic-chemolithotrophic bacteria) to molecular N. The energy gain in those reaction is slightly lower (ca. -5 %, Rohmann and Sontheimer, 1985) than in aerobic respiration. Denitrification thus only takes place below a threshold oxygen concentration that depends on the respective bacteria species as well as on the redox environment (Rödelsperger et al., 1991).

To reduce nitrate in aquifers, reduction potential within the aquifer is needed. Interaction of nitrate with reduced groundwater components such as Fe^{2+}, H_2S and CH_4 is possible (Otteley et al., 1997), but kinetic inhibitions can be encountered. Also, the reactions of nitrate with reduced species that are dissolved in the groundwater are rarely quantitatively significant for nitrate reduction in aquifers (Appelo and Postma, 1996). Substantial nitrate reduction can be provided by organic matter, pyrite and Fe(II)-silicates within the aquifer sediments (Eq. 2.10 to 2.13). Those substances have the thermodynamic potential for nitrate reduction. The principle reactions are as follows:

Nitrate reduction by organic matter (heterotrophic):

(2.10) $5\ CH_2O + 4\ NO_3^- \rightarrow 2\ N_2 + 4\ HCO_3^- + CO_2 + 3\ H_2O$

Nitrate reduction by pyrite oxidation (autotrophic):

(2.11) $5\ FeS_2 + 14\ NO_3^- + 4\ H^+ \rightarrow 7\ N_2 + 5\ Fe^{2+} + 10\ SO_4^{2-} + 2\ H_2O$

and

(2.12) $10\ Fe^{2+} + 2\ NO_3^- + 14\ H_2O \rightarrow 10\ FeOOH + N_2 + 18\ H^+$

Nitrate reduction by Fe(II) (autotrophic):

(2.13) $10\ Fe^{2+} + 2\ NO_3^- + 14\ H_2O \rightarrow 10\ FeOOH + N_2 + 18\ H^+$

The reduction of nitrate by organic matter as an important process in aquifers is often described in literature (Obermann, 1992, Smith and Duff, 1988 etc.). Here, not only solid organic phases (matrix) but also dissolved organic carbon (DOC) can be of importance (Star and Gilham, 1989).
Ongoing reduction processes in groundwater can be seen in the existence of intermediate products like NO_2^-, which eventually proceeds to N_2. Hardness is increased, and the nitrate concentration decreases in the same measure as HCO_3^- increases.

d) Soil retention (chapter 2.2)

There is little evidence for nitrate sorption on soils (Kendall and McDonnell, 1998). Owing to its positive charge ammonium (NH_4^+) rather than nitrate sorbs on clay mineralitic surfaces.

Only denitrification may serve as a major N-sink in the aquifer, as the other processes ((a), (b), (d)) only cause a temporary immobilization of nitrogen (Korom, 1992).

3 SITE DESCRIPTION AND AQUIFER CHARACTERISTICS

3.1 Location

The study area is situated on the Eastern fringe of the Kalahari between Serowe and Orapa in the Central District of Botswana, and covers about 21,000 km^2 (Fig. 3-1). Two pilot areas were chosen for detailed investigations. Area 1 is located WNW of Serowe and covers about 4090 km^2, area 2 is located WSW of Orapa and Letlhakane and covers about 5100 km^2 (Fig. 3-2). For simplification of designations, area 1 will be termed 'Serowe' in the following text, while area 2 will be termed 'Orapa'. The study area is characterized by a flat, slightly undulating topography at about 1000 to 1200 m above sea level; the only distinct topographic feature is the Eastern escarpment.

3.2 Climate

3.2.1 Recent conditions

The study area lies in a semi-arid region with low air humidity and mean annual rainfall between 200 mm/a in the Northwest and 450 mm/a in the Southeast, restricted to one annual rainy season from September to April (Fig. 3-3). However, there are extreme temporal and spatial variations in the distribution of precipitation. Isolated extremely heavy rainfall events that reach even up to 100 mm/d (Lubczynski, 2000) have been reported to reoccur in 10 to 12 year intervals. The return probability of these events is high, however, a real periodicity could not yet be established (Bäumle, 2003). Those years are suspected to constitute the principal mechanism for groundwater recharge (Lubczynski, 2000). Recharge is further discussed in chapter 3.5. In general, temperatures during summer can reach 35°C, while in winter less than 10°C can occur (Fig. 3-4).

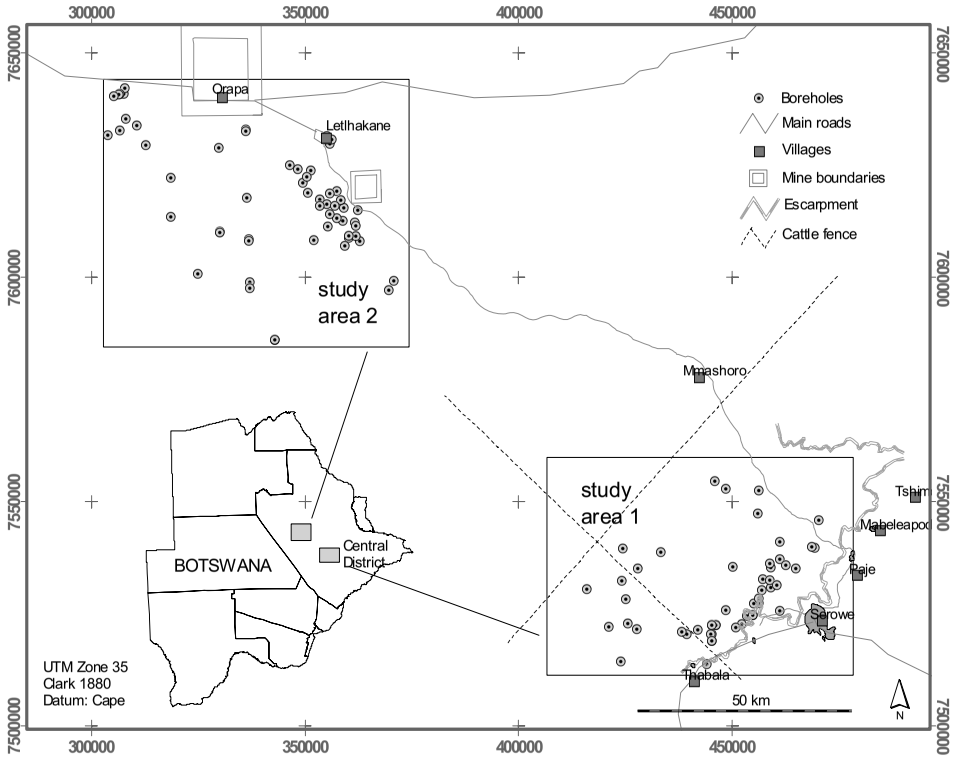

Fig. 3-1: Location of the study area in the Central District of Botswana (study area 1 = Serowe, study area 2 = Orapa). The used coordinate system and projection as given in this figure is also valid for subsequent maps.

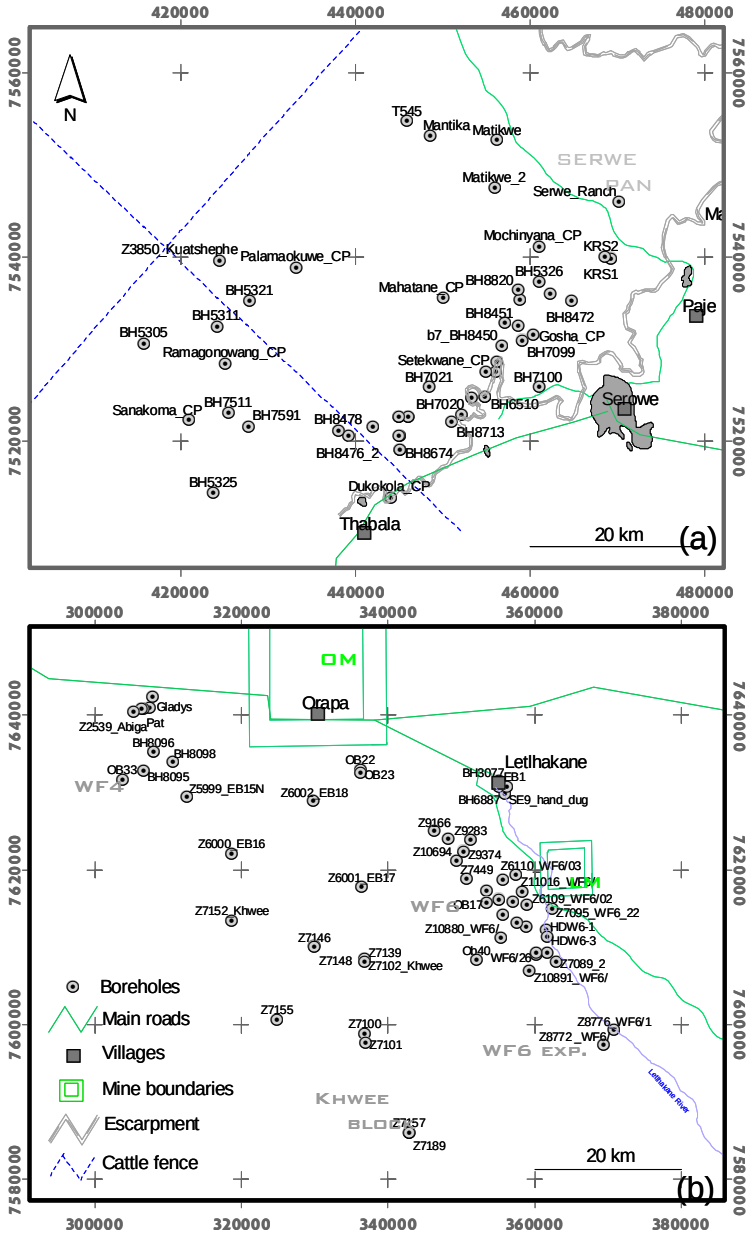

Fig. 3-2: Borehole location map of (a) study area 1 (Serowe) and (b) study area 2 (Orapa).Note the slight scale difference between the maps. Locations are referred to in the text of chapter 5 (WF= wellfield, WF exp. = wellfield expansion, LM = Letlhakane Mine, OM = Orapa Mine)

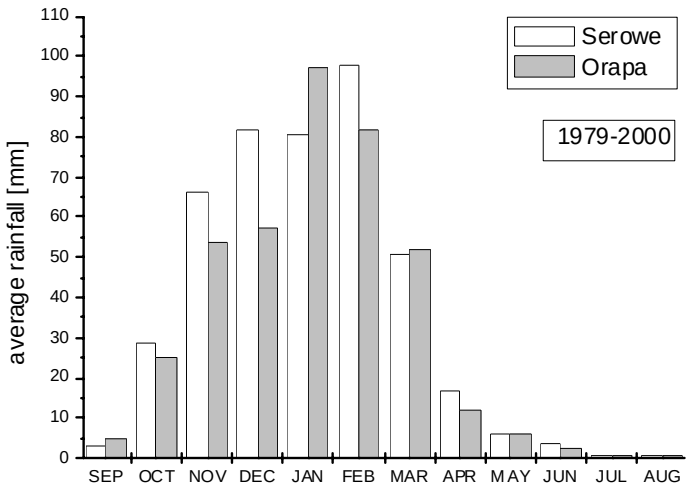

Fig. 3-3: Average monthly rainfall in Serowe and Orapa, Botswana (1979 to 2000).

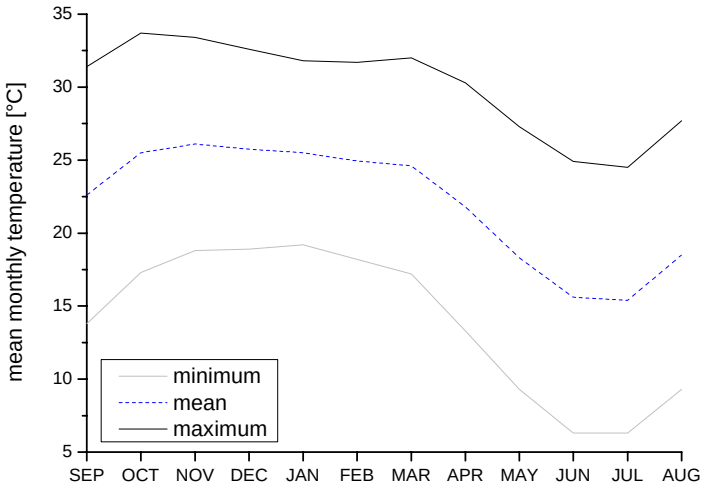

Fig. 3-4: Mean monthly temperatures in Letlhakane from 1994 to 2000.

3.2.2 Evapotranspiration

Potential evapotranspiration is in the order of 900 – 1200 mm/year (Lubczynski, 2000). Fig. 3-5 shows the average 10-day potential evapotranspiration and precipitation for the study area. As only rainfall records were available for Serowe, additional meteorological data were used from the nearest climate station that is located in Mahalapye about 100 km South of Serowe. Generally, monthly rainfall totals are consistently exceeded by potential evaporation (SGAB, 1988, and Fig. 3-5). This would indicate that recharge is not possible. However, due to the extreme rainfall conditions that may occur in short duration and high intensity, on a daily basis rainfall can exceed potential evapotransporation and lead to a potential recharge through transport via preferential flow paths (Selaolo, 1998, SGAB, 1984).

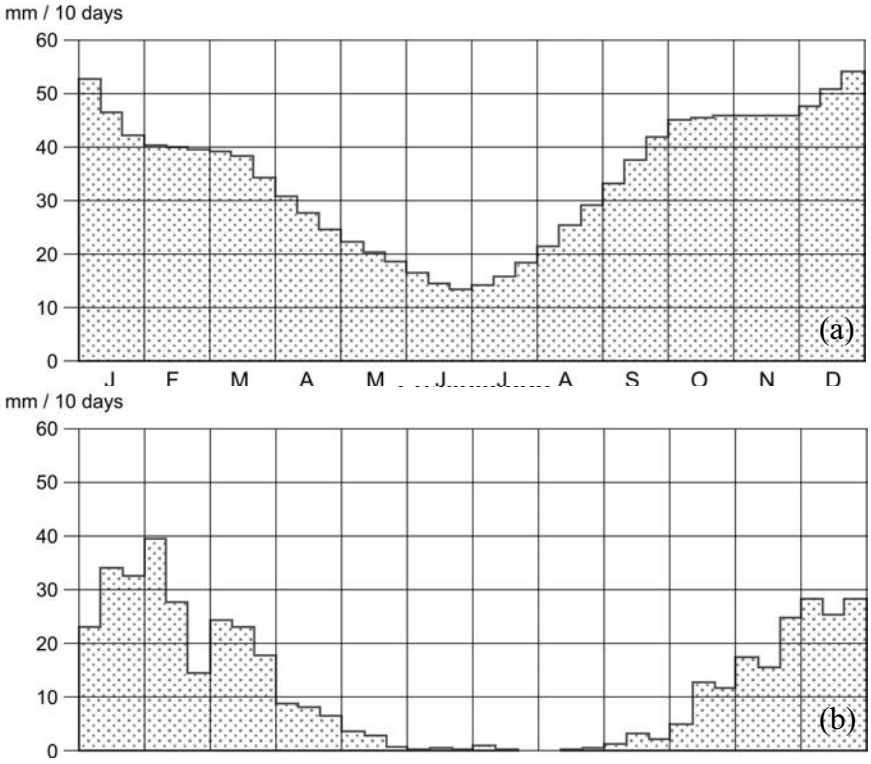

Fig. 3-5: Average 10-day (a) potential evapotranspiration (Mahalapye) and (b) precipitation (Serowe) after SGAB, 1998.

3.2.3 Paleoclimate

The fact that climatic changes have taken place in the Kalahari has already been suggested in the 1850s (Livingstone, 1858, in Thomas and Shaw, 1991). However, as data quality and resolution was poor, sometimes "climatic concepts were dictating the interpretation of evidence rather than vice versa" (Thomas and Shaw, 1991). For a long time only very scattered studies existed and directly dated evidence was lacking (Stokes et al., 1997), giving a lot of contrasting interpretations, and a lack of a chronological framework prevailed. Even today it is still difficult to interpret paleoclimatic data of the Kalahari, as interpretation can only be as good as the proxy data, which, in the case of the Kalahari, is very poor. The Kalahari Group sediments, which are mainly used in the investigations, are highly altered and difficult to differentiate. They contain only few fossils and have only low preservation levels of the contained organic matters. This hinders interpretation and dating.

In addition, there is only little material available for radiometric dating, most of which is calcrete. Calcrete dating can be problematic due to two factors: i) Data derived from calcrete provides the "youngest possible date" of the surrounding materials, as calcrete formation is not necessarily monogenetic (Netterberg, 1980). ii) Radiometric data obtained from calcrete analysis is prone to carbonate contamination. This shows that data from calcrete must be treated with caution in the interpretation and that this data can only be used as indicator rather than as stratigraphic marker (Thomas and Shaw, 1991). Other dating attempts, too, e.g. palynological methods, are often faced by the above mentioned problem of poor preservation of the material. In addition to those attempts, regional-scale interpretations are hampered by temporal and spatial heterogeneity of proxy data, at times giving only fragmentary information. Also, problems might be faced by the type and nature of the evidence that possibly creates different kinds of information. This information is likely to be accidentally interpreted as climatic effect while the true effect was maybe only masked by subsequent events. This can for example be the case in lake level reconstruction, or in poorly discriminated cave sinter deposits that are possibly misinterpreted, overestimating the indicated duration of periods of humidity (Thomas and Shaw, 1991). Despite all the criticism and the difficulties faced, general conclusions can be made, and investigation technologies have advanced. Generally, paleoenvironmental records of the Kalahari have been established by the investigation of river terrace sites, calcretes in fluvi-

atile and lacustrine terraces, cave sediments, sand dunes, pan depressions, shells and calcretes from dry valley systems and spring and tufa deposits. Recent studies apply e.g. luminescence-dating techniques to dune sediments (Thomas and Shaw, 2002), and investigate cave precipitates in more detail, revealing a more comprehensive record for time scales up to 50 ka – although further research is still required.

Quarternary paleoclimate in the Kalahari

An overview of available paleoenvironmental data is shown in Fig. 3-8 (200 ka before present (BP) to present) and Fig. 3-9 (10 ka BP to present), compiled by Thomas and Shaw (2002) from studies of different locations in the middle and Southern Kalahari. It is well visible that strong differences exist between the sites and that data remains fragmentary (Fig. 3-8, locations are shown in Fig. 3-6). 'Older' humid phases around 200 ka BP (Fig. 3-8, column f) as e.g. suggested by Brook et al. (1996) are the least reliable, due to their low environmental resolution, as criticized by Thomas and Shaw (2002). High discrepancies can also be found in the early part of the radiocarbon records around 50 to 20 ka BP (Thomas and Shaw, 1991). However, despite some data inadequacies, in total a number of general conclusions can be drawn.

Most of the sites indicate generally humid conditions around 45 ka and between 35 and 22 ka (with some drier periods within that period), with especially high levels of the Boteti River and Lake Makgadikgadi at 32 to 28 ka (Fig. 3-8, column g) preceded and followed by lake-bed calcretization. Only recently, newer findings of aeolian and cenote evidence suggest a propagation of aridity in some locations for the same period (Stokes et al., 1997) from the investigation of linear dunes in the Southwestern Kalahari (Fig. 3-8, column i). From around 20 to 18 ka BP cool, dry conditions of the last glacial maximum (LGM) prevailed, followed by wetter conditions in lakes and valleys in most of the Kalahari around 18 to 14 ka (Thomas and Shaw, 2002). This again was superseded by drier conditions that triggered calcrete precipitation through falling water tables around 13 to 10 ka BP. There is, however, contrasting evidence of different sites in the middle Kalahari around 14 ka, which reminds of the partially poor data resolution which is available for the region. Also, this again points to the fact that the shear location of the Kalahari creates conflict due to its position between the tropical summer rainfall and temperate winter rainfall belts, which even plays a role in today's rainfall distribution (Thomas and Shaw, 1991). In addition, the present situation of the Kala-

hari shows a regional-subdivision into areas of different moisture conditions. Active sand dunes are found in the Southwest while at the same time subtropical vegetation prevails between the Makgadikgadi depression and the Chobe area in the North. This shows that it is and presumably was not possible to encounter homogenic climate conditions throughout the entire Kalahari, making climatic reconstructions more challenging.

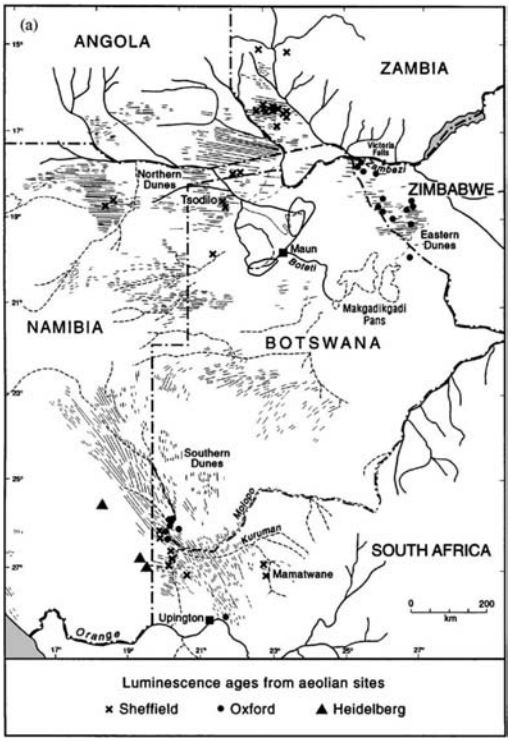

Fig. 3-6a: Distribution of numerically dated sites in the Kalahari: luminescence ages amended from Thomas and Shaw, 2002.

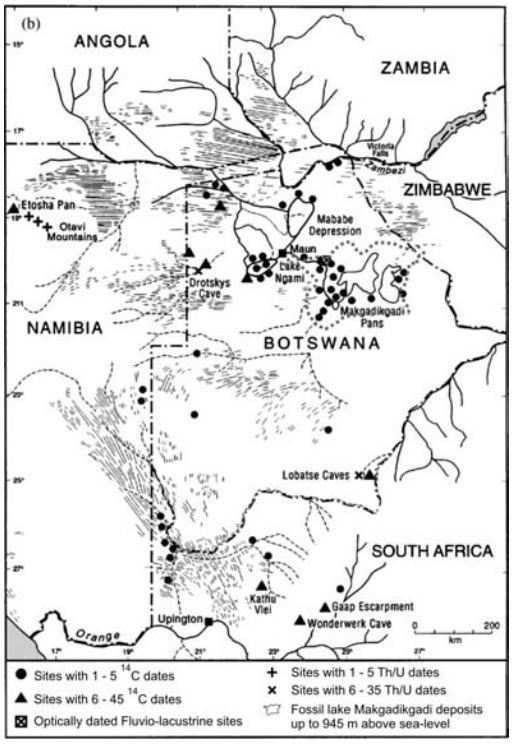

Fig. 3-6b: Distribution of numerically dated sites in the Kalahari: radiocarbon dates, amended from Thomas and Shaw, 2002.

To understand the local paleoclimate on a broader time scale, a short summary of climatic changes in Southern Africa is described in the following compiled from Tyson and Preston-Whyte (2000) and summarized in Fig. 3-7. From 25 to 15 ka BP moist conditions prevailed in most of Southern Africa, with regional drying in the Eastern and possible Southern part between 20 to 18 ka. This was followed by an arid phase in the African Tropics from 14 ka and in the Southern regions from 12 to 10 ka, following the LGM of 16 ka, after which temperatures began to rise rapidly (Fig. 3-7). Another wet phase in intertropical Africa occurred from 9 to 4 ka, however, the central and Western regions remained dry. As of 3 ka BP strong regional differences prevailed, with slightly wetter conditions in parts of the interior regions, though present-day dry areas such as the Namib and the Kalahari remain arid. A climatic shift

is not apparent over a longer period in any defined geographical direction. The regional differenciation as seen today seems to have existed throughout the past 10 ka.

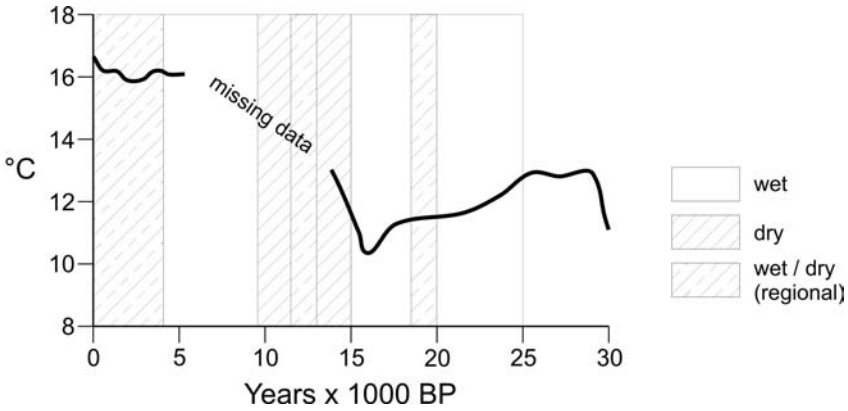

Fig. 3-7: Climatic framework of Southern Africa during the Holocene from Tyson and Preston-Whyte (2000). Temperatures inferred from stalagmites from Cango Cave, Southern Africa (after Talma and Vogel, 1992). Bars indicate overall moisture conditions. It should be noted that regional conditions vary greatly, such that this table represents only a broad climatic outline.

Holocene paleoclimatic conditions, as summarized in Fig. 3-9 also point to a number of conflicting pieces of evidence. But generally, increased temperature and precipitation was found in several locations from 10 ka to the Holocene optimum around 8 to 5 ka and a subsequent gradual drying (Thomas and Shaw, 2002). Subsequent short-term increases in precipitation were identified in some studies e.g in the middle Kalahari at 3.5 to 2.5 and 1.4 ka and in the Southern Kalahari at 1.8 to 1.2 ka (e.g. Nash et al., 1997). A comprehensive review of the newer paleoclimatic data of Southern Africa can be found in Thomas and Shaw (1991) and in Thomas and Shaw (2002).

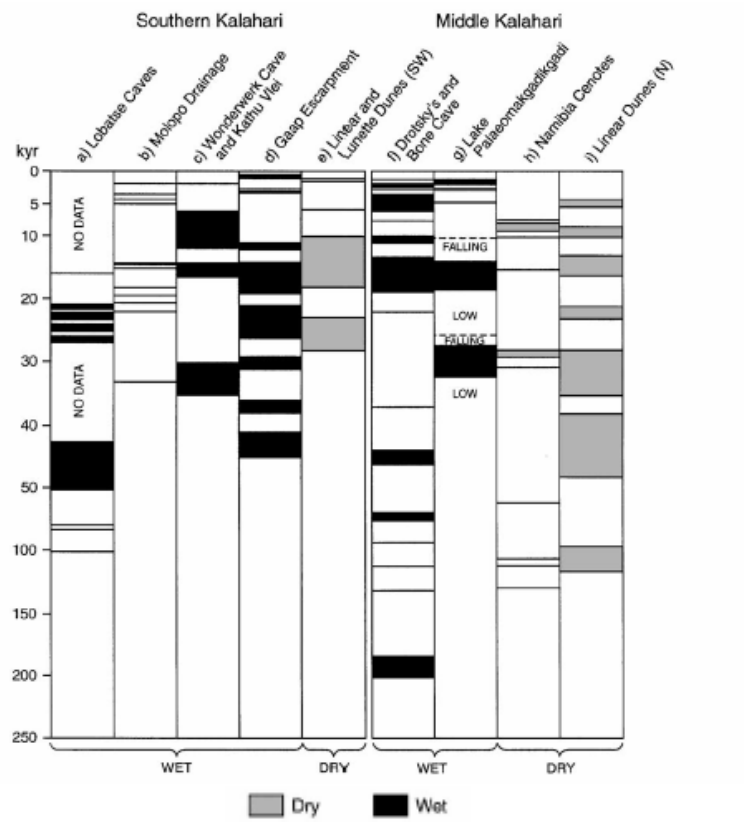

Fig. 3-8: Summary of paleoclimatic data for different locations in the Kalahari from 200 ka to present (taken from Thomas and Shaw, 2002).

Applicability of paleoclimatic findings to the study area

As indicated above, paleoclimatic data sets from different locations vary strongly, none of which is directly located within the study area (Fig. 3-6). In order to find the appropriate locations to compare, some general considerations about the groundwater formation in the different locations need to be made. Locations influenced by surface water of the Paleo-Makgadikgadi and Paleo-Okavango systems do not represent conditions comparable to an 'in-situ precipitation system' as it is (presently) occurring in the study area, which is located in the Central District between Serowe and Orapa. E.g. columns i) and j) in Fig. 3-9 represent groundwater that is influenced by inflowing surface

water and was replenished from precipitation from the Okavango Delta/Chobe catchment area about 200 km North of the area. That area is influenced by different wind and precipitation regimes, which are and probably were not comparable to that of the study area. In addition, an influence on the study area by the fossil Lake Makgadikgadi can be ruled out, as the lake shores at no time propagated onto the escarpment (Shaw et al., 1997). Also, the fossil shore lines follow today's morphology towards an Eastern direction and are not Southernly directed (M. v. Hoyer, personal comm.) and the maximum delimitation of the (fossil) lake Makgadikgadi as shown in Fig. 3-6 did not reach any part of the study area (Makadikgadi deliminations taken from Botswana Society, 1988). The study area was always upstream of the fossil lake.

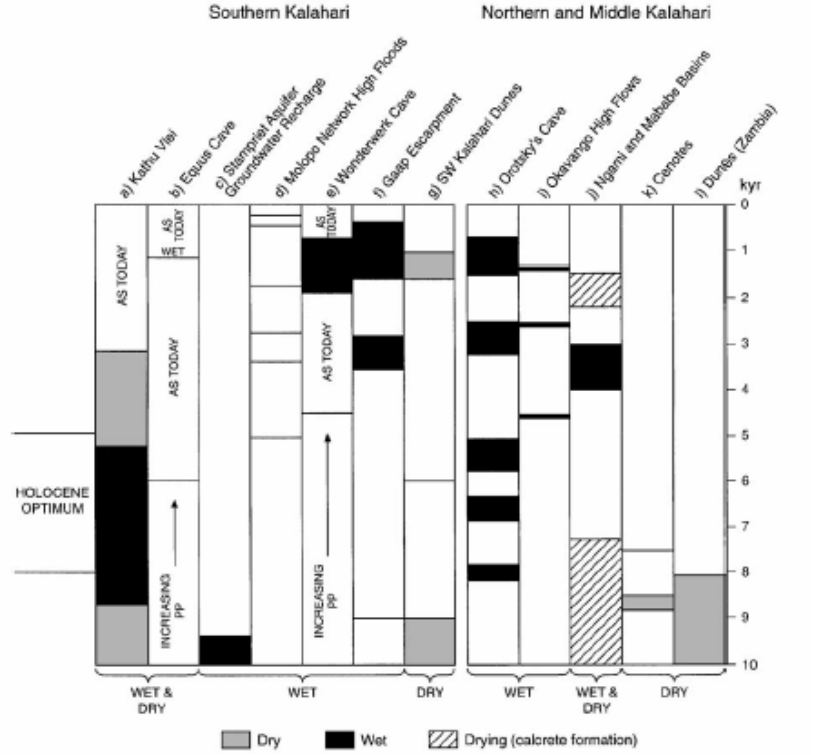

Fig. 3-9: Summary of paleoclimatic data for different locations in the Kalahari from 10 ka to present (taken from Thomas and Shaw, 2002).

Other locations e.g. the sand dunes in column g) of Fig. 3-9 represent yet another catchment area far away from the investigation area. The most comparable sites to the study area would be the Lobatse caves (Fig. 3-8, column a), and Drosky's caves (Fig. 3-8, column f and Fig. 3-9, column h), if the assumption is made that past general conditions resemble the ones presently observed. Today both sites receive precipitation of the similar general pattern as the study area and only vary in total precipitation amounts. The Lobatse caves, however, do not show a sufficient data resolution in the relevant time scale below 20 ka BP.

3.3 Soils, vegetation and land use

3.3.1 Soils

The main soil type of the Kalahari region is *Arenosol*, a deeply to very deeply developed soil type with a poor differentiation between the different soil horizons. On the Kalahari plateau, the Arenosol is formed in aeolian sediments from paleo-climatic dune sands. In the investigation area the Arenosol is mostly ferralic, its texture is medium to fine sandy with a yellowish-brown to dark red color, while its drainage capacity is moderately well to somewhat excessive (De Wit and Nachtergaele, 1990). However, most rainwater is consumed by the vegetation, leaving only small percentages for recharge to the aquifers. A region dominated by *Petric Calcisols* is found in the Northwestern part of the investigation area at Letlhakane and Orapa. This soil type region is bordered by the Makgadikgadi Pans where the saline soil type *Solonchak* is dominating. Throughout the study area *duricrusts,* like calcrete, silcrete and ferricrete crusts, are widespread. These hard layers occur in different soil depths (from several decimeters to decameters) reaching a vertical extension from several decimeters up to a few meters (Martini and Chesworth, 1992).

3.3.2 Vegetation and fauna

In shrub and tree savannas like the Kalahari plant communities on Arenosols are dominated by *Acacia* and *Terminalia* species, whereas *Mopane* trees are dominating the sites of calcareous soils (Thomas and Shaw, 1991, van Wyk, 2001). Vegetation is particularily dense during times of high rainfall. Recent detailed vegetation studies in the Kalahari were carried out e.g. by Ringrose et

al. (1998). Various kinds of termites are ubiquitous in the Kalahari. Their high number and biomass is playing an important role in the Kalahari ecosystem as collector and decomposer of wood, grass and organic litter (Lavelle and Spain, 2001).

3.3.3 Land use

The investigated area of the Kalahari region is scarcely inhabited (less than 1 person per 10 km^2, Thomas and Shaw, 1991). The study area is located on the fringe of the Kalahari, an area that is only used for extensive cattle grazing (ca. 11 ha/livestock unit, Mphinyane, 2001, Arntzen and Veenendaal, 1986). The area used to be purely occupied be wildlife, only in the 1950s cattle grazing started, expanding westward during subsequent years.

3.3.4 Geomorphology

The study area is located W to NW of the Kalahari escarpment as the edge of the *'Kalahari sandveld'* at an elevation of 1000 – 1200 m amsl. The escarpment signifies no specific geological junction, however, it basically outlines the limit of the Stormberg basalt (Wellfield, 2000) and marks a topographic edge. It represents the erosion fringe of the Kalahari basin, resulting from backward erosion reactivated by a post-glacial drainage system of the Limpopo River. The investigation area is characterized by a gently undulating relief with a gradient of about 0.001, only slightly tilting from West of Serowe towards the drainage direction of the Makgadikgadi Pans located over 220 km to the NNW. Lacking prominent features, the main geomorphological units of the area are pans and fossil dunes. The pans are shallow depressions of varying size which can be found in isolated locations of the investigation area, e.g. the Serwe Pan near Serowe, or, in very huge dimensions, to the North of the study area the Makgadikgadi Pans (Fig. 3-11). The pan floors are compacted and composed of calcareous clays, sand and possibly salt deposits. The clay causes relatively low permeability and high moisture retention capacities (Rabube, 2003). Pans are formed by processes of shallow-water lacustrine deposition, interrupted by periods of groundwater-controlled aeolian deflation (Thomas and Shaw, 1991). They tend to lack surface inflow. Often, they are associated with calcrete, or in case of calcium replacement silcrete. Due to the exceedingly flat topography of the study area, no prominent river beds cross the area (SGAB, 1988). However, fossil river beds can be found e.g. in the Letlhakane area, which can be best seen from aerial photographs or satellite

images, but are difficult to distinguish in the field. The Letlhakane River in area 2 is a remainder of a former bigger drainage system towards the paleolake Makgadikgadi, today's Makgadikgadi Pans. The paleolake used to connect the Paleo-Okavango with the Limpopo River that drains into the Indian Ocean. Today this connection is disrupted as a result to crustal movement of a prolonged arm of the East African Rift system. In addition, rainfall amounts decreased, rendering the necessity of additional drainage into the Limpopo less important.

Further geomorphologic features of the study area are fossil dunes. Those reflect paleo-wind directions. As for the fossil drainage systems, they can hardly be seen in the field without using satellite images. Further detailed descriptions of the geomorphological features of the Kalahari can be found in Thomas and Shaw (1991).

3.4 Geology

Intensive research on the geology of Serowe was conducted by the Swedish Geological Company (SGAB, 1988) and Wellfield Consulting Services (Wellfield, 2000). The geology of Orapa was investigated e.g. by Debswana Diamond Co. (Pty.) Ltd. (Debswana, 1997), and Anglo American Corporation (AAC, 1992). For a general framework, the geology of the Kalahari can be found in detail in Thomas and Shaw (1991). The lithostratigraphy and nomenclature of the Karoo Supergroup, which is the encompassed lithology of the study area, has been adopted from Smith (1984). In the following, a short overview of the geologic setting and a more detailed description of the Karoo strata is given.

3.4.1 Geological setting

Many interior basins in Africa, such as the Kalahari Basin, have formed as a result of subsidence and to a minor extent, of rifting within a shield area or craton of very ancient Precambrian rocks (Burollet, 1984). They mostly contain a great thickness of deposits as they experienced significant or intermittent sedimentation throughout the Phanerozoic. As evidenced by Permo-Carboniferous glacial tillites (Lower Karoo) that rest unconformably on the Precambrian basement rocks (Kaapvaal-Zimbabwe Craton), the Southern part of the Kalahari basin appears to have existed since the Paleozoic (Thomas and Shaw, 1991).

Karoo Supergroup
The Karoo Supergroup comprises successions of sedimentary and volcanic rocks, resting unconformably on Protorozoic basement, and formed during Carboniferous to Jurassic times within the Southern part of the Gondwana supercontinent. It includes the Dwyka-, Ecca-, Beaufort-, Lebung- and Stormberg Lava-Groups. The Karoo Supergroup is only poorly exposed, being unconformably overlain by the Tertiary to recent Kalahari Beds. A progression from glacial (Dwyka Group) to cool temperate (Ecca Group) into warmer semi-arid to arid (Lebung group) deposits can be found, probably as a result of the drifting of the Gondwana paleocontinent from high polar to lower latitudes (Smith, 1984). The Karoo sediments are covered by widespread basaltic lava eruptions, which are assumed to be caused by initial rifting phases and the progressive break-up of the Gondwana paleocontinent.

3.4.2 Regional geology of the Serowe-Orapa area

The lithostratigraphic units of the Serowe-Orapa area are shown in Tab. 3-1. In the following, only the Lebung Group of the Upper Karoo and younger successions are discussed, as those are of relevance to groundwater investigations in the studied system of Serowe to Orapa.

Lebung Group
In general terms, the Lebung Group consists of a sequence of massive fine to medium grained sandstone, silty fine grained sandstone, a basal conglomeratic sandstone, subordinate calcareous siltstone, muddy siltstone and sandy siltstone (Wellfield, 2000). It represents the final phase of Karoo sedimentation during mid- to late-Triassic times.

Mosolotsane Formation
The Mosolotsane Formation (Fm.) was deposited under fluviatile conditions. The formation generally consists of intercalated reddish coarse to fine-grained sandstones, siltstones and mudstones with well-developed cross-bedding. Pale grey or green bands or spots in which reduction has occurred, are common. Due to the depositional environment, the lithology of the Mosolotsane Fm. may be strongly heterogenic on a vertical and on a lateral scale. The Mosolotsane Fm. is overlain by the Ntane sandstone, but the contact between the two is commonly transitional, and cannot always be easily differentiated. It is

underlain by mudstones, siltstones and sandstones of the Tlhabala Formation of the Beaufort Group.

Ntane Sandstone Formation

The dominant rock types of the Ntane Formation are massive or well-bedded sandstones of red to pale-cream color that are fine-grained and mainly aeolian. Grains are variably cemented. The most part of the matrix is non-calcareous, but calcereous patches occur (SGAB, 1988). The deposition environment is a progression from semi-arid, aeolian and fluviatile processes with temporary lakes and alluvial flooding (producing mudstone/siltstone bands) to entirely aeolian (extensive dune fields with minor interdune fluviatile deposits). The Ntane sandstone is subdivided into two members (Smith, 1984): (a) The Upper Massive Member that consists of well-sorted, sub-rounded sand grains with occasional calcareous concretions and thin bands of siltstone. Its thickness is reduced in places where the Ntane Sandstone subcrops. (b) The Lower Transition Member, which comprises 30 to 40 percent of the total formation thickness. The transition between both members is gradational. The overall thickness of the Ntane Sandstone in the study area ranges from zero to 130 m. The contact to the lower-lying Mosolotsane Fm. is mostly gradational. The upper limit is an unconformable contact, commonly metamorphosed or baked with the overlying tholeiitic flood basalt of the Stormberg group. In some places intercalations of sandstone and basalt can be found. The Ntane Sandstone partly appears as a 'window' in the basalt, e.g. West of Serowe (Fig. 3-10).

Stormberg Lava Group

The Jurassic Stormberg Lava Group (Stormberg Basalt) consists of a very extensive, often very thick sequence of tholeiitic flood basalt, which put an end to the Karoo sedimentary succession. The thickness of individual flows amounts to several tens of meters. Those unconformably overlay the Ntane Sandstone Formation, and fill depressions of the former morphology (paleorelief). The base of a flow is often amygdaloidal, and the flows are chilled at top and bottom and have an internal massive zone. The color of the basalt is black to greenish-grey and in amygdaloidal zones reddish-brown. The large thickness variations that are observed in the study area (60 – 240 m) are partly inherent due to erosion, and considerably influenced by post-Karoo faulting. Weathering is usually mostly pronounced at the top of the basalt in the first 30 to 50 meters and at the base in the fractured contact immediately above the

sandstone (SGAB, 1988). Some interflow weathering and/or paleosoils have been observed locally (Wellfield, 2000).

Intrusives (dolerite dykes)
On a regional scale, two ages of intrusives can be found in the study area: i) pre-Karoo post-Shoshong dolerite intrusions, and ii) post-Karoo dykes that are emplaced in WNW-ESE trending faults (Fig. 3-10). The latter are the most prominent intrusives. Large dykes can have a thickness of up to tens of meters and consist of a fine-grained, very hard black to greenish grey dolerites. They have chilled margins and are frequently jointed. Their embeddig into the regional structure and the resulting hydrogeological implications are discussed in chapter 3.5.

Kalahari Beds (Kalahari Group)
The Kalahari Beds are post-Karoo superficial deposits that have accumulated in various episodes over the past 60 million years. They consist of a variety of aeolian sands and silts, alluvial soils, calcrete, silcrete, minor ferricrete, gravel and clays in variable thicknesses. The origin and stratigraphy of the Kalahari Group sediments has been subject of major geological debates (e.g. Grey and Cooke, 1977; Thomas and Shaw, 1991). In general, the sediments are mainly of continental origin and accumulated under a variety of depositional conditions including aeolian, fluviatile and lacustrine environments (Selaolo, 1998). Their thickness in the study area varies from few meters, e.g. 10 m near Letlhakane up to 140 m West of the Khwee block (Fig. 3-10). The general trend is, however, the occurrence of thick deposits up to greater than 100 m in the Central Kalahari Basin, and a reduced thickness on the Eastern Fringe (less than 15 to 60 m). The Kalahari Beds are marked by a lack of fossils and large lateral and vertical variations, rendering regional correlations complex. The prime components of the Kalahari Beds are discussed separately in the following.

Kalahari Sands
The Kalahari Sands consist of an upper zone of loose, fine to coarse grained sands of mainly aeolian origin and form a series of low-amplitude NNE-SSW trending dunes, which are stabilized in the study area by thick vegetation, and which can mainly be distinguished on satellite images. The underlying sand is a more complex unit of sandstones, duricrusts, and occasional mudstones and siltstones (SGAB, 1988).

Duricrusts

Duricrusts can be divided into calcretes, silcretes and ferricretes, of which the last are the least abundant. They have a tendency to follow the precipitation gradient and are associated with specific landforms, such as pan rims, drainage lines and specific horizons within the Kalahari strata. The duricrusts are of a polygenetic nature. In calcrete formation, pore water pressure (pF) plays an important role in the solution and precipitation of calcium carbonate. Increasing pF, encountered when groundwater ascends, leads to a loss of CO_2 and carbonate precipitation (Thomas and Shaw, 1991). The inverse occurs when groundwater descends, making fluctuating groundwater levels or evaporation from shallow groundwater or rainwater a production mechanism. The position and layer thickness of the calcretes depend on the evaporation conditions. Also, carbonates can precipitate close to the boundary of fresh and saline water by mixing near or at the interface. This can occur at greater depths and is not limited to near-surface conditions. Silcrete formation, too, is closely linked to groundwater processes involving alteration of sandstones, resilification of existing silcrete breccias or bidirectional replacement in existing calcretes (Shaw and DeVries, 1988). The silica source may be derived in situ from dissolution of host materials followed by reprecipitation, by sediment weathering in close proximity or by aeolian influx. Aeolian-transported quartz and alumosilicate grains are more susceptible to dissolution because of surface abrasion and due to an increased surface area to volume relation (Dixon, 1994). Silica solubility is highest at pH values above 9, but dissolution and transport appears to occur under neutral to low pH at normal temperatures. Different from calcretes, which for the most part form in areas with 200 to 500 mm of annual rainfall, silcretes occur under a range of climatic conditions from extreme arid to humid tropical (Goudie, 1985).

Structural framework

Located in the central part of the Southern African subcontinent and on the Southwesterly margin of the Archaean Zimbabwe Craton, the basement underwent a series of polycyclic events that resulted in a wide range of tectonic styles of the basement. From the end of the Upper Proterozoic most of the present African continent had formed and remained a stable cratonic area, and, in the area of the present Kalahari basin, was subsequently covered by the phanerozoic sedimentary Karoo cover. Subsequent widespread magmatism during the Phanerozoic, linked to the break-up of Gondwana and the subsequent development of the African Rift system took place, represented in

Botswana in form of basic dykes and kimberlites, e.g. the late Karoo ENE dyke swarm. The formation of the Karoo basin itself and the subsequent depositional history has been strongly influenced by renewed movements on former faults. In addition, Phanerozoic basinal warping and further dyke emplacement have played a major role in the structural development of the Karoo units.

Tab. 3-1: Lithostratigraphy of the Serowe Region (Wellfield, 2000).

Age	Super-group	Group	Formation	Lithological description
Cenozoic		Kalahari Group	Kalahari Beds	Soil, sand, calcrete and clay
Mesozoic to Upper Paleozoic (Late Carboniferous to Jurassic)		Stormberg Lava		Crystalline, massive, amygloidal basalts
	Karoo	Lebung	Ntane	Aeolian sandstone, medium to fine grained with minor mudstone intercalations, white, pink, red, brown, grey, green, yellow, partially fluviatile towards base.
			Mosolotsane	Fluvial red beds, siltstones, fine grained sandstone, red, purple.
		Beaufort	Tlhabala	Non-carbonaceous mudstones and siltstones with minor sandstones.
			Serowe	Carbonaceous mudstones, coals, siltstones, coaly carbonaceous mudstone, subordinate non-carbonaceous mudstones.
		Ecca	Morupule	Dull and heavy dull coal seams, black carbonaceous mudstone, subordinate siltstones, mudstones, micaceous.
			Kamotaka	White, massive, coarse to medium-grained sandstone, subordinate siltstones, mudstones, micaceous.

- continued -

Tab. 3-1 (continued): Lithostratigraphy of the Serowe Region (Wellfield, 2000).

Age	Super-group	Group	Formation	Lithological description
Upper Paleozoic			Makoro	Post glacial lacustrine mud-stones and siltstones marking the base of Ecca group.
		Dwyka	Dukwi	Base of Karoo sequence, tillites and shales, varved siltstones and mudstones.
Proterozoic		Palapye	Shoshong	Dolerite, siltstones, shales and quartzites
Archaean		Basement		Granite gneiss and amphibo-lite

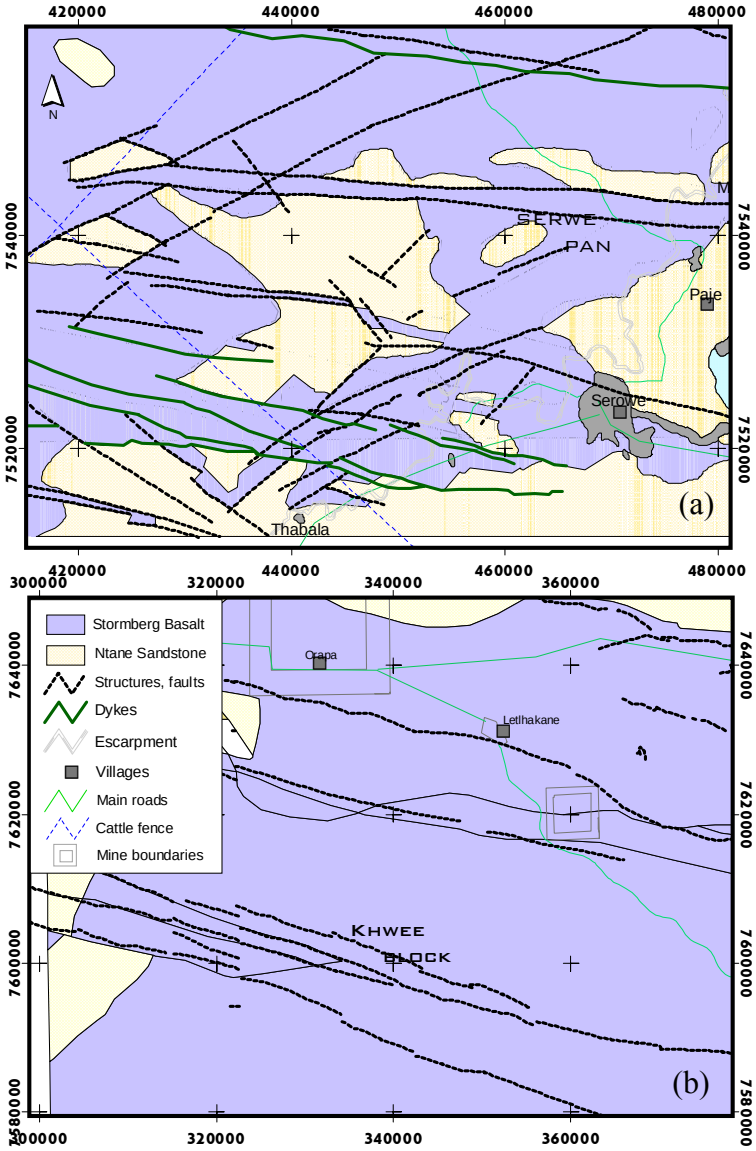

Fig. 3-10: Geology and structural features within (a) the Serowe area (without Kalahari Bed cover) and (b) the Letlhakane/Orapa area and the Khwee block areas (without Kalahari Bed cover).

3.5 Hydrogeology

3.5.1 Hydrogeological setting

The main aquifer is the Triassic Ntane Sandstone aquifer with an average thickness of 100 m, underlain by the less permeable Mosolotsane layers (mudstone, siltstone, sandstone). It is overlain by the Early Jurassic Stormberg basalt (SGAB, 1988). This basalt is of varying thickness and mostly confines the Ntane aquifer. The Stormberg basalt has no major significance as an aquifer, only structurally altered zones may contain significant amounts of water. The Ntane aquifer is covered by the Tertiary to recent Kalahari Beds, a group of superficial deposits of soil, sand, and clay, with locally extensive formations of calcrete, silcrete and ferricrete that have been formed along former drainage lines and in shallow pan depressions. Only locally perched aquifers within the Kalahari Beds are found. This was, however, only observed in the Northern part of the study area near Letlhakane along the ephemeral Letlhakane River, and in one location in WF4 West of Orapa (Fig. 3-2). The main regional groundwater flow is towards the lowest depression which is constituated by the Makgadikgadi Pans in the North (Fig. 3-11), making it an endorheic system. No other groundwater outcrops occur under the present climate. The mudstone layers at the base of the Ntane sandstone or within the underlying Mosolotsane formation that is dominated by mudstones represent the lowly transmissive aquitard to the Ntane system.

Hydrogeological significance of the structural setting

The hydrogeology of the entire area is strongly controlled by structural features. The general groundwater flow direction is ESE to WNW. However, the area is dominated by a large number of hydraulically influencing WNW-ESE trending tensional faults, which cut through the entire area, and some of which are intruded by lowly permeable dolerite dykes. Those divide the Karoo units into horst and graben structures of varying size. The structures in the study area are commonly less than 2 km wide, and exhibit down-throws from less than 10 m to more than 100 m. Significant structures of this kind can be found near Serwe Pan (Fig. 3-10a), and as an even more prominent feature, in form of the Khwee Block (Fig. 3-10b). A similar, but hydraulically less significant set of faults exists in the NE-SW and NW-SE directions (Wellfield, 2000). This setting leads to a series of blocks of varying size that may be partially or fully hydraulically isolated from each other. Local settings of individual struc-

tures are dependant on the thickness, competency and the local persistence of dolerite dykes in the area, as well as the magnitude of fault movements which may bring the aquiferous structures in juxtaposition (Wellfield, 2000).

3.5.2 Hydraulic properties

Kalahari Beds
The top aquifer is made of sands, calcretes, silcretes and sandstones of the Kalahari Beds. The layers of the unconsolidated sands act as a pore aquifer with a high primary porosity. The aquifer is quickly recharged during intensive rainfall periods. The Kalahari Beds do, however, not form an aquifer of possible economic value in terms of water supply (AAC, 1992).

Stormberg Basalt
The Stormberg basalt has been recognized as a potential aquifer in both study areas. The transmissivities are between $1.4 \cdot 10^{-4}$ and $9.2 \cdot 10^{-5}$ m^2/s. However, the nature of this aquifer is governed by the extent and degree of subvertical fracturing and weathering (Wellfield, 2000) and intergranual flow is virtually negligible. Fractures are present and mainly sub-vertical, but do not form a widespread, interconnected network and only locally enhance permeability (SGAB, 1988). This can be seen from the high transmissivities (see above) and a (very) low storage coefficient of $6.9 \cdot 10^{-6}$ (Tab. 3-2) which indicates fracture influences on the observed transmissivities. There are only few extensive horizontally developed zones of higher permeability on the top and/or bottom of individual lava flows, where weathering is usually highest. Observations of this kind of water occurrence have only been reported around Orapa. The Stormberg Basalt regionally behaves as a confining aquiclude, but locally it can possess the above mentioned enhanced fracture-induced permeability, creating a hydraulic connection to the Ntane sandstone.

Ntane Sandstone Aquifer
The Ntane Sandstone Aquifer is an aeolian sandstone with a porosity controlled by intergranular voids (primary porosity) and fractures and fissures (secondary porosity). Groundwater levels are at 30 to 100 m below the surface. Its transmissivity (T) ranges from $5.0 \cdot 10^{-5}$ to $2.1 \cdot 10^{-4}$ m^2/s (Wellfield, 2000), the confined storage coefficient in the range of $1.0 \cdot 10^{-4}$ to $9.8 \cdot 10^{-5}$ and the average yield of the boreholes ranges over a span of 2 – 30 m^3/h.

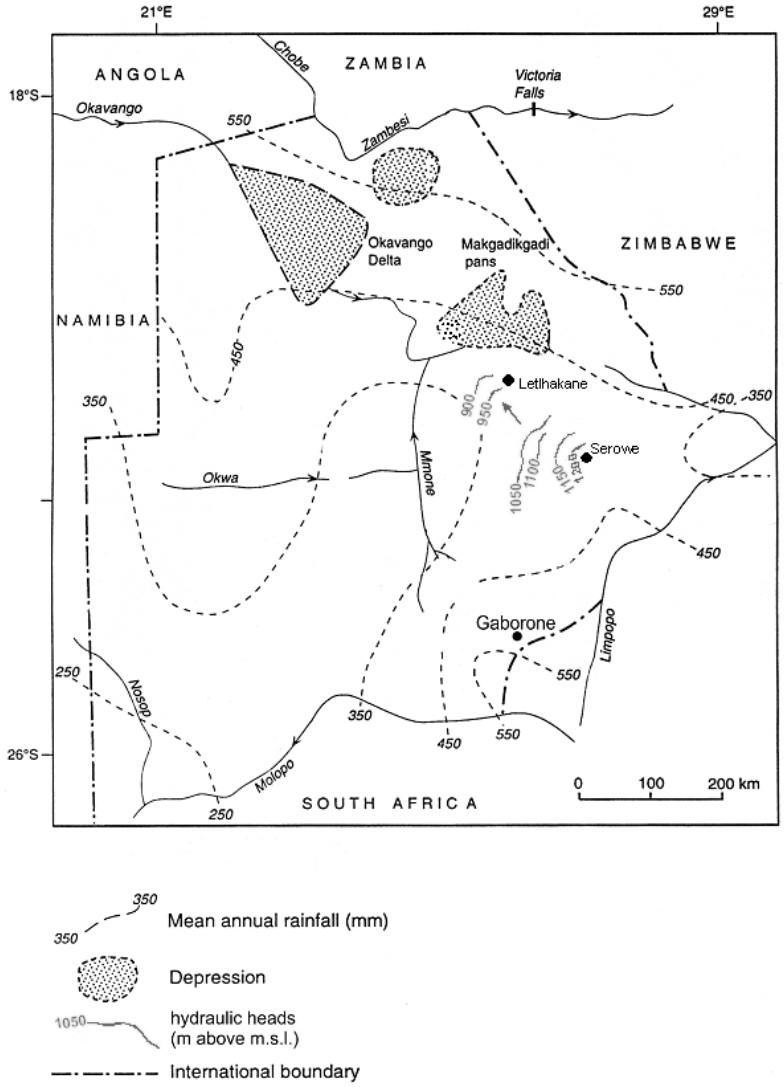

Fig. 3-11: Physiographical features of Botswana and hydraulic heads inferred from the Hydrogeological Reconnaissance Map of Botswana, 1:500 000, sheet 8 and own data (modified after DeVries et al., 2000).

Those parameters are of course strongly influenced by the location of the borehole in a fracture zone or away from it in a sparsely fractured block, which has been observed in varying yields, but transmissivity data that could confirm this is not available. In addition, a higher permeable upper contact zone to the overlying basalt has been observed that had been chilled during basalt deposition (Mazor et al., 1977).

Mosolotsane Formation
The permeability of the Mosolotsane sand- and siltstone is generally lower than that of the Ntane sandstone. In reports on the hydrogeology of Serowe, this 'aquifer' is not considered a significant resource (SGAB, 1992). However, a potential to provide considerable quantities of water was recognized, but the permeability of the aquifer is dependent on the local lithology which determines the local limits of aquifer potential. Investigations in Serowe gave only short term high yields, and boreholes were thus only drilled into the Ntane aquifer. Near Orapa, however, several boreholes reach the Mosolotsane Formation either due to a reduced cover of overlying lithologies, or due to the complete absence of the Ntane sandstone, as in the area of the Khwee block (Fig. 3-10). Transmissivities of the Mosolotsane Aquifer are in the range of 1.6 to 7.1 · 10^{-5} m^2/s (Anscombe, 2001), varying depending on the lithology and on encountered secondary porosity.

Dolerite dykes
Dolerite dykes may act as a hydraulic barrier, if they are perpendicular to the direction of groundwater flow. Yet, the barrier function is depending on their degree of fracturing due to cooling, and on their thickness. Thin dykes (less than 10 m) were observed to allow hydraulic continuity across different compartments, whereas thick dykes (about 10 to 40 m) serve as barriers (Wellfield, 2000). The only available transmissivity value from literature of 1.62 · 10^{-6} m^2/s appears be indicative for the barrier function a dolerite dyke with low to no fracturing.

3.5.3 Groundwater recharge

The occurrence of recharge by infiltrating rainwater in the Kalahari was contested in early studies (e.g. Foster et al. 1982, Boocock and Van Straten, 1961). Those studies suggested this is mainly due to the fact, that the dense vegetation, and thus high evapotranspiration, effectively takes out all available

moisture from retention storage accumulated by rainfall events. Other authors assigned the current groundwater gradient to residual levels of a past wet climate (DeVries, 1984). Subsequent isotope studies (mainly radiocarbon and tritium) provided evidence for recharge in the order of 1 to 10 mm/year, as compiled in Selaolo, 1998, or in Mazor et al., 1977. Within this low margin of recharge, regional differences, such as higher recharge rates at the fringe of the Kalahari than in the center were also suggested (e.g. DeVries et al., 2000, DeVries and von Hoyer, 1988). Spatial, and also temporal variability and/or episodic nature of recharge was supported by Lubczynski (2000) and Verhagen (1990).

Tab. 3-2: Compilation of hydraulic parameters of hydrologic units in the study area.

Hydraulic unit	**Horizontal hydraulic conductivity (m/s)**	**Storage coefficient**	**Transmissivity (m^2/s)**	**Data source**	**Remarks**
Kalahari	-		-		no data
Calcrete/	$1.9 \cdot 10^{-6}$		$5.6 \cdot 10^{-5}$	SRK,	Recovery
weathered	$2.7 \cdot 10^{-6}$	$9.6 \cdot 10^{-7}$	$7.8 \cdot 10^{-5}$	1981	CD* Pump
basalt					rate 1.5 m^3/h
Dolerite	$1.9 \cdot 10^{-9}$		$1.62 \cdot 10^{-6}$	SGAB,	
dykes				1988	
Basalt	$1.5 \cdot 10^{-6}$	$6.9 \cdot 10^{-6}$	$1.40 \cdot 10^{-4}$	SRK,	CD* pump
				1981	rate 13.6 m^3/h
	$1.0 \cdot 10^{-6}$		$9.16 \cdot 10^{-5}$		Recovery
	$1.8 \cdot 10^{-6}$				early
	$2.2 \cdot 10^{-6}$		$1.65 \cdot 10^{-4}$		Recovery late
				SGAB,	
				1988	
Basalt/	$8 \cdot 10^{-7}$		$7.81 \cdot 10^{-5}$	SRK,	CD* pump
Indurated				1981	rate 27.1 m^3/h
Ntane	$2.6 \cdot 10^{-6}$		$3.58 \cdot 10^{-4}$		Recovery
Contact	$2.2 \cdot 10^{-5}$				early
			$2.19 \cdot 10^{-4}$		Recovery late

- continued -

Tab. 3-2 (continued): Compilation of hydraulic parameters of hydrologic units in the study area.

Hydraulic unit	Horizontal hydraulic conductivity (m/s)	Storage coefficient	Transmissivity (m^2/s)	Data source	Remarks
Ntane Sandstone	$3.4 \cdot 10^{-6}$	$9.8 \cdot 10^{-5}$	$1.80 \cdot 10^{-4}$	SRK, 1981	CD* pump rate 25.5 m^3/h
	$3.0 \cdot 10^{-6}$		$1.59 \cdot 10^{-4}$	SGAB, 1988	Recovery early
	$4.1 \cdot 10^{-6}$		$2.11 \cdot 10^{-4}$		Recovery late
	$1.7 - 2.3 \cdot 10^{-6}$	$1.0 \cdot 10^{-4}$ - $5.0 \cdot 10^{-5}$	$1.6 - 1.8 \cdot 10^{-4}$ $5.0 \cdot 10^{-5}$	Wellfield, 2000	Constant rate
	$1.3 - 1.7 \cdot 10^{-6}$		$0.79\text{-}2.0 \cdot 10^{-4}$	own data	Recovery late
Mosolotsane	-	$7.6 \cdot 10^{-3}$	$3.52 \cdot 10^{-5}$	Anscombe, 2001	CD* Pump rate 9 m^3/h
		$4 \cdot 10^{-6}$	$7.08 \cdot 10^{-5}$		CD* Pump rate 9 m^3/h late
			$4.78 \cdot 10^{-5}$		CD* Pump rate 6 m^3/h
			$1.65 \cdot 10^{-5}$		CD* Pump rate 6 m^3/h late
			$3.83 \cdot 10^{-5}$		Recovery

3.5.4 Groundwater abstraction

Within both investigation areas groundwater is used as the main sources of water supply. Serowe operates 49 production boreholes to supply the village, 22 of which are located within the investigation area. Their current abstraction volume reaches roughly 2.5 million m^3 per year (G. Kago, DWA, personal comm.). Near Letlhakane and Orapa six wellfields are installed with an ap-

proximate abstraction volume of 8.9 million m^3 per year (2003). Their main purpose is to provide water supply for diamond mining (Orapa, Letlhakane and Damtshaa Mine), and to supply the villages of Orapa and Letlhakane. The boreholes of those wellfields mainly penetrate the Ntane Sandstone, but some also reach the Mosolotsane Formation, while boreholes in near Serowe are only drilled to the base of the Ntane sandstone. In addition, cattle post boreholes are found throughout both investigation areas that abstract small amounts of water for cattle watering. Groundwater abstraction in these areas exceeds by far the renewable amount (e.g. Maßmann, 2004). Around Orapa a usage conflict exists between the long-term groundwater usage for cattle watering and the short-term usage (20 to 30 years) for diamond mining. The higher rate of return of diamond mining is the justification for the present usage priority and this priority is authorized in Botswana's National Water Master Plan (BNWMP, 1991). In Serowe the same conflict arose and will remain, however within one population group: cattle owners as village inhabitants (and water users) and cattle owners as cattle post operators.

3.5.5 Conceptual hydrogeological model

Fig. 3-12 summarizes the hydrogeological setting in form of a hydrogeological concept model. The main groundwater recharge takes place near Serowe, where windows in the basalt enhance water influx from the unsaturated zone into the Ntane Sandstone Aquifer. The general flow direction follows the topographical gradient past Orapa towards the Makgadikgadi Pans that constitute the discharge area. The sandstone is mostly confined by the overlying basalt, and only locally recharge may pass through fractures along the flow path. Near Orapa perched aquifers within the Kalahari Beds allow additional recharge into the Ntane Sandstone Aquifer along structurally induced zones of higher hydraulic conductivity. The mudstone layers in the lower parts of the Ntane sandstone and throughout the Mosolotsane Formation provide the aquitard to the system.

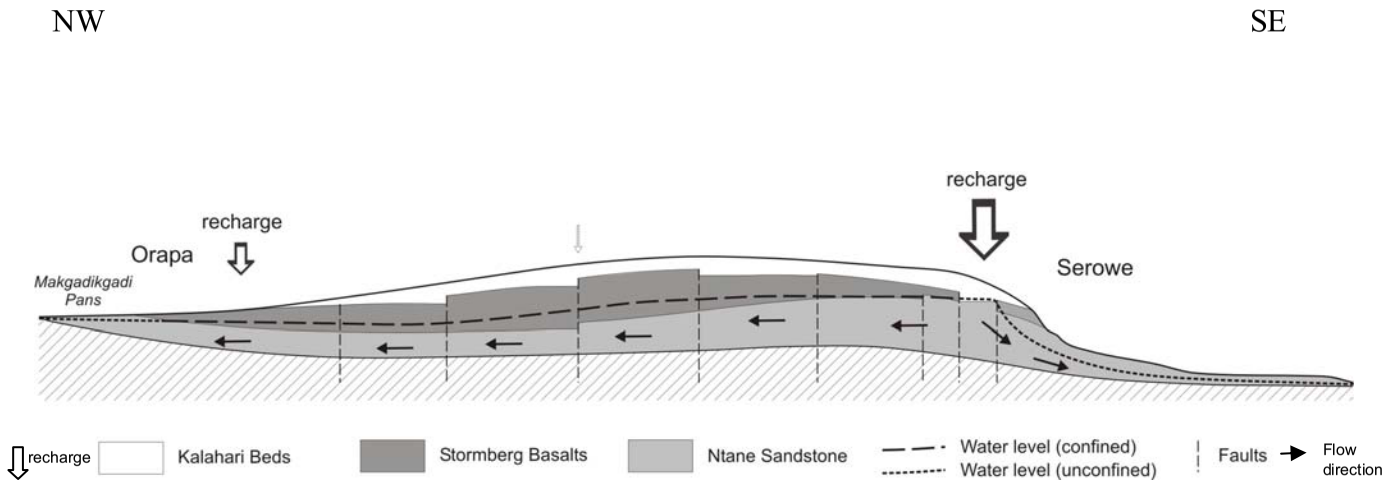

Fig. 3-12: Hydrogeological concept model of the investigation area between Serowe and Orapa (representing a flow distance of approximately 200 km). The size of the arrows indicates the relative significance of recharge.

4 MATERIALS AND METHODS

For this study, an integrative approach was used, combining many methods from hydrochemistry, lithological investigations and isotope hydrology. For many analyses standard methods could be applied which are summarized in the following.

4.1 Rock sampling

Lithological samples were analysed for N sources and sinks. XRF, CNS, eluate (dissolved NO_3) and organic carbon analyses were carried out at the BGR, Hannover, Germany. In addition, thin sections for the verification of core constituents and cementation investigation were prepared for transmitted and reflected light microscopy. Samples were analyzed as follows: Carbon-nitrogen-sulfur-analysis was performed with an *Elementar VarioMax* CNS analyzer, where 1 g of the pulverized rock sample was burned at 1150 °C. The determination limit is as follows: C = 0.012 %, N = 0.015 % and S = 0.02 %, according detection limits are at C = 0.004 %, N = 0.005 % and S = 0.007 %. Organic carbon (C_{org}) was determined indirectly via carbonate carbon and total carbon content measurements. Carbonate-C analysis was performed with a *Scheibler* apparatus with a detection limit of 1 %, following DIN ISO 10693. XRF measurements were conducted with a *PANalytical PW1480/2400* XRF in accordance with DIN 51418. The eluate samples for the determination of (releasable) dissolved nitrate were prepared following the DEV-S4 method according to DIN 38414, where 40 ml of distilled water was added to 4g of sample substance (grounded rock). The solution was shaken for 24 h. Samples were measured using a *DIONEX DX 500* ion chromatograph.

4.2 Regular groundwater sampling

4.2.1 Field methods

Sample abstraction

A total of 112 boreholes were sampled. The boreholes can be divided into four usage types:

(a) Production boreholes:
Government boreholes that are drilled for water supply, and that are equipped with pumps of a yield between 4.8 m^3/h (BH7101) and 19.8 m^3/h (BH7099). They run mostly 21 to 24 hours per day. Samples were collected 10 to 15 minutes after equipment setup, when field parameters had stabilized.

(b) Observation boreholes:
Government boreholes that are mainly used for water level monitoring. They are sealed and are not equipped with pumps. A *Grundfos SQ/SQ1-135* submersible pump was used for sampling, yielding approximately 1.2 m^3/h, depending on the abstraction depth. Two to three hours of pumping was needed to ensure that the stagnant water column in the borehole was exchanged at least once to twice. The field parameters were checked after 5, 10, 15, 30, and every 30 minutes thereafter to ensure that samples were taken at stable values.

(c) Cattle post boreholes:
Privately owned boreholes that were drilled for cattle watering. In most cases, the boreholes are equipped with small diesel pumps that are normally operated only few hours per day. The pump was activated for sampling purposes for 30 to 45 minutes only in order to avoid disturbances of the cattle watering scheme. These boreholes are generally drilled to shallower depths than the types (a) and (b).

(d) Hand-dug wells:
Very shallow boreholes that were manually dug into local perched aquifers in the Kalahari beds. This type of well was only encountered in the Orapa area. They were equipped with a very small diesel pump or only with a bucket connected to a rope.

The production and observation boreholes are mostly open boreholes where only the topmost 20 to 50 m within the Kalahari Beds Sediment and/or Stormberg Basalt are fully cased. The screen lengths are in the order of 80 to 100 m (see Fig. 11-1 and Fig. 11-2) and diameters are 203 to 303 mm. Some production boreholes have slotted screens instead of uncased ‘open hole’ screens (e.g. BH8819, BH7101, BH7102).

Field measurements and sample treatment
Including all different investigation methods, a total of 332 groundwater sample sets were taken at 112 boreholes. Field investigations included the measurement of pH, groundwater temperature, specific electric conductivity and redox potential (*WTW MultiLine 340i SET1* with pH-meter *Sentix 41*, oxygen sensor *CellOx 325*, EC probe *Tetracon 325* and redox-probe *SenTix ORP* (Ag/AgCl)) as well as the on-site photometric determination of nitrate, nitrite and ammonia (*WTW* filter photometer, *Photolab 12-A*). The measurement ranges were as follows:

- NO_3-N: 0.2 - 20.0 mg/l (equals 0.88 - 88.52 mg/l NO_3^-, conversion factor 4.426)
- NO_2-N: 0.005 - 1.0 mg/l (equals 0.02 – 3.28 mg/l NO_2^-, conversion factor 3.283)
- NH_4-N: 0.01 - 3.0 mg/l (equals 0.01 – 3.86 mg/l NH_4^+, conversion factor 1.286)

Abstracted samples were filtered with *Weissrand* filters (0.45 µm) and stored in a cool environment. HCO_3^- and CO_3^{2-} were determined by on-site titration with 0.1 n HCl (to pH 4.3), and 0.05 n NaOH (to pH 8.2), respectively. Samples for cation and trace element analysis were acidified with with 2 ml 1:1 HNO_3 per 100 ml sample.

On each borehole, the following (minimum) set of samples was abstracted:
- 500 ml for main elements, unfiltered
- 100 ml for cations, filtered (0.45 µm), acidified with 2 ml 1:1 HNO_3 per 100 ml sample.
- 125 ml PTFE bottle for trace element analysis, filtered (0.45 µm), 2 ml 1:1 HNO_3 per 100 ml sample
- 50 ml glass bottles, unfiltered, for TIC and DOC (with aluminium membrane)

4.2.2 Sample treatment, preparative and analytical methods

The samples were analysed at the BGR laboratories in Hannover, Germany. Nitrate, chloride and sulfate were determined using an ion chromatograph *DIONEX DX 500*. The determination limit is 0.05 mg/l, the calibration range

is up to 200 mg/l. The measurement range can be increased through sample dilution. Nitrite was was also determined with a *DIONEX DX 500*. The determination limit is 0.02 mg/l, the calibration range is up to 1 mg/l. The cations K, Na, Mg, and Ca were determined by an *ICP_OES Type SPECTRO CIROS*. The lower determination limits are approximately 0.02 mg/l, the calibration range of K is up 100 mg/l, Na up to 1000 mg/l, Mg up to 100 mg/l, Ca up to 200 mg/l. Trace elements (ca. 25) were as well determined by *ICP_OES Type SPECTRO CIROS*. The lower determination limits are element specific. Typical values are between 0.005 and 0.02 mg/l. The calibration range is element dependent between 5 mg/l and 25 mg/l.

4.3 Depth-related groundwater investigations

4.3.1 Multiparameter probe logging

Depth profiles of up to 200 m depth for 15 boreholes were recorded with an *Idronaut Srl Ocean Seven 303 CTD* multiparameter probe to obtain information on vertical stratification of hydrochemical field parameters. Calibration of probe sensors (DO, pH and redox) was performed daily in the field-laboratory prior to measuring. For static measurements the probe was manually lowered into the borehole with an approximate velocity of 0.1 to 0.2 m/s, data was continuously recorded every 10 seconds. Specific electric conductivity (EC) was measured at in-situ temperature. To distinguish between EC changes caused by changes in the hydrochemical composition of the water and EC changes caused by temperature variations only, measured EC values were recalculated to a reference temperature of 25°C. A function was found to approximate the empirical linear relation measured for the temperature range of 20 to 30°C (Fig. 4-1 and Fig. 4-2):

$$EC_{k25} = f(EC_{insitu}, T) \tag{4.1}$$

where EC_{insitu} denotes the measured EC at in-situ temperature at a depth z and EC_{k25} denotes the EC corrected to a reference temperature of 25°C. The empirical relation was determined for four different water types representing the range of water types found in the area (Fig. 4-1). Comparing downhole logs with upcast logs showed that EC and temperature were least sensitive to dis-

turbances caused by the turbulence of the measuring process. Upcast values for dissolved oxygen (DO), pH and redox were discarded due to intense disturbance of the water column. In support of those measurements, bailer samples were taken where different water types could be inferred from changes in the profile (next section).

Interpretation of multiparameter probe runs

Results from multiparameter probe logging yielded approximately 6000 data points per parameter at each borehole for logging section lengths between 100 and 200 m depending on groundwater level and depth of the borehole. In order to simplify data representation and to compare results from individual boreholes, mean gradients were calculated for each parameter x. To increase the signal to noise ratio, each gradient ($\Delta x/\Delta z$) was calculated for an interval of 51 data points. Results are comparable if smaller intervals are used. At each data point i the difference between i+25 and i-25 is calculated. The result is divided by the depth difference of both values (i+25 and i-25):

$$\frac{\Delta x}{\Delta z} = \frac{x(i+25) - x(i-25)}{z(i-25) - z(i-25)} \tag{4.2}$$

This calculated gradient is assigned to the mean depth z, assuming a nearly constant moving velocity of the probe. For example, at data point i = 250 this means:

$$z(250) = 0.5 \cdot (z(275) - z(225)) \tag{4.3}$$

The plots discussed in chapter 5.3 show a running average fitted to the calculated gradients using a data window of 50 values.

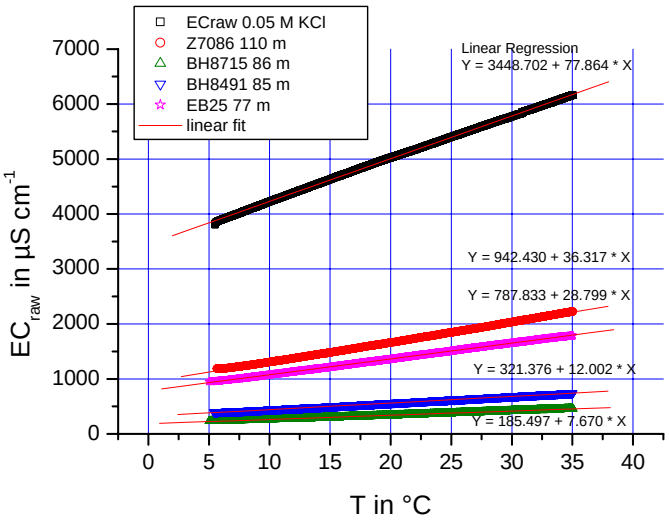

Fig. 4-1: Measured temperature dependence of specific electric conductivity (EC_{raw}) for four selected water types and a KCl reference.

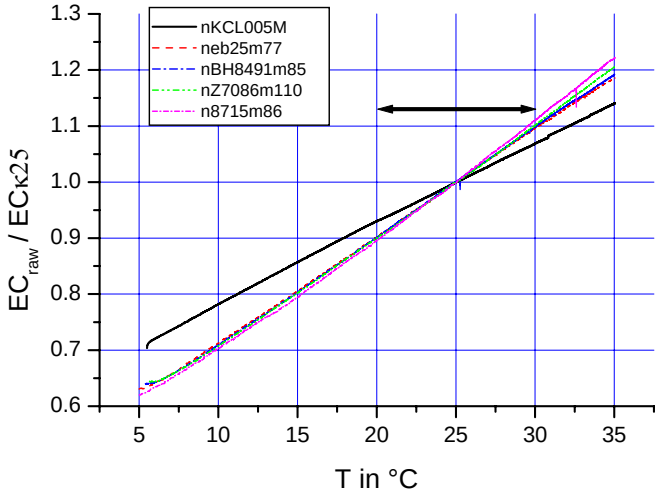

Fig. 4-2: Exemplary correction of the in-situ specific electric conductivity (EC_{raw}) to the reference temperature of 25°C at boreholes EB25, BH8491, Z7086 and BH8715. The arrow indicates the relevant temperature range for correction inferred from Fig. 4-1.

4.3.2 Depth-related sampling

As previous packer-testing only showed limited success in open hole-type boreholes in the investigation area (e.g. SGAB, 1998) and technical equipment was lacking, a *SEBA 4''* bailer was used to collect samples from specific depths. The system is based on a 1l-plexiglass tube that is lowered into the borehole at the desired depth. The closing mechanism is triggered by dropping a weight that activates a spring to close the tube. A detailed description can be found in Schnabel (2004).

4.4 Isotope hydrology

In the current study, the environmental tracers CFC/SF_6, ^{2}H, ^{3}H, ^{18}O, ^{14}C, ^{3}He, ^{4}He, ^{20}Ne and ^{22}Ne were investigated for the determination of mean residence times, and $^{15}N\text{-}NO_3^-$ and $^{18}O\text{-}NO_3^-$ for N-source determination. Samples were measured at the UFZ-Centre for Environmental Research Leipzig-Halle, Germany (^{2}H, ^{3}H, ^{18}O, ^{14}C, $^{15}N\text{-}NO_3^-$ and $^{18}O\text{-}NO_3^-$), at the Institute of Environmental Physics of the University of Bremen, Germany (^{3}He, ^{4}He, ^{20}Ne, ^{22}Ne, ^{3}H) and the *Spurenstofflabor Oster*, Wachenheim, Germany (CFC, SF_6). A short description of methods is given in the following. An overview over the different methods and applications in hydrology can be found in Cook and Herczeg (2000), Kendall and McDonnell (1998), Clark and Fritz (1997), Mazor (1991), Faure (1986), and Moser and Rauert (1980).

4.4.1 Stable isotopes (^{2}H and ^{18}O)

The determination of $\delta^{18}O$ and $\delta^{2}H$ (deuterium) is performed following the equilibration method (Knöller and Trettin, 2003). This method brings water samples in separate closed systems into isotopic equilibrium with a CO_2 gas for oxygen isotope measurement and a H_2 gas for hydrogen gas measurement. After reaching the equilibrium, the CO_2 and H_2 is abstracted from each system and is transferred to a mass spectrometer, where it is measured by the *Dual Inlet* principle (Knöller and Trettin, 2003). The $\delta^{18}O$ and $\delta^{2}H$ data is normalized to the *V-SMOW* standard (Tab. 6-1). The analytical accuracy is 0.1 ‰ for oxygen and 1 ‰ for deuterium.

4.4.2 Tritium (^{3}H)

Tritium measurements were carried out at two different institutions which used different methods. The UFZ Leipzig-Halle uses a liquid scintillation

counting (LSC) technique while the ^{3}He ingrowth method was applied at Institute of Environmental Physics of the University of Bremen. Both methods are summarized in the following.

Sample preparation (UFZ Leipzig-Halle)
The 1 l samples are pre-distilled and purified under a N_2 protective atmosphere to an electric conductivity below 100 µS/cm. In order to reach the detection limit of the natural water samples, the ^{3}H activity has to be enriched by electrolytical decomposition prior to the measurement. A commercially available scintillator cocktail (*Ultima Gold LLT*^{TM}) is added. A detailed description of the methods can be found in Taylor (1981) and Florkowski (1981).

Analysis (UFZ Leipzig-Halle)
Liquid Scintillation Counting (LSC) is used for tritium measurements, conducted on a *PerkinElmer Quantulus 1220* liquid scintillation spectrometer. Measurements are reported as Tritium Units (TU), which are the equivalent of one tritium atom among 10^{18} hydrogen atoms. One TU corresponds to an activity of $1.18 \cdot 10^{-4}$ Bq/ml. A detection limit of 0.3 TU is reached.

Sample preparation (University of Bremen)
Water samples are collected in 1 l bottles. For ingrowth of ^{3}He samples are degassed and stored for 4 to 8 months, after which the ^{3}He generated from ^{3}H decay is measured. Detailed descriptions of the methods can be found in Sültenfuß et al. (submitted).

Analysis (University of Bremen)
The ^{3}He ingrowth method is used for tritium measurements, conducted on a *MAP 215-50* sector field mass spectrometer, which is described in detail in Sültenfuß et al. (submitted). The measurement precision is typically ± 3% and the detection limit is 0.01 TU.

4.4.3 Chlorofluorocarbons (CFC) and sulfur hexafluoride (SF_6)

Field methods
The samples are filled in 600 ml glass flasks with glass stoppers contained in a sealable metal tin. This allows for an extra protective shelter of the sample against atmospheric chlorofluorocarbons.

Analysis
CFCs are quantitatively extracted from 10 to 30 ml water samples by a carrier gas (95 % argon, 5 % methane), followed by a concentration enrichment using purge and trap techniques. CFC determination is performed on a gas chromatograph with an Electron Capture Detector (ECD) according to Oster et al. (1996). The method achieves about 3% precision with minimum measurable concentrations of 0.01 pmol/l in water samples.

4.4.4 Radiocarbon (^{14}C)

Field methods
The dissolved inorganic carbon (DIC) content of the sample has to be determined in the field by titration of DIC species (see chapter 4.3.1). A total of greater than 1 g of C should be available in the sample, which generally result in samples of at least 60 l. Atmospheric contact needs to be avoided during sampling to prevent contamination by atmospheric CO_2. To extract the TDIC, carbonate-free $Ba(OH)_2 \cdot 8\ H_2O$ was added to increase the pH to 11 to transform all C into carbonate, and $BaCl_2$ to precipitate the latter. The sample precipitates over night and is decanted. The precipitate is transferred into 2.5 l sample bottles again avoiding atmospheric contact (Clark and Fritz, 1997).

Sample preparation
The measuring sample is generated from the precipitated carbonate through a synthesis to benzene (C_6H_6) via ethene (C_2H_2) synthesis which is then welded into a glass ampoule.

Analysis
^{14}C is measured by liquid scintillation counting in a *PerkinElmer Tri-Carb* scintillation spectrometer. The detection limit is about 1%-mod., where '%-mod.' equals the reference value of 'modern carbon' as given in chapter 6.2.1.

4.4.5 Helium ($^3He/^4He$) and neon ($^{20}Ne/^{22}Ne$)

Field methods and sample preparation
Samples are filled into copper pipes that are connected to the tubing in the field under slight pressure, while avoiding the influence of atmospheric air.

Analysis
The dissolved gases are extracted from the water samples. A cryogenic system removes all gases but helium (He) and neon (Ne). The samples are measured by a Quadrupol mass spectrometer for ^{4}He, ^{20}Ne and ^{22}Ne and with a magnetic sector mass spectrometer *MAP215-50* for ^{3}He and ^{4}He (Sültenfuß et al., submitted). The method achieves about ± 0.2% precision for the $^{3}He/^{4}He$ ratios, and ± 0.5 % or better for helium and neon concentrations.

4.4.6 Isotopic composition of dissolved nitrate ($^{15}N\text{-}NO_3^-$ and $^{18}O\text{-}NO_3^-$)

Field methods
Groundwater samples
For $^{15}N^{18}O_3$ analysis groundwater samples containing a minimum of 25 mg of nitrate were passed over 10 ml *Poly-Prep*-columns *(BioRAD)* with 5.5 g added anion exchanger (AG 2-x-8 Resin 100-200 mesh, chloride-form) to enrich nitrate and decrease the sample volume.

Soil samples
Soil samples were taken as bulk samples from a depth of 0 to 30 cm. 200 g soil samples were extracted with 200 ml distilled water. The samples were shaken for one hour and settled for at least 12 h. They were decanted and the fluid was then filtered through a 0.45 µm filter. For the calculation of the anion concentrations in the original solution the moisture content was measured (see also Schwiede, in prep.). The samples were subsequently treated like the above described groundwater samples.

Sample preparation
The fixed nitrate is extracted from the column by 3 M HCl. The hydrochloric solution is neutralized by the addition of silver oxide, where excess chloride is precipitated as AgCl. Further anions that could possibly falsify results especially during ^{18}O measurements (e.g. sulfate, phosphate) are precipitated by the addition of $BaCl_2$. The remaining filtrate is passed over a cation exchange column to remove excess barium, resulting in an acid nitrate solution that again is neutralized by the addition of Ag_2O. Filtration, freeze-drying and homogenization lead to a production of silver nitrate ($AgNO_3$) that is used for $\delta^{15}N$ and $\delta^{18}O$ analysis.

Analysis

$\delta^{18}O$ is determined using a high temperature pyrolysis system coupled to a continuous flow *IRMS delta S*. The $\delta^{18}O$ data are normalized to the *V-SMOW* standard. The measurement error is 0.4 ‰. $\delta^{15}N$ is measured online by the *Continuous Flow* procedure using a *delta XPplus* mass spectrometer. The sample gas is N_2 that is produced by an element analyser. The $\delta^{15}N$ data is normalized to the *Air* standard (Tab. 6-1). The measurement error is 0.2 ‰.

5 HYDROGEOCHEMISTRY

5.1 Nitrogen in rocks

5.1.1 Introduction

For the investigation of potential nitrate sources or reaction partners, four cores that penetrated the entire formation from the Kalahari Beds to the Tlhabana Formation were sampled. Of each core, about 15 samples were taken (Tab. 5-1). One exemplary core is discussed in the following (LGT 4).

Tab. 5-1: Locations of cores for bulk sample analysis (UTM).

Core-ID	Easting	Southing	Drill angle	Number of samples
LGT4	364249.82	7619365.22	55° (dip) and azimuth of 0	15
LDD12	363878.61	7619529.34	-40° (dip) and azimuth of 70	11
LDD13	364791.08	7620052.25	-40° (dip) and azimuth of 236	13
LDD21	364700.07	7619351.20	-43° (dip) and azimuth of 315	16

5.1.2 Results

General core description

The investigated cores penetrated mainly the Stormberg basalt and the Ntane Sandstone Fm. (see chapter 3.3 and Fig. 5-1). The microscopic investigation of the basalt samples showed that it consists mainly of plagioclase, clinopyroxene, partly transformed olivine and little magnetite. Depending on the location in the core, the basalt could be subdivided into tholeiitic diabase in

the center of a lava flow, or amygloidal or vesiculated basalt on the base of each flow. The investigated sandstone mainly consists of quartz, plagioclase and kalifeldspar, cementing is party composed of carbonate, clay minerals or is absent. Zones of mudstone, and siltstone occur within the profile. The mudstone mainly consists of quartz, phyllosilicates (mainly muscovite), clay minerals and hematite. Throughout the core no indications for sulphides were found, i.e. no pyrite, but oxides dominated. Evaporites were not found in the core, but would have been mainly expected to occur in the Kalahari Beds. Near the Letlhakane Mine, where the cores were drilled, the Kalahari Beds are, however, very thin or absent.

Apart from mineralogic investigations, element analyses have been conducted to establish element concentrations over depth. Fig. 5-2a shows the vertical distribution of carbon, nitrogen, sulfur and eluable dissolved nitrate in core LGT4. Sulfur contents are below the determination limit of 0.02 %. Carbon content is highest in samples of (weathered) basalt, reaching maximum contents of 3.35 %. In the sandstone, only values in the order of 0.02 % were found. Nitrogen in the core occurred predominantly in layers of mudstone occurrence. These are the only samples where nitrogen content is somewhat higher (up to 0.08 %) than the determination limit of 0.015 %. Calculated in maximum N-concentrations that could be theoretically released into the groundwater, a value of much greater than 2.5 g N/kg of rock would be reached. Nitrate measurements of the eluate sample showed only increased concentrations in the topmost samples, taken from the first 50 m of the profiles, there reaching contents of 0.0025 % (Fig. 5-2), representing nitrate concentrations of 25 mg/l in water.

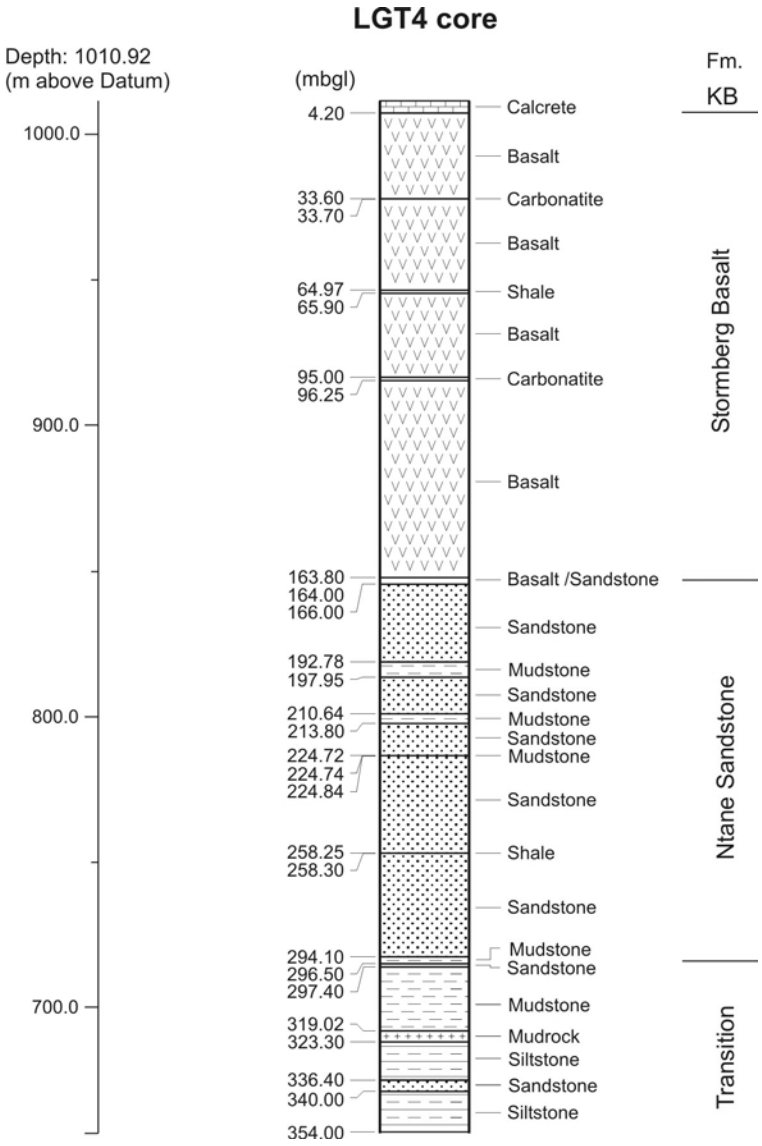

Fig. 5-1: Simplified lithological log of core LGT4. Detailed descriptions of the formations can be found in chapter 3.4.

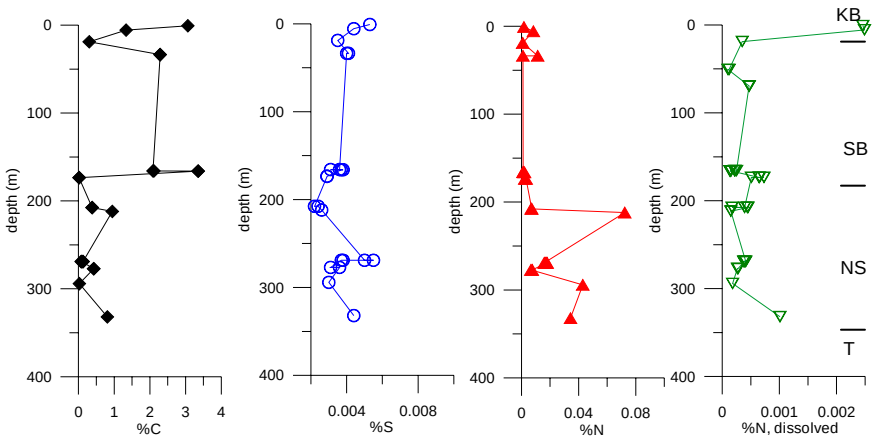

Fig. 5-2: Depth profiles of sulfur, nitrogen, carbon and dissolved nitrate-N in core LGT4 (KB = Kalahari Beds, NS = Ntane Sandstone, T = Transition as given in Fig. 5-1).

Nitrogen sources

From Fig. 5-2 it is visible that the highest N contents within the formation occur in mudstones. Transmitted and reflected light microscopy showed quartz as the main component, muscovite as a minor component, and some chlorite, feldspar, hematite and goethite. A direct determination of modal amounts via point counting was not feasible due to the extremely fine grain sizes. The component calculation from XRF data that was conducted on sample LM11 for verification resulted in quartz (approximately 30 wt.-%), muscovite (approximately 32 wt.-%), chlorite (approximately 12 wt.-%), hematite (approximately 2 wt.-%), apatite, calcite and TiO_2 (calculated as anatase). Quartz and hematite are rather unlikely to attach N, thus it is obvioulsy bound to muscovite and/or chlorite. Tab. 5-2 and plots of N versus K_2O (representative for muscovite; no other K-bearing phase present) and versus MgO (representative for chlorite; no other Mg-bearing mineral present) display increasing N with increasing oxides, but a better correlation between N and MgO (r = 0.79, see also Fig. 5-3). This correlation is even more expressed in the plot of N versus MgO/K_2O (r = 0.859; Fig. 5-3) suggesting a preferential bonding of N to chlorite.

Tab. 5-2: Chemical composition of typical mudstones (LM11, LM14, LM15), sandy mudstone (LM12) and sandstone (LM10).

Sample ID	wt.% SiO_2	%N (CNS)	wt.% K_2O	wt.%MgO	MgO/ K_2O·10
LM 10	84.03	0.007	1.87	0.63	3.37
LM 11	51.33	0.0723	4.332	2.32	5.36
LM 12	74.39	0.017	3.03	1.19	3.93
LM 14	55.54	0.0429	4.926	2.18	4.42
LM 15	57.32	0.0343	4.883	2.53	5.18

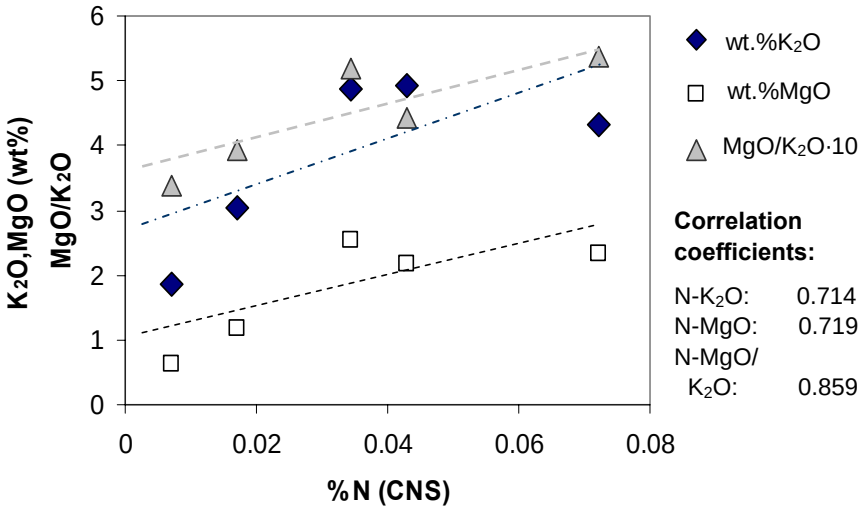

Fig. 5-3: Plot of N versus K_2O, MgO (wt.-%) and MgO/K_2O in typical mudstones, sandy mudstone and sandstone.

Nitrogen sinks

It was not only necessary to investigate sources, but also sinks for nitrogen in the aquifer. For this reason, the occurrence of pyrite (Eq. 2.7 and 2.8) and of organic carbon (Eq. 2.6) was investigated as potential reaction partners in the reduction of nitrate. Only small traces of pyrite occurred in the cores, not even in the basalt, where pyrite was most likely to occur. Organic carbon analysis

was performed on selected samples. In none of the samples detectable amounts of organic carbon were found (Tab. 5-3). Most of the carbon found in the cores stems from carbonate. In the basalt carbonate is mainly bound in amygloids and weathered parts at the base of each individual lava flow of the Stormberg basalt. In the sandstone, elevated carbon was only locally encountered (see section 'Porosity').

Tab. 5-3: Selected results of sample analysis for organic carbon content. Negative results are a consequence of the different measurements precision of the methods applied for total carbon and carbonate carbon.

sample ID LGT4	Carbonate-C (%C)	C_total (%C)	Difference = C-org (%C)
LM1	3.22	3.065	-0.155
LM2	1.27	1.335	0.065
LM4	2.47	2.227	-0.243
LM7-TP05	2.17	2.068	-0.102
LM8-TP04	3.5	3.286	-0.214
LM9-TP05	0.03	0.049	0.019
LM15	0.84	0.782	-0.058

Porosity

A further groundwater relevant aspect was an estimation of the pore volume of the aquifer. Although main results are deduced from pump tests, microscopic investigations were performed to support pump test results. In most of the sandstone samples a low porosity of less than 5 % was observed from microscopic investigations (e.g. LM9, LM10, LM12). None of the sandstone samples showed secondary silicification of the sand. The porosity varied from greater than 10 % associated with coarse graining, with partly carbonatic cementation and less than 5 % in finer grained zones. There, cementation is mainly made of clay minerals (see also Fig. 5-4).

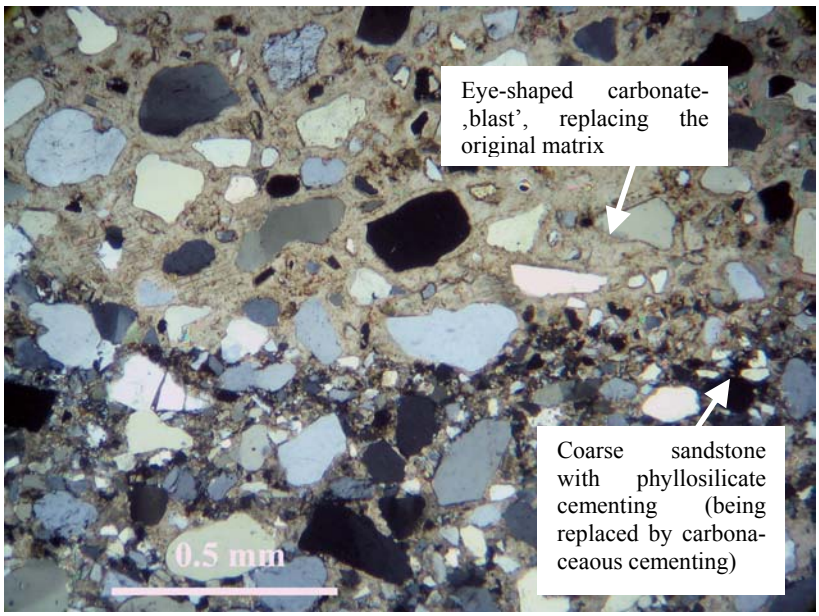

Fig. 5-4: Coarse sandstone with eye-shaped carbonate patch. The carbonate replaces the original phyllosilicate cementing (thin section of LM13-TP03).

5.1.3 Summary and conclusion

Concentrations of nitrogen were at a low 0 – 0.08 wt. % N throughout the core. The highest N concentrations were found in mudstone in the Mosolotsane Formation and in mudstone layers within the Ntane Sandstone. There, N is mainly bound to phyllosilicates (probably chlorite). Indications are that N from the host rock cannot be easily released into the groundwater. Elevated nitrate concentrations towards the top of the core from eluate measurements presumably reflect the position of the unsaturated zone. There, nitrate concentrations might be higher as a function of the (low) water content. In this zone it is possible that nitrate, as well as other water components, are temporarily fixed as salts on the surface of the solid component matrix (see chapters 2.2 and 2.3), which in the above example is mainly basalt. Deeper along the core, where saturated conditions prevailed, N salts would already be flushed out

due to their high solubility or they would simply never form. Water strike or water level data was, however, not available to confirm this.

N-sinks were not found within the lithology. Pyrite was not found in the samples, rendering the reduction of nitrate very unlikely in this lithology. The other expected reaction partner in the reduction of nitrate, i.e. organic carbon, did only occur in hardly detectable traces in the cores. The carbon that was found proved to be inorganic, mainly stemming from carbonate. Initially, organic carbon was expected between individual basalt flows, as they might host paleosoils that potentially may still contain organic matter of the former land surfaces. This was not the case on the investigated samples. Paleosoils could only be identified in one core sample, however, this proved to be a relatively pure sand soil without detectable amounts of organic matter.

Regarding porosity the results from conducted pump tests (chapter 3.5.2) could be generally confirmed. The Ntane sandstone exhibited an estimated porosity of less than 5 % from transmitted and reflected light microscopic observations. However, small-scale heterogeneities were found, where areas of coarser graining showed larger pore volumes of greater than 10 %, in addition to carbonaceous cementing, which was absent in most of the investigated samples.

5.2 General hydrochemistry

5.2.1 Introduction

To investigate the origin and fate of nitrate in the subsurface, a detailed knowledge of the hydrochemical and geochemical setting of the investigation sites is necessary. Due to a lack of sufficient data, a total of five own field campaigns were carried out from 2002 to 2004, during which spatial campaigns and depth-related sampling accompanied by multiparameter probe logging were performed. Hydrochemical data in study area 2 were supported by an MSc thesis at Karlsruhe University, Germany (Schnabel, 2004) that was carried out within this project.

5.2.2 Methods of data interpretation

To interpret data obtained from hydrochemical investigations, different methods were applied. The investigation of potential spatial distribution patterns and hydrochemical correlations related to nitrate behaviour was taken from field, standard and trace element data of the abstracted groundwater samples. Parameters for the description of potential vertical variations in groundwater chemistry due to hydraulic or reactive processes were obtained from multi-parameter probe logging accompanied by bailer samples for the determination of the total water chemistry. Reactive potential, sources and sinks from the lithology of and around the aquifer was inferred from investigations of core material in chapter 5.1.

Graphical representation of hydrochemical data

A selection of hydrochemical parameters in this chapter is represented as box-whisker plots to denote mean values and percentiles. The plot considers a normal distribution of the raw data and divides the data into four areas of statistical probability (Fig. 5-5), marked by percentiles. Further statistical methods that were applied can be found in textbooks such as e.g. Lozán and Kausch (1998) and were performed with the software packages *SPSS 10.0.5* and *Origin 6.0*.

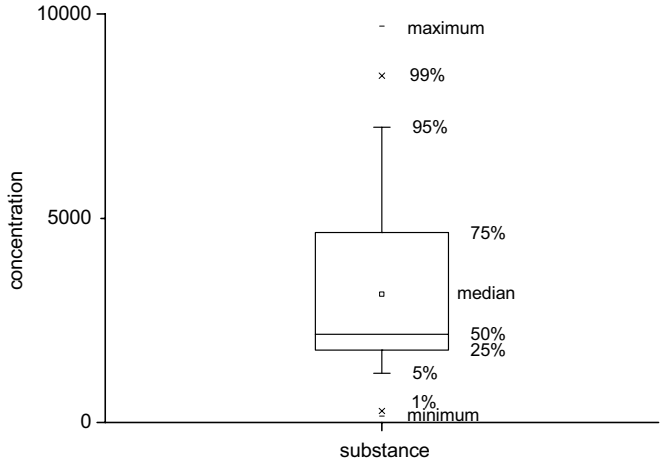

Fig. 5-5: Box-whisker plot to represent the range of measured parameters.

5.2.3 Results

5.2.3.1 General hydrochemical characterization of the area

The groundwater from the Ntane Aquifer is dominated by a Ca-(Mg-)HCO_3- to Na-HCO_3-chemistry and a Na-Cl water type towards the discharge area (Fig. 5-6 and Fig. 5-7). It has a moderate to very high ion content (range of specific electric conductivities (EC) 0.3 to 60 mS/cm), neutral to basic pH of 6.8 to 10.7, and temperatures of 26 to 28 °C. Specific electric conductivity and ionic concentrations generally increase from Southeast (Serowe) to Northwest (Orapa) following the flow pattern as a result of increased contact time for water-rock interaction (EC: $\tilde{x}_{Serowe}$ = 0.62 mS/cm and $\tilde{x}_{Orapa}$ = 2.34 mS/cm). Already near Serowe Ca-(Mg)-HCO_3 type waters evolve to Na-HCO_3 by cation exchange processes, raising the pH from 7.0 to 10.0 (alkalization) (Fig. 5-6). Along the flow path towards Orapa a trend can be observed that marks a development into a Na-HCO_3 to Na-Cl groundwater type (Fig. 5-7).

During the investigations significant differences were found between the recharge area Serowe (area 1) and the discharge area Orapa (area 2) especially relating to the electric conductivity, which is distinctly dominated by Na^+ and Cl^- only in Orapa (Fig. 5-8 and Fig. 5-9), reaching mean values of 35.9 and 40.2 mmol(eq)/l, while in Serowe concentrations reach only 3.2 and 1.2 mmol(eq)/l. This is supported by correlations of the electric conductivity with groundwater constituents. While EC near Serowe correlates strongly with Ca^{2+} (r = 0.803), Mg^{2+} (r = 0.842) and HCO_3^- (r = 0.708), dominant components towards Orapa are Cl^- (r = 0.982) and Na^+ (r = 0.953) (Tab. 5-4). Further correlations among the major groundwater constituents can be found in Tab. 5-4.

The observed nitrate (NO_3^-) concentrations reached up to 219 mg/l in Serowe groundwaters (BH8471). While the mean concentration was at 22.8 mg/l, the median only reached 8.4 mg/l, indicating a heterogeneous distribution of nitrate ranges (Fig. 5-10). In Orapa, maximum nitrate values were 244 mg/l in one hand-dug well (SE9) that appeared to be contaminated by surface inflow. Excluding this well, the maximum concentration was 93.7 mg/l (Z9058). The mean value of nitrate in Orapa is 30.6 mg/l and the median is 29.0 mg/l.

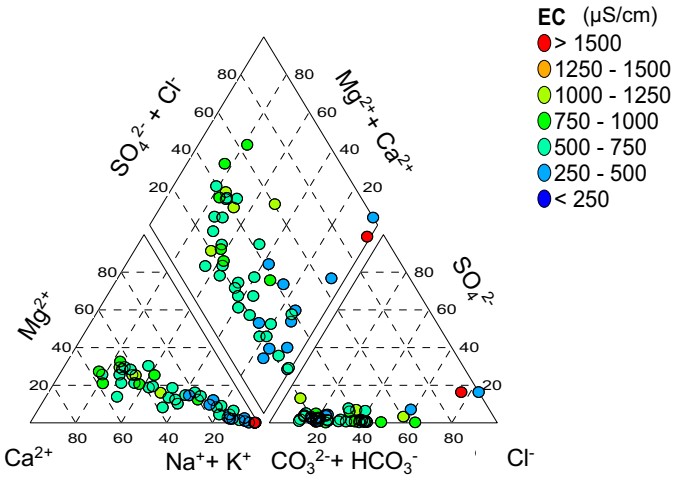

Fig. 5-6: Piper diagram of groundwater samples near Serowe, shading indicates specific electric conductivity ranges (µS/cm).

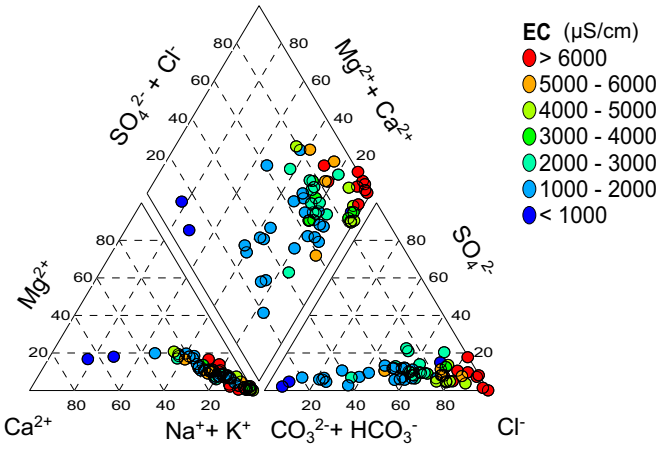

Fig. 5-7: Piper diagram of groundwater samples near Orapa, shading indicates specific electric conductivity ranges (µS/cm). Note the scale difference in electric conductivities as opposed to Fig. 5-6.

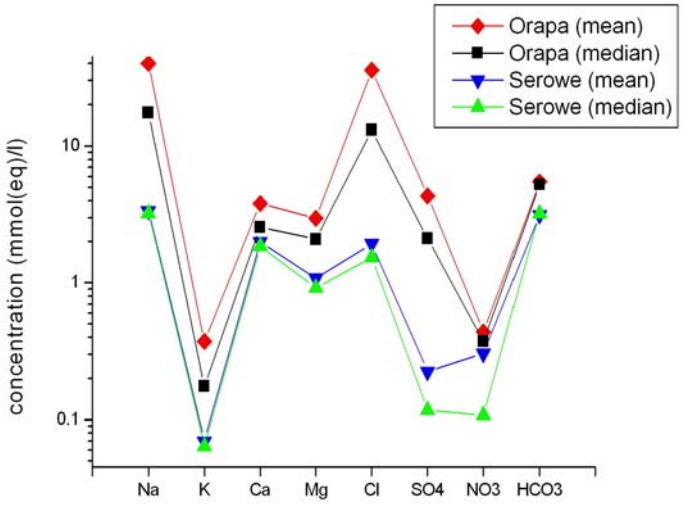

Fig. 5-8: Schoeller diagram of the two investigated locations Serowe (n = 51) and Orapa (n = 60). Mean and median values are shown.

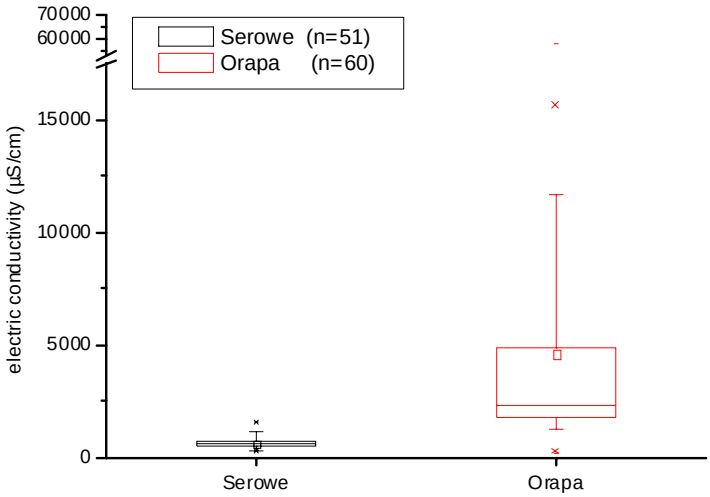

Fig. 5-9: Comparison of specific electric conductivities (µS/cm) from the two investigation areas.

This implies a more homogeneous range of nitrate concentrations in Orapa groundwaters compared to groundwaters from Serowe. In both areas, however, nitrate-free waters were also observed.

Tab. 5-4: Correlations after *Pearson* for (a) Serowe n=50, and (b) Orapa n=55 (significance level of p = 0.01 (2-site) for bold values).

(a) Serowe*

Parameter	EC	Ca^{2+}	Mg^{2+}	Na^{+}	Cl^{-}	SO_4^{2-}	NO_3^{-}	HCO_3^{-}
EC								
Ca^{2+}	**0.803**							
Mg^{2+}	**0.842**	**0.911**						
Na^{+}	0.057	**-0.491**	-0.400					
Cl^{-}	**0.645**	**0.571**	**0.511**	-0.152				
SO_4^{2-}	**0.463**	0.189	0.259	**0.437**	0.002			
NO_3^{-}	**0.577**	**0.580**	**0.582**	-0.212	0.139	0.035		
HCO_3^{-}	**0.709**	**0.586**	**0.662**	0.183	0.072	**0.621**	0.313	

*extreme values of the contaminated borehole Matikwe 2 were omitted in correlation calculations

(b) Orapa*

Parameter	EC	Ca^{2+}	Mg^{2+}	Na^{+}	Cl^{-}	SO_4^{2-}	NO_3^{-}	HCO_3^{-}
EC								
Ca^{2+}	0.333							
Mg^{2+}	**0.462**	**0.916**						
Na^{+}	**0.953**	0.041	0.188					
Cl^{-}	**0.982**	0.338	0.438	**0.928**				
SO_4^{2-}	**0.671**	0.141	0.228	**0.676**	**0.604**			
NO_3^{-}	0.068	**0.697**	**0.619**	-0.128	0.053	0.012		
HCO_3^{-}	0.045	0.139	0.273	0.027	-0.125	0.081	0.192	

*extreme values of boreholes Z7157, Z7101, Z7189, Z7155 and Z7100 from the Khwee block were omitted as they showed significant influence by Na-Cl type groundwater of the underlying Mosolotsane aquifer

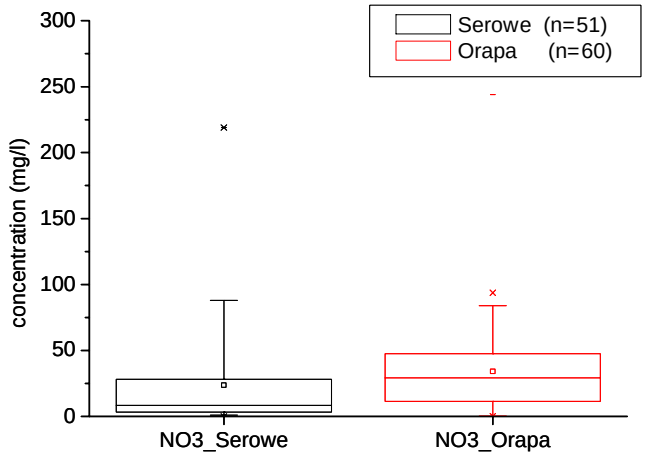

Fig. 5-10: Box-whisker diagram of nitrate concentrations in study area 1 (Serowe) and study area 2 (Orapa)

The distribution of nitrate is shown in Fig. 5-11. Elevated nitrate concentrations occur in a spatially scattered pattern, with localized clusters of elevated concentration. This is the case directly West of Serowe (Fig. 5-11a) and in the Western area near Letlhakane River and partially in wellfield 4 in the Orapa study area (Fig. 5-11b). Spatial designations that are referred to in the text can be found in the borehole location map in Fig. 3-2 and abbreviated in Fig. 5-11. However, in some cases in directly neighboring wells (distance less than 20 m) steep gradients can be observed (data not shown due to map resolution). An attempt to verify the pattern with hydraulic and hydrologic information indicated that the distribution of high nitrate cannot singularly be attributed to the flow path (chapter 6.1.2). The strong heterogeneity occurs both in the lateral and in the vertical direction (chapter 5.3.2).

However, water chemistry appears to play an important role for the nitrate distribution. Results from the analysis of Serowe groundwaters show clearly that elevated nitrate occurs in the context of Ca-(Mg-)HCO_3-type groundwaters, whereas waters with a Na-HCO_3 signature have low nitrate contents (Fig.

5-12). In the piper diagram of Orapa the Ca-HCO_3 dominated waters do not show elevated nitrate concentration, but rather show elevated concentrations in the order of 30 to 50 mg/l for Na-HCO_3-Cl groundwater types (Fig. 5-13). However, it has to be noted the three Ca-rich samples originate from the encountered perched aquifer in the Kalahari Beds which appears to behave and/or have formed differently (chapter 5.3.2.3) than Ca-HCO_3 water from the Ntane Sandstone Aquifer. In addition, the nitrate-free Na-Cl waters do not represent the general trend of Ntane groundwater as those stem from the 'Khwee Block' that is in parts hydraulically isolated and connected to the lower lying Mosolotsane layers, again representing waters formed under different boundary conditions.

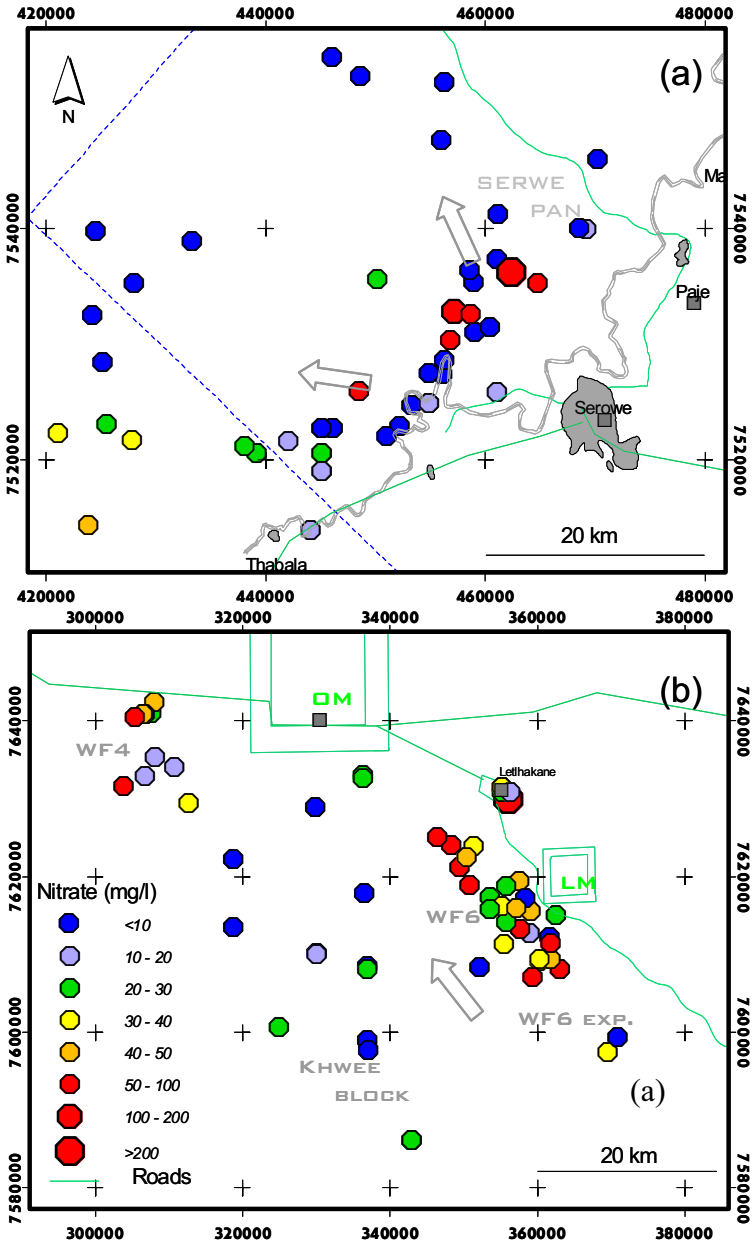

Fig. 5-11: Map of nitrate distribution (mg/l). (a) study area 1 (Serowe). (b) study area 2 (Orapa). Arrows indicate general flow directions. Abbreviations on locations as given in Fig. 3-2.

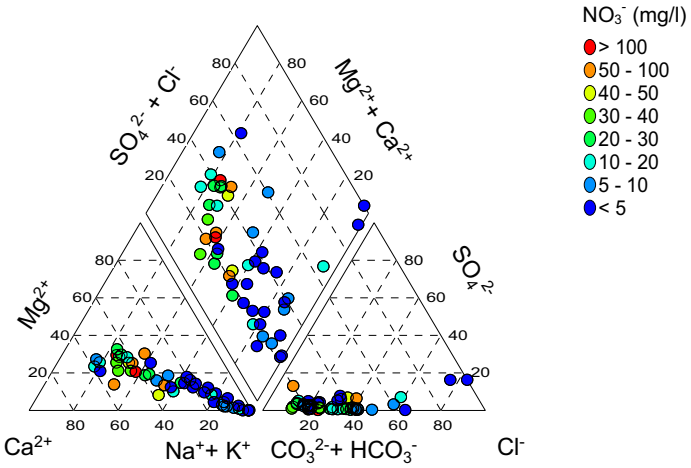

Fig. 5-12: Piper diagram of groundwaters from Serowe, shading indicates nitrate content (mg/l).

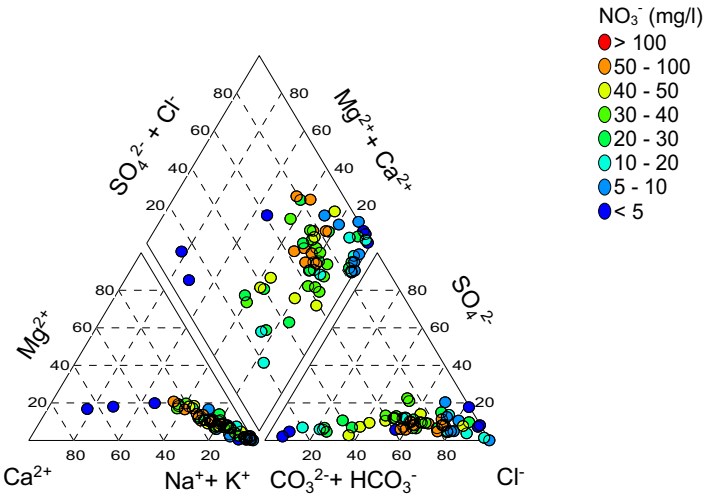

Fig. 5-13: Piper diagram of groundwaters from Orapa, shading indicates nitrate content (mg/l).

5.2.3.2 Genesis of chemical constituents in the groundwater

In order to understand processes that control the groundwater chemistry in the investigated Ntane Sandstone Aquifer, water-rock interaction, its influence on chemical constituents in the groundwater and the genesis of those constituents is discussed in the following. Of particular interest are:

- the redox environment and its impact on nitrate
- the carbonate chemistry
- redox-independent groundwater constituents and processes, i.e. cation exchange
- regional deviations and mixing

Supporting thermodynamic calculations were performed with *PhreeqC-2* (Parkhurst, 1995) using *PhreeqC.dat* as a reference thermodynamic database. Ammonia (NH_4^+) was changed from *Amm* to NH_4^+ to include it as a reactive species.

Theoretical background

Principles of aquatic chemistry relevant to this study are shortly summarized in the following.

The equilibrium of chemical reactions in water is described by the law of mass action. The species distribution at equilibrium for the reaction

(5.1) $aA + bB \leftrightarrow cC + dD$

is described by the equilibrium constant K:

(5.2) $$K = \frac{\{C\}^c \{D\}^d}{\{A\}^a \{B\}^b}$$

where bracketed quantities denote activities of the species. Activities of species describe the ‘effective’ concentrations of dissolved species in groundwater, as ion reactivity is reduced by electrostatic interactions with other ions (i.e. shielding effects). This effect gains more importance with increasing salinitiy.

Equilibrium constants can be calculated thermodynamically and are temperature dependent. The law of mass action is applicable for e.g. dissolution and precipitation reactions of minerals, relations between dissolved species and dissolution of gases (Appelo and Postma, 1996). By definition, the activity of water equals one ($a_{H2O} = 1$), and the activity of a pure solid equals one ($a_{ss} = 1$).

Solubility of minerals

For a solution of a mineral of a composition aA + bB ↔ aAbB the equilibrium constant is called the solubility product K_s which writes as

(5.3) $K_s = \{A\}^a \cdot \{B\}^b$

as defined by the law of mass action. Examples for equilibrium constants of common mineral phases are shown in Tab. 5-5.

Tab. 5-5: Equilibrium reactions and constants (K_s) for selected mineral phases at 25°C (Appelo and Postma, 1996).

Equation no.	Mineral	Reaction	Equilibrium constant (K_s)
(5.4)	Calcite	$CaCO_3 \leftrightarrow Ca^{2+} + CO_3^{2-}$	$10^{-8.3}$
(5.5)	Magnesian calcite	$(Ca_{1-x1}, Mg_{x1})CO_3 \leftrightarrow$ $1\text{-}x_1\ Ca^{2+} + x_1\ Mg^{2+} + CO_3^{2-}$	$10^{-8.4}$
(5.6)	Dolomite	$(Ca_{1-x2}, Mg_{x2})CO_3 \leftrightarrow$ $1\text{-}x_2\ Ca^{2+} + x_2\ Mg^{2+} + CO_3^{2-}$	$10^{-17.1}$
(5.7)	Gypsum	$CaSO_4 \cdot 2\ H_2O \leftrightarrow$ $Ca^{2+} + SO_4^{2-} + 2\ H_2O$	$10^{-4.6}$

$x_1 << x_2$

The ratio between the ion activity product IAP, which in aqueous solution is defined as the product of activities

(5.8) $IAP = \{A\}^a \cdot \{B\}^b$

and the solubility product K_s indicates the saturation state of a mineral. The saturation state is commonly expressed as the saturation index (SI), which is the logarithm of the saturation state. It writes as:

(5.9) $$\text{SI (saturation index)} = \log \frac{\text{IAP}}{K_s}$$

SI > 0 means supersaturation, indicating that precipitation is possible.
SI = 0 means equilibrium.
SI < 0 means undersaturation, where mineral dissolution is possible (Stumm and Morgan, 1996).

In the following, mineral solubility is discussed exemplarily by means of calcite solution. Carbonate reactions impose a large influence on the composition of groundwater and dominate over much slower silicate dissolution processes (Appelo, 1994). As indicated in Tab. 5-5 the solubility of carbonates in pure water is very low. However, the presence of CO_2 strongly impacts on the solubility equilibrium. CO_2 is taken up from the atmosphere and during infiltration from microbially mediated oxidation of organic matter in the soil (Stumm and Morgan, 1996), as shown in Equation 5.10.

(5.10) $CO_{2(g)} + H_2O \rightarrow H_2CO_3$

Carbonic acid (H_2CO_3) can dissociate in two steps. Each step releases one proton:

(5.11) $H_2CO_3 \rightarrow H^+ + HCO_3^-$
(5.12) $HCO_3^- \rightarrow H^+ + CO_3^{2-}$

(5.13) $\overline{H_2CO_3 \rightarrow 2\,H^+ + CO_3^{2-}}$

This CO_2-enriched water can dissolve silicates, $CaCO_3$ and $CaMg(CO_3)_2$, exemplarily given for calcite dissolution in groundwater:

(5.14) $CaCO_3 + CO_2 + H_2O \leftrightarrow Ca^{2+} + 2\,HCO_3^-$

If CO_2 is available, calcium will be dissolved, while degassing will cause a precipitation of calcite. Kinetics of carbonate dissolution can reach an equilibrium within hours or days (Merkel, 1992). Subsequent reactions such as ion exchange can fix the carbonate ions, thus trigger further carbonate dissolution in order to re-establish equilibrium conditions. Differences are found between

open and closed system dissolution, as in closed systems an initial CO_2 content is not replenished, limiting further carbonate dissolution.

Redox potential

In addition to the described reactions directly relating to the calcite equilibrium, redox reactions can influence the amount of inorganic carbon of a groundwater system that in turn can impact on dissolution and precipitation of minerals in the groundwater. In dissimilatory processes the **redox potential (Eh)** is the parameter that describes the hydrochemical environment and thus the possibility for microbes to catalyze reactions (Appelo and Postma, 1996). The reactions in Tab. 5-6 show a possible increase of HCO_3^- as a result of the oxidation of organic matter (CH_2O) with oxygen, nitrate, manganese, iron and sulfate. Detailed descriptions of the individual processes can be found in Appelo and Postma (1996) and Stumm and Morgan (1996). Eh ranges of important redox processes are shown in Fig. 5-14.

Tab. 5-6: Sequence of redox reactions in the presence of CH_2O (modified after Stumm and Morgan, 1996).

Equation number	Name	Reaction
(5.15)	Aerobic respiration	$CH_2O + O_2 \rightarrow H^+ + HCO_3^-$
(5.16)	Denitrification	$CH_2O + {}^4/_5\ NO_3^- \rightarrow {}^2/5\ N_2 + HCO_3^- + {}^2/_5\ H_2O$
(5.17)	Mn^{4+}- reduction	$CH_2O + 2\ MnO_2 \rightarrow 2\ Mn^{2+} + HCO_3^- + 2\ H_2O$
(5.18)	NO_3^- - reduction	$CH_2O + ½\ NO_3^- + H^+ \rightarrow ¼\ NH_4^+ + HCO_3^-$
(5.19)	Fe^{3+}- reduction	$CH_2O + 4\ Fe(OH)_3 + 7\ H^+ \rightarrow 4\ Fe^{2+} + HCO_3^- + 10\ H_2O$
(5.20)	SO_4^{2-}- reduction	$CH_2O + ½\ SO_4^{2-} \rightarrow ¼\ HS^- + ¼\ H_2S + ¼\ H^+ + HCO_3^-$
(5.21)	Methanogenesis	$CH_2O \rightarrow ½\ CH_4 + ½\ CO_2$

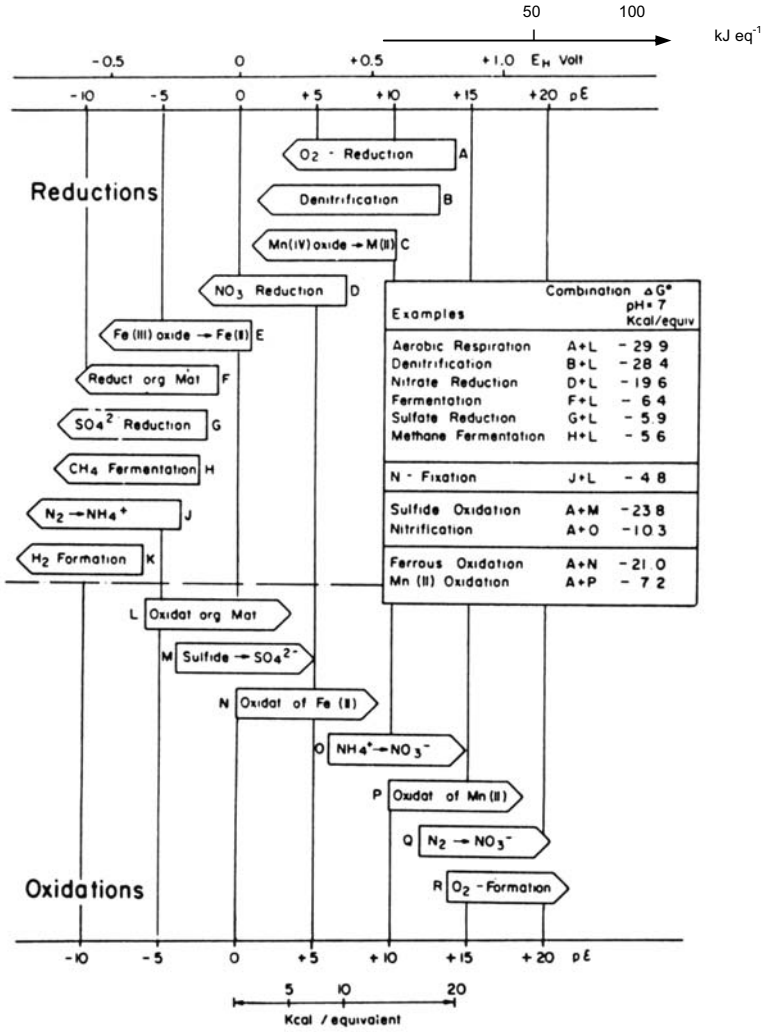

Fig. 5-14: Sequences of redox processes at pH 7 in natural systems (Stumm and Morgan, 1996).

Results

Redox environment and microbially catalyzed redox reactions

The measured redox potential (Eh) of groundwaters of study area 1 and 2 varies over a broad range between -94 mV and 357 mV. The relationship between selected dissolved species and Eh separated for the two areas is shown in Fig. 5-15. Oxygen concentrations are consistent with the redox potential. While Serowe groundwater samples show more oxic conditions, groundwater from Orapa appears to have developed to more reducing conditions at a lower Eh. The redoxcline appears to be located at an Eh around 200 mV, which lies slightly below the value proposed by Stumm and Morgan (1996) (Fig. 5-14). Manganese and iron exhibit a slightly more regular redox behavior in Orapa than in Serowe, as those parameters only exhibit very low concentrations in Serowe. Those values follow the expected sequences of redox processes (Fig. 5-14). In the investigated samples, the sulfate pattern is too scattered to be interpretable (data not shown). It should, however, be noted that in the investigated samples Eh values indicate nitrate reducing conditions but no reduction of sulfate.

The observed nitrate occurrence at the given Eh, however, cannot be explained by thermodynamic considerations alone. High nitrate concentrations appear to generally occur at a higher Eh in Serowe (between 300 and 400 mV), while nitrate concentrations greater than 50 mg/l already occur at more reducing conditions around 100 mV in Orapa (Fig. 5-15). This observation shows that hardly any nitrate reduction takes place in Serowe. The Eh values of several samples in Orapa (e.g. boreholes Z7089, Z7189, Z11048, Z11049) would, however, imply that nitrate is not reduced under nitrate reducing conditions. A possible explanation could be i) a lack of electron donors, which is unlikely from hydrochemical investigations of the groundwater, e.g. as to the presence of low amounts of organic carbon. ii) that the observed field Eh represents a random mixture of different groundwater components induced by the abstraction of the groundwater sample. On the one hand a mixture of anoxic groundwater with oxic groundwater leads to a rapid oxidation of ferrous iron that precipitates as FeOOH within seconds to minutes (e.g. Houben, 2004). On the other hand the thermodynamically feasible process of nitrate reduction is kinetically much slower (e.g. Ottley et al., 1997, Buresh and Moraghan, 1976) and is not likely to have the same influence as ferrous iron oxidation by O_2. Therefore O_2 is consumed much faster while NO_3^- becomes

preserved. In addition, deviations from the ideal redox conditions may appear in natural groundwater systems, as the observed potentials often represent a mixture of potentials (Appelo and Postma, 1996).

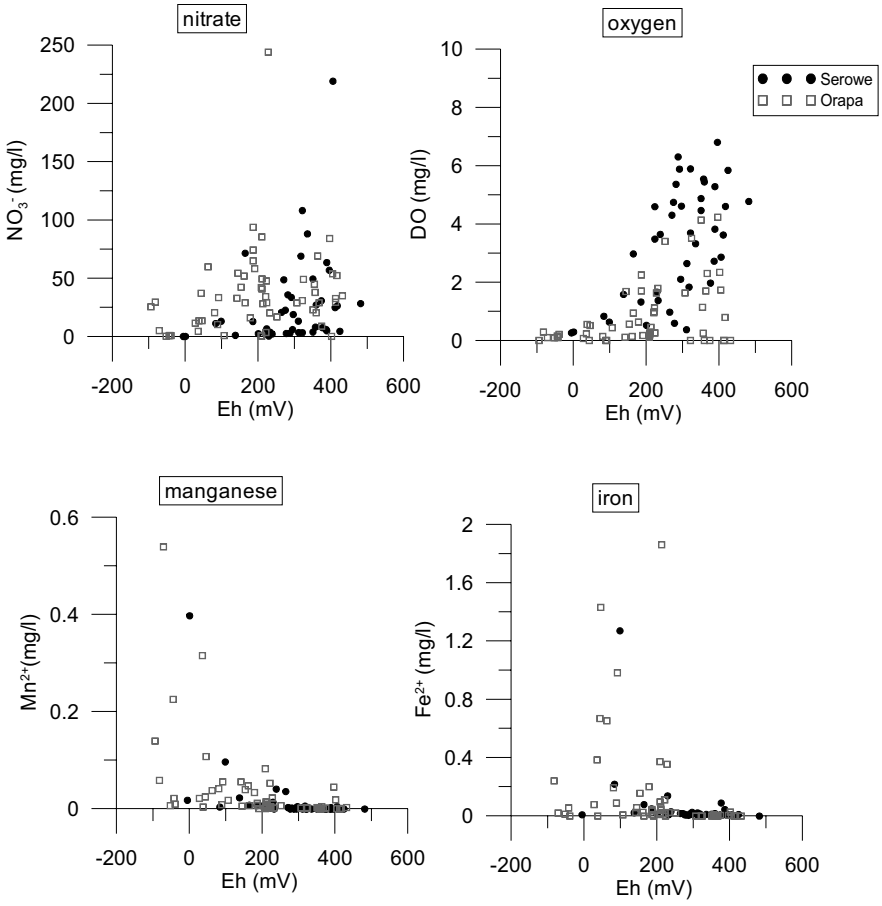

Fig. 5-15: Relationship between selected chemical parameters and redox potential (Eh) in groundwater from the Ntane Sandstone Aquifer near Serowe (filled symbols) and Orapa (open symbols).

Carbonate reactions

The investigated groundwaters contain high amounts of dissolved inorganic carbon (DIC), with mean concentrations of 4.3 mmol/l observed in Serowe and 7.0 mmol/l in Orapa, expressed as the sum of HCO_3^- and CO_3^{2-} in Fig. 5-16 a. The high carbon concentrations owe to a dominant open system carbonate dissolution in the unsaturated zone when infiltration waters pass calcretes, as replenishment of CO_2 in open systems allows a significantly higher dissolution of carbonates than under closed conditions (Eq. 5.10 to 5.13). Exemplary *PhreeqC-2* simulations of the pCO_2 for conditions in Serowe showed a good agreement with the above assumptions, indicating that pCO_2 values in the order of 10^{-2} bar are necessary to produce the observed DIC values. This is also consistent with the abundance of calcretes in the unsaturated zone. DIC concentrations are highest at circum-neutral pH values (Fig. 5-16b). Closed system processes mainly take place in the carbonatic matrix of the Ntane Sandstone Aquifer. Though no further CO_2 enters the system to re-equilibrate, kinetically inhibited reactions such as the dissolution and/or precipitation of minerals can fully proceed as the slowly flowing system constitutes no time-limit.

Most of the inorganic carbon that was found originates from the dissolution of calcretes (Eq. 5.4 to 5.6). The slightly higher DIC concentrations in Orapa probably relate to i) a higher abundance of calcretes near Letlhakane and Orapa. This higher abundance has been stated in reports (Debswana, 1997, AAC, 1992), but has, however, never been quantified; ii) longer contact times of the groundwater to surrounding rock, whereby further amounts of DOC (and DIC) can be released from the sandstone that can be converted into inorganic carbon as shown in Tab. 5-6. Even small amounts of less than 2% organic carbon which is typical for sandstones (Krauskopf and Bird, 1995) can theoretically account for a production of 425 mg/l HCO_3^-, at optimal pH and redox conditions. Own investigations of core samples showed even lower amounts of DOC (less than 1 %, chapter 5.1).

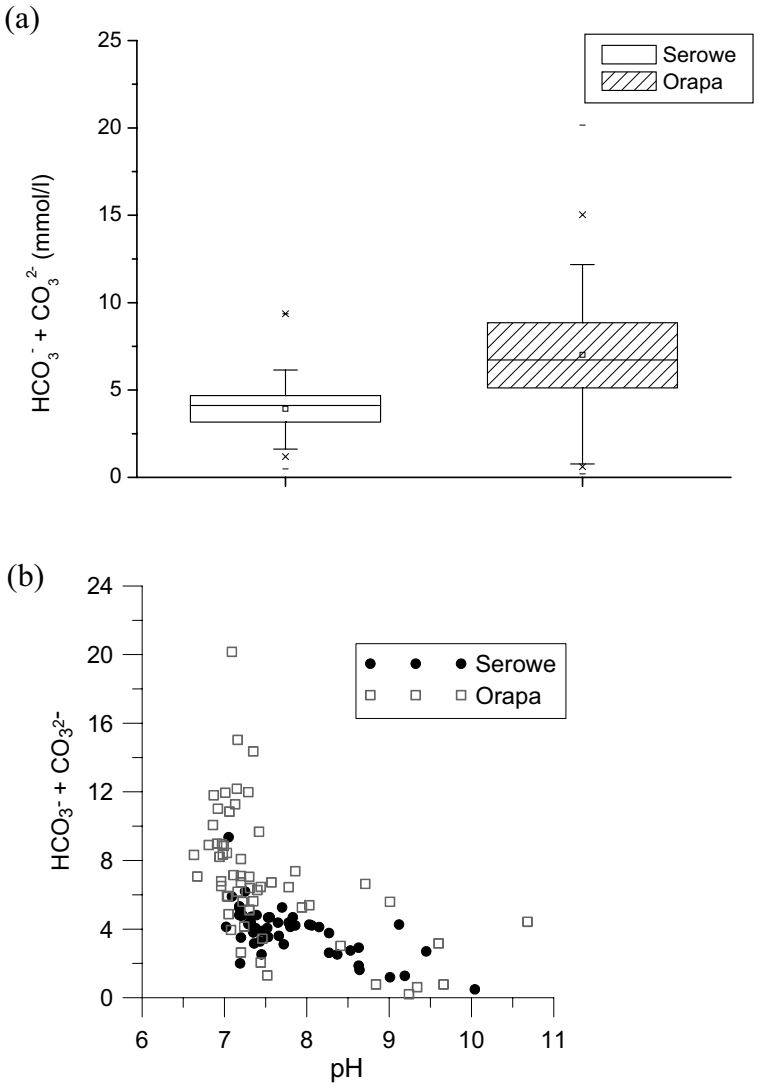

Fig. 5-16: Alkalinity of the study areas Serowe (n = 51) and Orapa (n = 60), expressed as (a) the sum of HCO_3^- and CO_3^{2-} in mmol/l and (b) with according pH values.

In the sampled groundwater only minor amounts of organic carbon (as NPOC: non-purgeable organic carbon) of less than 0.8 mg/l are found. Only in one hand dug well (HDW4) extremely elevated NPOC contents of 42 mg/l are found which point to anthropogenic pollution. In addition, borehole Z7157 shows NPOC contents of 8.3 mg/l. This borehole penetrates deeply into the Mosolotsane aquifer within the Khwee block and has very high electric conductivity values of 63.1 mS/cm. It may be the case that this borehole due to its position within the structural blockfaulting setting and due to its depth has contact to water that passed the very thin coaly layers within the mudstones of the underlying Thlabala layers. To support this, the redox potential at this borehole was found to indicate strongly reducing conditions of -71 mV. Apart from this specific location, influences of methanogenesis and sulfate reduction are not expected in the investigation area (Fig. 5-15). Further influence on carbon concentration can stem from local recharge influence that delivers further organic matter into the aquifer along the flow path with a subsequent transformation into inorganic carbon (Tab. 5-6). Due to the very low recharge amounts (chapter 3.5.3) this is expected to be a subordinate aspect to the DOC derived from lithology along the flow path.

Redox-independent groundwater constituents

Calcium and Magnesium

Measured calcium concentrations reach a mean value of 1.0 mmol/l in Serowe groundwaters and 1.9 mmol/l in Orapa, while magnesium concentrations reach mean concentrations of 0.54 mmol/l (Serowe) and 1.48 mmol/l (Orapa), respectively. As already indicated from the carbonate chemistry, calcium and magnesium mainly originates from the dissolution and precipitation of calcretes in the investigation area (Eq. 5.4 to 5.6). Further input during infiltration can stem from weathering of the overlying basalt. Incongruent dissolution of feldspars, mica and other silicates in the basalt can release large quantities of calcium, but also potassium and sodium (Eq. 5.23 and 5.24). The observed molar calcium to magnesium ratios in the study area range from 1.22 (median of Orapa) to 1.97 (median of Serowe). This indicates a dissolution of calcite ($CaCO_3$, Eq. 5.4) and dolomite ($CaMg(CO_3)_2$, Eq. 5.6) within calcretes during infiltration or within the carbonatic matrix of the Ntane or Kalahari Sandstones (chapter 5.1). At present conditions a near precipitation-dissolution equilibrium is reached ($SI_{calcite} \approx 0$). Long-term climatic changes as observed in the Kalahari (chapter 3.2.3) could lead to shifts in equilibrium, leading to enhanced calcite precipitation during more arid phases, while increased disso-

lution tends to be related to wetter phases. These calcrete formation mechanisms are described in detail in chapter 3 (duricrusts). Although the solubility of magnesium carbonates is generally higher than that of calcium carbonates, magnesium concentrations in groundwater are generally lower than calcium concentrations, as kinetics are approximately 100 times slower (Busenberg and Plummer, 1982). The prevalence of lower values in the study area is confirmed from the above mentioned molar ratios of calcium and magnesium. The trend of the relative increase of magnesium along the flow path owes to facilitated reprecipitation of calcite (Stumm and Morgan, 1996). Ratios may however be decreased due to heterovalent **ion exchange** of calcium with sodium (Eq. 5.22).

(5.22) $$\tfrac{1}{2}Ca^{2+} + Na - X \longrightarrow \tfrac{1}{2}Ca - X_2 + Na^{+}$$

The cation exchange capacity (CEC) is mainly given by clay minerals and humic substances. In the study area, the partially clay-mineralic matrix of the Ntane sandstone probably acts as the main exchanger. Due to their negative surface charge clay minerals sorb cations, while anions would react with Al- and Fe-hydroxides. Cation exchange capacity is, however, generally greater than anion exchange capacity (AEC) (Appelo and Postma, 1996). In the investigated samples ion exchange is a dominant process, as is already indicated from the piper diagrams (Fig. 5-6 and Fig. 5-7). However, exchange processes are more active in Serowe, while in Orapa the hydrochemical evolution has further developed and less calcium is available to be exchanged and/or the exchanger is saturated by sodium.

CEC is pH dependent. The simple exchange of calcium to sodium does not alter the pH. However, subsequent Ca dissolution impacts on the calcite equilibrium which in turn increases the pH (Eq. 5.4 to 5.6), as shown in Fig. 5-17 for a groundwater sample from Serowe. The figure shows a modeled development of pH and solution composition of an initial Ca-HCO_3 water type (representing a Serowe endmember) during cation exchange with sodium (NaX). An open system calcium equilibrium is assumed to represent calcrete dissolution. Subsequent exchange steps raise the pH from 7.2 to 8.8 and increase the calcium at the exchanger (CaX). Both calcium and sodium increase in solution. Once calcite ceases to be available, calcium concentrations in solution decrease, which eventually leads to a development of a sodium domi-

nated water (not shown). This may occur when the groundwater reaches closed system conditions in addition to limited calcite availability.

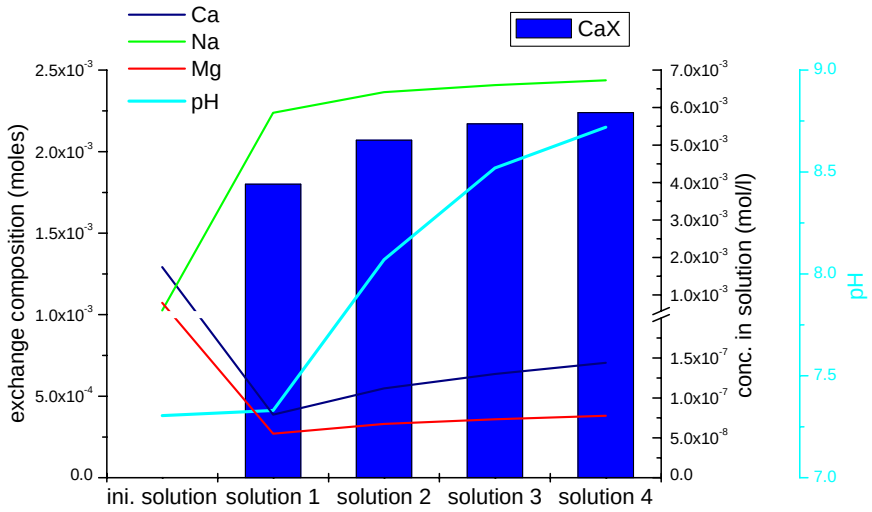

Fig. 5-17: Modeled development of a Ca-HCO_3 solution in contact with a sodium exchanger (NaX) in equilibrium with calcite.

Saturation state of minerals in the groundwater

At the measured pH most of the samples were saturated with respect to calcite and saturated to slightly undersaturated with respect to dolomite (Fig. 5-18a). Dolomite saturation is reached towards Orapa (Fig. 5-18b). Fe-phases were generally supersaturated but do not provide reliable results as the observed iron concentrations in the groundwater are generally lower than 0.1 mg/l in Serowe, and lower than 0.5 mg/l in Orapa. Only locally higher concentrations are found that might account for localized occurrences of ferricretes. From the consideration of the saturation indices of chalcedony and quartz of greater than 4 the possibility of silica precipitation e.g. in form of silcrete is suggested, though amorphous SiO_2 is undersaturated.

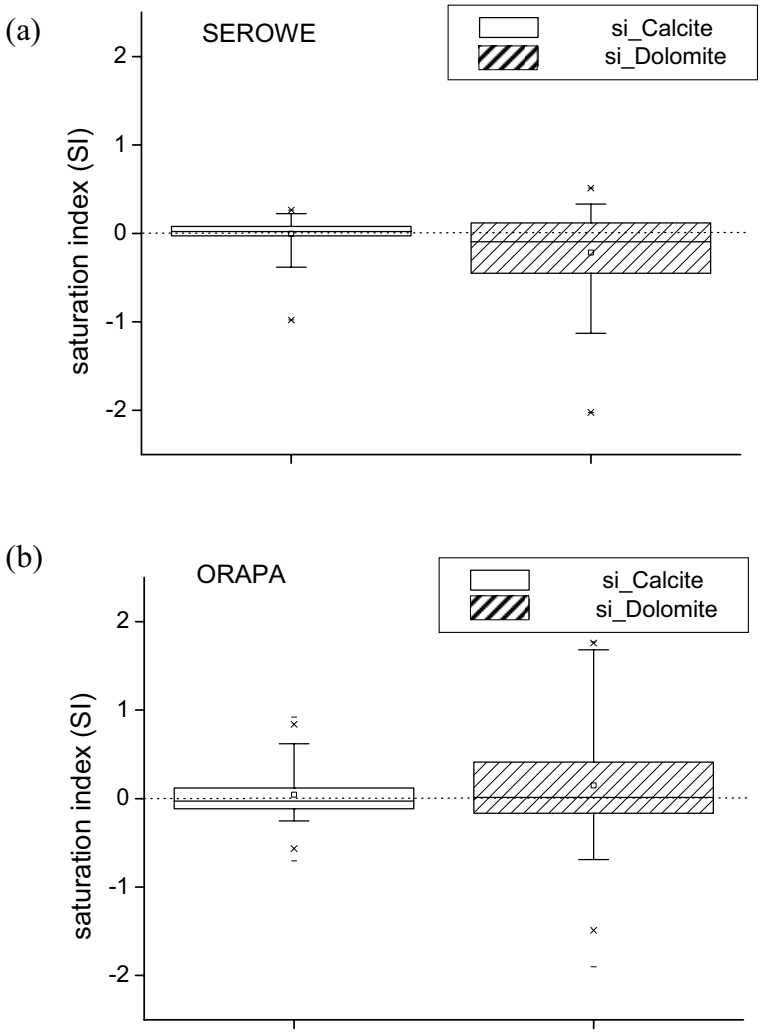

Fig. 5-18: Saturation indices of calcite (left) and dolomite (right) in (a) Serowe (n = 51) and (b) Orapa (n = 60).

Sodium

The **sodium** content of a given groundwater is defined by the availability of Na-bearing minerals, their resistance to weathering as well as to exchange processes (DVWK, 1996), as indicated in the previous subsection. Apart from input by precipitation, weathering of plagioclase is one of the main sources for the release of sodium into the groundwater, in the investigated system most likely during infiltration through the Stormberg Basalt, where feldspars are a common mineral phase, or in the Ntane Sandstone matrix (chapter 5.1). In a closed system, this leads to the formation of kaolinite and montmorillonite (Eq. 5.23).

(5.23) $Na_2Ca(AlSi_2O_6)_4$ (Plagioclase) + 14 H_2O + 4 CO_2
→ $Al_4[(OH)_8Si_4O_{10}]$ (Kaolinite) + 2 Na^+ + Ca^{2+} + 4 H_4SiO_4 + 4 HCO_3^-

If the solubility product of calcite is exceeded, Na-montmorillonite is formed (Eq. 5.24). Otherwise, Ca-montmorillonit is formed, leading to an increase of sodium in solution (DVWK, 1996).

(5.24) 2 $Na_2Ca(AlSi_2O_6)_4$ (Plagioclase) + 18 H_2O + 6 CO_2
→ $Na_2[(Al_4Si_6O_{15})_2(OH)_6]$ (Na-Montmorillonite) + 2 Na^+ + 2 Ca^{2+} + 6 H_4SiO_4 + 6 HCO_3^-

A diffuse inverse trend of sodium versus SiO_2 was found for some of the groundwater samples from Serowe, while the sum of calcium and magnesium correlated relatively well with SiO_2 in those samples (not shown). This implies silicate weathering from calcium-dominated feldspars in the basalt. It also implies that the sodium concentrations derived from basalt weathering stem from exchange processes on clay mineral surfaces rather than from the complete dissolution of Na-feldspars.

The measured increase in sodium from a 3.0 mmol/l in Serowe to greater than 40 mmol/l in Orapa owes to prolonged water-rock interaction along the flow path. In one regional subdivision of the Orapa study area (‘Khwee block’) further major sodium input originates from highly mineralized uprising groundwater from the lower-lying Mosolotsane aquifer, there reaching sodium concentrations of up to 636 mmol/l. The water mixes due to the structural

geological setting with the groundwater of the Ntane sandstone aquifer (next subsection).

Chloride

In general, **chloride** concentrations are lower in Serowe ($\tilde{x}$ = 1.5 mmol/l) than in Orapa ($\tilde{x}$ = 13.2 mmol/l) and follow the above described trend of prolonged water-rock interaction. The significant enrichment most likely owes to a number of processes: Generally, it originates from atmospheric input in form of dry fallout or as solute in precipitation, or from dissolution of evaporites (Külls, 2000). Chloride enrichment by ***evapotranspiration*** is likely to occur in the unsatured zone. Observations from soil water investigations indicate chloride concentrations in the order of several hundred mg/l in the soil solution at depth of 10 to 15 m below the surface (Schwiede, in prep.). These extremely elevated concentrations are higher than anticipated from the investigations of chloride in the groundwater, which averages around 1.7 mmol/l in Serowe. This suggests that either multiple recharge mechanisms transport water into the aquifer (and with it the conservative ion chloride) or that present boundary conditions of recharge are different than those under which the aquifer water was replenished. Else, the mechanisms may not be fully understood yet, as present recharge amounts are very low and infiltration conditions appear to strongly vary locally. Groundwater evaporation along the flow path is not expected to contribute to chloride enrichment in significant amounts, as the unsaturated zone thickness is very high (30 to 100 m). In addition, a possible minor influence of hyperfiltration (reverse osmosis) might be suspected to contribute to the tremendous increase of chloride along the flow path. It occurs when groundwater due to a hydraulic gradient flows across a clay layer, that may act as a semi-permeable membrane. Owing to their negative surface charge ions like chloride might be retained, increasing salinity on the inflow side (e.g. Post, 2004).

As already implied in subchapter ‘sodium’, one part of the Orapa study area around the ‘Khwee block’ exhibits exceptionally high electric conductivities, mainly dominated by sodium and chloride. The high concentrations are most likely a result of two processes: i) accumulation of dissolved solids along the flow path from Serowe over a time range of several thousand years, considering the matrix flow velocity in the order of few centimeters per year (chapter 3.5.2 and 6.1). And ii) the influence of the lower lying Mosolotsane Aquifer. The Mosolotsane Aquifer is dominated by mudstones and exhibits lower

transmissivities than Ntane lithology. Water from this aquifer is older and has developed into a Na-Cl type. Due to the fact that the Khwee block is highly structurally influenced, the hydraulic connection between the Mosolotsane and Ntane Sandstone Aquifer or their fracture systems, respectively, is facilitated. In addition, some boreholes in the Khwee block were observed where the Ntane Sandstone was absent. There, groundwater was of a distinct Na-Cl type (e.g. Z7157). In surrounding boreholes mixing is expected.

In the investigation area, additional input is likely from Cl-salts from minor salt pans in the area, and locally from the contamination by manure. Coupled with rapid downward transport either through direct well contamination or along fractures this is especially prominent near Letlhakane. This, however, mainly impacts on the perched aquifers in the Kalahari Beds and has no immediate influence on the groundwater from the Ntane Sandstone Aquifer (next subsection). Only a diluted signal may be found when water from the perched aquifers mixes with Ntane groundwater.

Regional deviations and mixing

Though ***mixing*** is implied from isotope hydrological investigations (chapter 7.2), groundwater samples from spatial sampling in Serowe seem to form a hydrochemically homogeneous group and only show an evolutionary trend from Ca-HCO_3 to Na-HCO_3 type waters as depicted from piper diagrams in Fig. 5-6 and Fig. 5-7. In the hydrochemically quite homogeneous groundwaters in Serowe a hydrochemical development cannot be easily distinguished from mixing processes as it could – if occurring - be 'masked' plotting in the piper diagram along the Ca-Na evolutionary trend. Groundwater in study area 2 (Orapa), however, shows signs of mixing in some areas. Exceptions from the described general trends of water development from Ca-HCO_3 to Na-Cl along the flow path can be found in wellfield 6 especially in the vicinity of Letlhakane River and in Wellfield 4 where local shallow groundwater occurrences have been observed (***perched aquifers***). The main composition of groundwaters from sampled shallow aquifers in Letlhakane is given in the following table (Tab. 5-7):

Tab. 5-7: Main constituents of groundwater from perched aquifers in the Kalahari Beds.

BH-ID*	EC (µS/cm)	pH	T(°C)	DO (mg/l)
SE9	5540	6.67	24.3	1.63
HDW4	156	7.52	22.9	2.34
HDW6-1	282	7.2	23.4	0.44
HDW6-3	4740	7.42	27.1	4.23
BH-ID*	**K^+ (mg/l)**	**Na^+ (mg/l)**	**Mg^{2+} (mg/l)**	**Ca^{2+} (mg/l)**
SE9	4.1	562	181	344
HDW4	3.6	3.9	3	19.5
HDW6-1	9.4	14	6.5	31.8
HDW6-3	5.8	584	119	238
BH-ID*	**HCO_3^- (mg/l)**	**Cl^- (mg/l)**	**SO_4^{2-} (mg/l)**	**NO_3^- (mg/l)**
SE9	431	1493	112	244
HDW4	79.4	4.6	3.4	0.1
HDW6-1	161	7	3	0.8
HDW6-3	590	1227	108	84

*BH-ID = borehole ID

It can be seen that the water chemistry of those samples is quite heterogeneous though two groups can be formed from the shown samples: group 1 groundwaters (SE9 and HDW6-3) are high EC Na-(Ca-)Cl waters around 5000 µS/cm with elevated nitrate and sulfate contents, while group 2 groundwaters (HDW 4 and HDW6-1) have very low specific electric conductivities of less than 300 µS/cm and are of a Ca-HCO_3 type. These two groups reflect quite well the main processes occurring in perched aquifers: group 1 appears to be influenced by surficial contamination which is especially marked by elevated nitrate, chloride and sulfate contents. These hand-dug wells are poorly protected as they represent approximately 1 x 1 m wide and about 7 to 11 m deep open shafts that are only provisionally covered that are thus very vulnerable to contamination. Group 2 also appears to be influenced by direct inflow. In this case, however, rain water directly entered the well, which is especially reflected in the very low electric conductivities and the Ca-HCO_3 type water. It was observed that processes seen from the two groups can occur subsequently in one borehole depending on the sampling time before or after a rainfall event. In one case a groundwater sample was taken at the same well (HDW-3)

during a rainfall event and two weeks later. The first sample yielded nitrate concentrations below the detection limit while a nitrate concentration of nearly 80 mg/l was measured in the second sample, apparently resulting from pollution. A possible reason for this sharp increase is the infiltration of animal manure or urea into the well, favored by the shallow water table. However, ammonium in the two samples was below the detection limit, indicating that - if infiltrated - it had already been oxidized to nitrate. If present, ammonium is an indicator of fresh contamination of the water by animal excreta. The infiltration process may as well occur in areas without shallow aquifers but cannot be seen as the chemical response in the groundwater is heavily delayed, owing to the long infiltration time through the thick unsaturated zone which is common in the study area. The shallow groundwater occurrences in wellfield 6 (WF6) near Letlhakane River and in wellfield 4 (WF4) probably locally influence groundwater along the flow path, resulting in a mixture between the two, possibly creating a Na-HCO_3 water type which is observed near Letlhakane River beside a Ca-HCO_3 type. The degree of mixing depends on the hydraulic connection between these perched aquifers in the Kalahari Beds and the underlying Ntane Sandstone Aquifer. Near Letlhakane River the transmissivity of the overlying Stormberg Basalt is likely to be higher, as the river follows a tectonic weak zone, thus facilitating water flow. Else, it may be possible that all processes described earlier that lead to a development from Ca-HCO_3 type towards Na-Cl water may occur locally and the abstracted sample chemistry depends on the shear location of sampling, but mixing is induced during the abstraction of the groundwater sample. However, the first explanation appears to be more plausible for the study area.

A further distinct deviation from the general water chemistry in Orapa is found in and near the ***Khwee block*** which exhibits extremely high electric conductivities up to 57.5 mS/cm (Z7157). These waters are mainly dominated by sodium and chloride and are strongly influenced by Mosolotsane groundwater. This is discussed in detail in the subsection ‘sodium’ earlier this chapter. It was not possible to sample water that only originated from the Mosolotsane mud- and siltstone layers. However, in some boreholes the Ntane Sandstone Aquifers was very thin, and boreholes penetrated deep into the Mosolotsane layers. The composition of a few exemplary boreholes is given in the following table (Tab. 5-8):

Tab. 5-8: Main constituents of groundwater from the Khwee block.

BH-ID*	EC (µS/cm)	pH	T(°C)	DO (mg/l)
Z7102	4420	10.68	30.7	0.12
Z7152	4720	8.41	31	0.98
Z7101	15640	9.24	29.8	0.1
Z7157	57500	8.84	29.1	0.1
BH-ID*	**K^+ (mg/l)**	**Na^+ (mg/l)**	**Mg^{2+} (mg/l)**	**Ca^{2+} (mg/l)**
Z7102	5.8	886	0.47	1.37
Z7152	14	836	37.4	32.4
Z7101	18.3	3526	9.9	213
Z7157	315	14622	144	461
BH-ID*	**HCO_3^- (mg/l)**	**Cl^- (mg/l)**	**SO_4^{2-} (mg/l)**	**NO_3^- (mg/l)**
Z7102	199	1076	88.5	0.4
Z7152	160	1280	74.6	3.4
Z7101	6.8	4890	1438	0.9
Z7157	47.3	23000	2758	5.1

*BH-ID = borehole ID

The water from the Khwee block generally has a Na-Cl signature of high specific electric conductivities, which coincides with Mosolotsane waters described in the vicinity of the study area (Rahube, 2003). The data sets in Tab. 5-8 also show that the amount of dissolved solids varies quite strongly as reflected by the electric conductivity ranges. Those are mainly governed by sodium, chloride and sulfate concentrations. Observed nitrate concentrations are generally low and remain less than 5 mg/l. This is, however, consistent with the observed reducing conditions. The ranges in specific electric conductivities probably reflect influences by Ntane water in areas where the geologic situation permits mixing. Helium isotopes also reflect that the Khwee groundwaters stem from a different source (chapter 6.2.3.5).

5.2.3.3 Conceptual hydrochemical model

In the conceptual hydrochemical model in Fig. 5-19 the pathway of water from infiltration into the Kalahari Beds through the Stormberg Basalt to replenishment into the Ntane Sandstone Aquifer is described and its fate within the aquifer is conceptually summarized for the study area. Near Serowe a slightly elevated precipitation rate as compared to Orapa enables the water to

be infiltrated into the soil. Together with the water nitrate from rain water enters the soil N cycle. Progressing deeper into the unsaturated zone, the water takes up additional nitrate from the dissolution of mineralized nitrogen (NH_4^+), raising the pH. The pH, is however buffered by HCO_3^- from the dissolution of calcretes in the Kalahari Beds. When passing into the Stormberg Basalt where the first saturated conditions occur in the aquifer no significant denitrification takes place as the basalt has no detectable to very low pyrite contents. The pyrite oxidation (and the presence of microbes) would trigger autotrophic denitrification, as it delivers sulfur (and iron) as a reactant. Once the Ntane Sandstone is reached the water undergoes heterovalent cation exchange of calcium to sodium. The observed water type is Ca-HCO_3 to Na-HCO_3 depending on the degree of exchange. Along the flow path towards Orapa only little additional recharge amounts enter the mostly confined aquifer. Redox conditions become more reducing along the flow path, making slight heterotrophic denitrification possible in the presence of small amounts of dissolved organic carbon. Along with this, a substantial increase in electric conductivity can be observed along the flow path, as the slow groundwater movement renders intense water rock-interaction possible. The Na-HCO_3 water partially develops to or mixes with Na-Cl water. Additional replenishment of the aquifer occurs in Letlhakane from locally existing perched aquifers within the Kalahari Beds. In locations where the latter are coupled with enhanced hydraulic conductivities (and shallow depths to the groundwater) the perched aquifers contribute further Ca-HCO_3 type water and/or chloride, sulfate, nitrate and sodium, depending on degree of pollution of the perched aquifers. The nitrate is partially reduced by DOC. Direct evidence for influence of H_2S and CH_4 in the denitrification has not been quantified, though it is suspected from olfactory observations at individual boreholes.

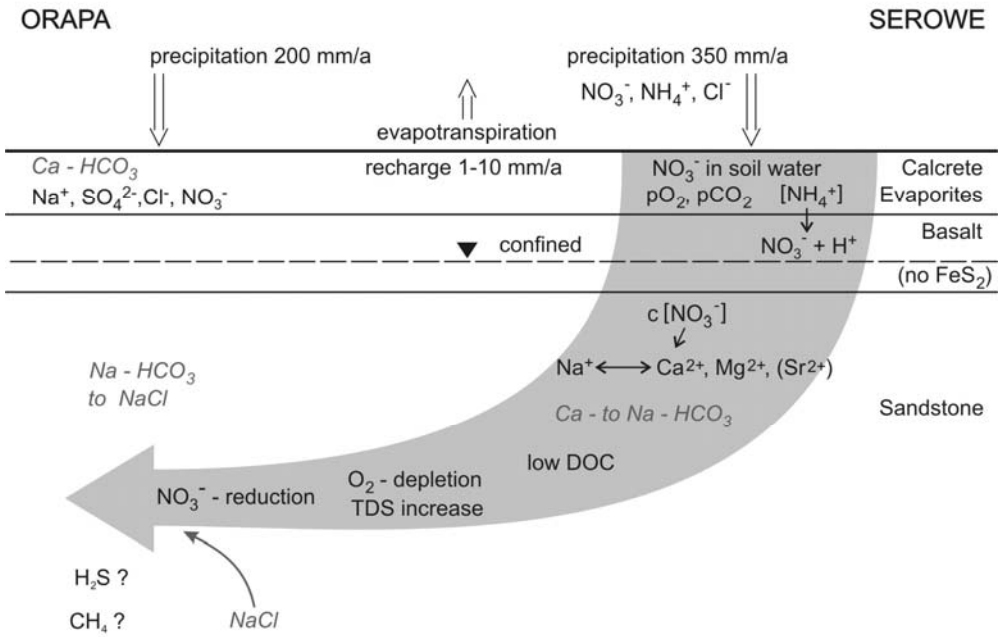

Fig. 5-19: Conceptual hydrochemical model of the chemical evolution of water in the Ntane Sandstone Aquifer between Serowe and Orapa. Question marks indicate processes that are suspected to occur, but where quantitative evidence is lacking.

5.2.4 **Summary and conclusion**

Groundwater in the Ntane Sandstone Aquifer is dominated by a Ca- to Na-HCO_3 character near the recharge area in Serowe and a Na-HCO_3 to Na-Cl type towards the discharge area in Orapa. The Na-HCO_3 signature of the groundwater is a result of heterovalent ion exchange of calcium from calcrete and sandstone matrix dissolution with sodium from plagioclase weathering, which is a dominant process in the aquifer. It can especially be found in groundwater near Serowe. Along the flow path, electric conductivities increase strongly from greater than 0.3 mS/cm to less than 60 mS/cm in Orapa.

High DIC concentrations are observed in the groundwater that result from open system dissolution processes. The system shows median DIC concentrations in the order of 4.3 mmol/l (Serowe) to 7.0 (Orapa) mmol/l that result from equilibrium with CO_2 from soil gas and/or mineral dissolution. The water is saturated with respect to calcite and slightly undersaturated with respect to dolomite.

Though implied from other investigations (chapter 5.3 and chapter 6.2), no indications for mixing were found from spatial sampling in Serowe. In Orapa mixing could be locally identified. There, a distinct Na-Cl type water can be found in the Southwestern part of the investigated area (Khwee block), where waters of the lower-lying Mosolotsane layers coupled with a partial absence of Ntane lithology result in abstracted water of extremely high salinities (EC up to 63.1 mS/cm). A further deviation to the hydrochemical evolutionary trend is found in a subsection of wellfield 4 and in wellfield 6 near Letlhakane River, where local occurrences of perched aquifers in the Kalahari Beds impact on water chemistry by either infiltrating dilute rain water or water contaminated by nitrate, chloride and sulfate.

Throughout the groundwater of both study areas, high nitrate concentrations occur in a spatially scattered pattern, with localized clusters of elevated concentration which cannot be associated with the general flow direction. Nitrate concentrations in Serowe range from less than 5 mg/l to 218 mg/l, with a mean concentration of 22.8 mg/l and a median value at 8.4 mg/l. In Serowe, the Ca-HCO_3 water type is associated with elevated nitrate concentrations of

greater than 30 mg/l up to 218 mg/l while Na-HCO_3 are connected to low nitrate concentrations in the order of 5 to 10 mg/l.

The general 'background' nitrate concentrations are higher in Orapa (median nitrate concentration of 22.8 mg/l) than in Serowe (median concentration of 8.4 mg/l). However, a narrower total range of concentrations was observed in Orapa that lies between 0 and 93.7 mg/l. This may result from the smoothing effect of denitrification, as suggested by the observed reducing redox conditions. It may, however, be the case that nitrate originating from the recharge area in Serowe is fully reduced along the flow path and that the observed concentration pattern is a function of nitrate input from perched aquifers. These aquifers are more common in the Orapa area and have been observed to partially carry elevated nitrate concentrations. In addition, the groundwater table is shallower in Orapa than in Serowe, enabling faster surficial input. A further observation was made in Orapa that supports the above theory: Higher NO_3^- concentrations in Orapa are not found in Ca-HCO_3 waters but rather in groundwaters with a Na-HCO_3Cl signature. This suggests that nitrate enters the aquifer along with chloride and sodium from the surface. Yet, the investigation of ^{15}N- and ^{18}O-NO_3^- suggests that this is not the dominant influence controlling nitrate concentrations (chapter 6.2). Also, mixing of different water types producing the Na-HCO_3Cl groundwaters cannot fully be ruled out, e.g. mixing of the incoming Na-HCO_3 groundwater from Serowe with chloride from the surface or from lower lying layers. A mixing of Ca-HCO_3 waters with Na-Cl type groundwater that could potentially rise from the lower lying Mosolotsane Aquifer seems, however, less probable. Na-HCO_3-Cl waters predominantly occur in oxic environments especially around the area around Letlhakane River where perched aquifers are common. A hydraulic connection to the Mosolotsane layers was not found in these areas. In addition, the Mosolotsane Aquifer carries low to absent nitrate concentrations. The available data does, however, not allow a quantification of water types. Though much higher specific electric conductivities observed in Orapa, nitrate does not necessarily need to be connected to electric conductivities unless dissolved from lithology. As seen from chapter 5.1 this was not the case.

5.3 Identification of vertical redox profiles

5.3.1 Introduction

Fluid logging with a moving multiparameter probe consists of continuous in-situ logging of electric conductivity (EC, µS/cm), temperature (T, °C), dissolved oxygen (DO, %), redox potential (Eh, mV) and pH (-). It was applied to investigate potential vertical stratifications within the Ntane Sandstone Aquifer. The probe was lowered manually at an average speed of 0.1 to 0.2 m/s. A total of 15 probe runs were conducted, 5 of which are exemplarily presented in the following. The runs recorded stagnant profiles in unpumped boreholes. Discussed depths notions are given as meters below the water table unless otherwise stated in the text. An overview of the presented probe runs is given in Tab. 5-9. All of the discussed profiles were recorded within uncased sections of the boreholes ('open hole') unless stated otherwise in the text.

Tab. 5-9: Summary of discussed multiparameter probe runs from October 2003 near Serowe.

BH-ID	Date	Total depth (mbgl)[#]	Logging depth (mbwl)[*]	Rest water level (mbgl)[#]	Bailer depths (mbgl)[#]
BH8475	Oct, 1st 2003	295.0	184.0	102.0	124, 185, 225, 264
BH8480	Oct , 2nd 2003	289.0	191.5	91.9	108, 189, 271
BH8479	Oct , 4th 2003	200.0	113.6	78.4	93, 128, 158, 178
BH8477	Oct , 2nd 2003	317.0	201.4	106.6	133, 185, 228, 283
BH8706	Oct , 6th 2003	248.0	141.3	91.9	107, 162, 270

[#] = meters below ground level [*] = meters below water level

5.3.2 Results and discussion

Most of the boreholes exhibit a distinct vertical stratification for the measured field parameters. Tab. 5-10 lists the median of minimum and maximum field parameter values for Serowe inferred from 15 profiles. Variability ranges of temperature, electric conductivity, pH and Eh for Serowe are summarized in Tab. 5-11. For all boreholes a thermal gradient could be observed over depth with mean temperature increases between 1.5 and 4.5°C/ 100 m. The gradient was generally higher up to a depth between 35 to 60 m. In deeper sections the gradient was shallower. No obvious relation could be found between the temperature gradient and changes in other parameters. Within individual profiles extreme differences in electric conductivity could be observed, with smooth or stepwise changes of electric conductivity. In some profiles multiple vertical zonations of specific electric conductivities could be found, with high values in shallower sections of the profiles, followed by lower values at increasing depth, and again superseded by water of high electric conductivities. Marked changes of pH over depth were found for circum-neutral waters around pH 7 and alkaline waters with pH 9.25 or higher. The strong differences in pH relate to different water types. Circum-neutral waters in Serowe tend to be Ca-(Mg-)HCO_3 waters, while more alkaline waters are Na-HCO_3 types. Significant redox potential changes were observed that generally proved to be in accordance with dissolved oxygen concentrations (DO). The DO data is not summarized in the tables due to frequent stability problems of the oxygen sensor caused by extreme heat, bumpy transport and low air humidity. Within each profile, relative oxygen content differences are, however, useful to support data interpretation and are thus included in the following interpretations of individual borehole logs.

A representative selection of boreholes is described in detail in the following (BH8475, BH8479, BH8480, BH8477, BH8706) that summarizes the types of vertical stratifications found in the Ntane Sandstone Aquifer. Most of the boreholes could be classified into three types according to the sequence of their parameter changes, later referred to as types A, B and C.

Tab. 5-10: Median of minimum and maximum values of physicochemical parameters from 15 profiles near Serowe, Botswana.

		T [°C]	EC [µS/cm]	pH	Eh [mV SHE]
Minimum (P50)	values	25.3	374	7.00	174
Maximum (P50)	values	28.4	733	9.25	322

Tab. 5-11: Summary of the vertical heterogeneities of T, EC, pH and redox potential derived from 15 profiles in open holes near Serowe, Botswana.

	T_{max} - T_{min}	EC_{max} - EC_{min}	pH_{max} - pH_{min}	Eh_{max} - Eh_{min}
Minimum vertical variability	1.86°C	116 µS/cm	0.28	74 mV SHE
Maximum vertical variability	3.95°C	1026 µS/cm	4.60	447 mV SHE

Borehole BH8475

A decrease of temperature gradient is observed at 55 m below the water table, which marks the boundary between basalt and sandstone in the investigated profile (Fig. 5-20a). A further subtle decrease in temperature gradient is observed at 120 m. Both gradients are as well reflected in the electric conductivities (EC), where a small EC decrease can be observed at 55 m that subsequently stabilizes, but drops sharply as of 90 m below the water table. Minimum conductivities of 450 µS/cm prevail for only few meters just below 120 m, followed by a strong increase to greater than 650 µS/cm can be observed. At the point of lowest EC at 120 m a strong negative gradient in dissolved oxygen (DO) is observed, reducing DO from greater than 60 % towards 0 %. A slightly less abrupt, but obvious change in pH from 7.5 to 8.7 is seen at the same depth as the oxygen depletion. The rise in pH is accompanied by a drop in redox potential (Eh) from 360 to 280 mV. Groundwater chemistry of bailer samples (Fig. 5-20b) reflects the same trends. Samples at 22 m and 83 m below the water table show a dominance of Ca-(Mg-)HCO_3, while in samples at

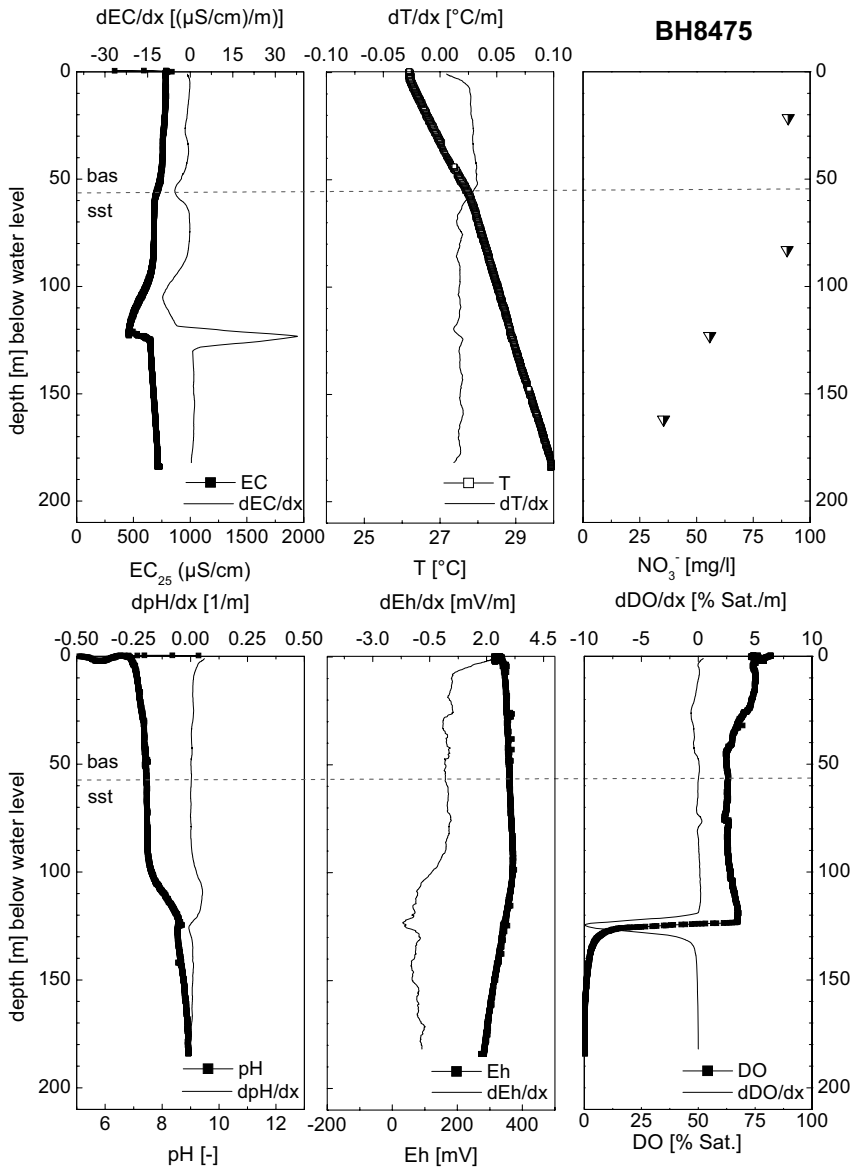

Fig. 5-20a: Multiparameter logging profile for BH8475. Measured values of temperature (T), electric conductivity (EC), dissolved oxygen (DO), pH, redox potential (Eh) and nitrate, and calculated gradients.

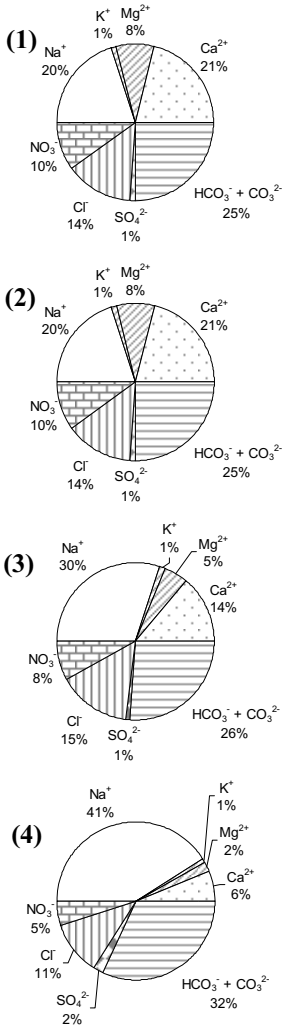

Fig. 5-20b: Groundwater chemistry of BH8475 obtained from selected depths. (1) 22 m, (2) 83 m, (3) 123 m, (4) 162 m below the water table, on the basis of percentage of total mmol(eq)/l.

123 m and 162 m increased sodium contents are found. Bicarbonate is highest in the sample at 162 m. In addition, the relative contents of chloride decrease. Along with these results, higher nitrate concentrations are found in shallower samples that reflect the Ca-(Mg-) HCO_3 type. The observed values of 90.4 mg/l nitrate in the shallowest sample, and 35.3 mg/l in the deepest sample, are however, quite high in comparison to median nitrate values of 8.4 mg/l observed from spatial sampling. Water strikes recorded during drilling indicate that a water inflow occurred at 57 and 98 m below the present groundwater table. Water inflow at 57 m reflects the confined nature of the Ntane Aquifer, where the first water is encountered at the basalt/Ntane Sandstone interface. The second water strike may explain the very subtle temperature and gradient in specific electric conductivity around 90 to 100 m below the groundwater level, marking localized inflow of water at a potential fracture zone or otherwise enhanced hydraulic conductivity within a limited section of the aquifer. This type of profile is referred to as *type A*.

Borehole BH8480

Borehole BH8480 (Fig. 5-21a) shows a change in temperature gradient at 54 m. A concurrent change in EC and slight changes in DO can be observed. This coincides with a transition of lithology from basalt to the sandstone aquifer at 54 m below the water table, and a water strike recorded during the drilling of the borehole. Another change in EC-gradient is observed at 85 m below the water table with a concurrent sharp rise in pH from 7.6 towards alkaline conditions around pH 8.8

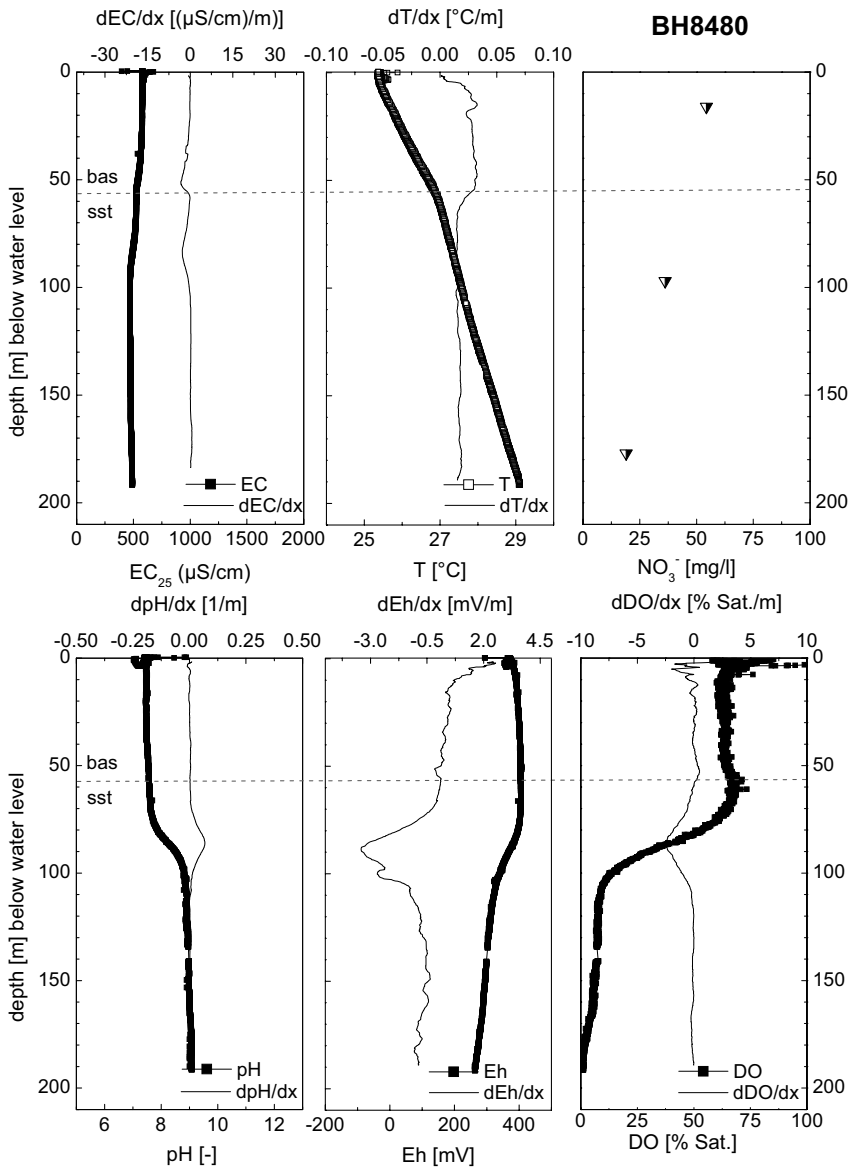

Fig. 5-21a: Multiparameter logging profile for BH8480. Measured values of temperature (T), electric conductivity (EC), dissolved oxygen (DO), pH, redox potential (Eh) and nitrate, and calculated gradients.

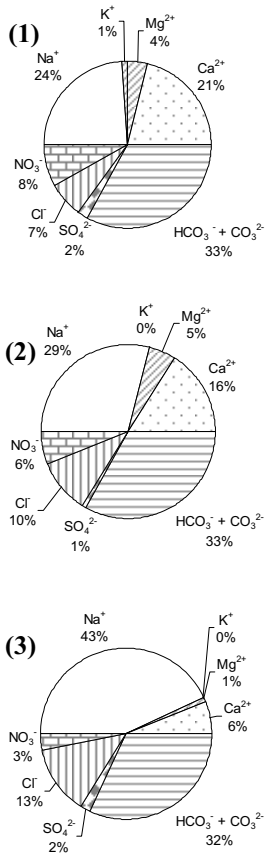

Fig. 5-21b: Groundwater chemistry of BH8480 obtained from bailer samples taken from selected depths: (1) 16 m, (2) 97 m, (3) 177 m below the water table, on the basis of percentage of total mmol(eq)/l.

This is accompanied by a change towards fully reducing conditions and a decrease in Eh. The zone between 54 and 85 m is interpreted as a wide hydrochemical transition zone between basalt and sandstone, where the upper part of the sandstone is more permeable and fissured and thus still receives more influence by waters from the basalt than the underlying sandstone. A differentiation into a lower and an upper Ntane member that have different hydraulic conductivities has also been suggested in a study by Mazor et al. (1977). This suggests that the physical heterogeneity of the aquifer induces a heterogeneous hydrochemistry. Although all boreholes are sealed, it cannot be fully ruled out that the redox potential within the borehole differs from the one in the aquifer, as e.g. surface water inflow or air contact may change conditions. The water chemistry of bailer samples shows concurrent changes over depth. For the sample from the shallowest depth at 16 m below the water table a slight dominance of the sum of calcium and magnesium over sodium can be observed. This trend changes into a dominance of sodium with 29 % in the intermediate sample at 97 m below the water table, and 43 % in the deepest sampling depth at the expense of calcium. In addition, an increase in chloride is observed towards deeper depths, though the water type remains a bicarbonate type at the same relative contribution of 32 % of the sum of HCO_3^- and CO_3^{2-} in all sampled depths. Nitrate concentrations in this profile are relatively high with 54.5 mg/l in the shallowest depth, and 19 mg/l in the deepest depth. High nitrate concentrations again coincide with higher calcium content. The described profile follows

processes analogous to the *type A* classification that was inferred from BH8475.

Borehole 8479

Measurements for borehole BH8479 (Fig. 5-22a) exhibit a decrease in temperature gradient at 40 m below the water table. This coincides with a change of lithology from basalt to sandstone. At a depth of 70 m a localized change to higher EC is found, rising from 400 to 470 µS/cm. Another marked stepwise increase is found at a depth of 100 m. The temperature and EC changes at 70 m are associated with a drop in pH from strongly alkaline to moderately alkaline conditions and a rise in redox potential. Reducing conditions are clearly present in the upper zones of the aquifer and DO from the surface is depleted at 25 m. Subsequent increases of DO concentrations at 70 m concur with the discussed inflow of higher mineralized groundwater. It contains residual DO concentrations of approximately 17 %. The sharp gradient points to the strong significance of fractures in the heavily pumped Ntane Sandstone Aquifer in parts of the Serowe study area (chapter 3.5.4 and 6.1). For bailer samples a relatively constant water chemistry is found in samples up to 80 m below the water table. There, the prevailing water type is Na-(Cl-)HCO_3. Only in the sample taken at 100 m below the water table a significant increase in total carbonate to 32 % is observed at the expense of chloride (12 %) as compared to the shallower sampling depth for which around 21 % of the main groundwater constituents is carbonate, and 22 % chloride. This is accompanied by slightly higher values in calcium, magnesium and sulfate at higher depth. In those samples, sodium is still the dominant cation, though it has decreased by 5 %. Within this profile, nitrate contents are quite homogeneous, with an average concentration of 11 mg/l. Groundwater level data recorded during drilling mark the first water strike at the basalt/sandstone interface at 43 m. Further water strikes, though suggested from the hydrochemical profile especially at 70 m were not recorded. However, water strike data are often filed incompletely in the drilling logs. This type of profile is referred to as *type B*.

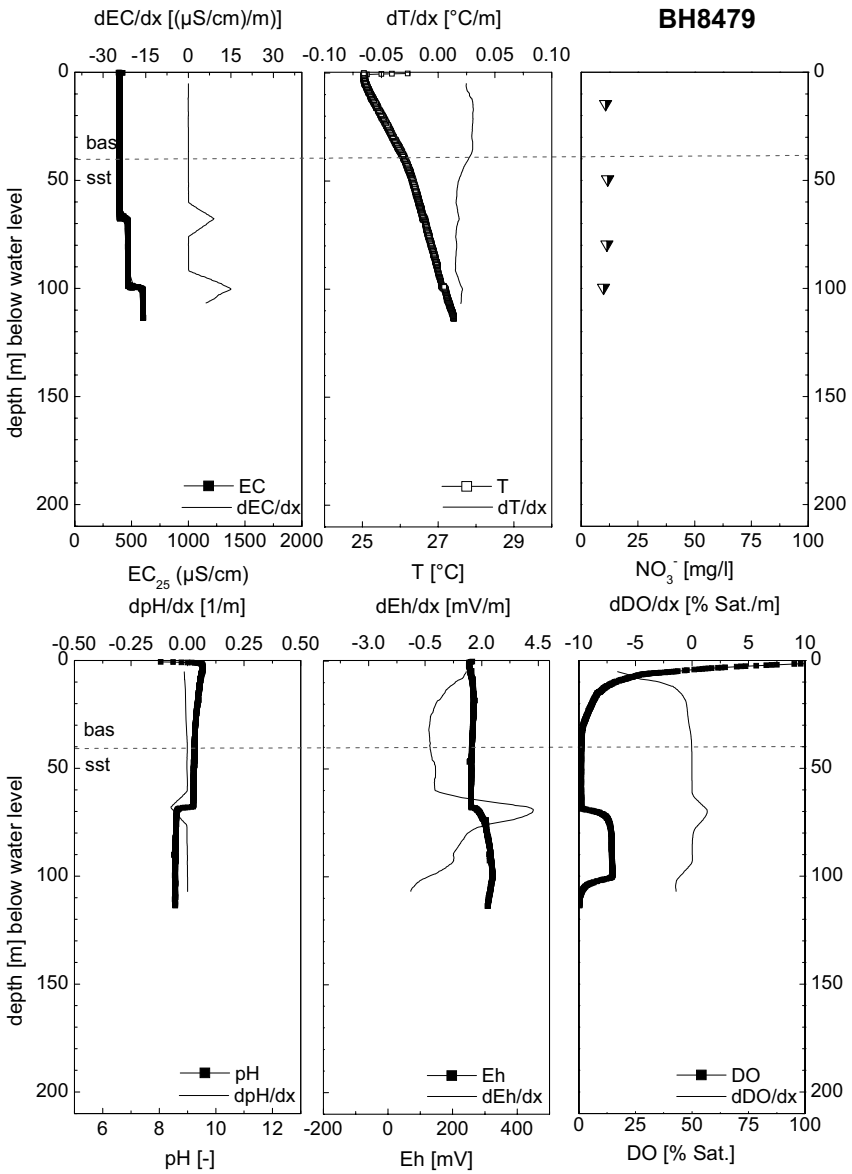

Fig. 5-22a: Multiparameter logging profile for BH8479. Measured values of temperature (T), electric conductivity (EC), dissolved oxygen (DO), pH, redox potential (Eh) and nitrate, and calculated gradients.

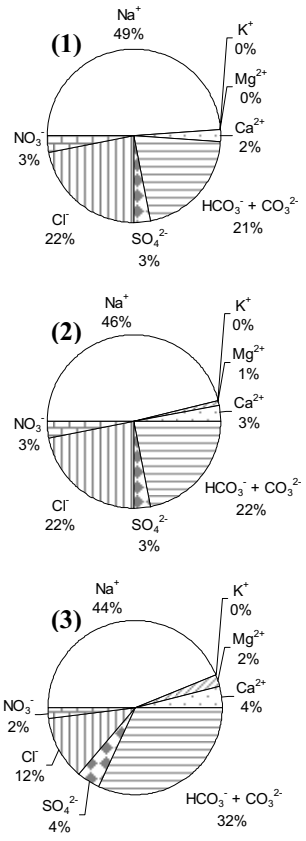

Fig. 5-22b: Groundwater chemistry of BH8479 obtained from selected depths. (1) 50 m, (2) 80 m, (3) 100 m below the water table, on the basis of percentage of total mmol(eq)/l.

Borehole BH8477

Logging profiles for borehole BH8477 show a peak for the temperature gradient at 60 m below the water table, which marks the lithological boundary between basalt and sandstone (Fig. 5-23a). Slightly deeper at 64 m below the present water table a water strike was noted during drilling. Along with the temperature change the electric conductivity abruptly increases from approximately 500 to 580 µS/cm, pH drops from 9.6 to 7.8, Eh rises from 300 to approximately 370 mV, and dissolved oxygen rises from around 20 to 70 %. Further down, all described parameters remain stable up to 95 m. At this depth a stepwise development can be observed similar to the changes at 60 m but with reverse trends back towards surface-near values. Further steps in the parameter profiles are found at 135 m, 155 m and 185 m. The only exception is the specific electric conductivity that as of the marked step at 135 m increases, and the gradual temperature increase over depth, which was, however, expected and confirmed in other profiles. The steplike parameter change at 145 m might be influenced by the water strike that was recorded at 135 m below the present water table. Though this is not described at exactly the same depth it is plausible that potential imprecision in rest water level measurements during drilling yield an inaccurate indication where a water strike occurs, and that the changes that are seen in the shown profile are influence by an inflow of water from a fracture that connects to the borehole at this depth.

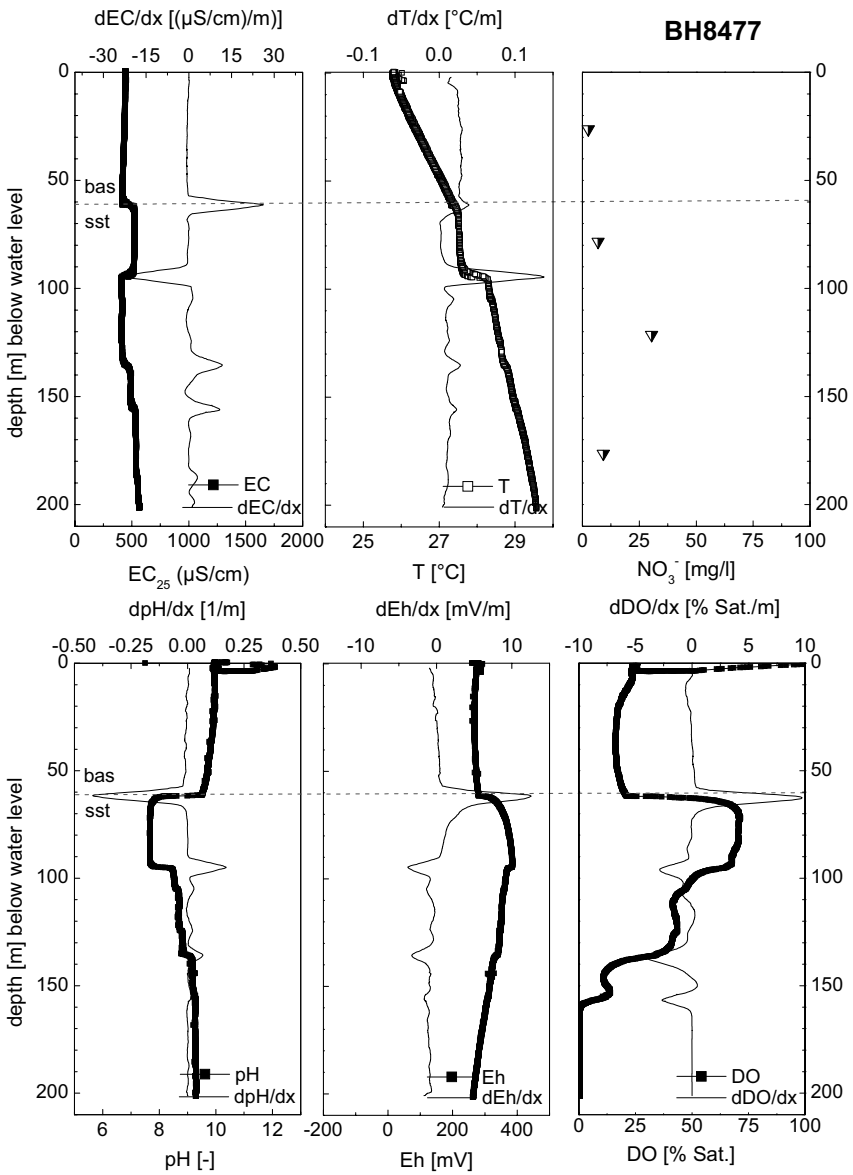

Fig. 5-23a: Multiparameter logging profile for BH8477. Measured values of temperature (T), electric conductivity (EC), dissolved oxygen (DO), pH, redox potential (Eh) and nitrate, and calculated gradients.

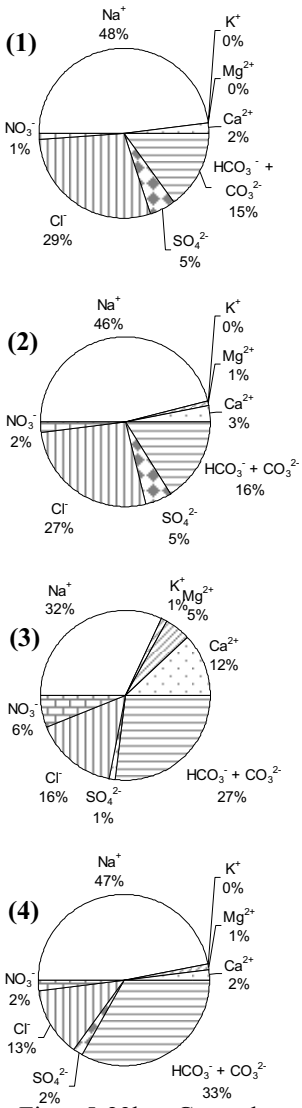

Fig. 5-23b: Groundwater chemistry of BH8477 obtained from selected depths. (1) 26 m, (2) 78 m, (3) 121 m, (4) 176 m below the water table, on the basis of percentage of total mmol(eq)/l.

Detailed lithological logs that include fractures are, however, not available to confirm this. In addition, a simple recording error in the borehole completion certificate cannot be ruled out. Water chemistry results from bailer sampling indicate a Na-Cl type water up to 78 m below the surface. Only in the sample at 121 m does a chemistry change occur were the total carbonat increases strongly from 16 to 27 %, and with it the sum of calcium and magnesium change from around 2 to 4 % to 17 %. This increase happens at the expense of sodium which decreases from greater than 46 to 32 % and chloride, which decreases from around 27 to 16 %. The sample taken at 176 m below the water table has again a similar chemistry to the ones at 26 and 78 m, respectively. However, instead of a Na-Cl type a Na-HCO_3 type water can be observed, as total carbonate increased at the expense of chloride.

Nitrate concentrations in this profile are less than 10 mg/l in all samples but the sample at 121 m below the water table. There, together with an increased calcium content of the water, elevated nitrate concentrations of 30.4 mg/l can be observed, while sodium dominated waters show lower nitrate concentrations. In this profile, individual processes inferred from the interpretation of BH8475 (*type A*) and BH8479 (*type B*) occur in a sequential order, where type B behavior prevails in depths less than 100 m below the water table, and type A behavior can be seen in the water column below a depth of 100 m.

BH8706

In borehole BH8706 a change in temperature gradient can be seen at 58 m. This marks the lithological boundary of basalt and sandstone (a). In this borehole, this also marks the end of a fully cased section, and the beginning of a slotted screen (Louvered), which in the other described boreholes only case off the topmost meters of loose sediments of the Kalahari Beds. Electric conductivities remain quite stable at relatively constant values around 300 µS/cm along the entire profile. The prevalence of only minor changes over depth is also reflected in the anoxic conditions throughout the borehole. pH as well does not change much throughout the profile. The pH value is slightly alkaline at around pH 8 and shows only slight decreases towards the center of the screened section. There, also Eh increases slightly. As opposed to previous profiles, Eh changes occur gradually and less marked. Low Eh matches the observed lack of DO, but the observed Eh rise between approximately 60 and 100 m cannot be reproduced by the presence of additional electron donors, e.g. nitrate. However, impacts of probe instabilities during measurement cannot be ruled out for the investigated profile. Water chemistry observations from bailer sampling indicate a similar chemistry of an Na-(Cl)-HCO_3 type from sampling depths of 15 m, 70 m and 135 m below the water table. Nitrate concentrations are very low and remain less than 0.2 mg/l, which was expected under fully reducing conditions. Borehole BH8706 is an example of a less distinct group referred to as *type C.*

Only subtle parameter changes can be seen over the entire depth of the profile. Water chemistry of the investigated samples may vary from one profile to another but not within one profile, and vertical zonations are hardly encountered. This may be the result of i) the lack of aquifer stratification in the investigated subsite ii) the result of homogenization of the water column through currents in the borehole, iii) a possible influence by the slotted screens or any other cased parts. Alternatively, iv) recorded profiles were not deep enough to reach any reactive or hydraulically influenced part of the boreholes. Some boreholes were more than 50 m deeper than the log length, but could not be fully measured due to mechanical obstacles that threatened to trap the probe. For reason number iv) two classes were introduced for type C: ‘shallow’, which marks logging depth of less than 100 m, and ‘deep’, which marks logging depths greater than 100 m, and which are the more representative boreholes of type C.

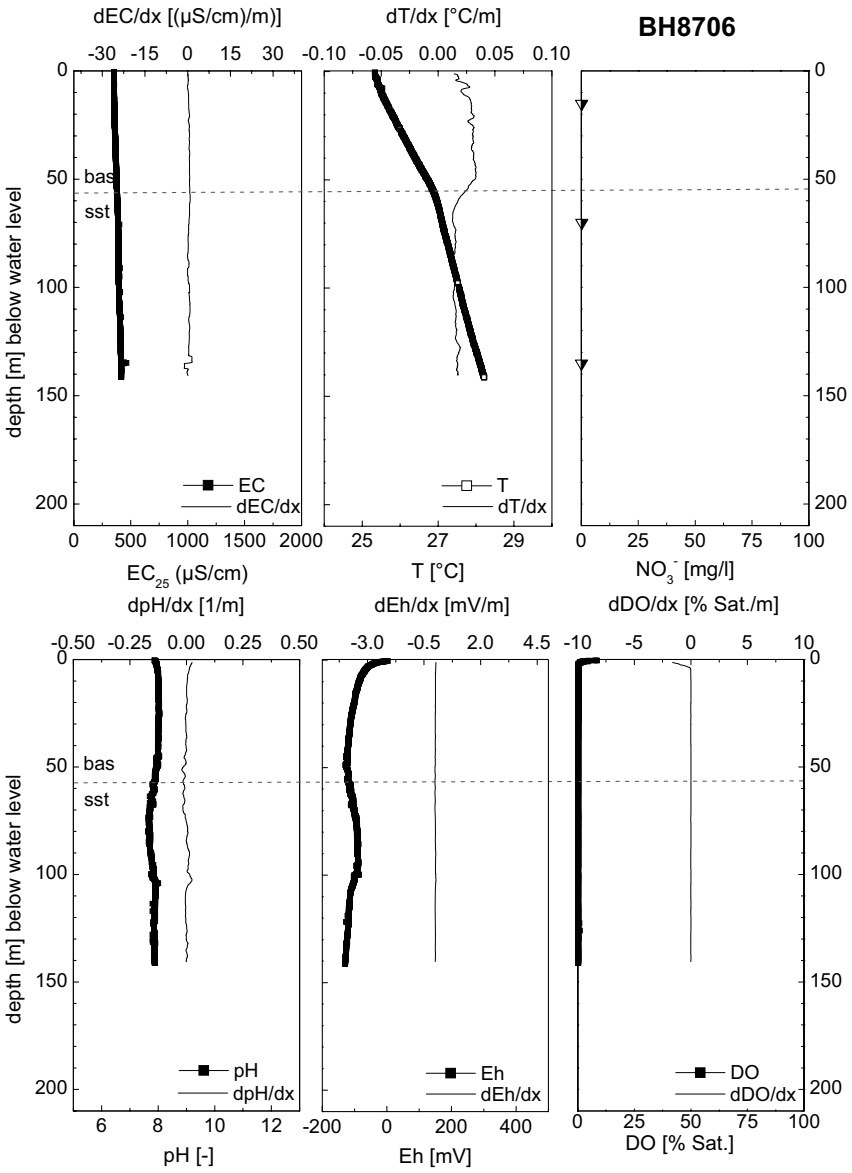

Fig. 5-24a: Multiparameter logging profile for BH8706. Measured values of temperature (T), electric conductivity (EC), dissolved oxygen (DO), pH, redox potential (Eh) and nitrate, and calculated gradients.

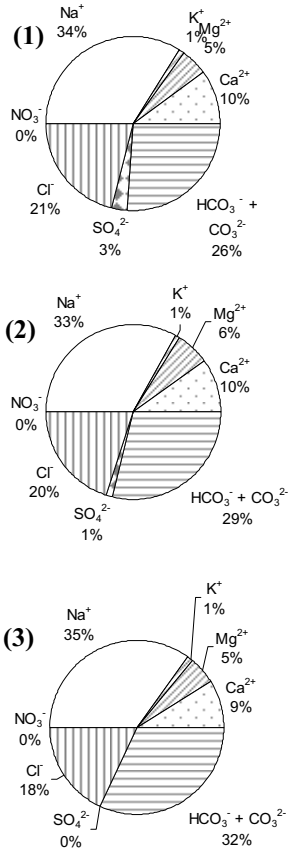

Fig. 5-24b: Groundwater chemistry of BH8706 obtained from bailer samples taken from selected depths (1) 15 m, (2) 70 m, (3) 135 m below the water table, on the basis of percentage of total mmol(eq)/l.

The remaining profiles are not discussed in detail but most of them can be classified into the described types A, B and C. All individual boreholes and their classifications are given in Tab. 5-12. Some boreholes have been ommited in the classification as their signal was too weak or sampling-or logging-induced disturbances occurred (e. g. BH8674^{s}). A regionalization of the classified types proved to be difficult, as several processes may mask the original profile type at the borehole. Masking could e.g. be induced by interference into natural groundwater flow directions through the installation and operation of wellfields. In addition, minor to major structural influences, e.g. fractures that connect boreholes, which are not all mapped in detail may influence the hydraulic system. But in total, a strong impact of aquifer hydraulics, often dominating over reaction processes, can be concluded from the multiparameter logs.

Tab. 5-12: Classification of boreholes according to sequences of field parameter changes.

Borehole ID	Logging depth (m) below surface	Classification type
BH8475, BH8480, BH8471, BH8477 (bottom)	184.0, 191.5, 127.5	A
BH8479, BH8492[s], BH8477 (top)	113.6, 156.8	B
BH8706[s], BH8491, BH8715[s], BH8708[s]	141.2, 105.8, 145.3, 104.6	C, deep (> 100 m below water table)
BH8451, BH8675[s], BH6510[s]	75.5, 91.1, 58.9	C, shallow (< 100 m below water table)

[s]screened (Louvered) sections instead of open hole conditions

5.3.3 Summary and conclusion

For many boreholes a distinct vertical stratification was found (Tab. 5-10, variability of parameters in Tab. 5-11) from multiparameter logging. A common feature of nearly all depth profiles was a relatively steep temperature gradient from the water table to depths between 35 and 60 m, followed by a subsequent shallower gradient. A wide range of values was found in thermal gradients, with values between 1.5 and 4.5 °C/100 m. Strong TDS (total dissolved solids, expressed in EC) variations were found within the same profile. Marked changes in pH with increasing depth were found in circum-neutral waters and alkaline waters. The large differences in pH are associated with Na-HCO_3 waters and Ca-dominated waters. Nitrate concentrations within the profiles appear to be higher in Ca-rich waters than in Na-rich waters. Distinct changes in redox potential were observed, generally in accordance with DO-profiles.

As indicated from the examples, based on multiparameter logs boreholes can be classified into different types. ***Type A*** (e.g. BH8475, BH8480, BH8477 (bottom)) describes results of an exchange process along flow lines that has already been observed from the spatial sampling results (earlier this chapter). A temperature gradient can be observed at the lithological boundary between

the Stormberg Basalt and the Ntane Sandstone. Specific electric conductivities remain relatively stable, though sometimes a decreasing trend can be observed. The pH rises over depth, with a concurrent decrease in redox potential. In general, a decrease of oxygen can be found towards deeper sections of the profiles. The topmost parts are Ca-Mg-dominated, but towards deeper depth sodium is the dominant cation. Throughout the profile, the water is of HCO_3^- type. The relative portion of carbonate may increase over depth.

Type B (e.g. BH8479) comprises profiles that show nearly inverse changes to those described above in type A. An exception is the temperature gradient change in shallow depths, which exhibits the same changes in most of the investigated profiles at depths where lithological boundaries occur. Specific electric conductivities increase gradually or stepwise over depth. At deeper levels pH decreases from alkaline to neutral with a concurrent Eh rise. This may coincide with increasing oxygen although at shallower levels anoxic conditions may prevail. In some profiles of this type, oxygen may however, behave differently. From the water chemistry, a bicarbonate content increase can be observed, leading to a chloride decrease. In addition, sodium may decrease concurring with a slight increase in calcium.

Type C (e.g. BH8706) is a less distinct profile type, where no significant changes occur over depth. Typical for this type is only the above mentioned temperature gradient at the basalt/sandstone boundary, a slight increase of electric conductivity and a relatively stable pH. Eh as well generally remains stable with a slightly decreasing trend in some boreholes. Chemistry varies within this type and depends on the prevailing Eh and pH conditions, but generally remains stable within the same borehole. Alkaline waters tend to be sodium dominated while neutral waters are rather Ca and Mg dominated. Potential disturbances of the water column through water circulation within boreholes, can however not be ruled out. This was especially suspected in boreholes of type C, as a distinctly high number of boreholes of this type had Louvered screened sections instead of ‘open hole’ conditions, and a plain casing that sealed off the basaltic sections of the borehole. Though screened sections generally have a similar length as the open hole sections of other boreholes, hydraulic influences cannot be ruled out. In addition, some boreholes may be influenced by surface inflow into the borehole, though boreholes are generally sealed and are only opened for sampling.

Investigations of boreholes by multiparameter logging, however, provided supportive information to regular groundwater sampling on stratifications within the aquifer. Some stratifications were reactively controlled (e.g. oxygen depletion with increasing depth and concurrent nitrate reduction), while other stratifications provided evidence for mixing processes, e.g. by the local inflow of water of different chemistry into the profile. From regular sampling campaigns it was not possible to distinguish mixing processes from evolutionary trends as both plot along the same trendline from calcium to sodium (e.g. Fig. 5-6). Using multiparameter logs revealed the dominance of mixing and the impact of aquifer hydraulics over reactive processes in the Serowe area. The mixing concept for Serowe is also confirmed from isotope analyses (next chapter).

6 FLOW AND TRANSPORT

6.1 Flow regime

6.1.1 Introduction

Species migration in the subsurface and eventually its distribution pattern is mainly controlled by the movement of the medium it is transported in, i.e. the groundwater flow. The natural flow direction in the study areas and the impacts on the flow pattern induced by groundwater abstraction are presented in this chapter, followed by a conceptual flow model of study area 1 (Serowe).

6.1.2 Regional groundwater flow

Though the study areas Serowe and Orapa represent natural conditions in terms of water chemistry, natural groundwater flow in the two areas is partially disturbed by groundwater abstraction. The two different areas are discussed separately in the following.

Serowe
The general flow is directed from a recharge mound to the East of the study area near Serwe Pan towards the WNW (Fig. 6-1). Groundwater contours at the SE part of the Serowe area follow the topographic gradient of the escarpment rim. A development of wellfields in the SE part of the Serowe study area started in the 1980s and strongly impacts local directions of flow. The abstraction (chapter 3.5.4) leads to decreasing groundwater levels in the order of few millimeters per year (e.g. Maßmann, 2004, SGAB, 1988), and resulted in ceased springs that used to exist at the base of the escarpment rim. Fig. 6-2 shows groundwater contour levels in 1988 which represent only moderately disturbed levels. Fig. 6-1 shows groundwater contours for the same area in 2002 after years of wellfield operation. Values were calculated from own measurements supported by data by DWA, and were interpolated by kriging. The general flow trend remains the same, though the Southern part of the area appears to have experienced deviations in flow direction. In order to identify areas mostly affected by water level and flow direction changes, a groundwater contour difference map was created for the Serowe area (Fig. 6-3).

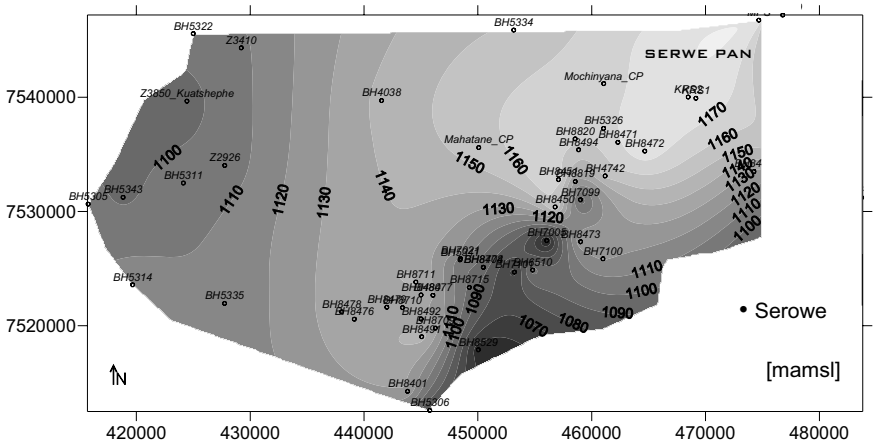

Fig. 6-1: Groundwater contours of Serowe in 2002 after wellfield operation (mamsl). Data was compiled from own measurements and supported by DWA data. Topographic information was derived from SRTM data.

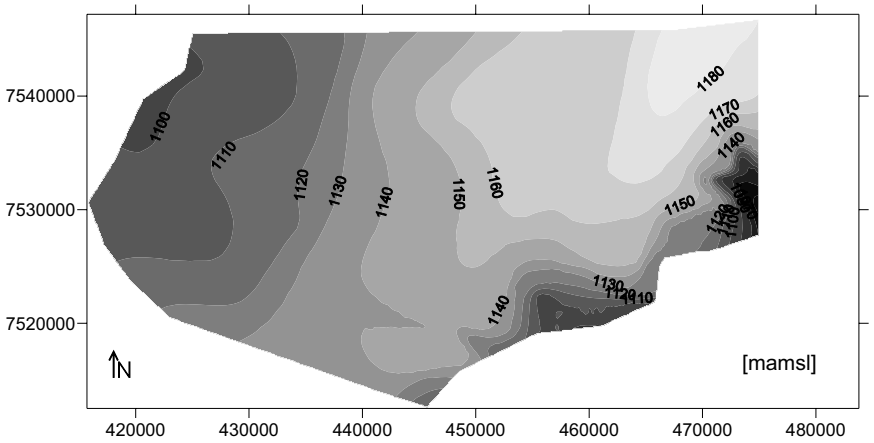

Fig. 6-2: Groundwater contours of Serowe in 1988 as digitized from SGAB (1988) (mamsl). Topographic references are based on geophysical investigations within the 1988 study.

Fig. 6-3 shows the areas that are mostly affected by the wellfield operation (hatched area). A striking feature is the westward shift of the groundwater divide from 1988 to 2002. There, groundwater experienced an inversion of flow direction. This may in turn affect observations in groundwater chemistry in boreholes located between the former and the present groundwater divide, as water is now attracted from different direction than before. If a point source of e.g. nitrate contamination used to be downstream of a defined borehole in this area, it may now be upstream and might affect the quality of the abstracted water. Reliable time series data for water chemistry and water levels to identify long-term water chemistry changes at individual boreholes were, however, not available.

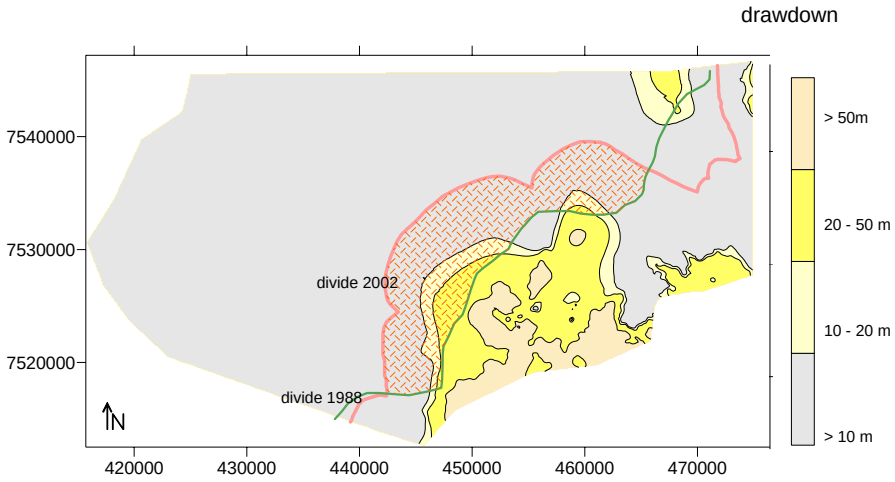

Fig. 6-3: Groundwater contour difference map, comparing 1988 and 2002 values. Note the shift in water divide. Dashed lines indicate potential imprecisions in the position of the divide as to slight variations in topographic reference levels.

Orapa

As discussed in chapter 3.5.5, the Orapa study area generally represents the discharge area of Serowe, and the general flow direction follows Southeast to Northwest. Before anthropogenic influences local disturbance of groundwater flow occurred only by hydraulic barriers (dykes, fracture zones, horst/graben structures) that locally redirect the flow. Increasing mining operations and the

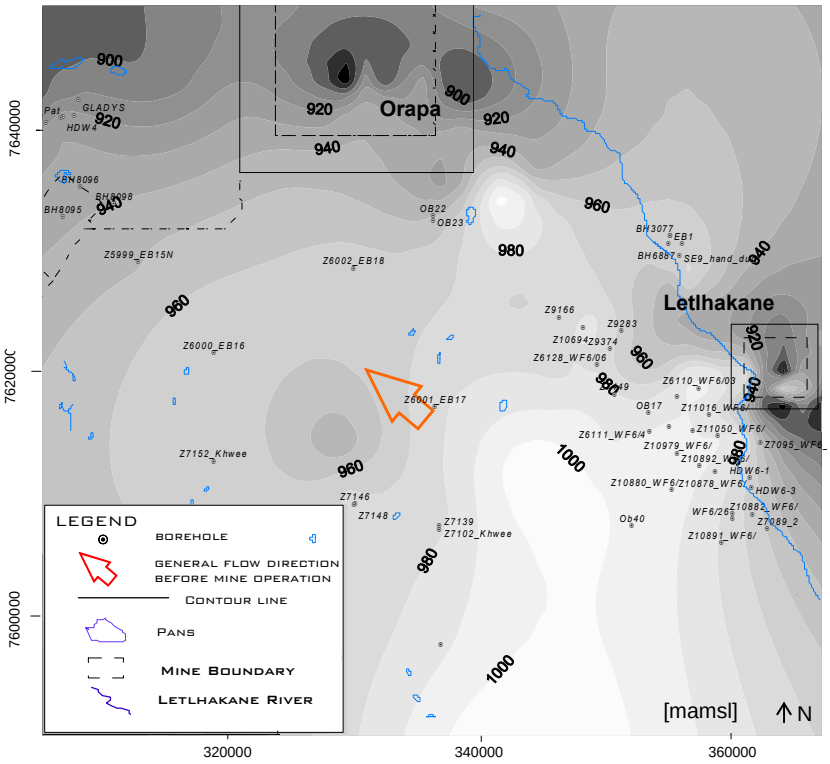

Fig. 6-4: Groundwater contours of Orapa and Letlhakane for the year of 2002 modified after Debswana, 2003. Contour labels are given in meters above mean sea level (mamsl). The arrow indicates the general flow direction before mining operations started in the 1960s. Note that contour lines are based on more boreholes than specified in the map.

growth of the villages and/or towns increased water demand and thus abstraction volumes. Both mines attract contours especially through dewatering activities in the Orapa and Letlhakane diamond mines (Fig. 6-4), and the recently opened Damtshaa mine as well has an increasing impact (not shown). Before mining, the flow direction in the Orapa study area was Southeast to

Northwest in the direction of the Makgadikgadi Pans. Fig. 6-4 shows a map of groundwater levels in the area of 2002 modified from Debswana, 2003. The arrow indicates the former direction of groundwater flow before mining impact. With current abstraction volumes of approximately 13 million m³/a (chapter 3.5.5) the shift in flow direction increased, especially in wellfields and dewatering rings around the open pits, leading to a further drawdown and attraction of the groundwater towards the mines.

6.1.3 Simulated groundwater flow and transport in the fractured aquifer

As flow and transport processes may not always be adequately represented by simple water level measurements in a system strongly affected by faults and dykes, conceptual studies of nitrate movement have been carried out exemplarily for study area 1 (Serowe) using the a finite element (FE) model (FEFLOW, Kolditz et al., 2001). In detail, this is described in an MSc thesis conducted within this project (Maßmann, 2004).

Flow and transport in a fractured porous medium

Flow in fractured porous media is characterized by relatively high flow velocities along the fractures compared to lower velocities within the porous matrix. In contrast, the fracture volume is relatively small compared to the matrix volume and contributes only little to the total aquifer volume. As a consequence, the flow field within fractured aquifers is controlled by a complex interaction between fractures and matrix. In the following the basic equations are briefly described. An extensive overview of the theoretical background can be found in e.g. Sahimi (1995), Bear et al. (1993), and Bear (1972).

Magnitude and direction of the flow velocity v at a given location in the aquifer are determined by the gradient of the hydraulic head h as

$$\vec{v} = -K \cdot \frac{\rho \cdot g}{\eta} \cdot \vec{\nabla} h \qquad (6.1)$$

with ρ as water density, η as water viscosity, and g as acceleration of gravity. For a fracture, the permeability K is given as

$$K = \frac{b^2}{12} \tag{6.2}$$

with *b* as the fracture aperture (Snow, 1965). These expressions are valid for laminar flow only (Reynolds numbers below 10) and do not consider effects caused by the fracture roughness. Inside the porous matrix, K is linked to the hydraulic conductivity k_f of the matrix using

$$k_f = K \cdot \frac{\rho \cdot g}{\eta} \tag{6.3}$$

Inserting Eq. 6.3 into Eq. 6.1 finally yields the expression known as Darcy's law.

Transport of dissolved species in an aquifer is determined by advective and dispersive/diffusive fluxes with changes in concentration *c* given as

$$\frac{\partial c}{\partial t} = -\nabla(\vec{j}_a + \vec{j}_d) + r \tag{6.4}$$

with the advective flux density

$$\vec{j}_a = \vec{v}_a \cdot c \tag{6.5}$$

describing the passive transport of species with the velocity of the fluid. The transport velocity v_a is related to the flow velocity via $\vec{v}_a = \frac{\vec{v}}{n}$ with n as the porosity of the medium.
The dispersive/diffusive flux density

$$\vec{j}_d = -(D_d + D_m) \cdot \vec{\nabla} c \tag{6.6}$$

describes mass fluxes due to either hydrodynamic dispersion (characterized by the dispersion coefficient D_d) or molecular diffusion (characterized by the diffusion coefficient D_m). The term *r* finally includes all sources and sinks caused by reactive processes. Inserting Eq. 6.5 and 6.6 into Eq. 6.4 then leads to the transport equation:

$$\frac{\partial c}{\partial t} = -\nabla\left(\vec{v}_a \cdot c + (D_d + D_m) \cdot \vec{\nabla} c\right) + r \ . \tag{6.7}$$

Flow and transport simulation

A 2-D steady state flow model of a 32 x 56 km area of the Ntane Sandstone Aquifer was simulated using the model package RockFlow (Kolditz et al., 2001), developed by the Institute of Fluid Mechanics and Computer Applications in Civil Engineering, University of Hannover, Germany. This FE model package was able to approximate the non-uniform geometry of the geological formations. Fractures and impermeable dolerite dykes were implemented as discrete 1-D features within a continuous porous medium aquifer. Simulations were performed with varying fracture permeabilites and matrix properties using parameter estimates given by geophysical investigations and pump-testing of boreholes during a previous intense investigation of the study area (Wellfield, 2000). The calibration occurred using a former FE model (Wellfield, 2000) and fitting well abstraction rates. Based on a steady-state flow field, transport of nitrate as a conservative tracer was simulated.

Results

Results showed that the simulated flow pattern was most sensitive to variations of permeabilities, especially to the difference between fracture and matrix permeability. The highest calculated velocities in the matrix are only a fraction of the calculated velocities in the fractures (Fig. 6-5 and Fig. 6-6). Two peaks can be found in the frequency distribution of flow velocities: a mean velocity of 0.06 m/a for the matrix and a mean velocity of 2,000 m/a for the fractures. This shows two processes: a) the rapid advection-dominated transport in fractures as opposed to b) the diffusive-dispersive controlled transport in the matrix. However, fracture property estimates hold many uncertainties and can only provide a tool to understand mechanisms. An exact simulation of the natural processes could not be elaborated as a detailed calibration of the model was not possible due to limitations in real data resolution.

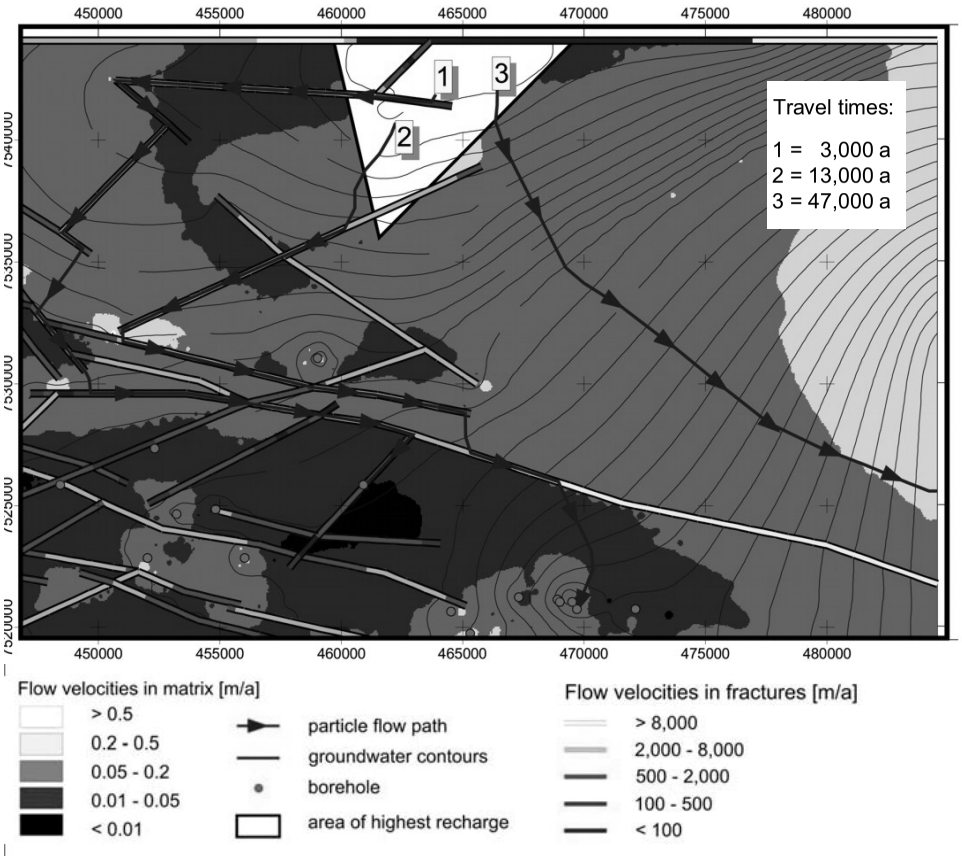

Fig. 6-5: Calculated heads and flow velocities in fractures and matrix in the Serowe study area. Potential flow paths of three inserted particles are shown with included approximate travel times (modified from Maßmann, 2004).

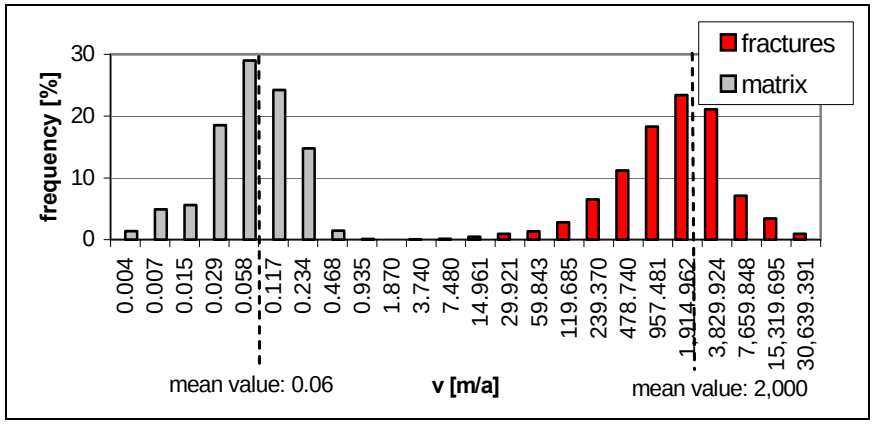

Fig. 6-6: Frequency distribution of flow velocities (v_f) in the Serowe study area taken from Maßmann, 2004.

Fig. 6-5 and Fig. 6-6 show flow velocities and directions of flow as a result of calculated heads. From the calculations approximate ranges of mean residence times of water in the system could be determined. This is exemplarily shown for three partices. They were inserted into the system in the area of highest recharge and terminate at an abstraction well at a boundary. The shown velocities are Darcy velocities (v_f). To obtain the transport velocities (v_a) the values were divided by a mean porosity of 0.07, resulting in a mean matrix v_a in the order of 1 m/a. These values were used in subsequent calculations. Fig. 6-5 shows flow distance and calculated travel times for the three particles. As can be seen from the table, the flow through the matrix strongly dominates the travel time. This in turn results in a broad range of travel times for the same distance. The order of magnitude of the mean residence time of water in the system is thus strongly dependent on the size of the unfractured matrix blocks and the fracture network. With an approximate size of the unfractured blocks between 2 to 20 km (Wellfield, 2000), a mean residence time of 1,000 to 10,000 years can be assumed. These values are in the order of magnitude of residence times observed from isotopic investigations (chapter 6.2).

6.1.4 Summary and conclusion

Regional water flow in the study areas is partially disturbed by anthropogenic activities. In Serowe this occurs by wellfield operation for the village water supply, and in Orapa by water abstraction for diamond mining and concurring dewatering activities. This leads to flow diversions up to local inversions of groundwater flow. To understand the flow pattern in the aquifer it has proven indispensable not only to create simple contour maps from interpolating measured groundwater levels but to include fault and dykes into the considerations. Results from the conducted modeling study reflect the inhomogenous structure of the aquifer, showing flow velocities of 2,000 m/a for the fractures and 0.6 m/a for the matrix, resulting in a broad range of residence times and flow directions. This may eventually account for a very heterogeneous distribution of nitrate: Even in case of an introduction from a relatively localized source nitrate could be spread unevenly in the aquifer owing to the different transport velocities from matrix and fractures at the given site. The same holds true for input through a bigger spatial source. Though the model only represents a conceptual approach it shows well the complexity of flow and transport as influenced by the fractured structure.

6.2 Isotope Hydrology

6.2.1 Introduction

The use of environmental isotopes in hydrogeology offers information on the origin and movement of groundwater and its constituents and can be of use for the evaluation of physical processes, such as evaporation, mixing of different sources, etc. (Geyh, 2000). A short overview of the principle concepts of isotope hydrology is given in the following, while detailed descriptions of applied principles can be found in e.g. Mook (2001), Cook and Herczeg (2000), Kendall and McDonnell (1998) and Clark and Fritz (1997).

The delta value

Due to the very little variation in isotopic abundances, stable isotope ratios are expressed as so-called δ-values in parts per thousand (‰) relative to a standard. The general expression is as follows:

$$\delta_x = \delta_{x-std} = \left[\frac{R_x}{R_{std}} - 1 \right] \cdot 1000 \qquad [‰] \tag{6.8}$$

where R denotes the ratio of the heavy isotope to the lighter isotope in compounds of the sample x and the standard 'std', respectively. Thus, negative δ-values indicate that the sample is depleted in heavy isotopes, positive values mean that it is enriched. Tab. 6-1 shows the internationally used standards that are referred to in this study.

Tab. 6-1: International standards of the isotopic systems oxygen, hydrogen, carbon and nitrogen.

Standard		Element	
V-SMOW	Vienna Standard Mean Ocean Water	O, H	$\delta^{18}O_{H2O}$, $\delta^{18}O_{NO3}$, $\delta^{2}H_{H2O}$
V-PDB	Vienna PeeDee Belemnite, Cretaceous, South Carolina	C	$\delta^{13}C_{DIC}$
Air nitrogen	Air	N	$\delta^{15}N_{N2}$

Isotopic fractionations

Isotopes are partitioned or fractionated by physical or chemical processes as a function of their mass differences (Cook and Herczeg, 2000). During reactions, the heavier isotope generally accumulates in the residual phase, while the lighter isotope tends to leave the system towards the more mobile phase. Kinetic isotope fractionation is usually greater than fractionation related to equilibrium processes and generally occurs in biological reactions. The fractionation can be expressed by the fractionation factor α which is defined as

$$\alpha_{A-B} = R_A / R_B \tag{6.9}$$

where R denotes the ratio of the heavy isotope to the lighter isotope in compounds A and B. An isotope enrichment factor ε can then be defined as

$$\varepsilon_{A-B} = \left(\alpha_{\text{A-B}} - 1\right) \cdot 1000 \tag{6.10}$$

For small values of ε, the difference in isotopic composition between two compounds A and B can be derived as (Kendall and McDonnell, 1998)

$$\varepsilon_{A-B} \approx \delta_A - \delta_B \approx 1000 \ln \alpha_{A-B} \tag{6.11}$$

Rayleigh distillation

The Rayleigh distillation process describes the relationship between the isotopic composition of reservoirs during reaction processes in stable isotopes. In finite reservoirs with a constant enrichment factor α, the isotopic ratios in the product and the reactant change continuously. For zeroth and first order reactions the development of the δ-values of the product and the reactant are described by the Rayleigh distillation equation:

$$R = R_0 \cdot f^{(\alpha - l)} \tag{6.12}$$

where R is the isotope ratio in the reactant, R_0 denotes its initial ratio, and α is the fractionation factor for the reaction ($\alpha_{\text{product-reactant}}$).

Radioactive decay
Radioactive isotopes are unstable owing to the composition of their nucleous and decay according to the following relation:

$$C = C_0 \cdot e^{-\lambda t} = C_0 \cdot e^{-\left(\frac{\ln(2)}{T} \cdot t\right)} \tag{6.13}$$

C_0 is the initial concentration of the radioisotope, C the concentration after time t, λ the decay constant and T=ln(2)/λ is the half-life. If the initial concentration C_0 of the investigated isotope is known, the measured concentration can be used to determine the radiometric age.

6.2.2 Description of applied methods

Of particular interest for the investigation of the fate of nitrate in the Ntane Sandstone Aquifer are the following investigations of isotopes and environmental tracers:

- The stable isotopes oxygen-18 and deuterium
- The transient tracers tritium, chlorofluorocarbons and sulfur hexafluoride
- The carbonate system carbon-13 and carbon-14
- The noble gases helium-3/helium-4 and neon-20/neon-22

Stable isotopes oxygen-18 and deuterium
In hydrology, stable isotopes are often used in recharge investigations and for a genetic distinction of groundwaters. They carry a fingerprint of the meterological processes they were produced in, thus providing information on the origin of the groundwater (Cook and Herczeg, 2000, Clark and Fritz, 1997). Stable isotopes are influenced by a number of factors, such as seasonal, latitude, altitude, continental and amount effects, as is well documented in the literature (e.g. Cook and Herczeg, 2000, Kendall and McDonnell, 1998, Clark and Fritz, 1997).

Meteoric water line
Stable isotope signatures of meteoric waters follow a linear trend, the so-called meteoric water line (MWL) (Craig, 1961). It nearly obeys the following

equation as generally fractionations of oxygen and hydrogen are affected in the same way:

$$\delta^2 H = 8 \cdot \delta^{18} O + d \tag{6.14}$$

d describes the 'deuterium excess' which usually equals 10, with slight regional differences due to fractionation. Stable isotopic ratios may locally represent different meteoric conditions and are described by a local meteoric water line (LMWL). LMWLs have a slight shift in slope and intercept from the global MWL. Deviations from the MWL can be triggered by reactive processes. These can be water/ water-vapor exchange reactions, or water-rock interaction. In the latter case (almost) only oxygen fractionation can be observed, as minerals contain more oxygen than hydrogen.

Tritium

Tritium (^{3}H) forms through interaction of ^{14}N with cosmic ray neutrons in the atmosphere (Craig and Lal, 1961):

$$^{14}\mathrm{N} + \mathrm{n} \rightarrow {}^3\mathrm{H} + {}^{12}\mathrm{C} \tag{6.15}$$

^{3}H has a half-life of 12.3 years (Lucas and Unterweger, 2000). Its activity is measured in TU (tritium units), where 1 TU equals one ^{3}H atom among 10^{18} hydrogen atoms (= 7.1 ^{3}H decays min^{-1} l H_20^{-1}) (Moser and Rauert, 1980). Tritium concentrations in precipitation are influenced by seasonal and continental effects (e.g. Cook and Herczeg, 2000, Kendall and McDonnell, 1998, Clark and Fritz, 1997). The natural, i.e. cosmogenic level of tritium in precipitation is only a few TU and as such would have a limited applicability. However, since nuclear weapon testing in the 1952s to 1961s levels rose to greater than 2000 TU in the Northern Hemisphere and greater than 200 TU in the Southern Hemisphere, which have now been reduced through decay and dilution with ocean water. This input can be used to estimate mean residence times in the hydrosphere. Strong variations in the global distribution of tritium occur due to circulation patterns in the stratosphere and due to the fact that most of the nuclear weapon tests were performed in the Northern Hemisphere, leading to lower ^{3}H concentrations in the Southern Hemisphere. Today's atmospheric background levels in the Northern Hemisphere are between about 5 and 15 TU, and in the Southern Hemisphere in the order of 3 TU (M. Butler,

personal comm.), challenging the use of ^3H as a dating tool in very young groundwaters.

Chlorofluorocarbons (CFC) and sulfur hexafluoride (SF_6)

Chlorofluorocarbons (CFCs) are used in dating young water (less than 50 years). They are anthropogenic tracers with a relatively well-known global input-function. CFCs have a wide range of industrial and refrigerant applications (Rowland, 1990) and were developed in the early 1930s. The production was followed by a release into the atmosphere and an incorporation into the hydrologic cycle (Fig. 6-7).

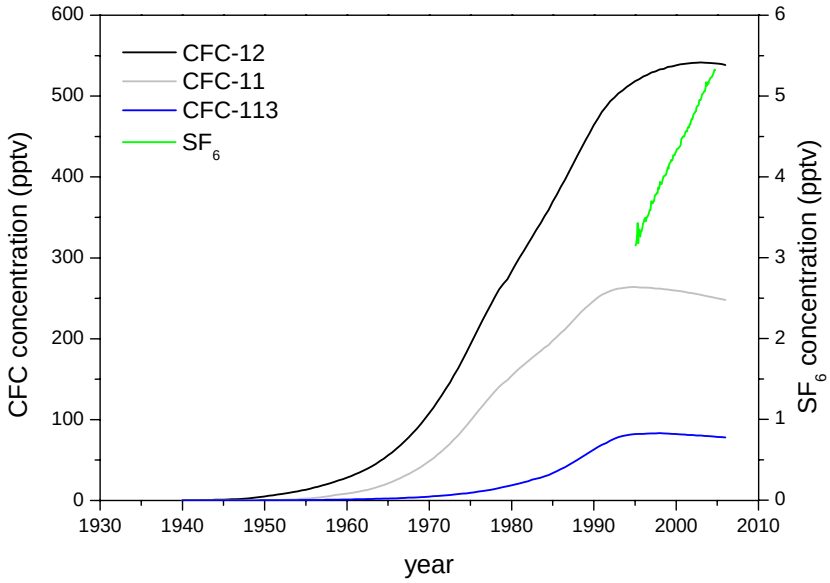

Fig. 6-7: Development of atmospheric concentrations of chlorofluorocarbons (CFCs) and sulfur hexafluoride (SF_6), as compiled from data available at NOAA (2005).

Trichlorofluoromethane CFC-11 (CCl_3F) and dichlorodifluoromethane CFC-12 (CCl_2F_2) were emitted early, whereas trichlorofluoroethane CFC-113 ($C_2Cl_3F_3$) has only been emitted since about thirty years. The only known

sinks in the atmosphere are photocatalytic processes in the stratosphere. A slight concentration decrease can occur under anaerobic conditions in the groundwater (Oster, 1994). Sulfur hexafluoride (SF_6) is predominantly used as isolation gas in high voltage engineering. The atmospheric life-span of this gas is larger than 3000 a, and its atmospheric concentration increases since the 1970s (Cook and Herzceg, 2000).

Carbon-13

Dissolved inorganic carbon (DIC) and ^{13}C evolution in groundwater starts with atmospheric CO_2 at a $\delta^{13}C$ of ~ -7 ‰ V-PDB (Tab. 6-1) and is followed by subsequent depletion during photosynthetic uptake. Photosynthesis fixes carbon which is stored in biomass (here given as CH_2O for simplification) in the soil as

(6.16) $$CO_2 + H_2O \rightarrow O_2 + CH_2O$$

Respiration by bacteria and roots decomposes biomass, much of which, beside producing organic matter, is oxidized to CO_2 that is recycled through photosynthesis.

(6.17) $$O_2 + CH_2O \rightarrow CO_2 + H_2O$$

Infiltrating water dissolves soil $CO_{2(g)}$. Some of it hydrates and dissociates into different DIC species according to Eq. 5.10 to 5.13, with the species distribution being pH dependent. In these processes, the fractionation amount of ^{13}C depends on the photosynthetic cycle that produced the primary organic matter (Fig. 6-8). The Calvin cycle (C_3) results in a mean $\delta^{13}C$ of soil CO_2 of ~ -23.5 ‰, the Hatch-Slack cycle (C_4) in a $\delta^{13}C$ value of ~ -9.6 ‰. The Crassulacean acid metabolism (CAM) yields a mixed signal, as it alternates between the C_3- and the C_4-cycle. C_3-plants dominate in most terrestrial systems (Clark and Fritz, 1997). Yet, plant composition varies as a function of climate, especially relating to humidity and light availability. Trees tend to be C_3-plants, while grass is a C_4-plant.

Depending on the 'openness' of a system, the $\delta^{13}C$ (and DIC) values develop differently as to isotopic exchange with the different reservoirs soil CO_2 and aquifer carbonate (Fig. 6-8).

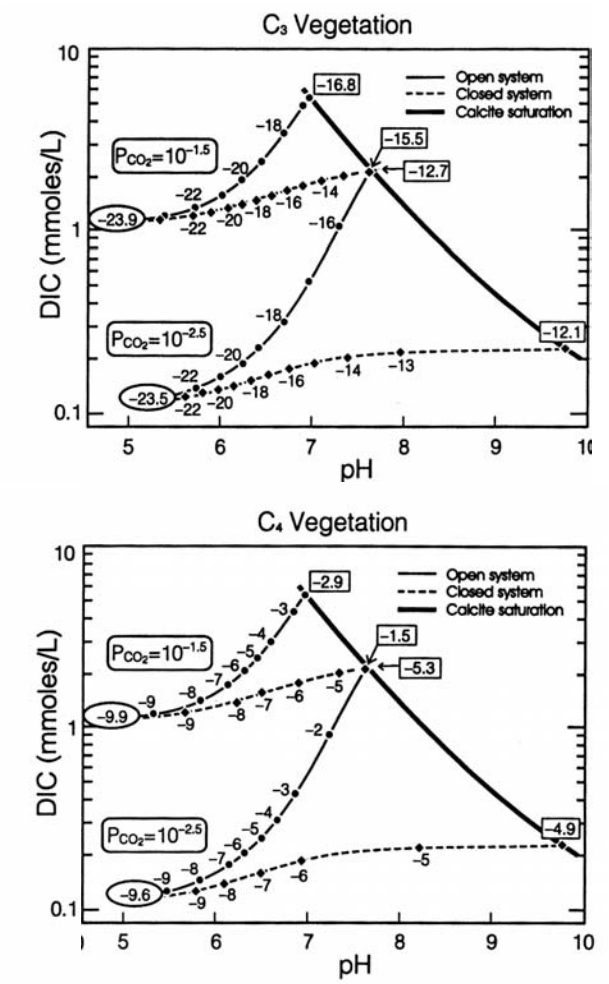

Fig. 6-8: Evolution of DIC and $\delta^{13}C$ in groundwaters as calcite is dissolved to the point of saturation in open and closed systems (Clark and Fritz, 1997). Open conditions maintain a fixed pCO_2 and reflect a continuous exchange with the soil CO_2, resulting in increased DIC amounts and heavier $\delta^{13}C$ signals as to the rise in pH and subsequent rise in fractionation factor ε due to carbonate species transformation. Closed systems reflect decreasing pCO_2 as calcite is dissolved and the $\delta^{13}C$ signal is diluted by that of carbonate.

The isotope fractionation factor ε of ^{13}C is carbonate species dependent (Clark and Fritz, 1997) and impacts on the $\delta^{13}C_{DIC}$ value as to the following relation:

$$\delta^{13}C_{DIC} \cdot m(DIC) = \delta^{13}C_{HCO_3^-} \cdot m(HCO_3^-) + \delta^{13}C_{CO_3^{2-}} \cdot m(CO_3^{2-}) + \delta^{13}C_{CO_2*} \cdot m(CO_2^*) \quad (6.18)$$

where dissolved CO_2 and H_2CO_3 are summarized as CO_2^*, and *m*(DIC) represents molar concentrations of dissolved carbon species.

Carbon-14

Radiocarbon (^{14}C) is produced in the upper atmosphere through collision of a neutron with ^{14}N as to the following reaction:

$$^{14}N(n,p) \Rightarrow ^{14}C \quad (6.19)$$

It enters the atmospheric carbon cycle in form of CO_2. Additional radiocarbon was produced through nuclear weapon testing during 1950s and 60s. The half-life of ^{14}C is 5730 years. Activities are expressed as percent of the reference value 'modern carbon' (activity a_C of ^{14}C related to 1950) abbreviated as '%-mod.'.

In order to calculate groundwater residence times based on ^{14}C data, several problems can be encountered. An overview can be found in e.g. Clark and Fritz (1997), Fontes and Garnier (1979) and Wigley et al. (1978). To obtain the initial ^{14}C activity of the samples, the measured %-mod. value must be corrected for alterations in the subsurface. Only this chemically corrected 'no decay' value is to be inserted into Equation 6.13. Several correction models have been elaborated to account for these effects, which are well documented in the literature (e.g. Clark and Fritz, 1997, Fontes and Garnier, 1979). The applied models are shortly summarized in the following.

The statistical model (Vogel, 1970) represents a simplified approach with an assumed dilution of the ^{14}C signal from decay by a factor q. q denotes the fraction of initial ^{14}C remaining after dilution and is usually between 0.65 and 1, depending on the type of rocks in the aquifer. The regular Pearson and Hanshaw model (e.g. Ingerson and Pearson, 1964) accounts for closed system

processes. It does not include calcite dissolution in the unsaturated zone, i.e. exchange with soil CO_2. As the investigated system is dominated by open system carbonate dissolution as suggested in chapter 5, this model is not suitable for data correction in this study. However, the modified Pearson and Hanshaw model, i.e. $\delta^{13}C$ mixing model (Clark and Fritz, 1997) was applied that describes open and closed system conditions and includes isotope exchange. The q factor is then obtained from an isotope mass balance as follows:

$$q_{\delta^{13}C} = \frac{\delta^{13}C_{DIC} - \delta^{13}C_{carb}}{\delta^{13}C_{rech} - \delta^{13}C_{carb}} \quad \text{with } \delta^{13}C_{rech} = \delta^{13}C_{soil} + \varepsilon_{DIC\text{-}CO2(soil)} \tag{6.20}$$

$\delta^{13}C_{DIC}$ denotes the measured ^{13}C in groundwater, $\delta^{13}C_{soil}$ is the ^{13}C value of the soil CO_2, and $\delta^{13}C_{carb}$ is the one of aquifer carbonate that is dissolved. $\delta^{13}C_{rech}$ is the initial $\delta^{13}C$ value in the infiltrating groundwater, which strongly depends on the pH value during recharge. $\varepsilon_{DIC\text{-}CO2(soil)}$ denotes the enrichment factor between aqueous carbon and soil CO_2. A further model by Fontes and Garnier (1979) appeared to be suitable for the current study as it describes the exchange between the gas reservoir, DIC and carbonate in the unsaturated zone. Assuming that the ^{14}C activity of the matrix carbonate is zero, the dilution factor $q_{F\text{-}G}$ in the Fontes and Garnier model is calculated as

$$q_{F-G} = \frac{mDIC_{meas} - mDIC_{carb} + mDIC_{CO_2-exch}}{mDIC_{meas}} \tag{6.21}$$

where m denotes molar concentrations, DIC_{carb} denotes matrix-derived carbonate defined as

$$mDIC_{carb} = mCa^{2+} + mMg^{2+} - mSO_4^{2-} + 0.5\,(mNa^{+} + mK^{+} - mCl^{-} - mNO_3^{-}). \tag{6.22}$$

This term includes corrections of carbonate contents for evaporite dissolution and cation exchange. It of course assumes an idealized and well-defined chemical composition of the evaporite. $DIC_{CO2\text{-}exch}$ is the matrix-derived DIC that exchanged with the soil CO_2 as described in the following equation:

(6.23) $mDIC_{CO2\text{-}exch} =$

$$\frac{\delta^{13}C_{DIC} \cdot mDIC_{meas} - \delta^{13}C_{carb} \cdot mDIC_{carb} - \delta^{13}C_{soil} \cdot \left(mDIC_{meas} - mDIC_{carb}\right)}{\delta^{13}C_{soil} - \varepsilon^{13}C_{CO_2 - CaCO_3} - \delta^{13}C_{carb}}$$

Here, $\varepsilon^{13}C_{CO2\text{-}CaCO3}$ denotes the isotopic composition difference between CO_2 and $CaCO_3$. As the Fontes and Garnier model does not distinguish between the species distribution of DIC and only differentiates between soil CO_2 and carbonate in its fractionation factor ε, and ε is strongly pH dependent, an application remained problematic.

Noble gases in groundwater

The dissolved concentration of noble gases in groundwater obeys Henry's law and therefore depends on temperature and their concentrations in air (Kendall and McDonnell, 1998). In contact with the atmosphere noble gas concentrations in precipitation equilibrate with noble gas concentrations in air. When water percolates through the unsaturated zone, noble gases reequilibrate with the mean annual temperature at the infiltration site. No further significant changes in concentration occur once they are in the groundwater as non-atmospheric sources of noble gases are usually negligible. The only exception is helium, which is discussed later this chapter. Noble gas concentrations can be used as paleothermometers as solubilities decrease with increasing temperature (e.g. Kipfer et al., 2002).

Helium-4 and Helium-3

The general concept of the ^4He method is that minerals release internally produced helium (He) from the decay of ^{238}U, ^{235}U and ^{232}Th into the groundwater. The longer the groundwater is in contact with the minerals, the higher is its He content. With a quantification of the He release rates and the assumption that external sources of ^4He are negligible e.g. from outside the aquifer, groundwater travel times can be established (Solomon, 2000). The measured total concentration of helium ($^4He_{tot}$) in groundwater consists of the following components (Schlosser et al., 1989):

(6.24) $$^4He_{tot} = {}^4He_{sol} + {}^4He_{rad} + {}^4He_{ea} + {}^4He_{mtl}$$

$^4He_{sol}$:	He from solubility equilibrium with air
$^4He_{rad}$:	radiogenic component of He
$^4He_{ea}$:	excess air component of He
$^4He_{mtl}$:	He mantle component

$^4He_{sol}$ is determined by estimating recharge temperature, elevation and solubility data, $^4He_{mtl}$ is assumed to be negligible. Measuring ***neon (Ne)***, an element without significant sources in the subsurface, determines $^4He_{ea}$. With these factors, $^4He_{rad}$ can be calculated (Weise and Moser, 1987) as to

$$^4He_{rad} = {}^4He_{tot} - {}^4He_{sol} - [Ne_{tot} - Ne_{sol}]\ R_{He/Ne} \quad (6.25)$$

where $R_{He/Ne}$ denotes the He/Ne ratio in the atmosphere and other subscripts equal those of Eq. 6.24.

Further helium in groundwater occurs in form of ^{3}He, expressed as (Sültenfuß and Massmann, 2004):

$$^3He_{tot} = {}^3He_{atm} + {}^3He^* + {}^3He_{nuc} + {}^3He_{mtl} \quad (6.26)$$

The subscript 'atm' denotes He of atmospheric origin, 'mtl' He of mantle origin, 'nuc' He produced by nuclear reactions in the subsurface, primarily by ^{6}Li neutrons produced from spontaneous fission (^{6}Li (n,α) → ^{3}H), and * denotes tritiogenic He. The relative abundance of ^{3}He and ^{4}He is distinct for various terrestrial reservoirs, enabeling it to be used as a tool for investigating the origin and fate of fluids (Cook and Herczeg, 2000).

6.2.3 Results and discussion

6.2.3.1 Isotope hydrological characterization of the investigated groundwaters

In the presented study a number of isotopic investigations have been applied in order to characterize the groundwater flow and transport regime in the Ntane Sandstone Aquifer as well as the recharge regime. For a comprehensive overview, the basic data is summarized in Tab. 11-1 to 11-3 and is discussed

in the following subchapters. Other isotopic data that was used to trace the origin of nitrate (^{18}O- and ^{15}N-NO_3^-) is presented in chapter 7.

6.2.3.2 Deuterium and oxygen-18

All δ^2H and $\delta^{18}O$ values of groundwater sampled from the Ntane Sandstone Aquifer near Serowe lie in a narrow range between -47.4 and -35.1‰, and -6.7 and -5.6 ‰, respectively (Fig. 6-9). The mean value of the δ^2H is -40.9 ‰, that of $\delta^{18}O$ is -6.1 ‰. The groundwater samples taken from Orapa denote a very similar range for δ^2H from -48.4 to -39.1 ‰ and a mean value of 43.4 ‰, and for $\delta^{18}O$ values of -6.8 to -5.9 ‰ (mean: 6.4 ‰) (Tab. 11-1). The values lie within the range observed in previous studies (e.g. Verhagen, 1991). A linear relationship between the different stable isotopes can be found for the samples, which is indicated in form of a regression line in Fig. 6-9. The samples group slightly below (and some samples on) the GMWL and significantly below the only available LMWL defined by precipitation from Lobatse (Selaolo, 1998), a location to the Southeast of the study area.

The displacement below the meteoric water line is likely to be the result of i) partial evaporation from soils and dilution by subsequent recharge as described e.g. in Allison et al. (1983) as a common feature of semi-arid regions. Long residence times of the infiltration water in the top few meters of the soil make it subject to partial evaporation. Water infiltrated in this manner is more enriched in heavy stable isotopes than water that enters the soil by direct infiltration. And/or ii) the observed stable isotope signatures are a result of evaporation already during rainfall through an atmosphere of lower humidity prior to infiltration (Yurtsever and Gat, 1981). With the lack or only little amount of surface runoff in the study area, rain water could be suspected to collect in surface depressions and undergo significant open surface evaporation as suggested by Verhagen (1995), which would show stronger enrichment, especially in $\delta^{18}O$. The latter can, however, not be confirmed from stable isotope data recorded in this study.

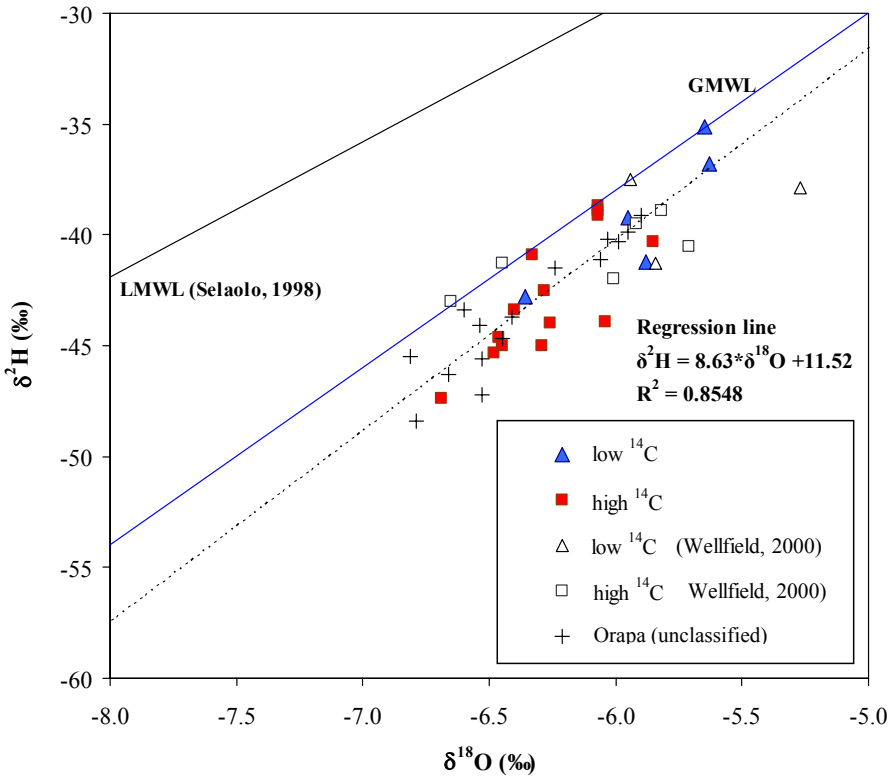

Fig. 6-9: $\delta^{18}O$ - $\delta^{2}H$ diagram of groundwater samples taken in the Serowe and Orapa area. The blue line represents the Global Meteoric Water Line (GMWL), given by $\delta^{2}H = 8 \cdot \delta^{18}O + 10$ ‰ V-SMOW, the black line represents the nearest Local Meteroric Water Line (LMWL) of $\delta^{2}H = 6.1 \cdot \delta^{18}O + 6.9$ ‰ (Selaolo, 1998). Open symbols represent external data from Wellfield (2000). Data from Orapa, where no ^{14}C data is available, have been included and denoted unclassified (cross symbols). The dotted line indicates a regression line of $\delta^{18}O$ - $\delta^{2}H$ from data of the current study. Symbol groups are in accordance with groups inferred from ^{14}C investigations.

The relatively close clustering of the groundwater samples suggests that there is little variation in formation conditions, neither in present nor in paleoclimatic conditions, as also confirmed by stable isotope data in previous studies in the area (e.g. Verhagen, 1992). Only when grouped according to their ^{14}C content slight trends can be observed. ^{14}C data is, however, only available for samples from Serowe as designated in Fig. 6-9. The bulk of ^{14}C rich groundwaters from the present study show a greater depletion in ^{18}O and ^{2}H relative to the groundwaters poorer in ^{14}C (Fig. 6-9 and Fig. 6-10). Given different recharge conditions as suggested by own ^{14}C and noble gas data (later this chapter) and in the literature (Verhagen, 1992, DeVries, 1984), the samples were expected to show a temperature effect, where waters replenished under warmer conditions would be enriched in heavy isotopes as opposed to those formed during colder and probably wetter periods. The earlier would be representing present semi-arid conditions (^{14}C rich samples), while the latter would represent water formed during pluvial phases (as assumed for ^{14}C poor samples). The last major pluvial phase was at the end of the Pleistocene, were noble gas studies have shown that temperatures were lower (e.g. Stute and Talma, 1997), followed by shorter periods of increased humidity (chapter 3.2.3) within generally dry conditions. However, a potential temperature effect, if present, appears to be covered by an extensive amount effect: Evaporation causes a greater enrichment in heavy isotopes in precipitation of small rainfall events than in large rainfall events (Dansgaard, 1964). This appears to dominate any temperature dependent evolution. Groundwater generally exhibits the ^{18}O signal of the mean annual precipitation. A comparison of own groundwater data with precipitation data (mean values in the order of -2 to -4 ‰, Selaolo, 1998) confirms the amount effect and shows that only high-intensity rainfall events replenish the aquifer. In addition, given the anticipated difference in temperature of 5°C between the Holocene and the Pleistocene as established by noble gas studies (Kulongowski et al., 2002, Stute and Talma, 1997), a 2 ‰ shift of the $\delta^{18}O$ values (Kipfer et al., 2002) would be observed. In contrast, Botswana rain waters were recorded to show amount effects of 5 to 7 ‰ (Selaolo, 1998), thus dominating the earlier effect.

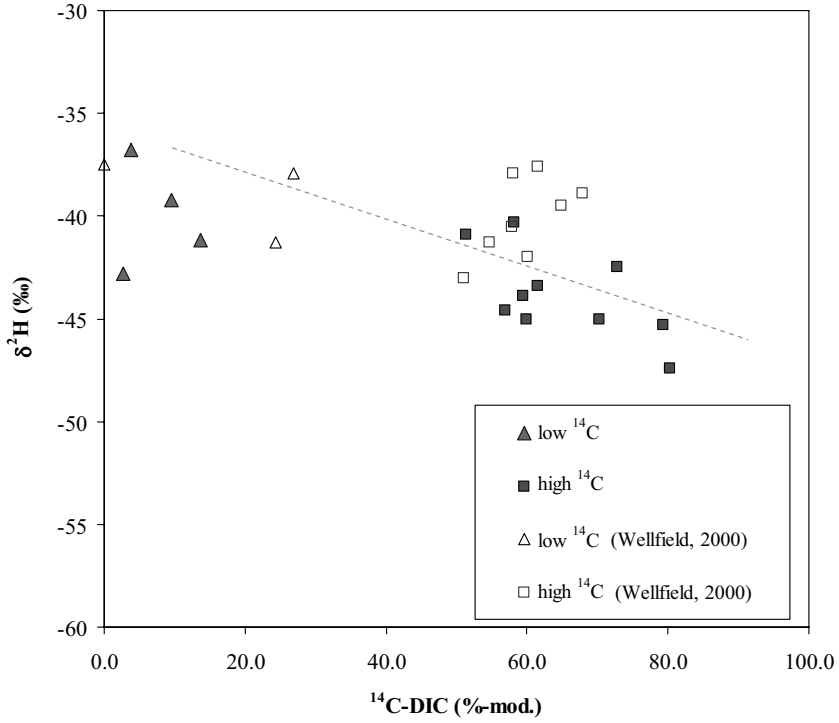

Fig. 6-10: Relations of ^{14}C content to δ^2H, indicating a greater enrichment in δ^2H for samples poorer in ^{14}C - especially in data recorded in this study. A poorer correlation of data from Wellfield (2000) was found. Symbol groups are in accordance with groups inferred from ^{14}C investigations.

6.2.3.3 The transient tracers tritium, chlorofluorocarbons and sulfur hexafluoride

All groundwater samples from the Ntane Sandstone Aquifer near Serowe and Orapa were practically tritium-free. Tritium contents of the samples were measured using two different methods owing to the different detection limits reached: liquid scintillation counting and ^3He-ingrowth (chapter 4.4.2). Using

the liquid scintillation counting method, the analysis of the first sampling set yielded tritium values less than the detection limit of 0.3 TU for all samples (Fig. 6-11 and Tab. 11-1). In order to verify the absence of tritium, the next sampling set was analyzed with the ^{3}He-ingrowth method that provided for a detection limit of 0.01 TU and a typical error of ± 3%. Two of the four samples of low detection limit from Serowe showed a very weak detectable signal (BH 7591: 0.009 ± 0.005 TU, BH 8673: 0.007 ± 0.005 TU). In Orapa, most of the samples lie slightly above the detection limit (Tab. 11-1). The very weak tritium signals indicate minimum travel times of the water of greater than 50 years, including transport in the unsaturated and the saturated zone (Zoellmann et al., 2001), since tritium reflects the time of the separation of the water molecule from the atmosphere. Most likely the tritium content of precipitation was much higher at the time of infiltration due to the long travel time of infiltration water through the thick unsaturated zone, which further reduces the percentage of young water. Considering the tritium content of current precipitation of 3 TU (M. Butler, personal comm.), the maximum percentage of young water in the investigated system would be in the order of less than 0.2 %, assuming that the modern component has a current atmospheric composition.

From tritium data alone one cannot distinguish between two processes: i) piston flow and increasing age of water during transport, leading to a decay of tritium, i.e. slow diffuse spatial recharge, or ii) mixing between a tritium-free (older than 50 years) component and localized recharge through preferential flow with then-atmospheric tritium content. As seen in Beekman et al. (1999) and Selaolo (1998) tritium contents generally decrease with increasing depth in the unsaturated zone, though some deep peaks occur that the authors attribute to preferential flow. The decrease of tritium through decay in the unsaturated zone is also supported by noble gas investigations (chapter 6.2.3.5). These investigations suggest the absence of tritiogenic helium in the investigated waters. Either this would imply that in the absence of tritium transport is slow, where formed tritiogenic helium could have entered the gas phase and left the water, as is suspected for the investigated groundwater samples. Or, for detectable tritium amounts this would indicate a rapid transport process, where tritium had no time to decay in the unsaturated zone and may only decay in the groundwater, where the decay product ^{3}He would be found.

However, the investigation of chlorofluorocarbons (for brevity the compounds CFC-11, CFC-12 and CFC-113 are collectively abbreviated as 'CFCs') showed that a detectable signal of CFC-12, CFC-113 and of sulfur hexafluoride (SF_6) is found in some of the investigated groundwaters (Fig. 6-11). Those three tracers yielded similar results in their signals, confirming atmospheric influence. CFC-11 shows much higher values which may represent contamination by degreasing agents in pump use or other contaminants, if not stemming from a natural (abiogenic) source, as e.g. reported in Schwandner et al. (2004). Such a source can, however, not be allocated for in the study area, and the CFC-11 source is not yet well understood. However, the data obtained from CFC-12, CFC-113 and SF_6 yield important information regarding water transport. While solute tracers are moved advectively with the seepage water, gas tracers pass the unsaturated zone relatively fast through the air phase (Zoellmann et al., 2001, Fulda and Kinzelbach, 1997, Katz et al., 1995, Busenberg and Plummer, 1992) and 'set their clock' at the groundwater table. Using the two tracer types gas and solute tracer, information on the different transport processes in the unsaturated and saturated zone, respectively, can be obtained. Assuming no further fractionation of the freons took place in the unsaturated zone, the fact that they are found in the groundwater shows that some water has recently replenished the aquifer. This confirms the assumption that the absence of tritium in groundwater is indeed a result of the long travel time of water (and solutes) through the thick unsaturated zone and does not necessarily indicate the absence of recharge, which demonstrates why effects of a thick unsaturated zone can lead to an overestimation of the age of the groundwater (Cook and Solomon, 1995).

In the quantification of young water components and/or residence times one needs to distinguish between i) freons that surficially enter the groundwater by diffusion and ii) an advective transport of freons into deeper parts of the aquifer. From semi-arid regions it is known that diffusion may play a role in the transport of CFCs. The penetration depth of CFC into the aquifer can be estimated using the relation (Crank, 1975, Gröning, 1994):

$$C(t,z) = C_0 \cdot \left(1 - erf\left(\frac{z}{2 \cdot \sqrt{(D \cdot t)}}\right)\right) \tag{6.27}$$

where C_O is the initial concentration of the CFCs, t denotes the time, D is the diffusion constant (max. 0.03 m^2/a for a free solution), z is the depth and *erf* denotes the Gaussian error function. For a diffusion of 50 years, less than 1% of the CFC concentrations found at the groundwater table, i.e. those in solubility equilibrium with the atmosphere, would reach a depth of 5 m, assuming (simplified) homogeneous conditions in the aquifer. Including porosity and tortuosity into the diffusion constant, which decreases the actual diffusion constant by an approximate factor 5 (Cook and Solomon, 1995), an even lower value would be reached. Considering screen lengths in the order of 100 m, only a proportion of less than 5 % of the CFCs could thus have been transported into the aquifer via diffusion, given the fact that the water table is in the screened section. If the water table is located in a cased section, diffusive CFC input would be even lower.

Considering the young water components as shown by the relative concentrations of freons in Fig. 6-, the dominance of advective transport appears more likely as values greater than 25 % of water of current atmospheric composition are reached, assuming that the young component has a recent atmospheric composition. This assumption is also suggested by Beekman et al. (1999) and is supported by another study (Wellfield, 2000) which in 1998 found detectable amounts of tritium in two boreholes that are part of the present investigations in Serowe (BH7099: 0.5 ± 0.2 TU and BH7021: 1.1 ± 0.2 TU), suggesting active localized recharge. It is also supported by radiocarbon investigations in that study. However, findings from this study and from the literature (DeVries and Simmers, 2002, Selaolo, 1999, Beekman et al., 1999, Verhagen, 1991, Gieske et al., 1995 and chapter 3.5.3) also show that exact processes in semi-arid environments are still not well understood.

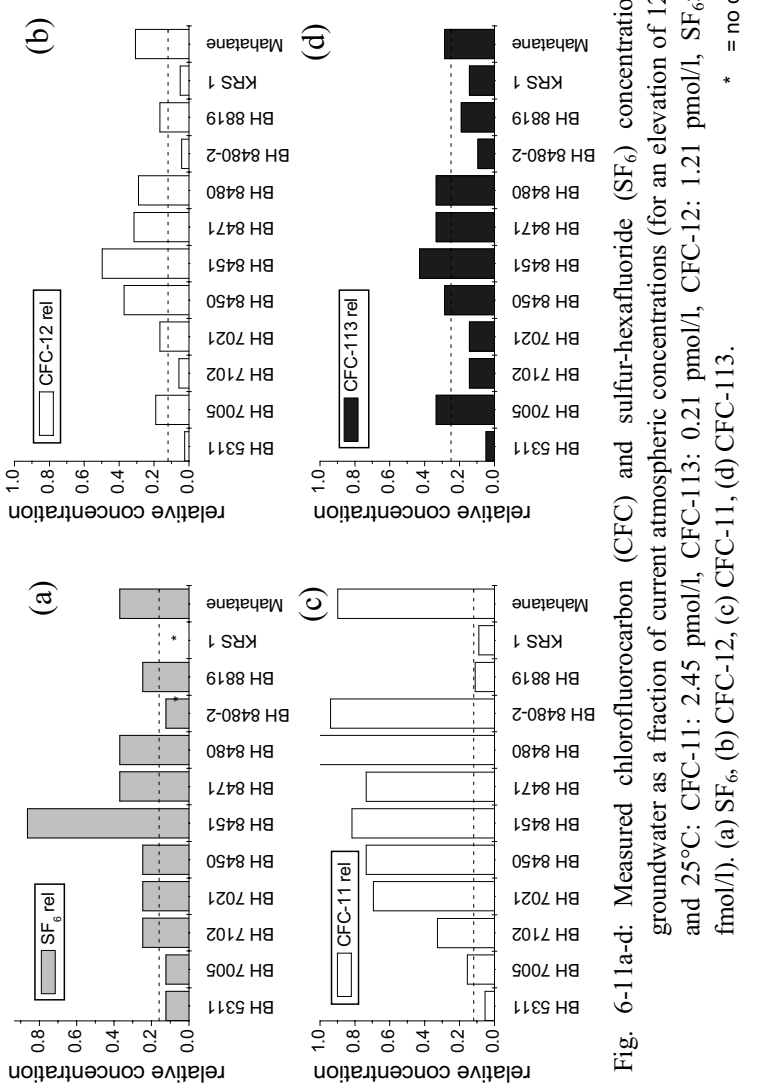

Fig. 6-11a-d: Measured chlorofluorocarbon (CFC) and sulfur-hexafluoride (SF_6) concentrations in groundwater as a fraction of current atmospheric concentrations (for an elevation of 1200 m and 25°C: CFC-11: 2.45 pmol/l, CFC-113: 0.21 pmol/l, CFC-12: 1.21 pmol/l, SF_6: 0.81 fmol/l). (a) SF_6, (b) CFC-12, (c) CFC-11, (d) CFC-113.

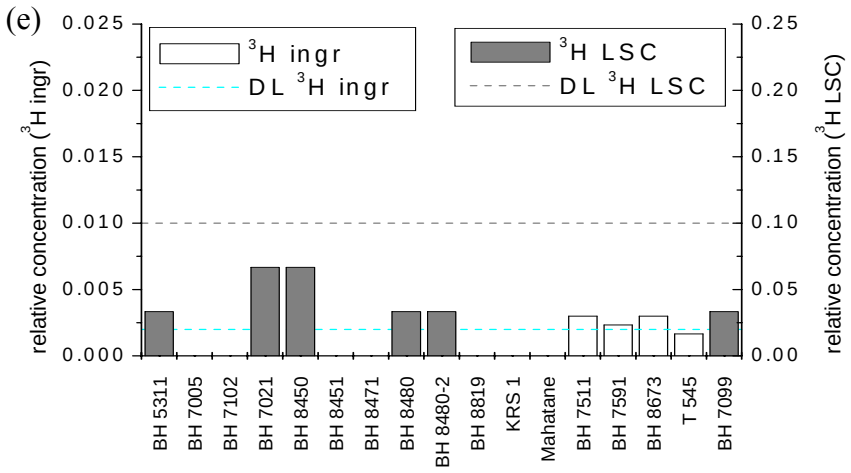

Fig. 6-11e: Measured tritium (^{3}H), concentrations in groundwater as a fraction of current atmospheric concentrations, separated into the two different analytical methods liquid scintillation counting (LSC) and ^{3}He ingrowth (ingr). Note the scale difference of the ^{3}H graph as opposed to (a) to (d). Dotted lines indicate the respective detection limits (DL), 'rel' denotes measured concentrations relative to current atmospheric concentrations.

6.2.3.4 The carbonate system

Relations of carbon-13 and carbon-14

Fig. 6-12 shows the observed ^{14}C-DIC values from Serowe, plotted against the measured δ^{13}C values, as ^{13}C can generally be used to trace the source of carbon (Clark and Fritz, 1997). Additional data from groundwater analyses of nearby study areas (Wellfield, 2000) have been inserted into the graph to validate the results from the current study. These additional data show a good agreement with own results. Own δ^{13}C data lie between -12.5 and -7.8 ‰. Two groups can be identified and are termed according to their ^{14}C content in ^{14}C-poor (less than 20 %-mod., group 1) and ^{14}C-rich samples (40 – 80 %-mod., group 2). ^{14}C-poor samples have a mean δ^{13}C signal of -9.1 ‰ (Fig. 6-

12). The ^{14}C-rich samples represent a narrow range of $\delta^{13}C$ values with a mean $\delta^{13}C$ value of -11.2 ‰.

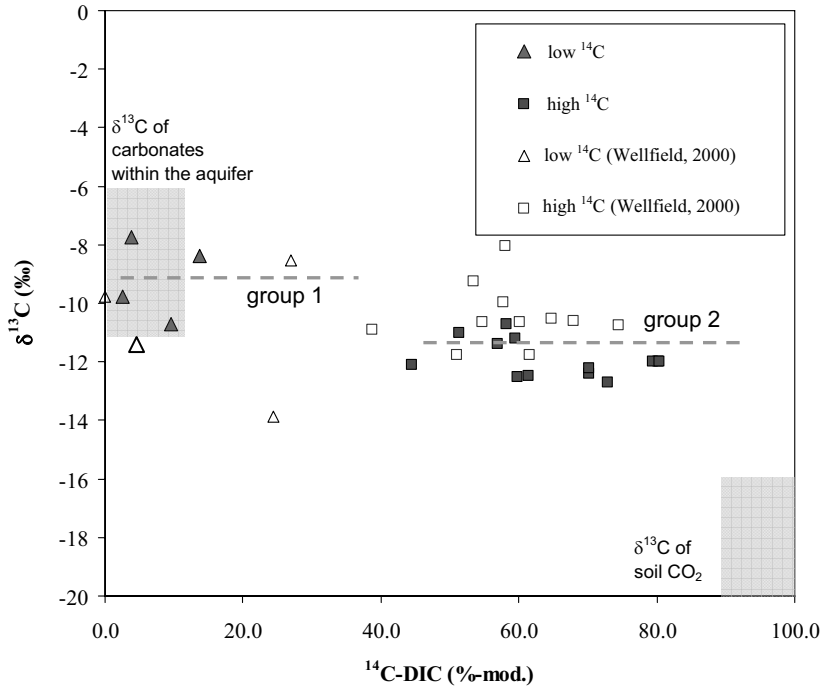

Fig. 6-12: Plot of ^{14}C activities of groundwater samples from Serowe in relation to their $\delta^{13}C$ values. Open symbols represent external data from Wellfield (2000). Group 1 represents ^{14}C-poor (< 20 %-mod.) and group 2 represents ^{14}C-rich samples (40 – 80 %-mod.).

Carbon-13

As seen from chapter 5, carbonate dissolution in the investigated system is controlled by soil CO_2 (chapter 5), which has implications on the amount of

DIC and the development of the δ^{13}C-DIC values (Fig. 6-8), in the following referred to as δ^{13}C. As indicated above, the δ^{13}C values found in the groundwater from Serowe are between -12.5 and -7.8 ‰ (Fig. 6-12). The encountered grouping of the δ^{13}C values may reflect that i) the samples were recharged under different conditions, ii) some of the samples progressed further in their geochemical evolution (regarding carbonate chemistry), or iii) they represent a mixed signal with varying contributions from C_3- and C_4-plants. In the Kalahari the predominant vegetation, such as acacias, are C_3-plants, while grass is a C_4-plant (Vogel, 1970). The proportion of each plant group is, however, not known.

Generally spoken, δ^{13}C signals lighter than those of the sediment matrix either point to an addition of organic matter into the system or to influence by methane, both of which are unlikely in the investigated system. Or else, the signals point to an isotopically light δ^{13}C value of the soil CO_2, indicating a production by C_3-plants mainly.

To derive possible constraints for the contribution of C_3- and C_4-plants to the ^{13}C signal measured in the groundwater, the potential initial ^{13}C value for dissolved CO_2 was estimated. The groundwater samples with isotopically heavier mean δ^{13}C values of -9.1 ‰ (group 1 in Fig. 6-12) represent a signal that is very similar to the one of the sediment matrix which hampers conclusions on the potential isotopic composition of soil CO_2. For the isotopically lighter samples of group 2 (Fig. 6-12) at a mean δ^{13}C value of -11.2 ‰ calculations could be performed. At the given pH range of the samples a ^{13}C fractionation between HCO_3^- and CO_2 occurs of ε = 7.9 ‰ at 25°C. This results in an initial value for CO_2 released from root respiration in the order of -1.1 ‰, assuming that the soil CO_2 was the main origin of DIC in groundwater. As indicated above, this sets an upper limit and would be the result of the vegetation being dominated by C_3-plants. Assuming δ^{13}C = -23.5 ‰ for the soil CO_2 produced by C_3-plants and δ^{13}C = -9.6 ‰ for C_4-plants (Fig. 6-8) suggests that within the assumption made the C_3-plants contribute by (at least) 90% to the soil CO_2 production. This seems plausible in the observed system as acacia trees are predominant year-round, while grass is only of importance in the rainy season.

Carbon-14

The investigation of radiocarbon is useful in establishing the residence time of groundwater and has been applied in previous studies in the Kalahari environment (Selaolo, 1998,, Verhagen, 1995, Vogel et al., 1982, Mazor et al., 1977). Yet, as indicated in chapter 6.2.2, difficulties can be encountered when attemping to calculate groundwater ages based on ^{14}C data. In the investigated system the ^{14}C signal may reflect either i) decay alone, ii) dilution of the ^{14}C content with groundwater containing 'dead' carbon (activity $^{14}a_C$ = 0 %-mod.) from carbonate dissolution, iii) interferences by matrix diffusion of ^{14}C in a fractured system, and iv) a disturbance of the originally infiltrated carbon amount through sulfate reduction, incorporation of geogenic CO_2 and/or methanogenesis. Even though the geochemical evolution of the groundwater samples could be satisfactorily reconstructed in this study (chapter 5) and point iv) can be neglected in the observed system, it proved difficult to obtain reliable ^{14}C 'ages' due to the partial overlapping of the $\delta^{13}C$ signal of the carbonaceous aquifer material with the $\delta^{13}C$ value of DIC in the groundwater (Fig. 6-12) and uncertainties in initial carbon chemistry. However, as will be illustrated in this chapter, corrected ^{14}C ages of the investigated groundwaters agree reasonably well with comparable ^{14}C dated groundwater from the Kalahari (Stute and Talma, 1997, Verhagen, 1991, Vogel et al., 1982). Noble gas temperature studies (NGT) in similar aquifers in the Kalahari (Kulongowski and Hilton, 2004, Stute and Talma, 1997) clearly show that a drop in temperature according to the transition from Holocene to Pleistocene coincides with corrected ^{14}C ages of about 12,000 to 15,000 years, proving the applicability of ^{14}C as a possible age indicator in the Kalahari system. In addition, advanced hydrochemical evolution with decreasing ^{14}C contents as well as high ^{4}He concentrations in waters of low ^{14}C contents support the assumption, that ^{14}C can at least represent a qualitative time scale. As will be illustrated in the following, two main factors control the ^{14}C contents in the Ntane aquifer: mixing between groundwater components of different radiocarbon content, and differences in residence times.

Carbon-14 as an indicator for mixing

Assuming that the observed ^{14}C contents of the groundwater samples represent a mixture between modern groundwater of a maximum content of 80.5 %-mod. (which is the highest ^{14}C content measured in the analyzed set of samples) with groundwater containing 'dead' carbon the observed values would not yield any information on residence times but rather on the degree of

mixing of different end members. Mixing was already implied from the observation of vertical hydrochemical profiles as discussed in chapter 5.3.

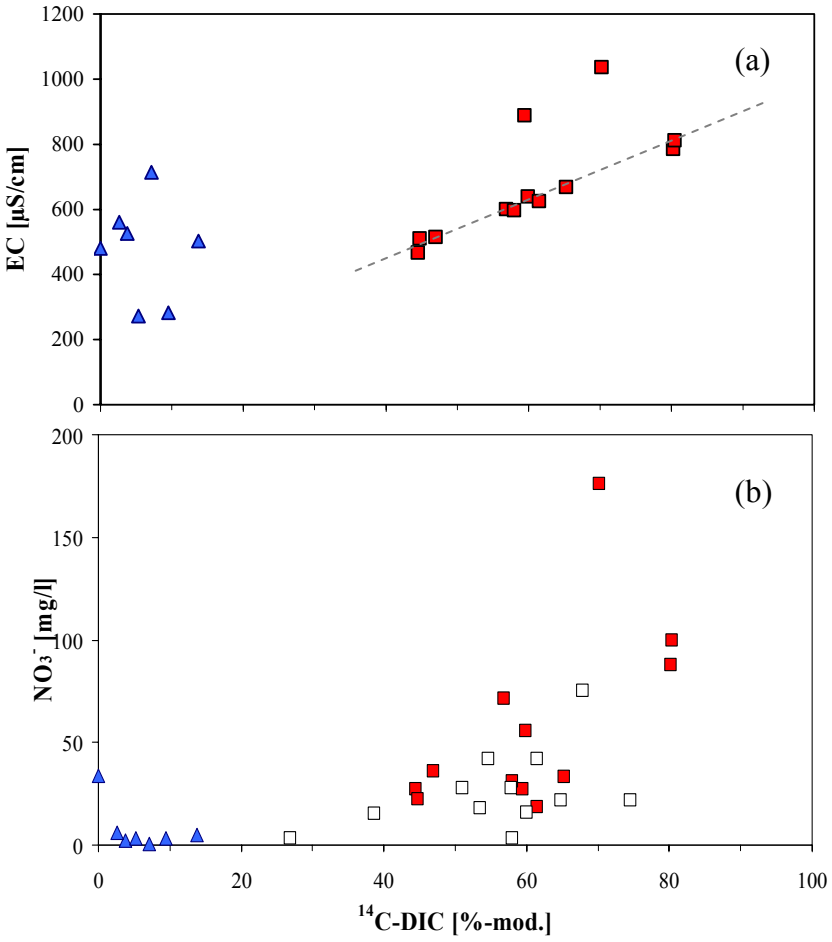

Fig. 6-13: (a) Relations of ^{14}C content and specific electric conductivities of groundwater samples of group 1 (triangles) and group 2 (squares), (b) Relations of ^{14}C content and nitrate concentration of groundwater samples of group 1 (triangles) and group 2 (squares). Open boxes represent external data from Wellfield (2000).

To verify the genetic relationship of samples of different ^{14}C content, the hydrochemical composition of the groundwaters was compared. As indicated earlier this chapter, the investigated groundwater samples can be divided into two groups. Groundwaters of group 1 were found to have higher sodium and slightly higher sulfate concentrations and to possess a Na-HCO_3 signature only. Groundwaters of group 2 with high ^{14}C content have higher concentrations of several major ions such as calcium, magnesium, chloride and nitrate. Within group 2, two end members can be identified, with the bulk of the remaining samples of this group plotting along a mixing line between the end members (Fig. 6-13a). A Ca-(Mg-)HCO_3 signature can be observed for ^{14}C-rich end members (e.g. BH8451), while a Na-HCO_3 signature was found in waters of lower ^{14}C contents in this group (e.g. BH8480). The development from a calcium to a sodium water type through ion exchange processes is hydrochemically plausible and describes a relative time sequence, where calcium-type waters are being formed prior to sodium-type waters (chapter 5.2). The assumption that group 1 developed from the modern group 2 end member is, however, contested as to the following observation: The EC distribution of the groundwater samples behaves adversely to an anticipated hydrochemical evolution. 6-13a shows the relation of ^{14}C to specific electric conductivities in the investigated samples. Given a hydrochemical evolution the specific electric conductivities should rise owing to prolonged water-rock interaction time and a resulting increased amount of dissolved solids in solution from the rock matrix. This is not the case in the investigated groundwater samples. A mixture of different water components with different recharge conditions, however, appears to be likely.

Carbon-14 as a residence time indicator

Assuming that the investigated carbon-14 in the samples stems from carbonate dissolution by carbon dioxide (as suggested in subchapter 'carbon-13') and subsequent decay of ^{14}C, calculations of apparent groundwater ages have been performed. Groundwater ages have been derived using different correction models. Measured $\delta^{13}C$ values have enabled corrections to be made for group 2 samples only as indicated in the subchapter 'carbon-13', using a ^{14}C value of 100 % modern carbon together with a $\delta^{13}C$ value of soil CO_2 of -21.6 ‰. For carbonate corrections an average literature value for terrestrial carbonates of -5 ‰ was used, as only one measured value from a study by Selaolo (1998) was available, which indicates a $\delta^{13}C$ of -9 ‰ for carbonates within the aquifer. This value lies within the upper values given in the literature (e.g.

Eichinger, 1983, Geyh, 2000, Kendall and McDonnell, 1998). Calculations for group 1 corrections have been included in the knowledge that the produced ages can only represent maximum ages, as the measured $\delta^{13}C$ values lie in the range of the sediment matrix so that isotope exchange processes cannot be quantified. A high apparent age range has been produced by the application of different models as depicted in Fig. 6-14. However, the models provide a tool in the qualitative age determination that is relevant to determine the fate of nitrate in the aquifer and results will be interpreted in their relative context only.

Of the tested correction models, the statistical model (Vogel, 1970) represents the most simplified approach with an assumed dilution of the ^{14}C from decay by 15 % of ^{14}C-free carbon. For the end members of group 2, represented by BH8451 (80.5 %-mod.) and BH8480 (40.5 %-mod.) apparent ages of 450 years and 5340 years, respectively, were calculated. This appears to provide a plausible estimate for groundwater samples that were recently exposed to modern (atmospheric) carbon, though theoretically an uncertainty in the order of 1700 years has to be assumed, as the initial ^{14}C content can only be limited to a range between 100 and the highest measured value of 80.5 %-mod. This uncertainty is especially significant for younger ages. The $\delta^{13}C$ mixing model (modified Pearson and Hanshaw model) (Clark and Fritz, 1997) is generally applicable as it describes open and closed system conditions and includes isotope exchange which may be expected in the observed system. However, this model requires the precise knowledge of the pH and therefore $\delta^{13}C$-DIC of the recharge water. This is a value which can only be estimated for the investigated system. Yet, due to the the narrow pH range between 6 and 7.2 that can be expected for the recharged water a plausible $\delta^{13}C$ range between 19 and 14 ‰ can be assumed, still yielding a possible error up to 2,000 years. The $\delta^{13}C$ mixing model approach then produces apparent ages between 28 (BH8451) and 5031 years (BH8480) for neutral pH ranges. Though expected to yield reasonable results, the Fontes and Garnier model (Fontes and Garnier, 1979) leads to an overcorrection of apparent ages. It yields apparent ages between -266 (BH8450) and 3665 years (BH8480) but generally overestimates exchanged amounts of DIC.

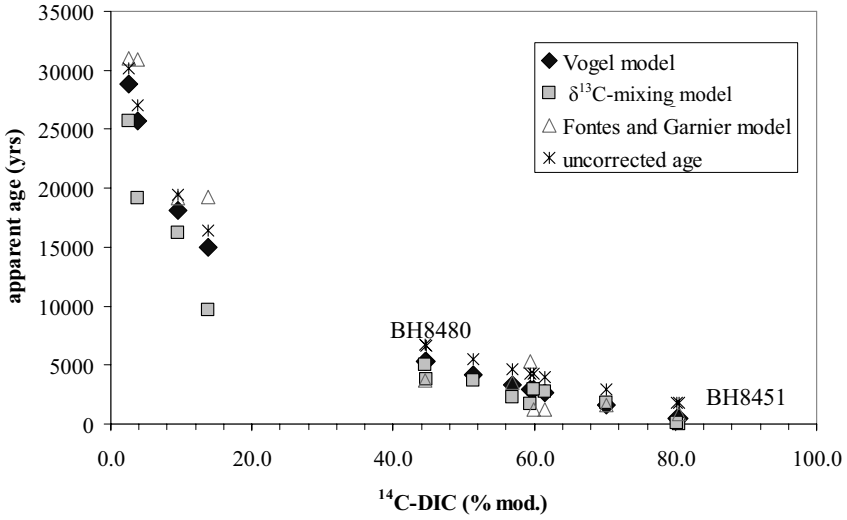

Fig. 6-14: Calculated ^{14}C apparent ages for selected groundwater samples from Serowe. Apparent ages were calculated using different models as designated in chapter 6.2.2.

To determine the impact of diffusion of ^{14}C from the groundwater table, the penetration depth z of diffusion can be calculated using

$$z = \sqrt{2 \cdot D \cdot t} \tag{6.28}$$

(Crank, 1975) where D represents the diffusion constant (max. 0.03 m^2/a for a free solution) and t the time estimated from the conventional age of the groundwater. For a least affected, i.e. deep borehole, exemplarily calculated for BH8480, a penetration depth of 18 m is reached by diffusion. As the screen length is in the order of 100 m, diffusive transport of ^{14}C can account for a ^{14}C content of about 20 %-mod. in the abstracted water, assuming an inflow of water over the entire screen length. This conventional calculation shows that ^{14}C values of 80 %-mod., which are the highest ^{14}C contents that are found in the aquifer, cannot be explained by diffusion, but require active recharge.

As can be seen from the presented data, neither correction model can satisfactorily be used to correct radiocarbon ages of all samples. Results must be considered as best estimates that yield qualitative age information only. However, as indicated in the introduction of this chapter, corrected ^{14}C ages of groundwaters of low ^{14}C contents agree reasonably well with the time of wetter conditions in the Kalahari (chapter 3.2.2), which in addition is in accordance with comparable ^{14}C dated groundwater from the Kalahari (Stute and Talma, 1997, Verhagen, 1991, Vogel et al., 1982).

For the investigated groundwater samples the influence of both mixing and differences in residence times is assumed, though direct evidence can only be reliably provided for mixing. Yet, though knowing that dilution processes suspected for group 1 may as well interfere with a precise determination of residence times, indicators were found that point to a confirmation of the relative 'age' sequence of the groundwater samples: i) Samples with a ^{14}C content of 80 %-mod. are continuously exposed to modern carbon, in this case atmospheric CO_2. These samples can be addressed as 'modern' and can be regarded as one end member. ii) The hydrochemical composition of the investigated groundwater samples provides a conceptual framework for the interpretation of the obtained ^{14}C data. They suggest Ca-HCO_3 type groundwater samples with high ^{14}C content to be formed later than the Na-HCO_3 groundwater samples with low ^{14}C content and/or their formation through different processes. In the investigated sytem this could be i) recharge through preferential pathways, resulting in a rapid replenishment of water into the groundwater. This could occur through macropores in the soil zone, which have been reported to occur (Schwiede, in prep.) in the study area. A further rapid flow enhancing feature in the unsaturated zone are fractures in the Stormberg Basalt that overlays the Ntane sandstone aquifer. ii) diffuse recharge through the soil and rock matrix. These processes coupled with the temporally and locally scattered rainfall distribution (chapter 3.2) might result in different recharge processes. Both processes are known to occur in semi-arid settings (Austin et al., 2004, DeVries and Simmers, 2002).

Relations of carbon-14 content to nitrate concentrations

A correlation of ^{14}C with nitrate concentrations was found in groundwaters near Serowe ($r^2 = 0.68$) (Fig. 6-13b). The more modern groundwater type of group 2 (40 to 80.5 %-mod.) shows an elevated nitrate content, while the water of group 1 (< 20 %-mod.) is associated with low nitrate concentrations.

If not due to anthropogenic activities, decreasing nitrate concentrations with lower ^{14}C content could either indicate denitrification processes or could be a result of a change in leaching conditions from the unsaturated zone and/or changed recharge mechanisms that transports nitrate into the groundwater. The latter is supported by the correlation of elevated nitrate with a Ca-(Mg-) HCO_3 water type as discussed earlier this chapter. This also points to mixing of different components. The scattered data points and outliers, however, might indicate that a simple two-component mixture may not adequately describe the data. The presence of at least one further component is suspected.

6.2.3.5 Dissolved noble gases

Helium-3 and Helium-4

The helium (He) isotopic composition for a selection of samples collected from Serowe and from Orapa was measured. The $^3He/^4He$ ratios ranged from $1.8 \cdot 10^{-8}$ to $1.23 \cdot 10^{-6}$ (Tab. 11-1). The ^4He content of the samples ranged from $4.6 \cdot 10^{-8}$ cm^3 STP/g to $1.3 \cdot 10^{-4}$ cm^3 STP/g. In order to reveal the genetic relationship and the relative residence times of the groundwater samples the measured $^3He/^4He$ ratio of the investigated groundwater samples from Serowe and Orapa was plotted as a function of the ^4He content (Fig. 6-15). It can be observed that the samples from Serowe and some of those from Orapa plot along a trend line starting with $^3He/^4He$ values that agree well with the air equilibrium ratio of $1.384 \cdot 10^{-6}$ and low ^4He concentrations of $3.8 \cdot 10^{-8}$ cm^3 STP/g, which corresponds to solubility equilibrium of ^4He at 25°C and 1200 m amsl. The trend develops towards typical ranges of crustal $^3He/^4He$ ratios in the order of $2 \cdot 10^{-8}$ and ^4He concentrations of greater than $1000 \cdot 10^{-8}$ cm^3 STP/g. Groundwater samples from Serowe plot closer to the air equilibrium values, while samples from Orapa show values that progressed further along the production line toward higher radiogenic influence. This trend may be generally used as a qualitative age indicator as the migration of radiogenic and/or mantle helium leads to a significantly increased ^4He content in the groundwater samples with increasing residence time (Kipfer et al., 2002, Osenbrück et al., 1998, Castro et al., 1998, Stute et al., 1992, Weise and Moser, 1987).

A quantitative age determination with ^4He is, however, generally hampered by the large variations of the estimated He flux from the continental crust and is difficult to determine (Castro et al., 1998, Stute et al., 1992) especially in case

of fractured systems present in Serowe. The latter makes estimations challenging whether the He flux is continuous, and complicates the correlation of ^{14}C and ^{4}He if small scales in the order of few kilometers are regarded. Minor amounts of helium might enter the aquifer through fracture connection from deeper aquifers. However, the fact that the observed ^{3}He values are relatively constant may lead to the assumption that helium input is homogenized at the investigated scale of greater than 10 to 100 km - a scale in the order of the size of the total study area. In addition, helium isotopes from the analysis of groundwater samples from Serowe qualitatively confirm the high age of ^{14}C-poor groundwater as those samples have high ^{4}He contents, indicating longer exposure to radiogenic helium, thus higher residence times within the aquifer (Fig. 6-15). The lower age of the ^{14}C-rich groundwater from Serowe is generally confirmed by helium isotope investigations as those samples plot closer to the air equilibrium values of ^{4}He and $^{3}He/^{4}He$, indicating shorter residence times (Fig. 6-15).

The groundwater samples from Orapa generally follow the trend of increased ^{4}He contents. However, the ratio of $^{3}He/^{4}He$ shows higher values up to the order of 10^{-7} (Fig. 6-15), which indicates the involvement of additional processes. It is suspected that these samples are influenced by an additional He source. Mantle helium has a high $^{3}He/^{4}He$ ratio in the order of $1.1 \cdot 10^{-5}$ which may account for the observed shift in ratio in the Orapa groundwaters. Alternatively, the water could be influenced by He from crustal material of a different composition than the one (of sandstone) found in the other groundwater samples, yielding different $^{3}He/^{4}He$ ratios. Those different values still fall within the range for He from crustal material reported in the literature (Kipfer et al., 2002, Andrews, 1985) despite the fact that $2 \cdot 10^{-8}$ is most often used as the crustal reference $^{3}He/^{4}He$ ratio (Kipfer et al., 2002). From hydrochemical investigations discussed in chapter 5 it is known that three of the samples (Z7092, Z7157 and BH6002) that show high ^{4}He, but do not lie on the discussed trend line are influenced by water from the lower lying Mosolotsane aquifer. This lower-lying aquifer is suspected to deliver helium with a mantle or amended crustal signature. The remaining two boreholes may reflect higher $^{3}He/^{4}He$ ratios as a result of a structural, i.e. hydraulic connection to the additional He source. The resolution of available data on structural geology is, however, too poor to verify this assumption. Atmospheric influence is ruled out for those samples as this should show in both the $^{3}He/^{4}He$ ratio as well as the ^{4}He content.

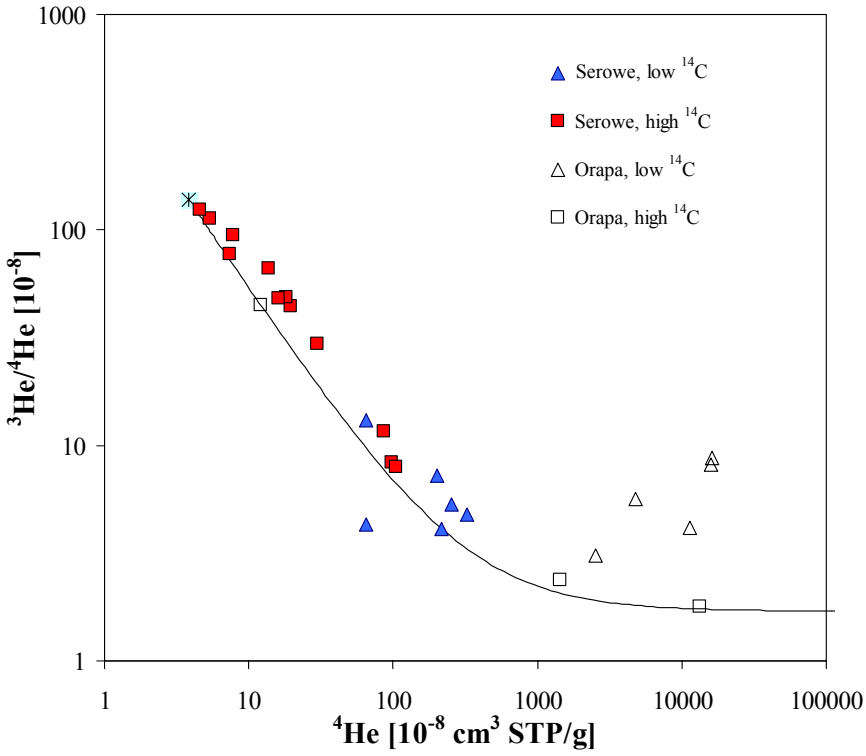

Fig. 6-15: Plot of measured ^{4}He and ^{3}He/^{4}He data of groundwater samples from Serowe and Orapa. Symbol groups are in accordance with groups inferred from carbon-14 investigations. The solid line represents the development, or mixing, respectively, of the ^{4}He content and ^{3}He/^{4}He ratio from water in equilibrium with air (^{3}He/^{4}He: $1.384 \cdot 10^{-6}$, ^{4}He: $3.8 \cdot 10^{-8}$ cm^3 STP/g) towards a radiogenic signature (in the order of ^{3}He/^{4}He: $2 \cdot 10^{-6}$, ^{4}He: $> 1 \cdot 10^{-5}$ cm^3 STP/g).

Neon-20 and nitrate

Neon (Ne) is found in excess of the solubility value of $1.6 \cdot 10^{-7}$ cm^3 STP/g in all groundwater samples, which is due to excess air dissolved in course of the

recharge process. Ne measured in groundwater samples consists of two components that have to be separated (Eq. 6.29).

(6.29) $$Ne_{sample} = Ne_{equi} + Ne_{excess}$$

with Ne_{equi} representing the Ne in equilibrium at the given conditions (Ne_{equi} = f(T, S, p)) and Ne_{excess} (ΔNe) being the so-called excess air component. In most aquifers noble gas concentrations are higher than the concentrations expected at atmospheric equilibrium, which is termed 'excess air'. Neon can be used to identify excess air, as Ne solubility is almost independent of temperature (Aeschbach-Hertig et al., 2000, Stute and Schlosser, 1993, Heaton and Vogel, 1981). The extent of excess air is influenced by the rate and extent of recharge and therefore may be used as an indicator to distinguish between dry and wet infiltration conditions (Beyerle et al., 2003; Stute and Talma, 1997; Heaton et al., 1983). Due to apparative constraints in Ne measurements the presented data shows only ^{14}C medium to high samples (next section).

A strong linear correlation of nitrate with dissolved neon content is found for the samples (Fig. 6-16), which confirms the impact of different recharge conditions. High nitrate contents in the groundwater correspond to low neon excess values, while low nitrate contents are related to high neon excess values. Lower Ne excess values suggest a low-rate recharge process where neon concentrations are maintained at solubility equilibrium, while higher Ne excess values are connected to high rate recharge, where air is captured below the water table. A quantification of the Ne excess could not be performed as the infiltration temperature and atmospheric helium content is not precisely known from the present data (see next subchapter). The determination of additional heavier noble gases (Ar, Xe, Kr) would be necessary to determine the infiltration temperature (noble gas temperatures) as e.g. described in Kipfer et al. (2002). However, the relation of neon and nitrate appears plausible due to the almost linear relation of excess air and Ne, independent of the applied correction model. The neon content can therefore be used as an indicator of excess air.

As explained above, the fact that high nitrate contents correspond to low neon excess values suggests its transport by a low-rate, potentially slow recharge process. Low nitrate concentrations in the groundwater on the other hand are connected to high rate recharge, suggesting wet conditions.

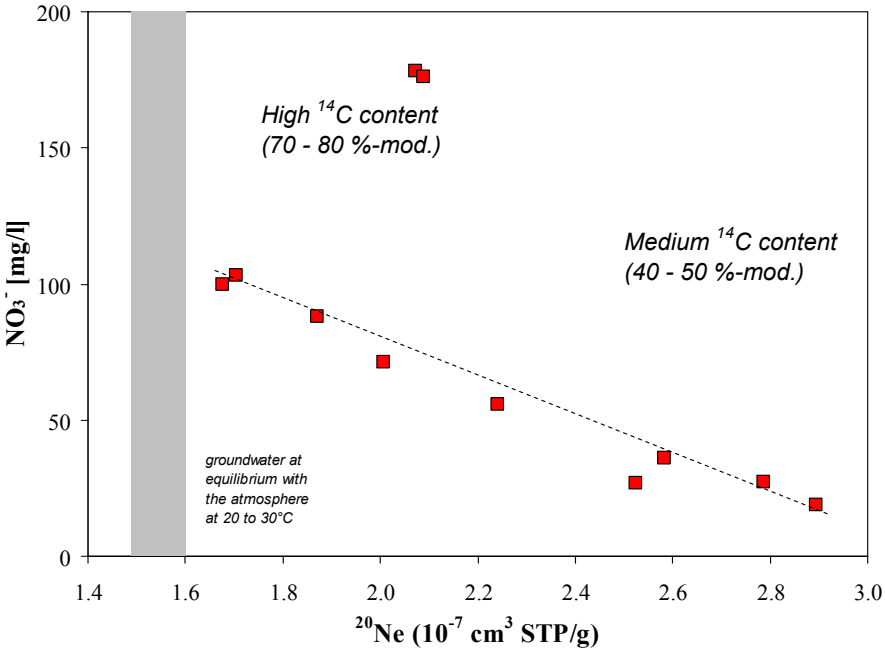

Fig. 6-16: Nitrate concentrations of Kalahari groundwaters from Serowe as a function of ^{20}Ne contents, showing a reasonable correlation (r^2 = 0.84). The presented data shows only ^{14}C medium to high samples.

However, whether the wet recharge conditions are related to a past humid climate period as suggested by high ^{14}C ages or are a consequence of a strong spatial variability of recharge cannot be distinguished from neon data alone. Yet, Fig. 6-17 implies a relation between ^{14}C and neon. The correlation of ^{14}C with neon is reasonably well and confirms the assumption of a relation of residence times and recharge rates. ^{14}C and neon, however, correlate slightly less than neon and nitrate. This owes to the fact that there is a physical relation between nitrate and neon as both species undergo the same process, a connection which is lacking for the neon-^{14}C relation. As other processes such as pCO_2, calcrete availability etc. impact on the carbonate chemistry and thus ^{14}C contents, a wider scattering of the data points may be caused.

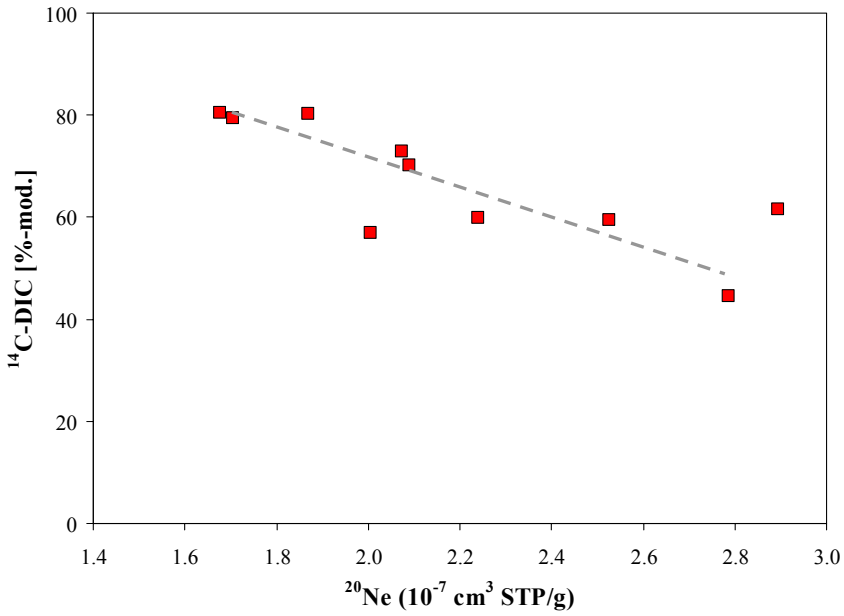

Fig. 6-17: ^{14}C contents of Kalahari groundwaters from Serowe as a function of ^{20}Ne contents. The presented data shows only ^{14}C medium to high samples.

The outlier BH8471 in Fig. 6-16, however, shows that a simple two component mixture cannot adequately describe the complex heterogeneous situation with at least three or more endmembers, in this case probably relating to inhomogeneous input pathways of nitrate.

Neon-20 and Helium-4

In order to verify assumptions derived from neon-nitrate relations, the plausibility of Ne-excess amounts was investigated using neon-helium relations. Ne measurements derived from groundwaters with He concentrations greater than approximately $1 \cdot 10^{-5}$ cm^3 STP/g could not be used in correction calculations as the samples had to be diluted strongly as to apparative constraints, hindering a precise determination of the low Ne values. As a result, Fig. 6-16 and

subsequent figures only show data for group 2 groundwaters. The used group designations are in accordance with groups inferred from ^{14}C investigations.

Fig. 6-18 shows the $^{20}Ne/^{4}He$ ratio as a function of the $^{3}He/^{4}He$ ratio. The data plot on a straight line between a radiogenic and a near atmospheric end member. With increasing ^{4}He content, the atmospheric contribution looses significance compared to radiogenic contributions. Though expected, the trend-line through the data does not intercept with the value of air saturated water at solubility equilibrium at a $^{20}Ne/^{4}He$ ratio of 0.364 and a $^{3}He/^{4}He$ ratio of $1.38 \cdot 10^{-6}$ at 25°C.

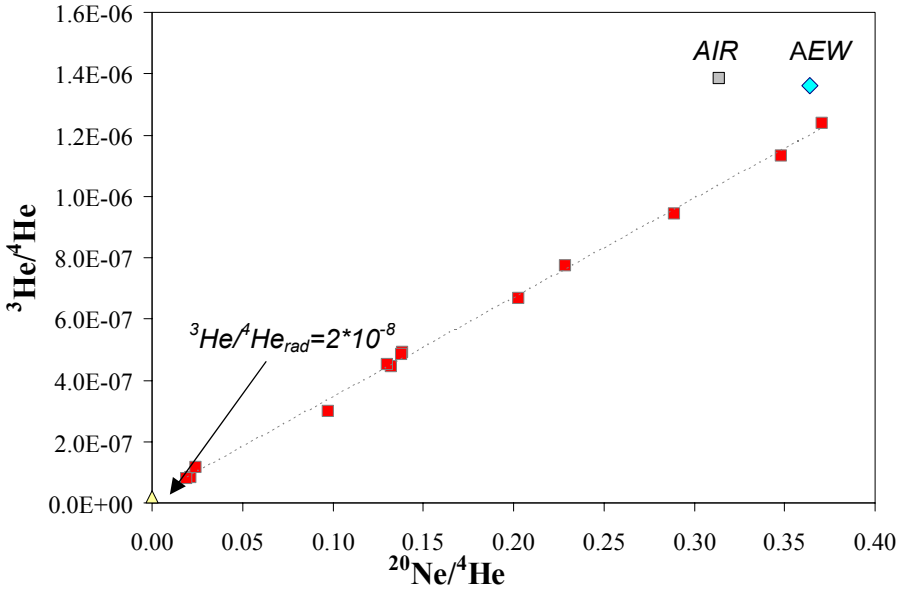

Fig. 6-18: Measured $^{3}He/^{4}He$ ratio versus the measured concentration ratio of Ne to He. The data define a mixing line between a radiogenic (triangle symbol) and an atmospheric end-member (AEW = air equilibrated water, AIR = atmospheric concentration), but appear to be influenced by excess air.

As previously indicated, this owes to the fact that the data has not been corrected for excess air. Depending on the correction model that is used to calculate excess air, the composition, i.e. noble gas pattern of the excess air may vary (Peeters et al., 2002, Holocher et al., 2002). The TD (total dissolution) model (e.g. Heaton and Vogel, 1981) assumes that initially the gas concentrations in the groundwater are at equilibrium with the atmosphere and that gas bubbles with atmospheric gas composition are trapped and completely dissolved. Gas excess may, however, exhibit systematic mass-dependent fractionation relative to atmospheric air. This concept is included in the PE (partial re-equilibration) model (Stute et al., 1995), which assumes a partial diffusive degassing of an initial excess with atmospheric composition across the groundwater table. While the PE model assumes that fractionation is solely due to the differences in molecular diffusivities between the gases and thus the degree of fractionation, the CE (closed-system equilibration) model (Aeschbach-Hertig et al., 2000) assumes an incomplete dissolution of the gas bubbles. The fractionation in the CE model depends on the initial air-water volume ratio and the pressure in the system, resulting in an enrichment of heavy noble gases relative to lighter gases.

Fig. 6-19 shows the application of the three different models (TD, PE, CE) to ^{4}He and ^{20}Ne data of the Serowe groundwater samples. The solid line with added temperatures shows the solubility concentrations of He and Ne for different temperatures (Salinity = 0, p = 0.876 hPa). The lines indicate excess air at 25°C which defines the assumed infiltration temperature. As can be seen from the plot, the application of the PE model produces an excess air composition within the range of the measured data. It provides an adequate description of the Serowe data and accounts for a faster diffusion of He than Ne. As found from the PE model, within the data group the degree of re-equilibration appears to be higher for boreholes with a higher ^{14}C content as represented by the dashed line in Fig. 6-19 than for those of a lower ^{14}C content (solid line). From this it might be assumed that the recharge conditions vary within the sample entity. The TD model leads to an overestimation of He concentrations, or an overcorrection of He concentrations, respectively. Using the CE model yields similar (overestimated) results.

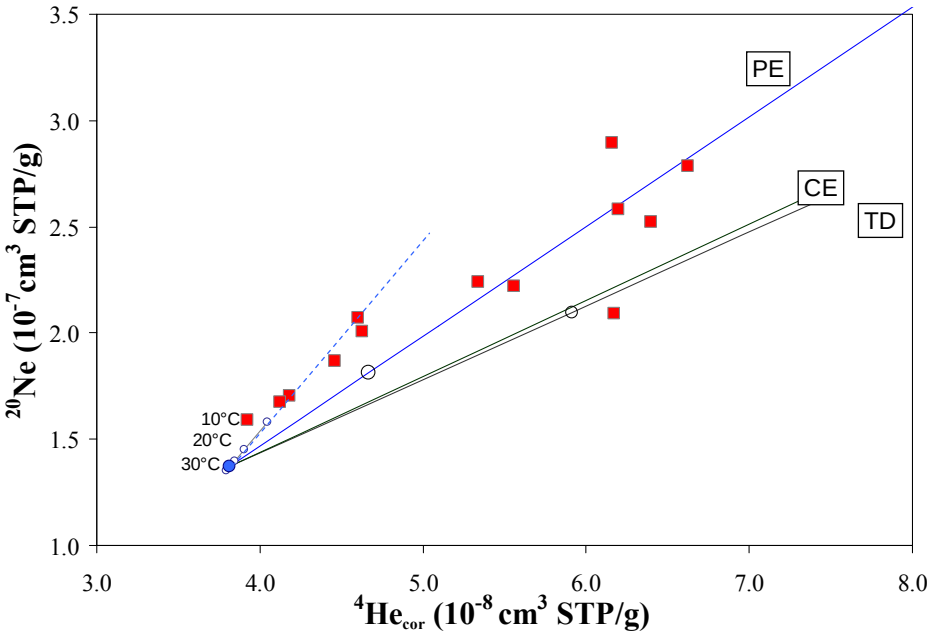

Fig. 6-19: Application of different excess air formation models to groundwater samples from Serowe. He_{cor} data is corrected for radiogenic He assuming a $^3He/^4He$ ratio of $2 \cdot 10^{-8}$. TD denotes the total dissolution (Heaton and Vogel, 1981), PE the partial re-equilibration (Stute et al., 1995) and CE the closed system equilibration model (Aeschbach-Hertig et al., 2000).

Despite the lack of exact quantification of ΔNe, Fig. 6-19 shows that excess air can be produced under the given semi-arid conditions. Assuming a partial re-equilibration of the noble gases seems plausible keeping in mind the slow transport of water through the unsatured zone and the low recharge rates observed in the investigation area (chapter 3.5.3). Though not precisely known from measurements, the estimated infiltration temperature ranges between 20 and 30°C which is also assumed in the literature for similar areas (Selaolo, 1998). This estimated infiltration temperature range has proven sufficient for a general understanding of the infiltration process.

6.2.3.6 Conceptual model inferred from isotope hydrology

Though individual findings may sometimes be ambiguous, combining the different indices yields a plausible scenario of recharge conditions and residence times in the aquifer. It leads to the following hypotheses (Fig. 6-20):

i) The investigation of stable isotopes in the groundwater showed an amount effect, which indicates that heavy rainfall events rather than small events supply water to replenish the aquifer, which is in accordance with other studies in the Kalahari (DeVries et al., 2000, Selaolo, 1998). Stable isotope investigations can, however, not reveal whether any groundwater is actually recharged or if all current rainfall is lost to evaporation and the groundwater found in the aquifer is paleowater.

ii) Infiltrating water is transported slowly through the thick unsaturated zone, resulting in the quasi-absence of tritium in the groundwater. However, some active recharge reaches the groundwater as suggested by the presence of freons. Model calculations show that these freons can reach the sampled groundwater depths not by diffusion alone. Advective transport and therefore at least some recharge (e.g. via individual preferential flow paths) is necessary to explain the freon results.

iii) While stable isotope data of the groundwater samples reflect the precipitation regime, excess neon revealed the presence of different infiltration mechanisms. One is a low-rate process where neon is maintained at solubility equilibrium with the atmosphere during (potentially slow) transport of water towards the groundwater table. This may be a process that delivers diffuse recharge as the recharge water slowly infiltrates through the rock matrix. A further process suggests recharge at much higher rates, preventing occasionally trapped and dissolved air bubbles from complete re-equilibration, which yields high concentrations of neon in the groundwater. Whether both processes exist under present climatic conditions or are a result of climatic change, i.e. are a function of time cannot fully be distinguished by the synthesis of stable isotope and freon results. If the processes mirror present-day conditions, then the rapid high-rate process could reflect preferential flow in the unsaturated zone, i.e. through the

Kalahari Bed cover and possibly through fractures in the overlying Stormberg Basalt.

iv) However, relations of neon and ^{14}C content suggest that the differences in recharge rate are a function of time, where groundwater samples of high ^{14}C content have a low excess air component. Higher recharge rates are associated with lower nitrate concentrations, while low recharge rates are connected with higher nitrate concentrations. The correlation of neon concentrations with ^{14}C contents favors the hypothesis that the difference in recharge mechanisms is triggered by climatic development. The groundwater component replenished by low recharge rates is a Ca-HCO_3 type, while high recharge rates surprisingly deliver Na-HCO_3 type groundwater. The latter observation can be explained by the relatively long residence times of these waters in the aquifer allowing for increased water-rock interaction after replenishment that amended the initial water type.

v) Accurate determinations of the water age could not be performed with radiocarbon data as to the limitations imposed by the (initial) $\delta^{13}C$ signal of the samples which is difficult to estimate due to uncertainties in the initial carbonate chemistry (relating to pH variations, similarity of the $\delta^{13}C$-DIC signal to that of the carbonaceous aquifer material, estimation of the soil gas-$\delta^{13}C$, pCO_2 and more). However, the relative age sequence of the groundwater samples as suggested by ^{14}C contents is confirmed by increased helium contents in waters of low ^{14}C contents, an advanced geochemical evolution with decreasing ^{14}C and results of comparable studies (e.g. Stute and Talma, 1997, Verhagen, 1991). Yet, slight deviations of the linear relationship between He and ^{14}C occur with high ^{4}He contents at medium ^{14}C content, which probably relates to the mixing of waters of different DIC content.

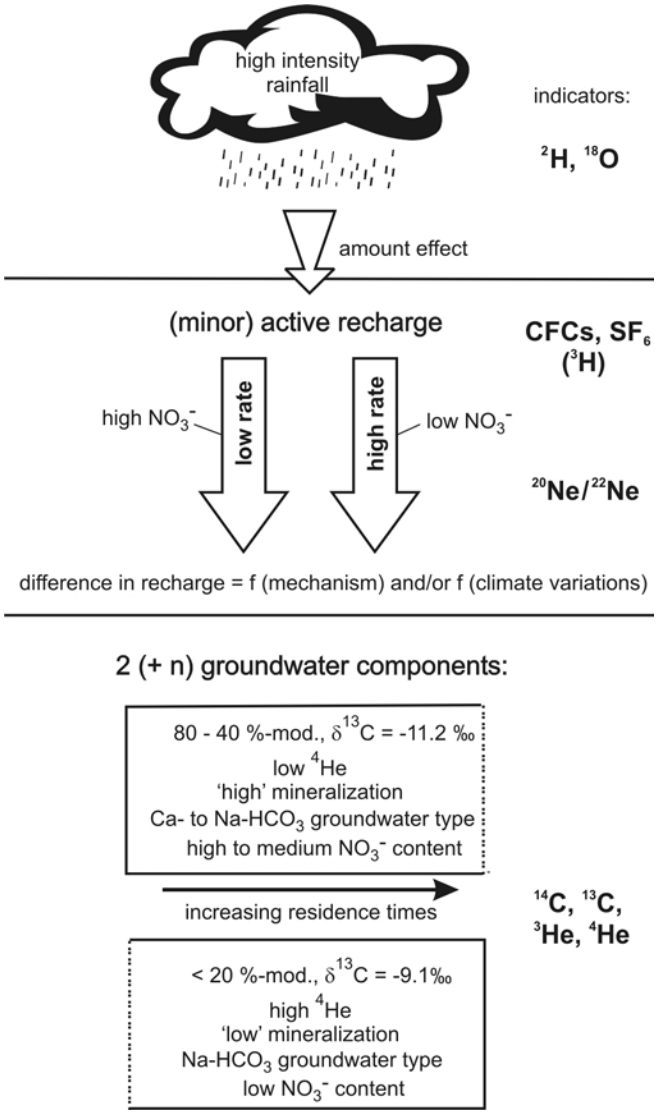

Fig. 6-20: Schematic overview of hydrogeological processes in the Ntane Sandstone Aquifer as derived from isotope hydrology. Associated processes are described in detail in the foregoing text.

6.2.4 Summary and conclusion

Natural isotope measurements of water and its solutes (^{2}H, ^{3}H, ^{18}O, ^{13}C, ^{14}C, $^{3}He/^{4}He$, and $^{20}Ne/^{22}Ne$) and of environmental tracers (CFC-12, CFC-113 and SF_6) proved useful in the interpretation of the hydrological processes that determine the fate of nitrate. The combination of multiple methods was crucial for the understanding of the system, as individual methods sometimes yielded ambiguous results. In total, results point to a complex system of high intensity rainfall, coupled with different recharge mechanisms, providing (minor) recharge amounts to the aquifer (Fig. 6-20), and the presence of independently formed groundwater types of different residence times in the aquifer.

Time scale

Though accurate age determinations by ^{14}C remained challenging, a comparison of ^{14}C results with ^{4}He data, the observed geochemical evolution in the aquifer and results of comparable studies (e.g. Stute and Talma, 1997, Verhagen, 1991) confirm the applicability of ^{14}C to distinguish relative time scales. The uncorrected ages of groundwaters of elevated ^{14}C (> 40 %-mod.) in this study show that their apparent ages are less than 10,000 years BP and fall within the Holocene, as uncorrected ages generally indicate maximum ages (Clark and Fritz, 1997). Though samples of lower ^{14}C content have proven to be older than those of elevated ^{14}C content, it cannot fully be distinguished whether samples of low ^{14}C (< 20 %-mod.) originated in the Pleistocene or Holocene. However, apparent ages calculated in this study show an agreement with ^{14}C results of similar studies (e.g. Stute and Talma, 1997). The corrected ^{14}C ages of those studies agree with a drop in temperature at the transition from Holocene to Pleistocene obtained by noble gas temperatures. As the end of the Pleistocene is marked by a pluvial phase (and as to short wetter periods during the Holocene), it seems likely that own samples low in ^{14}C were formed under those conditions, which is also implied by noble gas investigations and stable isotope data. Furthermore, the time scale obtained from corrected ^{14}C ages in the present study lies within the range of these wetter periods during the Holocene (possibly around 6,000 to 8,000 a BP) and the pluvial phase around 12,000 to 15,000 a BP implied by paleoclimatic findings (e.g. Kulongowski and Hilton, 2004, Thomas and Shaw, 2002).

Recharge
Combining the facts established from different methods, the recharge scenario can be summarized as follows: Even during the present semi-arid conditions active recharge takes place providing (minor) amounts of water to the aquifer. Younger waters were generally formed under heavy rainfall events, which is in accordance with findings in the literature (e.g. DeVries et al., 2000, Selaolo, 1998, Verhagen, 1985). This amount effect dominates an expected temperature effect which is suggested by noble gas investigations (e.g. Kulongowski and and Hilton, 2004). In addition, younger waters generally have a lower excess air component and have therefore received lower recharge rates, which in turn are related to high nitrate concentrations, while water formed by high rate recharge has low nitrate concentrations.

Water types
Within the aquifer, different water components of different ages have been identified that appear to have formed independently: A ^{14}C-poor group (< 20 %-mod.) with a mean $\delta^{13}C$ value of -9.1 ‰, and a ^{14}C-rich group (40 - 80 %-mod.) with a mean $\delta^{13}C$ value of -11.2 ‰. The first group is a Na-HCO_3 water type with low nitrate content, while the second group exhibits a development from Ca-HCO_3 to Na-HCO_3 water types with elevated nitrate concentrations. The assumption that the groundwater components formed independently is supported by a correlation of ^{14}C and specific electric conductivities that is in contrast to the expected geochemical evolution, as the groundwater samples show decreasing electric conductivities with decreasing ^{14}C content. A third component can be assumed from the correlation between the endmembers of the mixed water components which is lower than anticipated for a simple two-component mixture, and from the presence of outliers.

How the established recharge and residence time scenario exactly impacts on the migration of nitrate will be discussed in the following chapter.

7 SYNTHESIS OF THE ORIGIN AND FATE OF NITRATE IN GROUNDWATER OF THE KALAHARI

7.1 Introduction

Nitrogen input into the groundwater can be related to different processes. These can be of natural and/or anthropogenic origin as summarized in the introductory chapters. Apart from two boreholes in Letlhakane village, the selection criterion in this study was to sample uninhabited regions off the influence of anthropogenic activities, where impacts from nitrogen pollution such as sewage, fertilizer application and excreta do not directly affect groundwater chemistry. The only anthropogenically induced influence factor is the impact caused by extensive cattle grazing and resulting manure, which is included in the following discussion. Further natural input scenarios as well as nitrogen sinks are summarized in this chapter and verified with own data, based on the spatial distribution pattern of nitrate in groundwater established in chapter 5. This is followed by a discussion of aspects influencing the migration of nitrate into and within the aquifer.

7.2 Sources and sinks of nitrate

Input sources of nitrate into the groundwater into the Ntane Sandstone Aquifer can be classified into four types: i) surficial input by nitrogen through precipitation and/or contamination, ii) processes and point sources in the unsaturated zone, iii) nitrate from aquifer material and iv) groundwater-immanent nitrate input from overlying or underlying aquifers.

Nitrogen from contamination by manure

Nitrogen in excreted waste occurs mainly in the form of urea ($CO(NH_2)_2$), which is hydrolized by the enzyme urease and is subsequently converted to nitrate in the unsaturated zone (Eq. 7.1 and 7.2). From there, it is leached into the groundwater.

(7.1) $$CO(NH_2)_2 + H^+ + H_2O \xrightarrow{urease} 2\,NH_4^+ + HCO_3^-$$

and

(7.2) $$NH_4^+ + 2\,O_2 \longrightarrow NO_3^- + H_2O + 2\,H^+$$

The urea hydrolysis produces a temporary rise in pH that supports the formation of ammonium (NH_3), which is easily lost to the atmosphere (e.g. Widory et al., 2004). Depending on the redox conditions, i.e. a limited availability of oxygen as an electron acceptor, NH_4^+ may be found in the groundwater. Additional NH_4^+ may originate from dissimilatory NO_3^- reduction under highly reducing conditions, but this process normally plays a subordinate role (Appelo and Postma, 1996).

The groundwater samples from the study area contain no significant amounts of NH_4^+. Values are close to or below the WHO limit of less than 0.5 mg/l. In Serowe, values are generally below 0.6 mg/l. Groundwater samples from Orapa exceed the WHO limit for NH_4^+ in 4 boreholes (Z7100, Z7157, Z11016 and Z11049) but generally lie below 0.4 mg/l. The exceedences in these boreholes probably rather relate to highly reducing conditions in these boreholes than to contamination from the surface (chapter 5.2). However, nitrogen input as manure might not always be distinguishable as NH_4^+. As reaction kinetics allow a rapid oxidation of NH_4^+ to NO_3^- in the presence of oxygen, NH_4^+ input may not be identified separately and is measured as NO_3^-, too.

Along with elevated NO_3^- concentrations, groundwater influenced by manure (of cattle or wildlife) generally has elevated Cl^- concentrations. Na^+ and SO_4^{2-} from evaporitic deposits may also be found in manure-contaminated water as it is co-mobilized from the land surface. Such observation have been made locally for the groundwater in perched aquifers in the Kalahari Beds, but do not appear to be of quantitative importance as described later this chapter (cf. N from perched aquifers). In the Ntane Sandstone Aquifer, direct indications for NO_3^- contamination from manure were not found.

Nitrogen from rain water

Nitrogen from wet or dry fallout mainly occurs in the form of nitrate (NO_3^-) and ammonia (NH_4^+). Analyses of NH_4^+, NO_3^- and Cl^- in rain water in the investigation are summarized in Tab. 7-1. Assuming a complete oxidation of NH_4^+ in the soil as to Eq. 7.2, a total mean amount of 7.16 mg NO_3^- enters the soil per liter of rain. Considering rainfall amounts in the order of 450 mm/a, this would translate into an annual NO_3^- input of 32.2 kg/ha, which is subsequently taken up by flora and fauna and/or leached to the groundwater. Due to the lack of surface runoff, only little nitrate amounts are suspected to be lost surficially (chapter 3).

Tab. 7-1: Rain water analyses of Serowe and Orapa.

Date	**NO_3^- (mg/l)**	**NH_4^+ (mg/l)**	**Cl^- (mg/l)**	**Location**	**Source**
05.12.02	2.17	1.00	4.76	Serowe, Botswana	Schwiede, unpublished
07.12.02	2.61	0.77	1.33	Serowe, Botswana	Schwiede, unpublished
01.02.01	5.6	1.6	4.34	Orapa, Botswana	Matthes, 2002
Mean	3.46	1.12	3.47		

It has to be noted that these nitrate values rely on 3 measured samples only. As recharge is only in the order of 1 to 10 mm (DeVries and Simmers, 2002, Selaolo, 1998, and chapter 3.5.3), significant enrichment of nitrate through evaporation and evapotranspiration is expected in the study area. However, nitrate concentrations found in the groundwater are by far lower than expected, if strong evaporative enrichment is assumed to account for the big difference between rainfall amounts and recharge. Actual evaporation rates are not known for the study area to provide exact estimates. Average potential evaporation rates are higher than precipitation amounts and would not allow recharge. However, high intensity extreme rainfall events of short duration permit an exceedance of potential evapotransporation on a short-term basis and may lead to potential recharge through transport via preferential flow paths (Selaolo, 1998 and chapter 3.2). Empirical approaches such as the comparison of chloride values in rain with those in soil water of 1 m depth yielded an approximate enrichment factor of 30 for chloride during investigations in the Serowe area (Schwiede, unpublished), while nitrate enrichment yielded an approximate factor of 1.5, owing to reactive processes that influence nitrate in the soil (N cycle).

To investigate the role of evaporation in the development of nitrate concentrations in the subsurface nitrate concentrations were modeled with *PhreeqC-2* (Parkhurst, 1995) for different degrees of evaporation. Depending on the re-

charge process that is assumed, evaporation may play a major role. If a slow temporally and spatially homogeneous infiltration process is assumed, evaporation plays a more significant role than when assuming infiltration via preferential pathways and/or isolated heavy rainfall events. For the earlier scenario, rain water from the study area was used as an initial solution for calculation. An equilibrium with calcrete was assumed under open system conditions prior to evaporation. With increasing evaporation nitrate concentrations rose in solution. At 80 % evaporation the WHO threshold of 50 mg/l was exceeded. As of the point where approximately 90 % of the infiltrated rain water was evaporated, nitrate concentrations started rising sharply to concentrations of 110 mg/l. To account for 220 mg/l, which is near the observed maximum concentrations in the groundwater, an evaporation of 95 % needs to be assumed. At the same time, Cl^- would have risen to 43 mg/l (90 % evaporation) or 87 mg/l (95 %) respectively, which lies above the observed concentrations in the groundwater. As seen, the observed nitrate concentrations in the groundwater could theoretically be reproduced. It has to be noted, that the content of inorganic N of precipitation used in the calculations is rather in the upper range of values reported in the literature. Using lower N concentrations in rain water (e.g. 3 mg/l as given by Heaton (1984) from mean annual values) would necessitate a higher evaporation rate to reproduce the nitrate concentrations observed in the groundwater (98.5 %). This would then yield higher Cl^- values (283.6 mg/l), which in turn would be well above the observed Cl^- values in the groundwater. In addition, this process neglects that preferential-flow type recharge is likely to deliver lower concentrations of dissolved species, though this recharge type accounts for more than 50 % of the total recharge in semi-arid regions (DeVries and Simmers, 2002 and chapter 7.2). This would render the assumption that high nitrate values are only a function of evaporation more unlikely.

Yet, the assumption of evaporation alone neglects the role of the biogeochemical cycle in the soil. As can be seen from the investigation of the stable isotopes of nitrate (and the next section), most of the nitrate found in the water actively took part in the soil N cycle, which may theoretically reduce the nitrate amount that can be leached to the groundwater. However, additional N amounts are introduced to the soil by the fixation of air nitrogen by N-fixing plants in the study area (chapter 3.3.2). In addition, the N isotopic investigations show that nitrate from atmospheric deposition does not directly enter the groundwater, as established by the combined information from ^{18}O and ^{15}N in

the NO_3^- compound. Besides this, the investigation of the stable isotopes ^2H and ^{18}O in groundwater showed that evaporation of rain water plays a minor role for water that enters the aquifer. Both of the latter arguments point to the fact that nitrate enrichment in groundwater cannot exclusively stem from direct input though dry and wet fall from the atmosphere.

Nitrogen from soil

N in soil can occur in several forms: Fixed as N_{min}, as organic N in plants through fixation of atmospheric N and in bacteria associated with leguminoses, or in soil fauna (Eq. 2.4 to 2.7 and chapter 2.2). The transformation of organic N into nitrate leads to an acidification (Eq. 7.3).

(7.3) N from biomass + soil gas $\rightarrow NH_4^+ + 2\ O_2 \leftrightarrow NO_3^- + H_2O + 2\ H^+$

The drop in pH can be buffered by calcite equilibrium reactions in the soil and/or groundwater (Eq. 5.10 to 5.13). The so formed nitrate can be leached into the groundwater. To verify whether this process is likely to occur in the investigated groundwater system the process was modeled with *PhreeqC-2*. A solution of rain water composition was set in contact with nitrogen from biomass (Tab. 7-1). This water was subsequently put into equilibrium with calcite. Results show that though the N transformation leads to a drop in pH, and a subsequent buffering by calcite originating from calcretes leads to a rise in pH in the water. The modeled pH ranges in the order of 7.0 are consistent with measured values of Ca-HCO_3 type groundwaters from Serowe.

It has to be noted that oxic conditions are required to successfully perfom calcite buffering and a release of N from biomass in the described process, indicating that this process is likely to occur in the unsaturated zone where carbonate stems from calcretes. This also implies that this nitrogen source is not to be found under saturated, oxygen-limited conditions.

Investigations of natural soil background nitrate concentrations away from intense grazing areas yielded values of more than 100 mg/l in depths of greater than 10 m (M. Schwiede, personal comm.). This implies a vast pool of organic nitrogen that is potentially prone to leaching into the groundwater, which is in accordance with recent findings in the literature (Walvoord et al., 2003), and measured leachable fluxes of 4 to 40 kg/(ha·a) NO_3-N below the rooting zone in the study area (Schwiede, in prep., and later this chapter). In

the Kalahari, nitrate of natural origin was already suspected in a deep aquifer by Heaton (1983). Further evidence for the origin of nitrate in the unsaturated zone was found in the investigation of the stable isotopes of nitrate (next section).

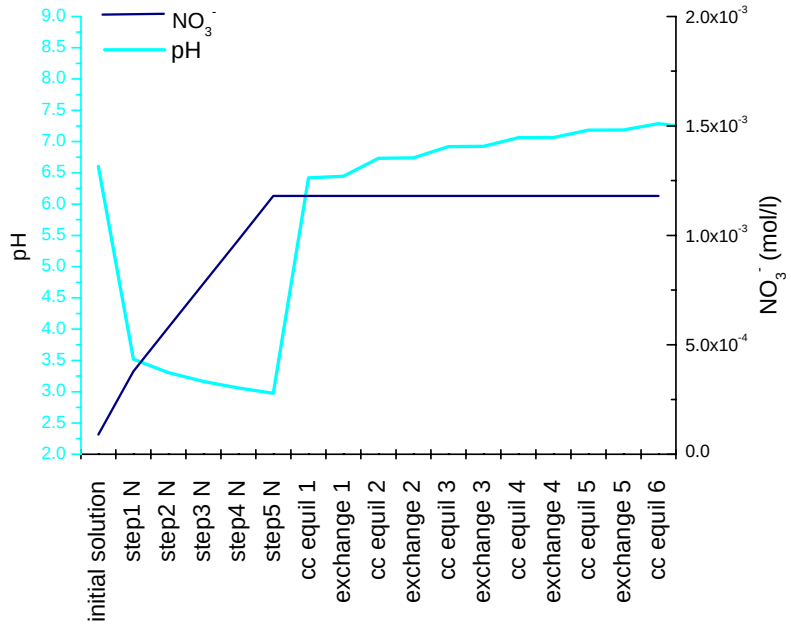

Fig. 7-1: Modeled N species and pH evolution during N_{min} oxidation in the unsaturated and saturated zone (addition of nitrogen from a total of 1.5 mmol biomass as $C_{10}H_{20}O_{10}N$ in 5 steps = 'step[number] N', calcite equilibrium = 'cc equi', ion exchange = 'exchange').

Stable isotopes of nitrate (^{15}N-NO_3^- and ^{18}O-NO_3^-) in groundwater

A useful tool in the investigation of nitrate sources is the analysis of the stable isotopes of nitrate ^{15}N-NO_3^- and ^{18}O-NO_3^- (Kendall and McDonnell, 1998, Clark and Fritz, 1997). The isotopic composition of nitrate in recharging

groundwater depends on source materials, reactions during formation and subsequent biogeochemical alterations (Böhlke, 2002). The combined information of ^{15}N and ^{18}O proved to be a useful tool for the identification of processes in the aquatic environment, as the individual signals are sometimes ambiguous (Kendall and McDonnell, 1998, Clark and Fritz, 1997). Atmospheric N_2 is defined as the ^{15}N standard ($\delta^{15}N_{Air}$ = 0 ‰). Microbial nitrogen fixation results in only minor fractionation in the order of 1 to 5 ‰. Further fractionation up to an additional 10 ‰ is found in manure as a result of volatilization of NH_3 as well as the passage of N through the food chain, resulting in heavier nitrogen isotopes in the residual waste. ^{18}O in biologically formed soil nitrate has empirically been proven to only contain one atom from atmospheric oxygen. The other two oxygen atoms in nitrate stem from water, which is considerably more depleted in ^{18}O. Isotope signatures are changed upon denitrification due to isotope fractionation. Denitrification appears to have lesser effects on ^{18}O in nitrate than on ^{15}N, with the change in $\delta^{15}N$ being about twice the change in $\delta^{18}O$ (Amberger and Schmidt, 1987). When denitrification occurs via organic carbon oxidation, a reciprocal $\delta^{18}O$ depletion in the DIC can be observed (Clark and Fritz, 1997). The individual fractionation fields for $^{15}N\text{-}NO_3^-$ and $^{18}O\text{-}NO_3^-$ are depicted in Fig. 7-2.

The $\delta^{15}N\text{-}NO_3^-$ of measured groundwater samples from Serowe form a relatively uniform group between 2.5 to 8.2 ‰ (Fig. 7-2) with a mean value of 5.4 ‰. The $\delta^{18}O\text{-}NO_3^-$ values generally range between 2.3 and 10.3 ‰ with a mean value of 7.1 ‰. The maximum values are consistent with the hypothesis that one oxygen atom of the ^{18}O from nitrate stems from air (+23 ‰) while two oxygen atoms stem from water (-6 ‰) (Kendall and McDonnell, 1998). Nitrate in groundwaters of this $\delta^{15}N$ range is likely to result from natural accumulation processes in the soil (Aranibar et al., 2003, Heaton, 1983). It appears that elevated nitrate concentrations that are found in the groundwater do not stem from enrichment through direct atmospheric dry or wet fall, as this process would show heavier $^{18}O\text{-}NO_3^-$ values. Neither can an influence of manure or of fertilizer be seen in the analysis of the groundwater samples. The lack of anthropogenic pollution is consistent with the observed long residence times in the unsaturated zone, as suggested by tritium below the detection limit in all investigated groundwater samples (chapter 6.2). Some Serowe samples have slightly higher $\delta^{15}N$ signals around 8 ‰, accompanied by slightly elevated $\delta^{18}O$ values of up to 10.3 ‰. These elevated $\delta^{15}N$ and $\delta^{18}O$ values indicate a moderate denitrification trend in those samples. This coin-

cides with the longer residence times of those waters suggested by their low ^{14}C contents as opposed to higher ^{14}C contents in waters containing more nitrate. The denitrification trend is, however, more pronounced in groundwater samples from Orapa, where $\delta^{15}N$ reaches 5.4 to 12.8 ‰ and $\delta^{18}O$ between 7.0 and 12.3 ‰.

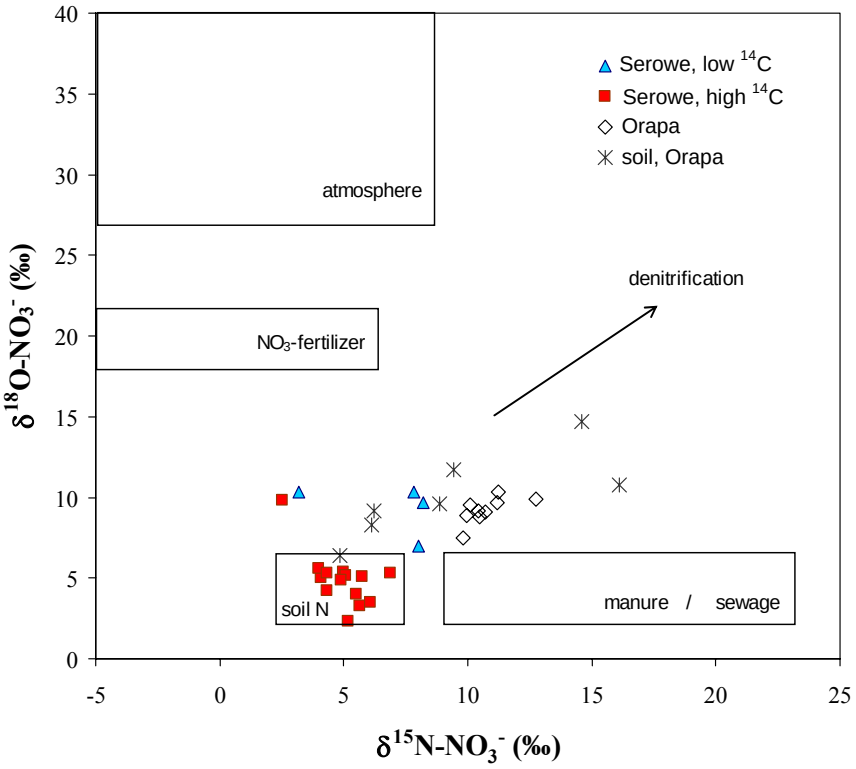

Fig. 7-2: Plot of $\delta^{15}N\text{-}NO_3^-$ versus $\delta^{18}O\text{-}NO_3^-$ for groundwater and soil water samples from Serowe and Orapa. Symbols are subdivided regionally and according to their ^{14}C content, where 'high ^{14}C' represents $^{14}C > 40$ %-mod. and 'low ^{14}C' represents $^{14}C < 20$ %-mod. The fractionation fields plotted in the diagram indicating the origin of nitrate are taken from Kendall and McDonnell (1998) and do not represent sharp boundaries but rather fields from empirical results.

As seen from Fig. 7-3 no significant correlations could be found between nitrate concentrations and ^{15}N as all samples behave quite homogeneously. Especially samples from Serowe show a very broad concentration range at a very narrow range of $\delta^{15}N$ values. The samples from Orapa show a slightly wider range. $\delta^{15}N$ - $\delta^{18}O$ relations indicate different degrees of denitrification for these samples. Yet, the nitrate concentration-$\delta^{15}N$ relation shows that some of the groundwater samples from Orapa exhibit high nitrate contents and appear to represent a mixed $\delta^{15}N$ -, $\delta^{18}O$-NO_3^- signal influenced by surficial nitrate input e.g. from manure. The lack of significant trends in relation to nitrate concentrations was also found for ^{18}O (not shown).

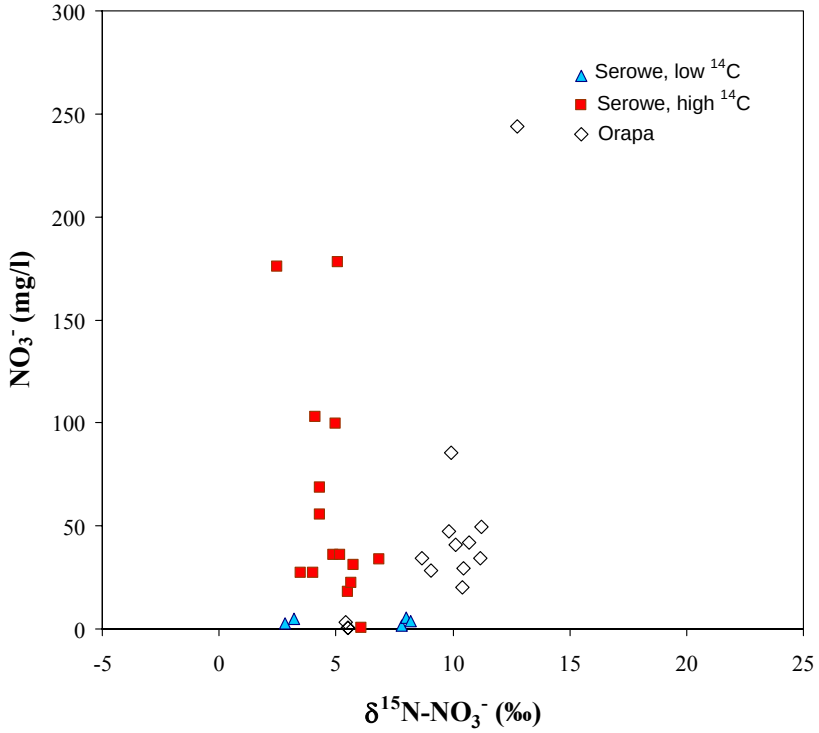

Fig. 7-3: Relations between $\delta^{15}N$-NO_3^- and nitrate concentrations (mg/l) for groundwater samples from Serowe and Orapa. Symbols are subdivided regionally and according to their ^{14}C content, where 'high ^{14}C' represents ^{14}C > 40 %-mod. and 'low ^{14}C' represents ^{14}C < 20 %-mod.

Stable isotopes of nitrate ($^{15}N\text{-}NO_3^-$ and $^{18}O\text{-}NO_3^-$) in the topsoil
Measured soil water samples show δ^{15}N-nitrate values between 4.8 to 14.6 ‰ and δ^{18}O-nitrate of 6.4 to 14.7 ‰ (Fig. 7-2). Those values lie off the fractionation field shown for soil. Interestingly, soil samples from the immediate vicinity of acacia trees and termite mounds showed a lighter signal in both ^{15}N and ^{18}O than samples taken close to small salt pans. The heavier ^{15}N and ^{18}O signals of soil samples from the pans may point to small-scale surface runoff, where minor amounts of organic matter may collect within the center of the pan. As to the lack of vegetation in this area that may consume nitrate, and to slower infiltration of water as to the concentration of small-sized material which may create reducing conditions, a denitrification signal can be found for the pan samples. However, soil samples were taken from very shallow depths (0 to 30 cm) and may show different signals than the groundwater nitrogen as they represent nitrogen that is still actively involved in soil N cycling. This nitrate might never reach the groundwater as it is retained or consumed by flora and fauna and is not leached to the groundwater. A different susceptibility to flushing of different nitrate pools is also suggested by Kendall and McDonnell (1998). These authors also consider artefact value production of soil water analyses caused by i) disturbance of the small biologically active pool caused by sampling or ii) by the extraction procedure or extractant, which cannot be fully ruled out in the case of the investigated samples.

Nitrogen from rocks
From the investigation of rock material from the Ntane sandstone aquifer as well as from overlying (Stormberg Basalt and Kalahari Beds) and underlying formations (Mosolotsane Fm.) low N contents of 0 to 0.08 % were found that do not appear to influence nitrate concentrations measured in the groundwater. Highest contents were recorded in phyllosilicates within mudstone layers in the lower parts of the aquifer, which however appear to be firmely bound to the minerals, as established in batch experiments (chapter 5.1). This is in accordance with literature findings that generally elevated nitrogen concentrations in rocks are associated with sediments (and metasediments) (Holloway and Dahlgren, 2002). Additional N occuring in the topmost core material within the Stormberg Basalts and Kalahari Beds was found to represent temporarily immobilized N salts, representing unsaturated conditions. If recharge takes place, those salts can be remobilized and are leached to the groundwater. Within the saturated zone, nitrate salts do not play a significant role, as they

would already be in solution and be discharged due to the high solubility product of nitrate (chapter 2.3). In addition, the N release from rocks is generally higher under surface conditions rather than in groundwater systems, as surface-exposed bedrock experiences stronger weathering rates (Lowe and Wallace, 2001). In the studied system, saturated conditions prevailed for several thousand years (Verhagen, 1991), making N release less likely. Hence, the aquifer material does not appear to contribute significantly to nitrate concentrations in the groundwater.

Nitrogen from uprising groundwater

Potential nitrate input can stem from uprising groundwater that enters the Ntane Sandstone Aquifer. In the investigated aquifer system groundwater from the lower lying Mosolotsane aquifer connects to the Ntane Sandstone Aquifer in parts of at least one study area (Orapa). The uprising groundwater is of a Na-Cl type as summarized in chapter 5.2.3.2 and confirmed by Rahube (2003). It has very high specific electric conductivities and has generally no observable to low nitrate concentrations. In areas where an enhanced hydraulic connection and/or the absence or thinning of Ntane layers was observed (chapter 3.4.2), the nitrate concentrations in the groundwater were very low. For this reason, potential nitrate input from lower-lying aquifers is assumed to be negligible in the study area.

Nitrogen from perched aquifers

Nitrate levels were found to be temporarily elevated in shallow perched aquifers in the Kalahari Beds as described in chapter 5.2 e.g. for hand-dug well HDW-3 in Orapa. Also, in Orapa some cattle post boreholes showed elevated nitrate concentrations, which proved to be influenced by surficial contamination. In Serowe these observations at cattle posts could not be confirmed. This is likely to owe to two reasons: i) the distance between surface and groundwater table being greater in Serowe than in Orapa. Even cattle post boreholes that tend to be only drilled into the topmost part of the aquifer are deeper in Serowe than in Orapa. Nitrate pollution thus takes longer to migrate into the groundwater. ii) Perched aquifers that are observed in the Orapa area have only rarely been reported in Serowe (only Dukokola CP) and thus appear to be of far less importance in the temporal storage of surficial nitrate contamination. Yet, they represent the possibility of additional N input to nitrate containing groundwater from the Ntane Sandstone Aquifer.

Significance of denitrification in the groundwater

Denitrification appears to play a minor role in the spatial distribution pattern of nitrate in groundwaters of the Ntane Sandstone Aquifer near Serowe. Autotrophic denitrification is rendered unlikely due to the quasi absence of pyrite as found from the investigation of rock samples from aquifer material to mediate denitrification (Eq. 2.11), in addition to the very low abundance of sulfate. In addition, a systematic decrease of nitrate along the flow path in Serowe is lacking. Heterotrophic denitrification would be possible in the aquifer, though sediment organic C content is low (less than 1 %). Assuming a porosity in the order of 7 % and a density of 2.65 g/cm^3 this would translate into the ability to reduce 0.55 mmol NO_3^-/l. Additional DOC input from leaching from soil horizons and burrowed organic material (Chapelle, 1993) may be expected locally, though evidence was only found of maximum concentrations of 0.8 mg/l in the groundwaters as NPOC. However, apart from slight indications for heterotrophic denitrification at one borehole (BH8471), the crucial constraint for denitrification in Serowe is the fact that oxygen is present in the groundwater as an electron acceptor. Groundwaters from Orapa, however, appear to provide appropriate conditions for nitrate reduction (especially where the influence of perched aquifers is lacking). This is inferred from the investigation of the stable isotopes of nitrate and from the absence of oxygen, the presence of carbon sources to mediate denitrification and appropriate redox potentials (chapter 5).

7.3 Migration of nitrate in the subsurface

Though often neglected in the investigation of natural nitrate enrichment mechanisms, the presence of secondary processes in the aquifer has proven to be of crucial importance in the distribution pattern of nitrate in the Ntane Sandstone Aquifer. One issue is the influence of the aquifer structure, which is often inadequately recognized in the investigation of the enrichment and fate of dissolved species (Cook et al., 2005). An even more important issue especially in water-limited semi-arid settings are recharge processes and rates (e.g. Austin et al., 2004, Stute and Talma, 1997), which impose crucial constraints in the studied system, where groundwater nitrate primarily originates in processes in the unsaturated zone. In the following, the dominant flow and transport processes relating to the Ntane Sandstone Aquifer and their impact on nitrate leaching and transport are discussed and evaluated. Most of the results shown here relate to study area 1 (Serowe), as this area was chosen as

the focus for studying flow and transport in this project. In addition, Serowe represents the recharge area of the investigated system, an understanding of which is crucial for the understanding of nitrate dynamics in the entire Serowe-Orapa groundwater system. Thus, samples from Serowe provide better information on the migration of nitrate towards the groundwater, whereas samples from study area 2 (Orapa) exhibit mixed signals influenced by processes in the unsaturated and the saturated domain of the subsurface.

Recharge mechanisms and residence times

The fact that nitrate stems from unsaturated zone processes (chapter 7.1) means that recharging water carries a nitrate load into the groundwater. The investigation of natural isotopes and environmental tracers in groundwater revealed the existence of ***active recharge*** (chapter 6.2) providing minor amounts of recharge to the aquifer. This is in accordance with results from other studies in the literature (Lubcyzinski, 2000, Verhagen, 1990, Mazor et al., 1977). The fact that active recharge takes place also shows that nitrate is carried to the groundwater under present conditions. This should be reflected in a correlation of nitrate with tritium as nitrate is transported advectively as a dissolved species in the (pore) water. However, tritium was quasi absent in the investigated groundwater samples and only little amounts just above the detection limit were found. This indicates that nitrate concentrations in the groundwater do not reflect very recent amounts of nitrate in the soil or present land-use conditions, but rather conditions at least more than 50 years ago. Yet, the investigation of chlorofluorocarbons and sulfur hexafluoride showed detectable amounts of these freons in the groundwater. Freons usually reflect diffusive gas transport through the unsaturated zone (Cook and Herczeg, 2000), which does not necessarily relate to the advective transport of a water body by which nitrate may migrate to the groundwater. However, calculations of diffusion lengths in the saturated zone gave evidence that advective transport of freons dominates in the saturated zone, indicating active recharge (chapter 6.2.3.3). Apparently, the weak signal given by tritium is diluted and thus not detectable.

To estimate whether present recharge conditions are suitable to explain the nitrate content found in the aquifer, an estimation of the time scale needed to refill the aquifer with present-day recharge rates was performed. Using an average aquifer thickness of 100 m with a porosity of 7 % (chapters 6.1 and 3.4) this simplified ***water balance*** calculation yielded reservoir exchange

times between 700 to 7000 years for typical recharge rates in the Kalahari between 1 mm/a and 10 mm/a (DeVries et al., 2000, Selaolo, 1998 and chapter 3.5.3) assuming steady-state conditions for the aquifer's water budget. Considering typical residence time scales of up to several thousands of years obtained from own ^{14}C data and conceptual (flow) modeling studies for the Ntane Sandstone Aquifer, the water balance calculations suggest that laterally averaged recharge rates tend to be in the lower range of the values reported in the literature. The calculated water body and the median nitrate concentrations in the order of 10 mg/l measured in groundwater from Serowe (chapter 5.2.3) translate into an approximate nitrate load of 700 kg/ha in the groundwater at the given aquifer thickness of 100 m. Considering this nitrate load with the calculated time needed to refill the aquifer an average mass flux of 0.1 to 1 kg/(ha·a) of nitrate would be needed to obtain the nitrate amounts observed in the aquifer. For comparison: Assuming the maximum nitrate concentration observed in the groundwater (approximately 200 mg/l) as representative concentration in the recharged water, a nitrate flux of 2 to 20 kg/(ha·a) could be achieved (for recharge rates of 1 to 10 mm/a). Taking into account mass balance calculations for the nitrate budget supplied by precipitation which yields 32.2 kg/(ha · a) as depicted earlier this chapter, a net accumulation of nitrate in the unsaturated zone by at least a factor 1.5 may be assumed – bearing in mind the simplifications in this approach, but confirming the existence of a nitrogen pool in the unsaturated zone.

However, one has to distinguish between the nitrogen pool provided by precipitation, and the nitrogen pool below the bioactive (rooting and surface) zone. Only the latter can actually reach the groundwater, as the earlier will be strongly impacted by contributions and withdrawal by soil flora and fauna which so far has been neglected in this approach. Yet, as shown in the first part of this chapter, the nitrate found in the groundwater has been actively involved in the soil cycle (chapter 7.1) which means that the biogeochemical cycle accumulates nitrate if steady-state conditions are assumed. In addition, Walvoord et al. (2003) found that in semi-arid to arid regions substantial amounts of nitrogen from the soil pool can be leached beyond the reach of roots, which the authors account for by deep-wetting events. Comparing their data with soil water nitrate concentrations from the literature these authors report on strongly varying amounts of nitrogen in the soil depending on the sampled location. Nitrogen pool magnitudes were in the range of 30 to 13,600 kg/ha NO_3-N, which corresponds to 132 to 60,000 kg/ha NO_3^-. Other authors

report that the values are only at lower ranges in the order of 200 to 500 kg/ha NO_3^- for semi-arid settings (Jackson et al., 2002, 2004). Still, these data demonstrate that nitrate pools in the unsaturated zone bear the capability for supplying sufficiently high nitrate fluxes into the groundwater for an extended period of time. In addition, estimates for the present study area yield nitrate fluxes of approximately 4 to 40 kg/(ha·a) being leached out of the soil root zone towards greater depths (Schwiede, in prep.). These numbers are in good agreement with the flux range estimated above based on groundwater concentrations and recharge rates, again implying that the nitrate found in the Ntane Sandstone Aquifer originates in a nitrate pool in the unsaturated zone. These calculations show that although challenged by heterogeneities imposed by e.g. the texture, structure and/or water content of the unsaturated zone, different recharge processes (i.e. diffuse processes vs. piston flow, e.g. DeVries and Simmers, 2002) and potential zones of higher nitrogen concentrations in the soil water caused by point sources and/or soil biota, it is generally possible to explain the nitrate leaching rate and the observed nitrate concentrations in the groundwater. With the assumption that the aquifer system has formed under (constant) conditions resembling those presently observed, the nitrate mass and concentrations may thus be explained.

However, this scenario cannot explain several facts found from the investigation of the groundwater, showing that the approach of constant (steady-state) conditions cannot readily explain the situation encountered in the Ntane Sandstone Aquifer. Those facts relate to the observed water chemistry and isotopic signatures of the groundwater, which are described in detail in chapter 6.2 and are shortly summarized in the following:

i) The existence of (at least) ***two groundwater types*** which contain different nitrate concentrations has been established in the groundwater. One groundwater type of low ^{14}C content (less than 20 %-mod., group 1), a Na-HCO_3 water type with low mineralization and low nitrate contents; and one group of elevated ^{14}C content (40 to 80 %-mod., group 2) of a Ca-HCO_3 type with high mineralization and high nitrate contents. Group two comprises two subgroups: A Ca-(Mg-)HCO_3 signature can be observed for ^{14}C-rich end members, while a Na-HCO_3 signature was found in waters of lower ^{14}C contents in this group, indicating mixing and/or increased ion exchange. The ^{14}C-rich end member is associated with higher nitrate concentrations than the ^{14}C-poorer end member of group 2. The investigation of ^{14}C and of the hydrochemical

evolution showed that the two components formed independently under different conditions. Observations such as low specific electric conductivities associated with group 1 as opposed to higher values for group 2 contest the assumption, that group 1 developed from the modern group 2. Though accurate age determinations remained challenged by uncertainties in the (initial) carbonate chemistry, ^{14}C could be used as a qualitative age indicator, supported by own noble gas investigations (chapter 6.2.3.5) and literature findings (Kulongowski and Hilton, 2004, Verhagen, 1991), indicating that elevated nitrate is associated with rather recent conditions in the order of hundreds to thousands of years as opposed to several thousand years, which was calculated for the samples of medium to poor ^{14}C content. Noble gas temperature studies from comparable aquifers in the Kalahari (Kulongowski and Hilton, 2004, Stute and Talma, 1997) and paleoclimatic development reconstructed from different climate proxies (chapter 3.2.3) in the Kalahari give evidence for ***climate transition*** from pluvial to more arid phases during the Pleistocene, with several wet phases in the Holocene. Comparing own data with these studies suggests a relation of wet climatic conditions with low nitrate concentrations, and a connection of drier conditions to higher nitrate concentrations in the groundwater, as corrected ^{14}C ages correspond reasonably well with the time of the last pluvial phase (12,000 to 15,000 years BP) and wetter phases in the Holocene, potentially around 6,000 to 8,000 years BP (chapter 3.2.3).

ii) Groundwater investigations revealed the presence of ***different recharge mechanisms***, as found from investigations of the dissolved ^{20}Ne content (chapter 6.2). One mechanism shows low recharge rates as revealed by low neon excess values that maintain neon concentrations at atmospheric solubility equilibrium, while the other mechanism is of a high rate as revealed by high neon excess values. Recharge under semi-arid conditions is usually anticipated to be discontinuous in space and time (Külls, 2002 and DeVries and Simmers, 2002) with only high intensity rainfall events providing infiltration to greater depths (Aeschbach-Hertig et al., 2000, Selaolo, 1998), which is also confirmed by own stable isotope investigations (chapter 6.2.3.2). Other authors attribute only greater than 50 % of the recharge to preferential flow, while the remaining portion migrates to the aquifer in a slow, diffuse process (DeVries and Simmers, 2002). With the present study it was found that the type of recharge mechanism is closely linked to the encountered nitrate content in the groundwater (chapter 6.2.3.5): High nitrate concentrations enter the

aquifer with low recharge rates, while nitrate concentrations are lower in higher recharge rates (chapter 6.2), showing that nitrate concentrations are closely linked to recharge dynamics. Whether these processes that yield different recharge rates co-occur at present conditions and only indicate different mechanisms (diffuse recharge or preferential flow), or if they are a function of time and consequently a function of (paleo)climatic development cannot be revealed from the investigation of neon isotopes alone.

However, a correlation of the neon data with ^{14}C was found, where high neon is associated with low ^{14}C, and low neon is associated with high ^{14}C content implying temporal relations. This indicates low rate recharge having high nitrate concentrations and high ^{14}C content, and high rate recharge having low nitrate concentrations and low ^{14}C content. Provided that ^{14}C can be used as a reliable age indicator, the different recharge trends imply temporal, and thus (paleo-)climatic relations, indicating an increasing trend in nitrate input concentrations in the recharged water from past wetter conditions towards present semi-arid conditions. As waters of high ^{14}C have high nitrate concentrations, this indicates that under present conditions high nitrate concentrations enter the groundwater. Surprisingly, neon-nitrate relations indicate that those high nitrate containing waters have low excess air contents and have been formed under low rate recharge. Today, most of the recharge occurs via preferential flow (DeVries and Simmers, 2002) and only to a lesser extent by diffuse infiltration. Preferential flow was suspected to constitute the high rate process, as prefential flow appears to be the principal recharge mechanism in semi-arid regions (DeVries and Simmers, 2002 and DeVries, 1984). Yet, excess neon contents in groundwater can only be used to distinguish recharge processes of different rates, but cannot be used to identify the exact process. Maybe preferential flow addressed in the literature cited above only occurs in the topmost meters of the unsaturated zone and does not provide any information on the recharge mechanism within the remaining part of the unsaturated zone. Thus, the total travel time of the recharge to the groundwater table is not a function of processes within the uppermost part of the unsaturated zone. The measured neon contents are apparently more sensitive to total recharge amounts (or average annual recharge rates) rather then specific recharge mechanisms. The latter would explain the low neon content found in the younger fractions of the groundwater as annual recharge rates supposedly dropped between former wetter conditions and the semi-arid conditions found today.

Including the groundwater types and recharge regimes into the earlier developed scenario would require a greater nitrate flux to groundwater at present day conditions as less time would be available to provide for the nitrate load in the aquifer, and, consequently, an increased average pore water concentrations for the recharged water. However, calculations earlier this chapter showed that using present day recharge rates and peak concentrations found in groundwater a nitrate flux of 2 to 20 kg/(ha·a) could be achieved. This would allow to deliver the nitrate mass that is presently found in the aquifer within 35 to 350 years, only. This again might lead to the assumption that the presently leached nitrate pool - if not stemming from a former very large pool - is constantly refilled. In total, this scenario can explain all observations found from the investigation of groundwater in the Ntane Sandstone Aquifer. It explains nitrate concentrations, the nitrogen mass in the aquifer, but also isotopic signals that reflect recharge regimes and residence times as well as the identified water types. However, this scenario still has to be considered a best estimate, as nitrogen fluxes, especially related to the vegetation and soil nitrogen cycle in semi-arid setting still often lack quantitative evidence (Walvoord et al., 2003). Also, water fluxes in the unsaturated zone under semi-arid conditions still need to be understood in detail, as they strongly impact on the subsurface transport of dissolved species (Austin et al., 2004). In addition, heterogeneities in the unsaturated zone may occur, that result in strong spatial variabilities of nitrogen input rates, which contribute to the clustered concentration distribution in the aquifer (cf. outliers as discussed in the neon-nitrate relations in chapter 6.2). In addition to heterogeneities in nitrate input induced by unsaturated zone processes as discussed above, the Ntane Sandstone Aquifer is not only characterized by low recharge and deep groundwater levels, but also is a fractured aquifer, which again induces more (spatial and temporal) heterogeneity to the system as will be explained in the following.

Nitrate transport in the fractured aquifer

The Ntane Sandstone Aquifer is characterized by a structural complexity in the form of hydraulically influencing faults and lowly permeable dolerite dykes (chapter 3.4.2) that divide the region into horst and graben structures (SGAB, 1988). Own investigations indicate that there is a complex exchange between highly permeable fracture zones, dykes and sparsely fractured bedrock (chapter 5.3 and 6.1). The structural complexity prohibits a simple interpolation between single sampling points to derive the spatial distribution patterns of nitrate to reconstruct the nitrate sources. Yet, results from a concep-

tual modeling study using the FE model package Rockflow (Kolditz et al., 2001) were able to reproduce the inhomogeneous structure of the aquifer, resulting in a broad range of residence times and flow directions which are mainly controlled by the ***different velocities*** inferred from ***fractures*** (2,000 m/a) and ***matrix*** (0.6 m/a). The different velocities may account for the observed heterogeneous distribution of nitrate concentrations and challenge the distinguishment between autochthonous and allochthonuous sources. Remote recharge areas that potentially deliver water from other geological conditions that differs from the one of the Ntane Sandstone Aquifer can be ruled out as to the flat topography of the Kalahari Basin, the observed relative hydrochemical homogeneity and the limited flow distance as indicated by the presence ^{14}C in all groundwater samples. The range of residence times obtained by the model is confirmed by results from isotope hydrology (chapter 6.2). Yet, it has to be noted that the times obtained from the investigation of isotopes represent mean residence times of dissolved substances rather then real ages of water (Cook et al., 2005). ***Matrix diffusion*** leads to a retardation of dissolved substances in immobile parts of the aquifer (dead pores and within the pore volume), that only exchange by molecular diffusion with mobile water (Pfingsten, 1990, Neretnieks, 1980). However, for the investigation of nitrate this approach is suitable, as nitrate is transported as dissolved substance in the water body, and measured concentrations only reflect the mobile nitrate.

Besides through modeling studies, the impact of the fractured aquifer has also been revealed in the investigation of vertical hydrochemical zonations (chapter 5.3). The investigations identified inflow of water from fractures into existing redox zonations. Depending on the fracture connection to different aquifer zones, nitrate may e.g. be delivered from near the water table into deeper parts of the aquifer, which obscures the original nitrate content in that part of the aquifer.

Temporal variations of nitrogen concentrations

Reliable historical time series of nitrate concentrations of several months to years were unfortunately not available for the study area to yield the desired information on nitrate development. Existing data from other studies often lacks adequate ionic balances, and recording long-term data was beyond the scope of this study. Yet, to obtain some temporal information, during the project, short-term observations of nitrate concentration development in groundwater from the Ntane sandstone aquifer were made during five 72-hour

pumping tests at a maximum pumping rate of 15 m^3/h. Results showed little or no variation of nitrate concentrations as a function of pumping time. Most of the boreholes did not show significant changes in any chemical parameter. The borehole (BH8480) that exhibited the most differences of water chemistry as a function of time is shown in Fig. 7-4.

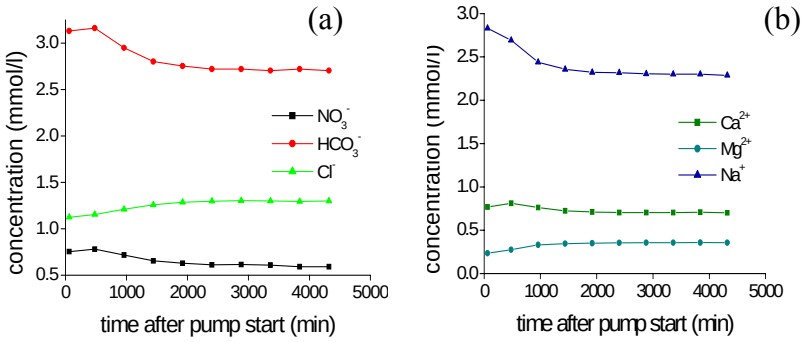

Fig. 7-4: Example of results from a chemical pump test at BH8480 (pump rate: 15 m^3/h, test duration: 72 h). Different water chemistry is attracted after 1000 min of pumping, shown for a) selected anions and b) selected cations. The data is shown for a Na-HCO_3 groundwater type.

For the shown borehole a slight decrease in nitrate concentrations can be seen, which however coincides with a stronger decrease in specific electric conductivities, indicating a higher total mineralization at the beginning of the pump test than at the end. If occurring, chemical variations of the water abstracted during the time-scale of these chemical pumping tests are expected to rather represent the attraction of water from fissure and fracture zones as opposed to pore water of the Ntane Sandstone (depending on the fracture connection of the individual borehole) than provide information on long-term development of nitrate concentrations in the aquifer. At most, the tests reflect the attraction of different components of the local groundwater stratigraphy as established in chapter 5.3. This is the case for the shown borehole, indicating mixing of groundwater components having different nitrate contents as inferred from aquifer stratifications at the sampled location, and not a short-term nitrate evolution in the aquifer. The chemical trend shown here represents an attrac-

tion of vertical hydrochemical zonation observed in the aquifer as a temporal sequence (chapter 5.3.2, Fig. 5-21) induced by pumping.

As described in chapter 5.2 stronger short-term variations of nitrate levels were found in some perched aquifers during this project, which are a result of the direct impact of rainfall events on the (shallow) wells, diluting former nitrate concentrations or providing nitrate input by contamination from the surface. Yet, the present data did not permit similar conclusions for groundwater from the Ntane sandstone aquifer.

7.4 Summary and conclusion

Hydrochemical and isotopic data from groundwater investigations of the Ntane Sandstone Aquifer in the Kalahari of Central Botswana suggest a close link between nitrate concentrations, residence times of groundwater and recharge conditions. High nitrate concentrations were recharged under drier (i.e. semi-arid) conditions while lower nitrate concentrations appear to be recharged under much wetter conditions. It is suggested that the differences are related to climatic change, as observed residence time differences lie within the ranges of past wetter phases. Results, however, also point to the existence of different recharge mechanisms: i) low-rate recharge delivering high nitrate concentrations and ii) higher rate recharge with low nitrate concentrations. Though higher rates were expected to be associated with preferential flow processes, which appear to be the principal mechanisms under present semi-arid conditions, ^{14}C investigations showed, that under present conditions high nitrate concentrations enter the groundwater. Thus the flow mechanisms controlling the recharge process in the topmost part of the unsaturated zone have less impact on the nitrate fluxes towards the groundwater compared to the dependency of the nitrate fluxes on the total (averaged) annual recharge amounts.

Despite the inhomogeneous distribution of nitrate concentrations in the aquifer very uniform ^{15}N- and ^{18}O-NO_3^- signatures were found in the groundwaters. These ^{15}N- and ^{18}O-NO_3^--signatures agree well with the typical range for naturally occurring soil nitrate (Kendall and McDonnell, 1998), which is in agreement with the absence of nitrogen sources within the aquifer. Neither is the bulk of nitrate concentrations recorded in groundwater in the Ntane Sandstone Aquifer significantly influenced by groundwater entering from over- or

underlying aquifers. If at all an influence is observed, then the nitrate concentration in the Ntane Sandstone Aquifer is diluted by the nitrate-free groundwater of the Mosolotsane Aquifer. This, however, only occurs in one local section of the Orapa study area. The aquifer material as well does not deliver additional nitrogen to the groundwater. The evidence of the active involvement of the nitrogen found in the groundwater in the soil nitrogen cycle, together with results from rock analysis suggests the existence of a nitrate pool in the unsaturated zone. It appears that the elevated nitrate concentrations that are found in the groundwater do not stem from enrichment through evaporation or from direct atmospheric deposition, as these process would be reflected in the ^{18}O and ^{2}H signatures of the groundwater and would show heavier $^{18}O\text{-}NO_3^-$ values and higher total mineralization.

The heterogeneous nitrate concentration distribution appears to be only little influenced by reactive processes within the aquifer. In groundwater samples from Serowe, denitrification appears to be of minor importance, which is in accordance with the predominantly oxic conditions and the absence of reaction partners, both of which do not favour denitrification. Consequently, only few samples showed a slight denitrification trend in their isotopic signal. The slightly denitrified samples have lower ^{14}C contents, indicating longer residence times (chapter 6). Samples from Orapa show a stronger denitrification trend (chapter 5), which is consistent with observations from hydrochemistry (higher reducing conditions) and from isotope hydrology (longer residence times).

However, detailed processes of nitrogen buildup in biomass or enrichment as point sources in the unsaturated zone could not be established within the scope of the present study. Yet, this issue is still under complex discussion in the literature especially for semi-arid settings (e.g. Aranibar et al., 2004, Walvoord et al., 2003). Soil processes that lead to a nitrogen enrichment are investigated in detail in a further PhD study within this project (Schwiede, in prep.) investigating the same study area. From the combination of both PhD studies it is clearly demonstrated that the unsaturated zone represents a long-term reservoir of nitrate, and that surface-near input concentrations are retarded but slowly leached into the groundwater.

8 SUMMARY AND CONCLUSION

In the presented study the origin and fate of nitrate in the Ntane Sandstone Aquifer in the Kalahari of Botswana was investigated, as elevated concentrations were reported that were suspected to stem from natural sources. A complex distribution of nitrate was found in the groundwater, with concentrations ranging from 0 to 219 mg/l. The occurrence of high nitrate concentrations is very heterogeneous and cannot be singularly attributed to the main flow path, especially not in the investigated fractured aquifer which is additionally affected by groundwater abstraction. Natural processes in the unsaturated zone have been identified to be the source of the nitrate found in the groundwater. The evidence of the active involvement of the nitrogen found in the groundwater in the soil nitrogen cycle suggests the existence of a nitrate pool in the unsaturated zone. This has proven not to stem from direct dry and well fall from the atmosphere evaporation alone as shown by the investigation of the ^{15}N- and ^{18}O-NO_3^- and by the investigation of ^{2}H-H_2O and ^{18}O-H_2O. Initially suspected contributions from the aquifer lithology as well as from uprising groundwater or inflow from perched aquifers into the Ntane Sandstone Aquifer have proven to be negligible. Also, present land-use does not (yet) influence the nitrate concentrations in the groundwater as concluded from slow travel times of water through the unsaturated zone.

An intense literature review reflected the importance of water transport in the unsaturated zone in the investigation of nutrient migration in semi-arid settings, a fact that also proved to be valid for the location investigated in the present study. In addition, the literature review showed that elevated nitrate concentrations that exceed the WHO guideline of 50 mg/l in the groundwater appear to be an often reported phenomenon in the literature in semi-arid regions. Though frequently resulting from anthropogenic pollution, several cases of elevated nitrate in groundwater have been reported, that are suspected to stem from natural sources.

The investigated Ntane Sandstone Aquifer is characterized by a double porosity, a strong heterogeneity in fracture patterns and low recharge in the order of 1 to 10 mm. The aquifer is mostly confined and is covered by a thick unsaturated zone (up to 100 m). The Ntane Sandstone is overlain by the Stormberg Basalt, which in turn is covered by the Kalahari Beds sand(stone) to siltstone

cover with local occurrences of calcretes and silcretes. The sandstone is mainly composed of quartz, plagioclase and kalifeldspar, with a partly carbonaceous, partly clay mineralitic and party absent cementation. Nitrogen sources in this lithology have proven to be negligible. Only in mudstone layers towards the base of the aquifer elevated nitrogen concentrations have been found to be bound to phyllosilicates, but which proved to be not easily releasable from the rock and thus do not contribute to the nitrate concentrations found in the groundwater. The hydrochemistry of the groundwater from the Ntane Sandstone Aquifer is quite homogeneous. It is dominated by a Ca- to Na-HCO_3 character near the recharge area in Serowe and a Na-HCO_3 to Na-Cl type towards the discharge area in Orapa. The Na-HCO_3 signature of the groundwater is a result of heterovalent ion exchange of calcium (from calcrete and sandstone matrix dissolution) with sodium from plagioclase weathering. Along the flow path, specific electric conductivities increase strongly from greater than 0.3 mS/cm to less than 60 mS/cm in Orapa. Only the multiparameter depth logging of hydrochemical parameters and the application of a wide range of environmental tracers revealed the presence of at least two independently formed groundwater components in the aquifer, which can mainly be hydrochemically distinguished by their calcium, sodium and nitrate content as well as specific electric conductivies. One groundwater component shows low specific electric conductivities, has low to absent nitrate contents and a Na-HCO_3 character, while the other groundwater component has a Ca- to Na-HCO_3 signature, elevated specific electric conductivities and higher nitrate concentrations. Hydrochemical profiles obtained from multiparameter depth logging in Serowe could be classified into three types: i) an ion exchange type of a Ca-HCO_3 signature at the top and a Na-HCO_3 signature and according redox conditions at depth, ii) an inverse sequence of type i) with a Na-HCO_3 groundwater type at the top and a Ca-HCO_3 type at the bottom of the profile, and iii) a type of insignificant changes over depth, where the observed chemistry is uniform over the entire borehole depth and where the chemistry encountered in the boreholes depends on the site location alone. In some profiles the impact of fracture induced water inflow into existing redox profiles was identified. High nitrate concentrations in the profiles were associated with a Ca-HCO_3 groundwater type. In Serowe, low nitrate concentrations proved to be determined by the water type rather than being a result of denitrification. Denitrification was only of quantitative importance in the Orapa study area.

Isotopic data from groundwater investigations of the Ntane Sandstone Aquifer, especially the investigation of ^{14}C data, confirmed the existence of the above discussed different groundwater components, their formation under different conditions, and the link between high nitrate concentrations, high ^{14}C content and a Ca-HCO_3 groundwater type (while low nitrate concentrations are connected to low ^{14}C content and a Na-HCO_3 type). It is suggested that the differences are related to climatic change, as observed residence time differences established by ^{14}C and noble gas investigations lie within the range of past wetter phases. The range of travel times of nitrate in the groundwater inferred from isotope analyses has also been confirmed in Rockflow modeling studies performed within this project. Results from the investigation of dissolved neon in groundwater, however, also suggest a close link between recharge mechanisms and nitrate concentrations: Low-rate recharge delivers high nitrate concentrations, while high-rate recharge delivers low nitrate concentrations. While the low-rate recharge processes agree with the present climatic conditions and with hydrochemical and isotopic findings from the groundwater sampled in this study, the scenario of locally high recharge rates under the same present climatic conditions is difficult to explain as the driving force for the introduction of lower nitrate concentrations into the groundwater. This again favors a climatic shift as an explanation for the different nitrate input concentrations to the groundwater.

As found from the investigation of the transient tracers chlorofluorocarbons, sulfur hexafluoride and tritium, evidence for (minor) active recharge was found in the aquifer, reflecting that nitrate is transported into the aquifer under near present conditions. Stable isotopes in the groundwater revealed that water for recharge is only supplied by heavy rainfall events (amount effect) rather than from minor events. A connection of this amount effect to ^{14}C content was found, pointing to the fact that younger waters are generally formed under heavy rainfall events.

From the reported findings, the resulting scenario for nitrate migration into the aquifer is as follows: Nitrate enters the aquifer via the groundwater recharge. The processes leading to an enrichment of nitrate in the recharge are related to the flushing of nitrate pools in the unsaturated zone during heavy rainfall events. In the recharge water, nitrate concentrations are higher at present semi-arid conditions than during wetter conditions in the past when recharge rates were higher. The contribution of different flow mechanisms (preferential

flow or diffuse flow) to the total groundwater recharge determines the heterogeneity of nitrate fluxes but does not seem to determine the total flux of nitrate into the groundwater. Nitrate is absent in very old waters, either due to denitrification or because it has not been in those waters at all.

For future groundwater management the developed scenario represents a great challenge, as the presently recorded nitrate concentrations will increase as caused by the present semi-arid climate conditions. In addition, further nitrate contamination, that so far only penetrated the topmost meters of the unsaturated zone will eventually reach the groundwater and will further raise nitrate concentrations.

9 OUTLOOK

Though this study was able to explain and qualitatively describe natural processes related to nitrate enrichment in groundwater in semi-arid settings, it showed that these settings still pose a challenge in the interpretation of individual findings due to the encountered heterogeneities and the lack of quantitative data. This study showed that for the investigation of the origin of nitrate in groundwater an understanding of the water transport in both the saturated as well as in the unsaturated zone is crucial. Further research should therefore be conducted with the following focus:

» A better understanding of species migration coupled to water transport throughout the full thickness of the unsaturated zone, especially related to preferential flow processes, should be targeted. Though studies exist that investigate the subsurface up to depths of 12 to 15 m (e.g. Schwiede, in prep., Obakeng, 2000), additional studies that investigate larger depths beyond the rooting zone up to the water table (e.g. up to 100 m below the ground such as in the study area) should be conducted to fully understand and quantify water transport in the unsaturated zone. This could e.g. be enhanced by isotopic studies in the unsaturated zone (^{3}H, CFCs, SF_6).

» To quantify heterogeneities and to understand local flow dynamics, more tracer experiments, as e.g. in Gieske et al. (1995) should be conducted in pilot plots within the study area. Accompanied by suction cup application - which might however be problematic with the given low water content in semi-arid setting - this would yield information on chemical fluxes.

» As to the close coupling of the nitrogen and carbon cycle a detailed knowledge of the vertical development of carbon chemistry in the unsaturated zone should be aimed at. A crucial aspect in this is to understand the role of plants for element cycling in semi-arid settings. Depending on the rooting depth the pCO_2 is affected by CO_2 root respiration. Especially for nitrogen investigations indications are that nitrogen input into (shallow) groundwater may occur through roots (e.g. Verhagen et al., 2004, 2003, Jackson, 2002), too. Though

such issues were often investigated in surface-near settings (e.g. Aranibar et al., 2003, Ringrose et al., 1998), more studies that investigate deeper levels are needed as was already suggested for the water transport investigations in the unsaturated zone, as often the exact depth of the rooting zone is not clear. So far thick unsaturated zones as occurring in the investigated study area (up to 100 m) are often treated as 'black box' and processes within these 'black boxes' have been neglected – also remaining a challenge in this study. The understanding of the carbonate chemistry also relates to isotopic signals, e.g. including the verification of the ^{13}C-signal in the soil gas.

» To verify the time scales suggested by ^{14}C data, more data needs to be recorded to establish the ^{13}C-signal of aquifer material. In this context, it would be desirable to establish noble gas temperatures (to determine infiltration temperatures) in the Ntane Sandstone Aquifer to verify the time scale and the paleoclimatic implications for the study area. There is, however, still the need to establish further paleoclimatic proxies for the study area, a task which even with today's tools available for research remains problematic.

» To obtain a more detailed understanding of the fractured aquifer, a better description of the impact of the fractured structure on the water movement in the saturated zone on various length scales would be desirable. With the data available in this study and the given fracture pattern, only a conceptual model seemed appropriate that could be refined with additional data.

Though some studies exist that investigate parts of the above discussed issues (e.g. Lubczynski, 2000, Selaolo, 1998), focussing the investigations to selected sites should be desired as to strong heterogeneities observed in those systems (Jackson et al., 2004, 2002). As a final remark it is suggested to establish long-term monitoring networks to record temporal nitrate trends, which are often lacking in similar settings. Ideally, those networks would be of high spatial and temporal resolution. As this study clearly points to a natural origin of nitrate in combination with strong impacts imposed by the semi-arid setting, similar studies in different locations of the same conditions should be conducted. A first step could be investigating, whether e.g. observed neon-nitrate relations as well as ^{14}C-nitrate relations can be established

in other areas, too, to validate the climatic connection of nitrate in groundwater of other aquifers in semi-arid regions. And last but not least, one should try to avoid additional nitrate input through anthropogenic activities that might eventually add up to the natural nitrate pool, as water is a limited resource in semi-arid settings.

Acknowledgements

I would like to thank the BGR for financing the project, conducting laboratory measurements and scientifically accompanying the project. Especially M. v. Hoyer and T. Himmelsbach and the very supportive section B1.17 (groundwater protection, groundwater quality) are gratefully thanked, and section B4.16…. I would also like to kindly acknowledge Prof. H. Hötzl (University of Karlsruhe) for making this PhD thesis possible and the AGK for strongly supporting me (special thanks goes to M. Ruff and D. Rettenmaier). In addition, I would like to thank Prof. Balke (University of Tübingen). And of course I want to thank the Department of Geological Survey (DGS), Botswana, for their tremendous logistical support during field work, especially P. Phofuetsile, M. Magowe, O. Obakeng and K. Keipeile, F. Dithapo and O. Bapege. And definetely H. Vogel (BGR/DGS) for making the impossible possible…A further big 'thank you' goes to Debswana, especially P. Khutwje, M. Mokgaotsane, A. Doorgapershad and P. Kesebonye and to everyone who assisted me during field work, as well as to the Department of Water Affairs, Botswana, especially M. Manatoko, N. Singo and G. Kago. Within the regional cooperation it was very fruitful and enjoyable to work with CSIR Pretoria (S. Talma) and Stellenbosch (G. Tredoux and P. Engelbrecht), South Africa and MAWRD Namibia (J. Wrabel). I hope discussions will continue… also with W. Duijnisveld and M. Schwiede of section 4.26 and the Soil Science Dept. of the University of Hannover. Thanks! Another big 'thank you' goes to the Isotope Hydrology Department of the UFZ Leipzig-Halle, especially to K. Osenbrück (and his patience) and S. Weise, and to A. Suckow of GGA Hannover (presently IAEA Vienna). J. Sültenfuß of the Institute of Environmental Physics, University of Bremen, and H. Oster, Spurenstofflabor Wachenheim: Thanks! Of course I would also like to acknowledge the (then-) MSc students S. Schnabel and J. Maßmann for the nice results they produced. S. Babinka is acknowledged for very 'isotopic' conversations, and C. and C. Franzen for more than 'mineralogical' support. U. Gersdorf and M. Kosenko are gratefully thanked for graphical support, and K.P. Burgath and R. Kringel for their scientific support. Also G. Houben and T. Krekeler: Thanks! And of course I want to thank my parents and friends (and my new colleagues at the Technical University Bergakademie Freiberg) who helped me through busy times, and especially M. Thullner. And I would like to thank every animal in the Kalahari that did not attack me.. and the big and final thank you goes the

numerous other people who were involved in this project, who are not listed, though their help was highly appreciated..!

Ke itumeletse go direla mo Botswana fela thata. Ke leboga botlhe ba ba nthusitseng mo tirong yame le go nthuta ka lefatshe le le ntle la Botswana, la batho ba ba pelontle.

Ke a leboga.

10 REFERENCES

AAC (Anglo American Corporation of Southern Africa Ltd.) (1992): Orapa 1992 Water supply investigation. Volume I – main report, CED/068/92. Internal report for Debswana Diamond Co. (Pty.) Ltd. Orapa and Letlhakane Mines.

Addiscott, T.M., Whitmore, A.P., Powlsen, D.S (1991): Farming, fertilizers and the nitrate problem. – CAB international, Wallingford. 170p.

Aeschbach-Hertig, W., Peeters, F., Beyerle, U., Kipfer, R. (2000): Paleotemperature reconstruction from noble gases in ground water taking into account equilibrium with entrapped air. – Nature, 405: 1040-1044.

AGSO Research Newsletter 19 (1993): High nitrate groundwater in the Australian arid zone: Origin of nitrate, and possible denitrification technology - Research Newsletter 19(1993), Australian Geological Survey, Canberra, 16p.

Allison, G.B., Barnes, C.J., Hughes, M.W., Leaney, F.W.J. (1983): Effect of climate and vegetation on oxygen-18 and deuterium in soils. – Isotope hydrology. IAEA.Vienna: 105-123.

Amberger, A., Schmidt, H.L. (1987): Natürliche Isotopengehalte von Nitrat als Indikatoren für dessen Herkunft. - Geochim. Cosmochim. Acta, 51: 2699-2705.

Andrews, J.N. (1985): The isotopic composition of radiogenic helium and its use to study groundwater movement in confined aquifers. - Chem. Geol., 49: 339-351.

Anscombe Groundwater (Pty) Ltd, (January 2001): The drilling and test testing of five "In-Pit" Dewatering Boreholes at Letlhakane Mine, December 2000, LMD1-LMD5. Internal report.

Appelo, C.A.J., Postma, D. (1996): Geochemistry, groundwater and pollution. Balkema. Rotterdam. 536p.

Appelo, C.A.J., Beekman, H.E., Oosterbaan, A.W.A. (1994): Hydrochemistry of springs from dolomite reefs in the southern Alps of Northern Italy. – in: Erikksen (ed.): Hydrochemical balances of Freshwater Systems, Proc. Uppsala Symp. 1994, IAHS Publ. 150: 125-138.

Aranibar, J. N, Anderson, I.C., Ringrose, S., Macko, S.A. (2003): Importance of nitrogen fixation in soil crusts of southern African arid ecosystems: acetylene reudction and stable isotope studies. - J.Arid Env., 54: 345-358.

Arntzen, J.W., Veendendaal, E.M. (1986): A profile of environment and development in Botswana. – Report of the Institute for Environmental Studies (IES), Free University of Amsterdam, The Netherlands and the National Institute of Development, Research and Documentation (NIR), Gaborone, Botswana.

Austin, A.T., Yahdjian, L., Stark, J.M., Belnap, J., Porporato, A., Norton., U., Ravetta, D.A, Schaeffer, S.M. (2004): Water pulses and biogeochemical cycles in arid and semiarid ecosystems. – Oecologia, 141: 221-235.

Baard, J.A.J. (1992): Written communication. Elsenburg Agricultural Development Institute. Elsenburg, S.A. - in Tredoux, G. (2000): Research Proposals for the Orapa Area and Elsewhere, submitted to the DGS, Lobatse, CSIR report ENV-S-C2000-024.

Barnes, C.J., Jacobsen, G., Smith, G.D. (1992): The origin of high nitrate ground waters in the Australian arid zone. – J. Hydrol., 137: 181-197.

Bäumle, R. (2003): Geohydraulic characterisation of fractured rock flow regimes. Regional studies in granite (Lindau, Black Forest, Germany) and dolomite (Tsumeb Aquifers, Northern Namibia). - PhD thesis at the University of Karlsruhe, Germany.

Bear, J., Tsang, C.-F., Marsily, G. (eds.) (1993): Flow and contaminant transport in fractured rock. Academic press, San Diego. 560p.

Bear, J. (1972): Dynamics of fluids in porous media. Elsevier, New York. 761p.

Beekman, H.E., Selaolo, E., De Vries, J.J. (1999): Groundwater recharge and resources assessment in the Botswana Kalahari. Executive Summary GRES II, Geological Survey of Botswana and Faculty of Earth Sciences, Vrije Universiteit, Amsterdam, The Netherlands. 48p.

Beyerle, U., Ruedi, J., Leuenberger, M., Aeschbach-Hertig, W., Peeters, F., Kipfer, R., Dodo, A. (2003): Evidence for periods of wetter and cooler climated in the Sahel between 6 and 50 kyr derived from groundwater. - Geophys. Res. Lett. 30, DOI 10.1029/2002GLO16310.

BGW (Bundesverband Gas-Wasser) (2004): BGW Wasserstatistik. http://Bundesverband-gas-wasser.de 08.12.04.

Blight, G.E. (1995) Ground-water pollution from a landfill in a semi-arid climate. - Proc. Sardinia 95 Fifth Intern. Landfill Symposium, 2-6.10.1995, Cagliari, Italy: 593-599.

BNWMP (1991): Botswana National Water Master Plan. Final Report. Vol. 5, Hydrogeology. - Snowy Mountains Engineering Corporation Ltd.

WLPU Consult. Swedish Geological International AB. Report for the Department of Water Affairs (DWA) Gaborone, Botswana.

Böhlke, J.-K. (2002): Groundwater recharge and agricultural contamination. – Hydrogeology Journal, 10: 153-179.

Boocock, C., Van Straten, O.J. (1961): A note of the development of potable water supplies at depth in the Kalahari. Bechuanaland Protectorate. Records Geological Survey, 1957-1958: 11-14.

Boring, L. R., Swank, W. T., Waide, J. B., and Henderson, G. S. (1988): Sources, fates and impacts of nitrogen inputs to terrestrial ecosystems: review and synthesis. - Biogeochemistry, 6: 119-159.

BOS (2000): Botswana Bureau of Standards: BOS 32:2000 Botswana Standard: Water quality Drinking water – Specification BOS 32:2000.

Botswana Society (1988): Social studies Atlas, ISBN 99912-60-11-X.

Brook, G.A., Cowart, J.B., Marais, E. (1996): Wet and dry periods in the southern African summer rainfall zone during the last 330 kyr from speleothem, tufa and sand dune age data. Palaeoecology of Africa, 24: 147-158.

Buresh, R.J., Patrick, W.H. (1978): Nitrate reduction to ammonium in anaerobic soils. – Soil Sci. Soc. Am. J., 42: 913-918.

Buresh, R.J., Moraghan, J.T. (1976): Chemical reduction of nitrate by ferrous iron. – Journal of Environmental Quality, 5 (3): 320-325.

Burollet, P.F. (1984): Intercratonic and pericratonic basins in Africa. - Sedimentary Geology, 40: 1-10.

Burt, T.P., Heathwaite, A.L., Trudgill, S.T. (1993): Nitrate. Processes, patterns and management. Wiley, Chichester. 444p.

Busenberg, E., Plummer, L.N. (1992): Use of chlorofluorocarbons (CCl_3F and CCl_3F) as hydrologic tracers and age dating tools – The alluvium and terrace system of central Oklahoma. – Water Resources Research, 28 (9): 2257-2283.

Busenberg, E. , Plummer, L.N. (1982): The kinetics of dissolution of Dolomite in CO_2-H_2O systems at 1.5°C to 65°C and 0 atm to 1 atm pCO_2. – American Journal of Science, 282 (1): 45-78.

Canter, L.W. (1997): Nitrates in groundwater. - Boca Raton, CRC Press Inc., 263p.

Careeira, J.A., Niell, F.X. (1995): Mobilization of nutrients by fire in a semiarid gorse-scrubland and ecosystem is Southern Spain. – Arid Soil Research and Rehabilitation, 9 (1): 73-89.

Castro, M.C, Goblet, P., Ledoux, E., Violette, de Marsily, G. (1998): Noble gases as natural tracers of water circulation in Paris Basin 2. Calibration of a groundwater flow model using noble gas isotopic data. - Water Resources Research, 34: 2467-2483.

Chapelle, F. (1993): Ground-Water Microbiology and Geochemistry. John Wiley and Sons, Inc., New York. 424p.

Clark, I.D, P. Fritz (1997): Environmental Isotopes in Hydrogeology. Springer, Berlin, Heidelberg, New York. 350p.

Colvin, C. (1999): Increased risk of methaemoglobinaemia as a result of bottle feeding by HIV positive mothers in South Africa. – IAH Congress, Bratislava.

Comly, H.H. (1945): Cyanosis in infants caused by nitrates in well water. – J. Am. Med. Ass., 129: 112-116.

Cook, P., Love, A.J., Robinson, N.I., Simons, C.T. (2005): Groundwater ages in fractured rock aquifers. – Journal of Hydrology, 308: 284–301.

Cook, P., Herczeg, A.L. (2000) (eds.): Environmental Tracers in Subsurface Hydrology. Kluwer Academic Press, Boston. 552p.

Cook, P.G., Solomon, D.K. (1995): Transport of atmospheric trace gases to the water table: Implications for groundwater dating with chlorofluorocarbons and krypton 85. – Water Resources Research, 31(2): 263-270.

Craig, H. (1961): Isotopic variations in meteoric waters. – Science, 133: 1702-1703.

Craig, H., Lal, D. (1961): The production rate of natural tritium. – Tellus, 13 (1): 85-105.

Crank, J. (1975): The Mathematics of Diffusion. Clarendon Press, Oxford. 424p.

Dahlgren, R.A., Holloway, J. (2002): Geologic nitrogen as a non-point source of nitrate in natural waters. - Proc. 17th WCSS, 14-.21. Aug. 2002, Thailand, Paper no. 83.

Dansgaard, W. (1964): Stable isotopes in precipitation. – Tellus, 16 (4): 436-468.

Davison, K.L., McEntree, K., Wright, M.J. (1964): Nitrate toxicity in dairy heifers. I. Effects on reproduction, growth, lactation and vitamin A nutrition. – J. Dairy Sci., 47: 1065-1073.

Debswana (2004): Wellfields groundwater monitoring report. Number 32, 1 January to 31 December 2003. Internal report compiled by A. Doorgapershad and P.Khutjwe.

Debswana (2003): Wellfields groundwater monitoring report. Number 31, 1 January to 31 December 2002. Internal report compiled by B. Baane and P.Khutjwe.

Debswana (2001): Orapa and Letlhakane Mines: Letlhakane Mine Groundwater Control Phase 1 Report. Debswana/KLM Consulting Services (Pty) Ltd, internal report, November 2001.

Debswana (1997): Orapa groundwater model review 1997. Final report November 1997. Internal report of Debswana Diamond Co. (Pty.) Ltd. Orapa and Letlhakane Mines.

DeVries, J.J, Simmers, I. (2002): Groundwater recharge: an overview of processes and challenges. – Hydrogeology Journal, 10: 5-17.

DeVries, J.J., Selaolo, E.T., Beekman, H.E. (2000): Groundwater recharge in the Kalahari, with reference to paleo-hydrologic conditions. – Journal of Hydrology, 238: 110-123.

DeVries, J.J., von Hoyer, M. (1988): Groundwater recharge studies in semiarid Botswana – a review. In: Simmers (Ed.): Estimation of Natural Recharge. Nato ASI series C222 Reidel, Dordrecht: 113-136.

DeVries, J.J. (1984): Holocene depletion and active recharge of the Kalahari groundwaters – A review and an indicative model. - Journal of Hydrology, 70: 221-232.

De Wit, P.V., Nachtergaele, F.O. (1990): Soil Mapping and Advisory Services Botswana: Explanatory Note on the Soil Map of the Republic of Botswana (Typifying Pedons and Soil Analytical Data"); Gaborone, December 1990.

DIN ISO 10693 (Deutsches Institut für Normung) (1997), Ausgabe 05: Bodenbeschaffenheit - Bestimmung des Carbonatgehaltes - Volumetrisches Verfahren. (Soil quality - determination of carbonate content - volumetric method).

DIN 51418-1 (Deutsches Institut für Normung) (1996), Ausgabe 09: Röntgenspektralanalyse - Röntgenemissions- und Röntgenfluoreszenz-Analyse (RFA) - Teil 1: Allgemeine Begriffe und Grundlagen Titel (en): X-ray spectrometry - X-ray emission- and X-ray fluorescence analysis (XRF) - Part 1: Definitions and basic principles.

DIN 38414 (Deutsches Institut für Normung) (1984): Deutsche Einheitsverfahren zur Wasser-, Abwasser- und Schlammuntersuchung (German Standard Methods for the Examination of Water, Waste Water and Sludge).- Sludge and Sediments Group S4, Determination of Leachability of Water.

Dixon, J.C. (1994): Duricrusts. – In: Abrahams, A.D. and Parsons, A.J.(eds): Geomorphology of desert environments. Chapman and Hall, London: 82-105.

D'Odorico, P., Laio, F. Porporato, A., Rodriguez-Iturbe, I. (2003): Hydrologic controls on soil carbon and nitrogen cycles. II. Case study. – Advances in Water Resources, 26: 59-70.

DVWK (1996): Hydrochemische Stoffsysteme Teil 1, Schriftenreihe des Deutschen Verbandes für Wasserwirtschaft und Kulturbau e.V. (DVWK) Heft 110, Bonn. 288p.

Edmunds, W.M., Gaye, C.B. (1997): Naturally high nitrate concentrations in groundwaters from the Sahel. J. Environ. Qual., 26: 1231-1239.

Edmunds, W.M., Wright, E.P. (1979): Groundwater recharge and paleoclimate in the Sirte and Kufra Basins, Libya. - J. Hydrol. 40: 215-241.

Eichinger, L. (1983): A contribution to the interpretation of ^{14}C groundwater ages considering the example of a partially confined sandstone aquifer. – Radiocarbon, 25: 347-356.

Ericksen, G.E., Hosterman, J.W., Amand, P.S. (1988): Chemistry, mineralogy, and origin of the clay-hill nitrate deposis, Armagosa River valley, Death Valley region, California, USA. – Chem. Geol., 67: 85-102.

Ericksen, G.E. (1981): Geology and origin of the Chilean nitrate deposits. – U.S. Geol. Surv. Prof. Pap. 1188: 6p.

European Parliament (2000): Report on Implementation of Directive 91/676/EEC on Nitrates, Final A5-0386/2000.

Faillat, J.P., Rambaud, A. (1991): Deforestation and leaching of nitrogen as nitrates in underground water in intertropical zones: The example of Côte d'Ivoire. – Environ. Geol. Water Sci., 17: 133 – 140.

Faure, G. (1986): Principles of isotope geology. John Wiley, New York, Chichester, Brisbane, Toronto, Singapore. 589p.

Favreau, G., Leduc, C., Seidel, J.-L., Ousmane, S.D., Mariotti, A. (2003): Land clearance and nitrate-rich groundwater in a Sahelian aquifer, Niger.- Proc. Hydrology of the Mediterranean and Semiarid Regions, Montpellier, April 2003, IAHS Publ. no. 278: 163-167.

Favreau, G. (2002): Le déboisement: origine d'une hausse durable de la recharge des nitrates en aquifère libre semi-aride (Sahel, Niger).- Pangea 37/38: 25-34.

Fenchel, T., King, G.M., Blackburn, T.H. (1998): Bacterial geochemistry: the ecophysiology of mineral cycling. – Academic Press, San Diego. 307p.

Feral, C.J.W, Epstein, H.E., Otter, L., Aranibar, J.N., Shugart, H.H., Macko, S.S., Ramontsho, J. (2002): Carbon and nitrogen in the soil-plant system along rainfall and land-use gradients in Southern Africa. – Journal of Arid Environments, 54: 327-343.

Florkowski, T. (1981): Low-level tritium assay in water samples by electrolytic enrichment and liquid scintillation counting in the IAEA laboratory. – In: Methods of low-level Counting and Spectrometry, International Atomic Energy Agenca, Vienna: 335-353.

Fontes, J.C., Garnier, J.M. (1979): Determination of the initial ^{14}C activity of the total dissolved carbon: A review of the existing models and a new approach. – Water Resources Research, 5 (2): 399-413.

Foster, S.D.D. (1985): Groundwater pollution protection in developing countries. – in: Matthess, G, Foster, S.S., Skinner, A.C.(eds.): Theoretical background, hydrogeology and practice of groundwater protection zones.- IAH International Contributions to Hydrogeology, 6: 167-200.

Foster, S.D.D, Bath, A.H., Farr. J.L., Lewis, W.J. (1982): The likelihood of active groundwater recharge in the Botswana Kalahari - Journal of Hydrology, 55: 113-136.

Fulda, C., Kinzelbach, W. (1997): Datierung junger Grundwässer im Gebiet Sindelfingen-Stuttgart mit Hilfe eines neuen Tracers - Schwefelhexafluorid. Die Stuttgarter Mineralwasserherkunft und Genese. Amt für Umweltschutz, Stuttgart, Germany.

Garrett, D. E. (1985): Chemistry and origin of the Chilean nitrate deposits. – In: Schreiber, Ch. and Harner, H.L. (eds.) "Sixth International Symposium on Salt", 24.05. – 28.05.1983 Toronto, Canada: 285-302.

Geyh, M. A., (2000). An overview of ^{14}C analysis in the study of groundwater. - Radiocarbon 42 (1): 99–114.

Gieske, A., Selaolo, E.T., Beekman, H.E. (1995): Tracer interpretation of moisture transport in a Kalahari sand profile. IAHS Publication, 232 (Application of Tracers in Arid Zone Hydrology): 378-382.

Girard, P., Hillaire-Marcel, C. (1997): Determining the source of nitrate pollution in the Niger discontinuous aquifers using the natural 15N/14N ratios. – Journal of Hydrology 199: 239 – 251.

Goudie, A.S. (1985): Duricrusts and landforms. – In: Richards, K.S., Arnett, R.R., Ellis, S. (eds): Geomorphology and soils. George Allen and Unwin Publishers Ltd, London. 441p.

Grey, D.R.C., Cooke, H.J. (1977): Some problems in the Quarternary evolution of the landforms in northern Botswana. - Catena, 4: 123-133.

Grobbelaar, N., Rösch, M.W. (1981). Biological nitrogen fixation in a Northern Transvaalsavanna. - Journal of South African Botany, 47: 493–506.

Gröning, M. (1994): Edelgase und Isotopentracer im Grundwasser: Paläo-Klimaänderungen und Dynamik regionaler Grundwasserfließsysteme, PhD thesis, University of Heidelberg, Germany.

Hadas, A., Sagiv, B., Haruvy, N. (1999): Agricultural practices, soil fertility management modes and resultant nitrogen leaching rates under semi-arid conditions. – Agricultural Water Management, 42: 81-95.

Heaton, T.H.E. (1984): Sources of the nitrate in phreatic groundwater in the Western Kalahari. – Journal of Hydrology, 67: 249-259.

Heaton, T.H.E., Talma, A.S., Vogel, J.C. (1983): Origin and history of nitrate in confined groundwater in the Western Kalahari. – Journal of Hydrology, 62: 243 – 262.

Heaton, T.H.E, Vogel, J.C. (1981): Excess air in groundwater. - Journal of Hydrology 50, 201-216.

Hesseling, P.B. (1991): An epidemiological survey to assess the effect of well-water nitrates on infant health at Rietfontein in the Northern Cape Province, South Africa. – S.A. Jounal of Science, 87: 300-304.

Holocher, J., Peeters, F., Aeschbach-Hertig, W., Hofer, M., Brennwald, M., Kinzelbach, W, Kipfer, R. (2002): Experimental investigations on the formation of excess air in quasi-saturated porous media. – Geochimica et Cosmochimica Acta. 66 (23): 4103-4117.

Holloway, J., Dahlgren, R.A. (2002): Nitrogen in rock: Occurrences and biogeochemical implications. – Global biogeochemical cycles, 16 (4), 1118: 65-1 – 65-17.

Holloway, J.M., Dahlgren, R.A., Hansen, B., Casey, W.H. (1998): Contribution of bedrock nitrogen to high nitrate concentrations in stream water. – Nature, Vol. 395: 785-788.

Ingerson, E., Pearson, F.J. (1964): Estimation of age and rate of motion of groundwater by the ^{14}C-method. – in: Miyake, Y., koyama, T. (eds.): Recent Researches in the Fields of Hydrosphere, Atmosphere and

Nuclear Geochemistry. Nagoya, Water Research Laboratory, Tokyo: 263-283.

Jacks, G., Sefe, F., Carling, M, Hammar, M., Letsasmao, P. (1999): Tentative nitrogen budget for pit latrines – eastern Botswana. – Environmental Geology, 38: 199-203.

Jacks, G, Sharma, V.P. (1983): Nitrogen Circulation and Nitrate in Groundwater in an Agricultural Catchment in Southern India. – Environmental Geology, 5 (2): 61-64.

Jackson, R.B., Berthrong, S.T., Cook, C.W., Jobbágy, E.G., McCulley, R.L. (2004): Technical comment abstracts: Comment on a Reservoir of Nitrate Beneath Desert Soils". - Science, 304 (5667): 51.

Jackson, R.B., Banner, J.L., Jobbágy, E.G., Pockman, W.T., Wall, D.H. (2002): Ecosystem carbon loss with woody plant invasion of grasslands. – Nature, 418: 623-626.

Katz, B.G., Lee, T.M., Plummer, N., Busenberg, E. (1995): Chemical evolution of groundwater near a sinkhole lake, northern Florida. 1. Flow patterns, age of groundwater, and influence of lake water leakage. - Water Resources Research, 31 (6): 1549-1565.

Keipeile, K. (2004): Environmental Hydrogeology of Letlhakane, Central District, Republic of Botswana. - Internal report of the Environmental Geology Section of the Department of Geological Survey, Botswana in cooperation with the Federal Institute for Geosciences and Natural Resources, Germany.

Kendall, C., McDonnell, J.J. (1998): Isotope Tracers in Catchment Hydrology. Elsevier, Amsterdam, 839p.

Kipfer, R., Aeschbach-Hertig, W., Peeters, F., Stute, M. (2002): Noble Gases in Lakes and Ground Waters. - in: Porcelli, D.P., Ballentine, C.J., Wieler, R. (eds): Noble gases in geochemistry and cosmochemistry. - Reviews in Mineralogy and Geochemistry, 47: 615-700.

Knöller, K., Trettin, R. (2003): Isotopenanalytische Bewertung des Sulfathaushaltes in landwirtschaftlich genutzten Wassergewinnungsgebieten. – UFZ Bericht 16/2003, ISSN 0948-9452. 157p.

Kolditz, O., Habbar, A.; Kaiser, R., Rother, T.; Thorenz, C.; Kohlmeier, M., Moenickes, S. (2001): ROCKFLOW User´s Manual Release 3.5. Institut für Strömungsmechanik und Elektronisches Rechnen im Bauwesen, Universität, Hannover : Juni 2001.

Korom, S.F. (1992): Natural denitrification in the saturated zone: A review. – Water Resources Research, 28 (6): 1657-1668.

Krauskopf, K.B., Bird, D.K. (1995): Introduction to geochemistry. 3rd ed. McGraw Hill, Inc., New York, USA. 647p.

Külls, C. (2000): Groundwater of the North-Western Kalahari, Namibia. – Estimation of Recharge and Quantification of the Flow Systems. PhD thesis, University of Würzburg, Germany.

Kulongowski, J.T., Hilton, D.R. (2004): Climate variability in the Botswana Kalahari from the late Pleistocene to the present day. – Geophysical Research Letters, 31, L10204: 1-5.

Lafthouhi, N.-E., Vanclooster, M., Jalal, M., Witam, O., Aboufirassi, M., Bahir, M. Persoons, E. (2003): Groundwater nitrate pollution in the Essaouira Basin (Morroco). – C.R. Geoscience, 335: 307-317.

Lagerstedt, E., Jacks, G., Sefe F. (1994): Nitrate in groundwater and N circulation in eastern Botswana. – Env. Geol. 23: 60-64.

Lagerstedt, E. (1992): Nitrate contamination in the groundwater and nitrogen circulation in an area of south-east Botswana. A minor field study. MSc Degree Study, Dept. of Physical Geography, Stockholm University, Sweden.

Lavelle, P., Spain, A.V. (2001): Soil Ecology. Kluwer Academic Publishers, Dordrecht, The Netherlands, 514p.

Lawrence, C.R. (1983): Nitrate-rich groundwaters of Australia – Dept. of Research and Energy, Australian Water Resources Council, Research Project no. 74/58, Techn. Paper 79. 110p.

Lichtenberg, E., Shapiro, L.K. (1997): Agricultural and nitrate concentrations in Maryland community water system wells. - Journal of Environmental Quality, 26 (1): 145-153.

Livingstone, D. (1858): Missionary Travels and Researches in South Africa. Ward Lock: London. - in: Thomas, S. G., Shaw, P .A. (1991): The Kalahari Environment. Cambridge University Press. Cambridge. 284p.

Lowe, M., Wallace, J. (2001): Evaluation of potential geologic sources of nitrate contamination in ground water, Cedar Valley, Iron County, Utah, with emphasis on the Enoch area. – Utah Geological Survey special study 100. ISBN 1-55791-660-8. 50p.

Lozán J.L., Kausch, H. (1998): Angewandte Statistik für Naturwissenschaftler, 2. überarbeitete und ergänzte Auflage; Parey Buchverlag, Berlin, Germany. 287p.

Lubczynski, M.W. (2000): Groundwater evapotranspiration – Underestimated component of groundwater balance in a semi-arid environment - Se-

rowe case, Botswana. - Groundwater: Past Achievements and future challenges. Balkema, Rotterdam: 199-204.

Lucas, L.L, Unterweger, M.P. (2000): Comprehensive Review and Critical Evaluation of the Half-Life of Tritium. – Journal of Research of the National Institute of Standards and Technology, 105 (4): 541-549.

Marrett, D.J, Khattak, R.A., Elseewi, A.A., Page, A.L. (1990): Elevated nitrate levels in soils of the eastern Mojawe desert - J. Environ. Qual., 19: 658-663.

Martini, I.P., Chesworth, W. (1992): Weathering, soil and paleosols. - Development in Earth Surface Processes, 2: 309-377. Elsevier, Amsterdam.

Maßmann, J. (2004): Simulation der Nitratverteilung in einem klüftig-porösen Grundwasserleiter in Botswana. - MSc thesis at the University of Hannover, Germany.

Matthes, L. (2002): Environmental Hydrogeology of Orapa, Central District, Republic of Botswana. - Internal report of the Environmental Geology Section of the Department of Geological Survey, Botswana in cooperation with the Federal Institute for Geosciences and Natural Resources, Germany.

Mazor, E. (1991): Applied chemical and and isotopic groundwater hydrology. Hallsted Press John Wiley, New York. 274p.

Mazor, E., Verhagen, B.Th., Sellschop, J.P.F., Jones, M.T., Robins, N.E., Hutton, L.G., Jennings, C.H.M. (1977): Hydrologic, isotopic and chemical studies at Orapa, Botswana. - Journal of Hydrology, 34: 203-234.

Merkel, B. (1992): Modellierung der Verwitterung carbonatischer Gesteine.- Berichte 55, Geol. Paläont. Inst., University of Kiel, Germany. 224p.

Mokokwe, K. (1999). Occurence of groundwater with high nitrate content – Orapa wellfields. – Inception report, DGS, Lobatse.

Mook, W.G. (ed.) (2001): UNESCO/IAEA Series on Environmental Isotopes in the Hydrological Cycle – Principles and Applications. http://www.iaea.org/programmes/ripc/ih/volumes/volumes.htm

Moser, H., Rauert, W. (1980): Isotopenmethoden in der Hydrogeologie. - in: Lehrbuch der Hydrogeologie, Band 8. Gebrüder Bornträger, Berlin, Stuttgart, Germany. 400p.

Mphinyane, W. N. (2001): Influence of livestock grazing within piospheres under free range and controlled conditions in Botswana. - PhD thesis at the Department of Plant Production and Soil Science, Faculty of

Natural and Agricultural Sciences of the University of Pretoria, South Africa.

Murray, L.R., Siebert, B.D. (1962): Nitrate in underground waters of central Australia. - Aust. J. Sci., 25: 22-23.

Nash, D.J., Meadows, M.E., Shaw, P.A., Baxter, A.J., Gieske, A. (1997): Geomorphological and chronostratigraphic evidence for late Holocene environmental change in the Ncamasere Valley, Okavango Delta, Botswana: preliminary results (special edition). - South African Geographical Journal: 93-100.

Neretnieks, I. (1980): Diffusion in rock matrix: An important factor in radionuclide retardation? - Journal Geophys. Research, 85: 4379-4397.

Netterberg, F. (1980): Geology of Southern African calcretes: 1. Terminology, description, macrofeatures and classification. – Transactions of the Geological Society of South Africa 83: 255-83.

Nkotagu, H. (1996): Origins of high nitrate in groundwater of Tanzania. - J. African Earth Sciences, 21 (4): 471-478.

NOAA (2005): National Oceanic and Atmospheric Administration, Global Monitoring Division, http://www.cmdl.noaa.gov/infodata/ftpdata.html.

Obakeng, O. (2000): Groundwater recharge and vulnerability: a case study at the margins of the south- east central Kalahari sub basin, Serowe region, Botswana. - MSc thesis at the University of Botswana in cooperation with the International Institute for Geo-Information Science and Earth Observation (ITC), Enschede, The Netherlands.

Obermann, P. (1982): Hydrochemische/hydromechanische Untersuchungen zum Stoffhaushalt von Grundwasser bei landwirtschaftlicher Nutzung. - Besondere Mitteilungen zum deutschen gewässerkundlichen Jahrbuch 42, Düsseldorf, Germany.

Offer, Z.Y., Goossens, D., Shachak, M. (1992): Aeolian deposition of nitrogen to sandy and loessial ecosystems in the Negev Desert. – J. Arid Environ. 23: 355-363.

Osenbrück, K., Lippmann, J., Sonntag, C. (1998): Dating very old pore waters in impermeable rocks by noble gas isotopes - Geochim. Cosmochim. Acta 62: 3041-3045.

Oster, H., Sonntag, C, Münnich, K.O. (1996): Groundwater age dating with chlorofluorocarbons. – Water Resources Research 32 (10): 2989-3001.

Oster, H. (1994): Datierung von Grundwasser mittels FCKW: Voraussetzungen, Möglichkeiten und Grenzen. - PhD thesis, Institute of Environmental Physics, University of Heidelberg, Germany.

Otteley, C.J., Davison, W., Edmunds, W.M. (1997): Chemical catalysis of nitrate reduction by iron (II). – Geochim. Cosmochim. Acta 61 (9): 1819-1828.

Pacheco, J., Marin, L., Cabrera, A., Steinich, B., Escolero, O. (2001): Nitrate temporal and spatial patterns in 12 water supply wells, Yucatan, Mexico. - Env. Geol. 40 (6): 708-715.

Packham, R.F. (1991): Public health and regulatory aspects of inorganic nitrogen compounds in drinking water. - International workshop, Inorganic Nitrogen Compounds and Water Supply, Hamburg, Nov. 1991.

Parkhurst, D.L. (1995): User's guide to PHREEQC – A computer program for speciation, reaction path, advective transport and inverse geochemical calculations. U.S. Geological Survey, Water Resources Investigations Report 95-4227, Lakewood, Colorado.

Payne, W.J. (1981): Denitrification. John Wiley and Sons, New York.

Peeters, F., Beyerle, U., Aeschbach-Hertig, W., Holocher, J., Brennwald, M., Kipfer, R. (2002): Improving noble gas based paleoclimate reconstruction and groundwater dating using $^{20}Ne/^{22}Ne$ ratios. – Geochim.Cosmochim. Acta, 67 (4): 587-600.

Peterjohn, W.T., Schlesinger, W.H. (1990): Nitrogen loss from deserts in the southwestern United States. - Biogeochemistry, 10: 67-79.

Petri, H. (1976): Nitrate und die Trinkwasserverordnung. – in: Aurand, K, Hässelbarth, U., Müller, G, Schumacher, W, Steuer, W. (1976): Die Trinkwasserverordnung, Erich Schmidt Verlag, Berlin: 40-46.

Pfingsten, W. (1990): Stofftransport in Klüften mit porösen Gesteinen. –. PhD thesis at the University of Hannover – Mitteilungen des Instituts für Wasserwirtschaft, Hydrologie und Landwirtschaftlichen Wasserbau, Heft 73. Hannover.

Porporato, A., D'Odorico, P., Laio, F., Rodriguez-Iturbe, I. (2003): Hydrologic controls on soil carbon and nitrogen cycles. I. Modelling scheme. – Advances in Water Resources, 26: 45-58.

Post, V.E.A. (2004): Groundwater salinization processes in the coastal area of the Netherlands due to transgressions during the Holocene. – PhD thesis at the Vrije Universiteit Amsterdam, The Netherlands.

Postma, D., Boesen, C., Kristiansen, H., Larsen, F. (1991): Nitrate reduction in an unconfined aquifer: Water chemistry, reduction processes, and geochemical modelling. – Water Resources Research, 27: 2027-2045.

Rahube, T.B. (2003): Recharge and groundwater resources evaluation of the Lokalane-Ncojane Basin (Botswana) using numerical modelling. - MSc. Thesis, International Institue for Geo-Information Science and Earth Observation. Enschede, The Netherlands.

Razowska-Jaworek, L., Sadurski, A. (eds.) (2004): Nitrate in groundwaters.- IAH Hydrogeology Selected Papers, 5: 247-258.

Ringrose, S., Chipanshi, A.C., Matheson, W., Chanda, R, Motoma, L., Magole I., Jellema, A. (2002): Climate - and human – induced woody vegetation changes in Botswana and their implications for human adaptation. - Environmental management, 30 (1): 98-109.

Ringrose, S., Vanderpost, C., Matheson, W. (1998): Analysis of soil organic carbon and vegetation cover trends along the Botswana Kalahari transect.- Journal of Arid Environments, 38 (3): 379–396.

Rödelsperger, M., Rohmann, U., Frimmel, F.H., Sontheimer, H. (1991): Untersuchungen zur natürlichen Denitrifikation im Grundwasserleiter und deren Einfluß auf die Grundwasserzusammensetzung. – in: DFG Forschungsbericht: Schadstoffe im Grundwasser. Band 1: Wärme und Schadstofftransport im Grundwasser.

Rödelsperger, M., Rohmann, U., Wertz, A. (1984): Stickstoffgehalt und Umsetzungen unterhalb des Wurzelraums und der gesättigten Zone. - Literaturstudie im Auftrag des Ministeriums für Ernährung, Landwirtschaft, Umwelt und Forst Baden-Württemberg, Karlsruhe, Germany.

Rohmann, U., Sontheimer, H. (1985): Nitrat im Grundwasser. Ursachen, Bedeutung, Lösungswege. - DWVG Forschungsstelle, Karlsruhe. 468p.

Rosenthal, E., Margaritz, M., Ronen, D., Gilead, D. (1988): Groundwater contamination by nitrates and chlorides washed out from phosphorite ores in the Negev desert, Israel. – J. Cont. Hydrol., 3: 27-36.

Rosenthal, E., Margaritz, M., Ronen, T., Roded, D. R. (1987): Origin of nitrates in the Negev Desert, Israel. – Applied Geochemistry, 2 (3): 347-354.

Rowland, F.S. (1990): Stratospheric ozone depletion by chlorofluorocarbons. - Ambio, 19: 281-191.

Saâdi, Z., Maslouhi, A. (2003): Modeling nitrogen dynamics in unsaturated soils for evaluating nitrate contamination of the Mnasra groundwater. – Advances in Environmental Research, 7: 803-823.

Sahimi, M. (1995): Flow and transport in porous media and fractured rock. VCH Verlagsgesellschaft, Weinheim, Germany. 482p.

Sanchez, J.P., Lazzari, M.A. (1999): Impact of fire on soil nitrogen forms in central semiarid Argentina. - Arid Soil Research and Rehabilitation, 13 (1): 81-90.

Scheffer, F., Schachtschnabel, P. (2003): Lehrbuch der Bodenkunde. Enke Verlag, Stuttgart, Germany. 491p.

Schlesinger, W.H. (1997): Biogeochemistry – An Analysis of Global Change. Academic, San Diego, California. 588p.

Schlosser, P., Stute, M., Sonntag, C., Münnich, K.O. (1989): Tritiogenic ^{3}He in shallow groundwater. - Earth. Planet. Sci. Lett., 94: 245-256.

Schnabel, S. (2004): Hydrochemical characterization of a stratified aquifer in the semi-arid region of Orapa/Letlhakane, Botswana. - MSc thesis at the University of Karlsruhe, Germany.

Schwandner, F.M., Seward, T.M., Gize, A.P. (2004): Diffuse emission of organic trace gases from the flank and crater of a quiescent active volcano (Volcano, Aeolian Islans, Italy). – Journal of Geophysical Research – Atmospheres 109 (D4): D04301.

Schwiede, M. (in prep.): Erkundung der Prozesse der Nitratanreicherung in Aauiferen des südlichen Afrikas – Ermittlung von Ursache und Ausmaß der Nitratauswaschung aus Böden ins Grundwasser im Projektgebiet Serowe/Orapa. - PhD thesis at the University of Hannover, Germany.

Selaolo, E.D. (1998): Tracer studies and groundwater recharge assessment in the Eastern Fringe of the Botswana Kalahari. The Lethlakeng – Botlhapatlou Area. – Ph.D. thesis at the Vrije Universiteit te Amsterdam (ISBN 99912-9-3), The Netherlands. 228 p.

SGAB (Swedish Geological Survey) (1988): Serowe – Groundwater resources evaluation project. – Internal report. DGS-Botswana, Lobatse.

Shaw, P.A., Stokes, S., Thomas, D.S.G., Davies, F.B.M., Holmgren, K. (1997): Pealeoecology and age of a late Quartenary high lake level in the Makgadikgadi Basin of the Middle Kalahari, Botswana. – South African Journal of Science: 273-276.

Shaw, P.A., DeVries, J.J. (1988): Duricrust, groundwater and valley development in the Kalahari of southeast Botswana. - J. Arid Environments, 14: 245-254.

Sheard, M.J. (1982): Sources of nitrate ions in underground waters throughout central Australia: a discussion. – Geol. Surv. South Aust., Q. Notes, 84: 11-15.

Shushu, D.D. (2000): Blue-green algae as indicators of changes in soil conditions in semi arid Botswana. - in: Ringrose, S. & Chanda, R. (eds.): Towards Sustainable Management in the Kalahari Region-Some Essential Background and Critical Issues. Gaborone, Botswana: University of Botswana: 120–124.

Skarpe, C., E. Henriksson (1986): Nitrogen fixation by cyanobacterial crusts and by associative-symbiotic bacteria in the Western Kalahari, Botswana. – Arid Soil Research and Rehabilitation, 1: 55-59.

Smith, R.L., Howes, B.L., Duff, J.H. (1991): Denitrification in nitrate-contaminated groundwater: occurrence in steep vertical geochemical gradients. – Geochim. Cosmochim. Acta, 55: 1815-1825.

Smith, R.L., Duff, J.H. (1988): Denitrification in contaminated groundwater. - Applied and Environmental Microbiology, 54: 1071-1078.

Smith, R.A. (1984): The lithostratigraphy of the Karoo Supergroup in Botswana. - Botswana Geological Survey Bulletin 26. 239p.

Snow, D.T. (1965): A parallel plate model of fractured permeable media. – PhD thesis, University of California, Berkley, USA.

Solomon, D.K. (2000): ^{4}He in groundwater. - in: Cook, P, Herczeg, A.L. (2000) (eds.): Environmental Tracers in Subsurface Hydrology. Kluwer Academic Press, Boston: 425-439.

Speijers G.J.A., Van Went, G.F., Van Apeldoorn, M.E., Montizaan, G.K., Janus, J.A., Canton, J.H., Van Gestel, C.A.M., Van der Heijden, C.A., Heijna-Merkus, E., Knaap, A.G.A.C., Luttik, R., De Zwart, D. (1989): Integrated criteria document nitrate; effects. Appendix to RIVM Report No. 758473012. Bilthoven, Rijksintituut voor de Volksgezondheid en Milieuhygiëne (National Institute of Public Health and Environmental Protection), The Netherlands (RIVM Report No. A758473012).

SRK Consulting (1981): Report on the Letlhakane Mine Dewatering System for DeBeers Botswana. Report No. CL.2439/2.

Starr, R.C., Gillham, R.W. (1989): Controls on denitrification in shallow unconfined aquifers. – in: Kobus, H.E., Kinzelbach, W. (ed.): Contaminant transport in groundwater. Balkema, Rotterdam: 51-56.

Stokes, S., Thomas, D.S.G., Washington, R. (1997): Multiple episodes of aridity in southern Africa since the last interglacial period. - Nature, 388: 154-158.

Stumm, W., Morgan, J.J. (1996) Aquatic Chemistry. - Wiley Interscience, New York. 1022 p.

Stute M., Talma S. (1997): Glacial temperatures and moisture transport regimes reconstructed from noble gases and $\delta^{18}O$, Stampriet aquifer, Namibia. - in: Isotope Techniques in the Study of Environmental Change, IAEA, Vienna, Austria: 307-320.

Stute, M., Förster, M., Frischkorn, H., Serejo, A., Clark, F.J., Schlosser, P., Broecker, W.S., Bonani, G. (1995): Cooling of tropical Brasil (5°C) during the Last Glacial Maximum. - Science, 269: 379-383.

Stute, M., Schlosser, P. (1993): Principles and applications of the noble gas paleothermometer. - in: Swart, P.K., McKenzie, J., Savin, S. (eds.): Climate Change in Continental Isotopic records, 78. American Geophysical Union, Washington D.C.: 88-100.

Stute, M., Sonntag, C., Deák, J., Schlosser, P. (1992): Helium in deep circulating groundwater in the Great Hungarian Plain: flow dynamics and crustal and mantle helium fluxes. - Geochim. Cosmochim Acta, 56: 2051-206.

Super, M. (1981): An epidemiological study of well water nitrates in a group of Nambian infants. – Water Res., 15: 1265-1270.

Sültenfuß, J., Roether, W., Rhein, M. (submitted): The Bremen Mass Spectrometric Facility for the Measurement of Helium Isotopes, Neon, and Tritium in Water. – IAEA International Symposium on Quality Assurace for Analytical Methods in Isotope Hydrology, IAEA CN-119.

Sültenfuß, J., Massmann, G. (2004): Datierung mit der ^{3}He-Tritium-Methode am Beispiel der Uferfiltration im Oderbruch. – Grundwasser, 4: 221-234.

Talma, A.S., Vogel, J.C. (1992): Late Quaternary paleotemperatures derived from a speleothem from Cango Caves, Cape Province, South Africa. - Quaternary Research, 37: 203-213.

Taylor, C.B. (1981): Present status and trends in electrolytic enrichment of low-level tritium in water. – In: Methods of low-level Counting and Spectrometry, International Atomic Energy Agenca, Vienna: 303-325.

Terblance, A.P.S. (1991): Health hazards of nitrate in drinking water. - Water SA, 17 (1): 77-82.

Thomas, D.S.G., Shaw, P.A. (2002): Late Quartenary environmental change in central southern Africa: new data, synthesis, issues and prospects. – Quarternary Science Reviews, 21: 783-797.

Thomas, S.G., Shaw, P.A. (1991): The Kalahari Environment. Cambridge University Press. Cambridge. 284p.

Tindall, J.A., Petrusak, R.L., McMahon, P.B. (1995): Nitrate transport and transformation processes in unsaturated porous media. – J. Hydrol., 169: 51-94.

Tredoux, G., Engelbrecht, P., Talma, S. (2004): Nitrate in groundwater in arid and semi-arid parts of Africa. – in: Vogel, H., Chilume, C. (eds.): Proc. of the International Workshop on Environmental Geology in semi-arid environments, Nov. 11-12, 2004, Selebi-Phikwe, Botswana.

Tredoux, G., Engelbrecht, J.F.P., Talma, A.S. (2001): Nitrate in groundwater of Southern Africa. - in: Seiler and Wohnlich (eds): New Approaches Characterizing Groundwater Flow, Swets and Zeitlinger Lisse, ISBN 902651 848 X: 663-666.

Tredoux, G. (1993): A preliminary investigation of the nitrate content of groundwater and limitation of the nitrate input. Report to the WRC by the Groundwater Programme, Division of Water Technology, CSIR, WRC Report No: 368/1/93, CSIR Project No: 670 26328, Stellenbosch, SA.

Tredoux, G., Kirchner, J. (1985): The occurrence of nitrate in groundwater in South West Africa/Namibia. Paper presented at the conference "Nitrates in Water", Paris.

TrinkwV (2001): Trinkwasserverordung vom 21. Mai 2001, BGBl I 2001: 959.

Tyson, P.D., Preson-Whyte, R.A. (2000): The weather and climate of Southern Africa. Oxford University Press, Cape Town, South Africa. 408p.

US EPA (2002): National Primary Drinking Water Regulations (NPDWRs or primary standards), http://www.epa.gov/safewater/consumer/pdf/mcl.pdf

US EPA (1994): National Water Quality Inventory. 1992 Report to Congress. EPA-841-94-001. Office of Water, Washington.

Van Wyk, P. (2001): Southern African trees - A photographic guide. Struik Publishers (Pty.) Ltd., Cape Town, South Africa. 144p.

Verhagen., B.Th., Butler, M.J., van Wyk, E. (2004): Isotopes and chemistry suffest natural processes for high nitrate in Limpopo Province ground water - Water Institute of Southern Africa (WISA), Biennial Conference, 2-6 May 2004, Cape Town, South Africa.

Verhagen., B.Th., Butler, M.J., van Wyk, E. (2003): Isotope data point to natural processes in the production of high nitrate concentrations in

groundwater. - Isotope Hydrology and Integrated Water Resources Management. Int. Sym. Vienna, 19-23 May 2003 (IAEA-CN-104/P-50)

Verhagen, B.Th. (1995): Semiarid zone groundwater mineralization processes as revealed by environmental isotope studies. – in: Adar, E., Leibundgut, C. (eds.): Application of Tracers in Arid Zone Hydrology - IAHS Publication 232: 245-266.

Verhagen, B.Th. (1992): Detailed geohydrology with environmental isotopes. A case study at Serowe, Botswana. – in: Isotope Techniques in Water Resources Development: 345-362.

Verhagen, B.Th. (1991): The isotope geohydrology of the Karoo Basin underlying the Kalahari Thirstland, Southern Africa. - in: Proc. Int. Conf. on Groundwater in Large Sedimentary Basins. Perth, W. Australia, July 2004. Australian Water Resources Council, Cof. Series 20: 390-402.

Verhagen, B.Th. (1990): Isotope hydrology of the Kalahari: Recharge or no recharge? – Paleoecology of Africa, 21: 143-158.

Verhagen, B.T. (1985): Isotope hydrology of ground waters of the Kalahari, Gordonia. - South African Journal of Geology, 88 (3): 517-522.

Vogel, J.C., Talma, A. S., Heaton, T.H.E. (1982): The age and isotopic composition of Groundwater in the Stampriet Artesian Basin, SWA. – Internal report: CSIR National Physical Research Laboratory Proj. No. 400/90615.

Vogel, J.C. (1970): Carbon-14 dating of groundwater. - Isotope Hydrology: 225-239, Vienna, IAEA.

Wakida, F.T., Lerner, D.N. (2005): Non-agricultural sources of groundwater nitrate: a review and case study. – Water Research 39: 3-16.

Walvoord, M.A., Philips, F.M., Stonestrom, D.A., Evans, R.D., Hartsough, P.C., Newman, B.D., Striegl, R.G. (2003): A reservoir of nitrate beneath desert soils. – Science, 302 (7): 1021-1024.

Weise, S.M., Moser, H. (1987): Groundwater dating with helium isotopes. - in: Isotope techniques in water resources development. IAEA Vienna: 105-126.

Wellfield (Wellfield Consulting Services) (2000): Serowe Wellfield 2 Extension Project (TB10/3/10/95-96). Final Report. - Internal report for the Ministry of Minerals, Energy and Water Affairs, Department of Water Affairs, Botswana.

WHO (2004): Rolling Revision of the WHO Guidelines for Drinking-Water Quality - Draft for review and comments. Nitrate and nitrite in drinking water. http://www.who.int/water_sanitation_health/dwq/chemicals/nitratesfull.pdf.

WHO (1998): Guidelines for drinking-water quality, 2nd ed. Appendum to Vol. 2. Health criteria and other supporting information. Geneva, World Health Organization: 64-80.

WHO (1996): Toxicological evaluation of certain food additives and contaminants. Prepared by the Forty-Fourth Meeting of the Joint FAO/WHO Expert Committee on Food Additives (JECFA). Geneva, World Health Organization, International Programme on Chemical Safety (WHO Food Additives Series 35).

WHO (1985a): Guidelines for the study of dietary intake of chemical contaminants. Geneva, World Health Organization (WHO Offset Publication No. 87).

WHO (1985b): Health hazards from nitrate in drinking-water. Report on a WHO meeting, Copenhagen, 5–9 March 1984. Copenhagen, WHO Regional Office for Europe (Environmental Health Series No. 1).

Widory, D., Kloppmann, W., Chery, L., Bonnin, J., Rochdi, H, Guinamant, J.-L. (2004): Nitrate in groundwater: an isotopic multi-tracer approach. – Journal of Contaminant Hydrology, 72: 165-188.

Wigley, T. M.L., Plummer, L.N., Pearson, F.J. (1978): Mass transfer and carbon isotope evolution in natural water systems. - Geochim. Cosmochim. Acta 42: 1117-1139.

Williams, A.E., Johnson, J.A., Lund, L.J, Kabala, Z.J. (1998): Spatial and Temporal Variations in Nitrate Contamination of a rural aquifer, California. – J. Environ. Qual., 27: 1147-1157.

Yurtsever, Y., Gat, J.R. (1981): Atmospheric Waters. – in: Stable Isotope Hydrology. Tech. Report Series No. 210 IAEA, Vienna: 103-142.

Zoellmann, K., Kinzelbach, W., Fulda, C. (2001): Environmental tracer transport (^3H and SF_6) in the saturated and unsaturated zones and its use in nitrate pollution management. – Journal of Hydrology, 204: 187-205.

11 APPENDIX

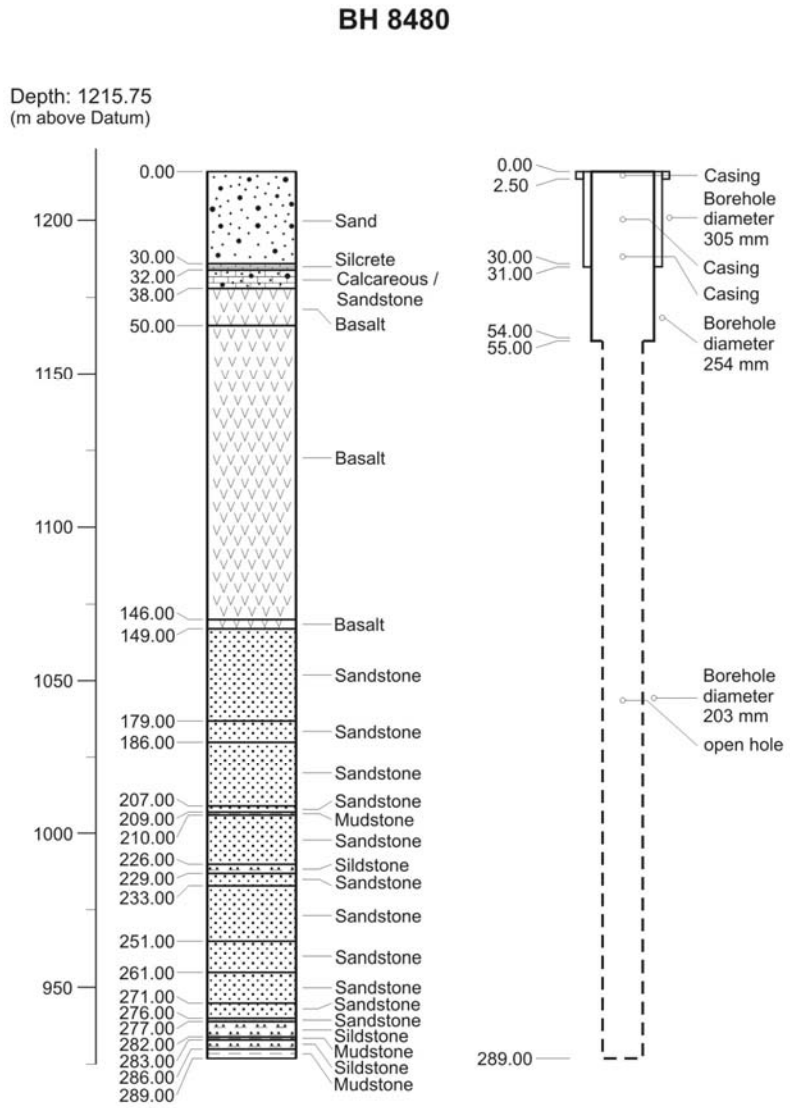

Fig. 11-1: Exemplary borehole (open hole)

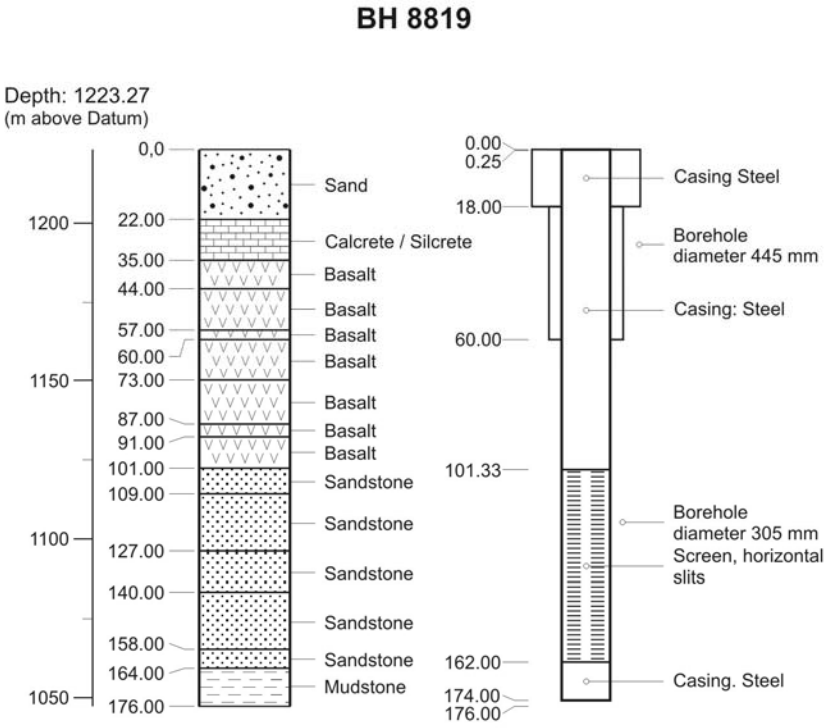

Fig. 11-2: Exemplary borehole (with screen)

Tab. 11-1a: Data of dissolved noble gases (^{4}He, ^{3}He/^{4}He, ^{20}Ne, ^{22}Ne) and tritium (^{3}H) in groundwater samples from Serowe, grouping is according to ^{14}C content. Different numbers of digits in tritium results owe to different detection limits applied (see methods).

BH-ID	**^{4}He** (10^{-8} cm^3 STP/g)	**^{3}He** (10^{-14} cm^3 STP/g)	**^{3}He/^{4}He** (10^{-8})	**^{20}Ne** (10^{-7} cm^3 STP/g)	**^{22}Ne** (10^{-7} cm^3 STP/g)	**^{22}Ne/^{20}Ne** (10^{-8})	**^{3}H** (TU)	**error** (TU)
Serowe: Group 1								
BH 5311	65.4	8.5	13.0	2.41	0.24	0.101	0.1$^+$	± 0.3
BH 7005	217.4	8.9	4.1	1.51	0.15	0.102	0.0$^+$	± 0.3
BH 7099	65.3	1.7	4.3	2.69	0.27	0.101	0.1$^+$	± 0.3
BH 7102	202.6	14.6	7.2	2.05	0.20	0.096	0.0$^+$	± 0.3
T 545	325.7	15.6	4.8	-	-	-	0.005$^\#$	±0.006
Serowe: Group 2								
BH 7021	7.8	7.2	94.3	2.24	0.22	0.097	0.2$^+$	± 0.3
BH 8450	5.4	6.1	113.2	1.87	0.18	0.097	0.2$^+$	± 0.3
BH 8451	7.3	5.7	77.4	1.68	0.16	0.097	0.0$^+$	± 0.3
BH 8471	86.5	10.0	11.6	2.09	0.21	0.098	0.0$^+$	± 0.3
BH 8480	13.7	9.1	66.6	2.79	0.27	0.097	0.1$^+$	± 0.3
BH 8819	104.3	8.3	7.9	2.01	0.19	0.096	0.0$^+$	± 0.3
KRS 1	29.7	8.8	29.8	2.90	0.29	0.099	0.0$^+$	± 0.3
Mahatane	18.2	8.9	49.0	2.53	0.25	0.097	0.0$^+$	± 0.3
BH 7591	16.1	7.8	48.3	-	-	-	0.009$^\#$	±0.005
BH 8673	-	-	-	-	-	-	0.007$^\#$	±0.005
Sanakoma	-	-	-	-	-	-	0.009$^\#$	±0.015

$^+$detection limit = 0.3 TU $^\#$detection limit = 0.01TU - = no data

Tab. 11-1b: Data of measured radiocarbon, ^{13}C and stable isotopes in groundwater samples from Serowe, grouping is according to ^{14}C content.

BH-ID	**$\delta^{13}C$-DIC** (‰)	**^{14}C-DIC** (%-mod.)		**error**	**$\delta^{2}H$** (‰)	**$\delta^{18}O$** (‰)
Serowe: Group 1						
BH 5311	-7.8	3.8	±	0.8	-36.8	-5.63
BH 7005	-9.8	2.6	±	0.5	-42.8	-6.36
BH 7099	-10.7	9.5	±	1.3	-39.2	-5.95
BH 7102	-8.4	13.8	±	0.6	-41.2	-5.88
T 545	-8.9	7.2	±	0.5	-35.1	-5.65
Serowe: Group 2						
BH 7021	-12.5	59.9	±	1.1	-45.0	-6.29
BH 8450	-12.0	80.2	±	1.5	-47.4	-6.69
BH 8451	-12.0	80.5	±	1.4	-45.4	-6.48
BH 8471	-12.4	70.2	±	1.2	-42.5	-6.28
BH 8480	-12.1	44.5	±	1.1	-44.0	-6.26
BH 8819	-11.4	56.9	±	1.3	-44.6	-6.46
KRS 1	-12.5	61.5	±	1.6	-43.4	-6.40
Mahatane	-11.2	59.4	±	1.0	-43.9	-6.04
BH 7591	-11.0	47.0	±	1.0	-38.7	-6.07
BH 8673	-12.3	58.0	±	7.2	-40.9	-6.33
Sanakoma	-10.4	65.3	±	1.0	-39.1	-6.07

Tab. 11-2: Stable isotope and tritium data of groundwater samples from Orapa/Letlhakane

BH-ID	**δ^2H**	**$\delta^{18}O$**	**^3H**		**error**
	(‰)	(‰)	TU		TU
Letlhakane					
Gladys	-48.4	-6.79	0.011	±	0.006
Barbara	-47.2	-6.53	0.005	±	0.005
Z7102	-44.1	-6.54	0.014	±	0.005
Z7152	-44.7	-6.45	0.009	±	0.005
Z6000	-43.7	-6.41	0.030	±	0.015
Z6001	-45.6	-6.53	0.013	±	0.005
Z6002	-46.3	-6.66	0.007	±	0.005
Z6109	-41.5	-6.24	0.009	±	0.005
Z6110	-43.4	-6.60	0.008	±	0.005
Z7092	-39.9	-5.95	0.012	±	0.005
Z6128	-45.5	-6.81	0.007	±	0.005
Z8879	-39.1	-5.90	0.011	±	0.015
Z8778	-40.2	-6.03	0.008	±	0.005
WF6/26	-40.3	-5.99	0.010	±	0.006
Z7095	-41.1	-6.06	0.017	±	0.005

Tab. 11-3: Chlorofluorocarbon and sulfur hexafluoride data of groundwater samples from Serowe.

BH-ID	**CFC-12 (CCl_2F_2)** (pmol/l)	**error**	**CFC-11 (CCl_3F)** (pmol/l)	**error**	**CFC-113 ($C_2Cl_2F_2$)** (pmol/l)	**error**	**SF_6** (fmol/l)	**error**
Serowe:Group1								
BH 5311	0.03	± 0.05	0.13	± 0.05	0.01	± 0.05	0.10	± 0.10
BH 7005	0.23	± 0.05	0.38	± 0.05	0.07	± 0.05	0.10	± 0.10
BH 7102	0.07	± 0.05	0.80	± 0.05	0.03	± 0.05	0.20	± 0.10
Serowe:Group2								
BH 7021	0.20	± 0.05	1.70	± 0.20	0.03	± 0.05	0.20	± 0.10
BH 8450	0.45	± 0.05	1.80	± 0.20	0.06	± 0.05	0.20	± 0.10
BH 8451	0.60	± 0.10	2.00	± 0.30	0.09	± 0.05	0.70	± 0.10
BH 8471	0.38	± 0.05	1.80	± 0.20	0.07	± 0.05	0.30	± 0.10
BH 8480	0.35	± 0.05	2.60	± 0.60	0.07	± 0.05	0.30	± 0.10
BH 8480-2	0.05	± 0.05	2.30	± 0.30	0.02	± 0.05	0.10	± 0.10
BH 8819	0.20	± 0.05	0.27	± 0.05	0.04	± 0.05	0.20	± 0.10
KRS 1	0.06	± 0.05	0.22	± 0.05	0.03	± 0.05	0.10	± 0.10
Mahatane	0.37	± 0.05	2.20	± 0.30	0.06	± 0.05	0.30	± 0.10

Tab. 11-4a: Main hydrochemical composition of selected groundwater samples from Serowe (part 1).

BH_ID	pH	T	DO	EC	E_H (SHE)	K	Na	Cl
	(-)	(°C)	(mg/l)	(µS/cm)	(mV)	(mg/l)	(mg/l)	(mg/l)
BH8450	7.2	26.0	3.32	832	336	3.0	57.8	55.3
BH5305	7.7	28.1	1.58	785	138	4.4	133.0	82.2
BH5311	7.8	26.9	0.52	526	201	3.8	81.6	45.8
BH5321	7.9	26.9	3.48	575	224	3.6	104.0	46.1
BH5325	7.1	27.5	4.87	1068	351	3.4	78.1	124.0
BH5326	7.4	27.5	1.85	1037	207	4.1	108.1	195.0
BH6510	7.1	27.2	1.83	1164	318	1.4	99.2	29.4
BH7005	8.0	26.4	2.10	560	295	1.4	122.0	46.7
BH7020	9.5	28.4	6.30	385	288	0.2	87.4	19.8
BH7021	7.5	27.1	6.80	645	396	2.9	52.6	49.4
BH7099	8.4	26.1	3.69	283	322	1.3	58.4	13.1
BH7100	7.3	28.6	1.32	685	186	2.0	92.5	79.9
BH7101	9.1	28.4	0.59	568	278	0.3	133.0	36.0
BH7102	7.8	26.5	0.83	549	84	1.3	107.0	27.5
BH7511	7.5	26.5	4.74	510	275	3.0	50.7	35.2
BH7591	7.3	25.7	5.36	515	282	3.1	43.2	22.5
BH8451	7.2	26.3	5.89	811	322	3.9	68.5	56.0
BH8471	7.2	25.9	2.86	1207	406	4.7	62.9	123.0
BH8472	7.4	25.8	5.28	707	389	2.8	47.3	79.7
BH8476	7.4	26.5	4.60	627	418	3.0	64.1	32.9
BH8477	10.0	27.3	1.37	428	233	0.3	81.4	72.4
BH8478	7.7	27.1	3.62	560	412	2.4	78.9	27.9
BH8479	9.0	26.8	0.37	390	311	0.6	75.0	59.0
BH8480	7.5	26.8	4.30	554	271	2.2	66.3	34.5
BH8491	7.2	26.2	4.77	742	482	2.2	42.9	73.1
BH8492	7.4	27.9	29.8	619	374	2.0	35.5	76.0
BH8494	8.5	27.8	2.72	454	387	1.4	87.5	54.4
BH8672	8.6	27.7	0.26	349	-5	2.1	54.3	48.7

- continued -

Tab. 11-4a (continued): Main hydrochemical composition of selected groundwater samples from Serowe (part 1).

BH_ID	**pH**	**T**	**DO**	**EC**	**E_H (SHE)**	**K**	**Na**	**Cl**
	(-)	(°C)	(mg/l)	(µS/cm)	(mV)	(mg/l)	(mg/l)	(mg/l)
BH8673	7.7	28.2	0.97	585	265	2.1	33.5	75.4
BH8674	7.0	26.6	0.63	648	99	2.1	43.5	73.9
BH8706	7.2	27.2	0.29	379	1	2.0	47.9	50.2
BH8713	8.6	28.6	5.54	304	358	0.9	56.6	38.8
BH8714	8.1	26.8	5.84	522	425	2.1	102.0	36.3
BH8819	7.5	25.6	2.97	601	165	2.5	74.5	35.1
BH8820	8.6	25.8	2.64	403	312	1.2	87.1	33.5
Dukokola[CP]	-	-	-	-	207	2.2	36.0	99.1
Gosha[CP]	8.3	27.3	3.82	340	389	1.8	56.6	25.2
KRS1	7.2	-	4.61	625	297	3.3	24.9	80.8
KRS2	7.4	15.4	-	845	207	3.9	28.7	138.0
Mahatane[CP]	7.2	24.7	5.44	889	360	4.1	44.2	111.0
Mantika	7.5	25.9	0.24	767	207	3.6	115.4	86.0
Matikwe	7.6	24.5	2.00	565	207	2.7	76.2	34.6
Matikwe_2	9.2	27.6	0.38	1573	207	0.8	314	358.0
Mochi-nyana[CP]	7.7	25.0	4.59	673	224	13.3	72.6	95.6
Palamao-kuwe[CP]	7.3	22.3	3.64	765	239	4.6	74.2	51.2
Ramagono-wang[CP]	7.8	26.8	4.46	542	351	3.0	84.5	32.7
Sanakoma[CP]	7.3	25.6	5.88	668	291	2.8	45.8	56.0
Serwe_Ranch	7.5	25.0	5.07	770	207	3.1	32.5	159.0
Setekwane[CP]	8.3	23.9	1.97	471	377	1.0	96.9	33.2
T545	8.2	26.5	1.66	714	230	4.4	141.0	79.6
Kuatshephe	-	-	-	-	207	4.9	85.8	68.0

- = no data

[CP] = cattle post

Tab. 11-4b: Main hydrochemical composition of selected groundwater samples from Serowe (part 2).

BH_ID	Mg (mg/l)	Ca (mg/l)	SO_4 (mg/l)	HCO_3 (mg/l)	Fe(II) (mg/l)	Mn (mg/l)	NO_3 (mg/l)	NH_4 (mg/l)	NO_2 (mg/l)
BH8450	23.3	75.6	4.0	325	0.009	<0.001	88.0	<0.01	<0.01
BH5305	10.8	21.7	12.7	321	0.020	0.022	1.0	0.02	<0.01
BH5311	11.2	22.2	9.9	252	0.009	0.005	2.4	0.02	<0.01
BH5321	6.4	13.4	12.0	257	0.013	0.001	1.7	<0.01	<0.01
BH5325	33.5	92.1	33.6	360	0.010	0.001	49.3	0.01	<0.01
BH5326	19.0	67.8	15.2	232	0.027	0.014	8.4	<0.01	<0.01
BH6510	39.6	106.0	73.5	571	0.012	0.005	68.9	<0.01	<0.01
BH7005	1.0	8.7	6.4	260	0.009	<0.001	5.9	0.02	<0.01
BH7020	0	1.0	3.8	137	0.003	<0.001	2.8	<0.01	<0.01
BH7021	23.7	42.5	3.1	248	0.006	<0.001	56.8	0.01	<0.01
BH7099	1.1	7.13	2.8	154	<0.003	<0.001	3.2	0.01	-
BH7100	8.5	41.2	6.5	262	0.047	0.006	12.8	0.01	<0.01
BH7101	0.2	1.1	7.1	237	0.005	<0.001	2.5	0.01	<0.01
BH7102	6.2	16.8	14.3	286	0.216	0.003	11.1	<0.01	<0.01
BH7511	12.2	41.3	2.5	237	0.010	0.001	22.5	<0.01	<0.01
BH7591	14.3	48.6	2.4	267	0.004	0.001	35.7	<0.01	0.02
BH8451	20.5	68.5	0.7	294	0.003	<0.001	108.0	<0.01	<0.01
BH8471	41.7	107.0	1.7	293	0.006	0.004	219.0	0.02	<0.01
BH8472	11.5	74.9	18.0	193	0.007	0.002	63.4	0.01	<0.01
BH8476	15.3	47.3	13.7	294	<0.003	<0.001	26.3	0.01	0.01
BH8477	0.1	2.9	19.2	-	0.007	<0.001	3.7	<0.01	<0.01
BH8478	10.3	28.2	9.5	267	<0.003	<0.001	24.7	<0.01	0.01
BH8479	0.4	3.6	9.7	59.7	0.005	<0.001	13.1	0.02	<0.01
BH8480	5.4	41.1	5.6	216	0.015	0.002	48.6	0.01	0.01
BH8491	25.5	66.6	2.7	292	<0.003	<0.001	28.2	0.02	<0.01
BH8492	18.7	57.9	3.5	200	0.005	<0.001	30.6	0.01	<0.01
BH8494	1.2	8.9	2.1	168	0.042	<0.001	6.0	<0.01	<0.01
BH8672	4.8	8.8	1.6	114	0.006	0.017	0	0.58	<0.01

- continued -

Tab. 11-4b (continued): Main hydrochemical composition of selected groundwater samples from Serowe (part 2).

BH_ID	Mg (mg/l)	Ca (mg/l)	SO_4 (mg/l)	HCO_3 (mg/l)	Fe(II) (mg/l)	Mn (mg/l)	NO_3 (mg/l)	NH_4 (mg/l)	NO_2 (mg/l)
BH8673	20.5	49.7	2.4	190	0.015	0.035	20.7	0.01	<0.01
BH8674	22.4	54.4	2.1	252	1.269	0.096	13.0	0.02	0.26
BH8706	6.0	15.7	1.1	122	4.725	0.397	0	0.05	<0.01
BH8713	0.8	6.49	2.2	99	0.009	<0.001	8.0	<0.01	<0.01
BH8714	3.0	16.4	7.1	257	0.008	<0.001	4.4	0.01	<0.01
BH8819	9.9	39.8	1.3	237	0.076	0.007	71.4	<0.01	0.02
BH8820	1.3	3.8	8.6	178	0.019	0.002	3.3	0.01	<0.01
Dukokola[CP]	26.3	109.0	2.9	375	0.014	0.015	18.2	0.01	<0.01
Gosha[CP]	4.0	11.2	1.4	160	0.008	<0.001	4.9	0.02	0.02
KRS1	19.3	68.8	0.9	214	0.023	0.004	18.8	<0.01	<0.01
KRS2	26.9	91.3	1.5	247	0.004	<0.001	9.2	0.02	<0.01
Mahatane[CP]	34.6	77.1	2.9	319	0.015	0.002	27.0	<0.01	<0.01
Mantika	11.4	30.7	22.1	285	0.010	<0.001	1.0	0.07	<0.01
Matikwe	8.9	35.4	9.4	286	0.092	0.008	3.9	<0.01	<0.01
Matikwe_2	0.1	4.1	104.0	62	0.019	<0.001	3.0	0.01	<0.01
Mochi-nyana[CP]	14.9	37.2	1.3	220	0.019	0.004	6.6	<0.01	<0.01
Palamao-kuwe[CP]	24.6	52.3	19.2	378	0.027	0.040	2.1	<0.01	<0.01
Ramagono-wang[CP]	9.6	20.0	8.1	267	0.006	<0.001	3.8	<0.01	0.01
Sanakoma[CP]	18.0	69.3	4.8	288	0.013	0.001	33.5	0.03	0.31
Serwe_Ranch	17.8	80.4	0.9	154	0.013	<0.001	3.6	0.06	<0.01
Setekwane[CP]	2.7	10.2	5.6	230	0.087	<0.001	7.5	<0.01	<0.01
T545	5.8	10.9	27.2	230	0.136	0.013	0.3	<0.01	<0.01
Kuatshephe	13.6	25.2	15.8	241	0.018	0.006	2.8	<0.01	0.01

- = no data

[CP] = cattle post

Tab. 11-5a: Main hydrochemical composition of selected groundwater samples from Orapa (part 1).

BH_ID	pH	T	DO	EC	E_H (SHE)	K	Na	Cl
	(-)	(°C)	(mg/l)	(µS/cm)	(mV)	(mg/l)	(mg/l)	(mg/l)
BARBARA	7.2	28.0	1.79	2420	232	6.3	500	374
BH8095	7.1	28.3	3.40	1340	252	3.9	262	114
BH8096	7.3	29.3	0.00	1392	89	4.3	298	70
BH8098	7.1	30.1	0.51	3270	46	11.3	611	671
EB1	7.9	28.9	0.07	4870	28	5.5	1050	1251
GLADYS	7.0	28.3	1.12	5380	223	11	890	1390
HDW4	7.5	22.9	2.34	156	402	3.6	3.9	4.6
OB22	7.2	28.4	0.00	2430	413	5.5	516	326
OB23	7.0	30.2	0.00	1573	360	6.4	298	140
OB33	7.1	29.3	1.68	5060	145	28.1	1072	841
Pat	6.9	27.7	1.14	3800	355	9.2	700	886
Z2539	6.8	27.9	1.73	3940	405	7.0	643	947
Z5999	6.9	30.2	0.00	7430	92	36.7	1332	1986
BH3077	7.0	29.5	0.79	1522	417	6.3	235	212
BH6887	7.0	29.4	2.30	1152	368	4.3	173	101
BH6888	7.0	30.4	0.00	1336	413	4.8	211	146
HDW6-1	7.2	23.4	0.44	282	107	9.4	14	7
HDW6-3	7.4	27.1	4.23	4740	397	5.8	584	1227
OB17	6.9	29.5	4.13	1204	351	5.9	174	114
OB40	7.4	31.2	0.23	2180	36	7.0	398	534
Z10694	6.6	28.2	1.70	5710	364	15.4	772	1384
Z10878	8.0	30.1	0.63	1729	179	5.4	332	349
Z10880	7.1	30.5	0.11	2060	142	8.3	323	483
Z10882	7.2	29.5	0.00	2040	432	7.3	373	374
Z10891	7.2	30.4	0.17	2070	191	8.3	386	404
Z10892	7.0	29.4	0.14	1876	162	5.0	314	375
Z10979	7.3	30.3	0.14	1664	81	6.1	265	355
Z11016	7.3	29.3	0.15	1669	-44	3.9	167	321
Z11048	7.4	20.5	0.00	1849	44	5.6	381	410
Z11049	7.5	30.6	0.00	1796	-94	4.7	225	446

- continued -

Tab. 11-5a (continued): Main hydrochemical composition of selected groundwater samples from Orapa (part 1).

BH_ID	**pH**	**T**	**DO**	**EC**	**E_H (SHE)**	**K**	**Na**	**Cl**
	(-)	(°C)	(mg/l)	(µS/cm)	(mV)	(mg/l)	(mg/l)	(mg/l)
Z11050	7.0	29.3	0.56	2160	154	9.7	289	500
Z6111	7.3	31.3	1.63	1826	307	6.1	347	387
Z7100	9.3	30.2	0.21	11630	-39	20.9	2601	3850
Z7101	9.2	29.8	0.10	15640	-42	18.3	3526	4890
Z7139	7.8	29.8	0.26	3960	224	6.5	867	1036
Z7146	8.7	31.8	0.09	4570	-52	9.2	1042	1292
Z7148	7.9	33.9	0.55	4650	38	9.0	1045	1250
Z7155	7.4	29.0	0.94	9700	165	19.3	2280	2600
Z7157	8.8	29.1	0.10	57500	-71	315.0	14622	23000
Z7189	7.4	31.6	0.29	13850	-82	47.4	3047	4450
Z7449	7.0	28.5	1.70	1882	187	7.5	297	379
Z8772	7.4	31.5	0.25	2530	357	6.8	511	486
Z8776	6.9	26.6	0.00	6180	375	14.7	1026	1758
Z9058	7.2	29.3	2.25	1873	187	9.7	331	379
Z9166	7.0	28.8	-	2120	187	9.1	360	450
Z9283	7.2	29.5	0.00	1481	322	2.7	252	298
Z9374	6.9	27.1	3.51	1770	325	4.6	259	229
SE9_hand_dug	6.7	24.3	1.63	5540	228	4.1	562	1493
WF6/26	7.3	29.9	0.95	2160	221	6.8	382	394
Z6000	9.0	29.9	0.11	8490	208	9.9	1715	2263
Z6001	9.7	20.7	0.22	7230	210	20.2	1470	2222
Z6002	9.6	29.6	0.18	3740	209	6.1	781	931
Z6109	7.2	30.7	0.29	2310	211	5.9	405	407
Z6110	7.1	31.2	0.26	5210	210	11.7	825	1483
Z6128	7.1	30.4	0.25	2590	210	6.9	453	508
Z7089	7.4	29.4	-	-	63	7.3	223	261
Z7092	7.6	29.0	0.15	1917	209	4.7	368	333
Z7095	7.2	28.7	0.45	1653	213	3.0	311	246
Z7102	10.7	30.7	0.12	4420	209	5.8	886	1076
Z7152	8.4	31.0	0.98	4720	222	14.0	836	1280

- = no data

Tab. 11-5b: Main hydrochemical composition of selected groundwater samples from Orapa (part 2).

BH_ID	Mg (mg/l)	Ca (mg/l)	SO_4 (mg/l)	HCO_3 (mg/l)	Fe(II) (mg/l)	Mn (mg/l)	NO_3 (mg/l)	NH_4 (mg/l)	NO_2 (mg/l)
BARBARA	23.9	37.3	96.6	743	0.022	0.001	20.2	<0.01	<0.05
BH8095	21.1	44.2	42.4	662	0.018	0.006	16.8	<0.02	0.06
BH8096	15.0	26.0	50.3	731	0.087	0.008	10.2	<0.02	0.09
BH8098	44.6	62.8	114.0	688	1.430	0.107	13.5	0.07	2.30
EB1	9.3	28.5	309.0	321	0.076	0.021	11.4	<0.02	2.04
GLADYS	63.1	137.0	205.0	546	0.014	0.004	47.6	<0.01	<0.05
HDW4	3.0	19.5	3.4	79.4	0.025	0.018	0.1	<0.02	1.46
OB22	26.5	40.4	87.0	917	<0.003	-	29.3	0.04	<0.01
OB23	23.4	43.6	55.9	729	<0.003	<0.001	20.3	<0.02	<0.01
OB33	29.8	33.6	249.0	1230	0.055	0.005	54.3	<0.02	<0.01
Pat	52.9	101.0	184.0	614	0.001	0.001	44.8	0.04	<0.01
Z2539	66.1	125.0	170.0	543	0.001	-	53.7	<0.02	<0.01
Z5999	129.0	125.0	280.0	720	0.981	0.055	33.3	0.03	<0.01
BH3077	36.2	55.9	54.0	509	<0.003	-	52.2	<0.02	<0.01
BH6887	30.4	51.3	34.9	540	<0.003	0.000	28.9	<0.02	0.04
BH6888	30.3	53.5	72.2	515	<0.003	<0.001	32.6	<0.02	<0.01
HDW6-1	6.5	31.8	3.0	161	0.005	0.017	0.8	<0.02	2.06
HDW6-3	119.0	238.0	108.0	590	0.003	0.044	84.0	0.07	<0.01
OB17	29.9	65.1	28.7	548	<0.003	0.002	22.9	<0.02	0.04
OB40	15.9	59.2	210.0	125	0.383	0.315	4.4	<0.02	0.81
Z10694	112.0	248.0	289.0	508	<0.003	0.004	69.0	0.04	<0.01
Z10878	13.8	27.1	98.9	329	0.199	0.033	16.0	0.06	1.92
Z10880	32.0	74.2	92.9	297	0.023	0.055	32.8	0.05	0.47
Z10882	25.8	42.7	126.0	433	<0.003	0.002	34.9	<0.02	0.18
Z10891	23.0	39.5	117.0	410	<0.003	0.000	58.2	0.03	0.13
Z10892	25.1	70.3	110.0	359	0.023	0.047	51.8	<0.02	0.18
Z10979	24.4	62.3	82.7	313	0.192	0.041	20.4	0.08	2.48
Z11016	38.7	109.0	44.5	390	20.8	0.225	0.6	-	<0.01
Z11048	7.4	34.9	75.2	343	0.667	0.024	37.1	0.30	1.36
Z11049	41.1	83.1	53.7	210	10.700	0.139	25.5	4.06	0.27

- continued -

Tab. 11-5b (continued): Main hydrochemical composition of selected groundwater samples from Orapa (part 2).

BH_ID	**Mg** (mg/l)	**Ca** (mg/l)	**SO_4** (mg/l)	**HCO_3** (mg/l)	**Fe(II)** (mg/l)	**Mn** (mg/l)	**NO_3** (mg/l)	**NH_4** (mg/l)	**NO_2** (mg/l)
Z11050	46.4	114.0	68.0	397	0.154	0.039	42.2	<0.02	1.32
Z6111	17.1	42.1	97.4	311	<0.003	0.001	28.8	<0.02	<0.01
Z7100	14.1	20.0	419.0	24	<0.003	0.009	0.7	6.10	<0.01
Z7101	9.9	213.0	1438	7	0.053	0.021	0.9	0.29	<0.01
Z7139	3.5	21.0	155.0	393	<0.003	0.003	29	0.05	<0.01
Z7146	3.1	5.5	97.1	376	0.010	0.006	0.2	<0.02	<0.01
Z7148	2.7	11.2	107.0	450	<0.003	0.003	13.4	<0.02	<0.01
Z7155	27.5	34.2	744.0	876	<0.003	0.006	28.9	<0.02	<0.01
Z7157	144.0	461.0	2758	47	0.018	0.539	5.1	0.97	<0.01
Z7189	45.9	154.0	684.0	383	0.239	0.058	29.5	0.02	<0.01
Z7449	33.4	70.2	53.4	414	0.043	0.006	64.9	<0.02	0.07
Z8772	22.2	37.2	257.0	394	0.007	-	37.8	<0.02	<0.01
Z8776	127.0	147.0	143.0	501	0.003	0.001	8.8	<0.02	<0.01
Z9058	23.8	55.2	49.2	377	0.008	0.007	93.7	0.07	<0.01
Z9166	25.0	59.3	78.4	362	0.033	0.011	74.2	<0.02	0.27
Z9283	11.5	39.0	42.0	253	<0.003	0.002	30.7	<0.02	0.04
Z9374	40.3	71.9	24.0	672	<0.003	0.001	49.0	<0.02	<0.01
SE9_hand_dug	181	344.0	112.0	431	0.353	0.022	244.0	0.24	0.72
WF6/26	25.6	41.5	135.0	430	0.110	0.004	34.2	<0.01	<0.05
Z6000	22.2	4.9	402.0	275	0.371	0.082	0.3	0.01	<0.05
Z6001	3.2	41.0	46.3	28	0.017	0.006	0.2	0.68	<0.05
Z6002	7.6	6.4	212.0	114	0.017	0.005	0.5	-	0.59
Z6109	20.2	58.2	238.0	341	0.045	0.001	49.4	<0.01	0.28
Z6110	53.4	153.0	184.0	241	0.061	0.009	40.7	<0.01	<0.05
Z6128	26.2	51.3	113.0	436	0.037	0.014	85.4	<0.01	0.17
Z7089	40.8	65.9	27.6	478	0.652	0.037	59.8	0.62	0.29
Z7092	14.5	26.1	104.0	410	0.095	0.001	42	<0.01	0.18
Z7095	15.8	40.0	74.9	493	1.860	0.013	28.1	<0.01	<0.05
Z7102	0.5	1.4	88.5	199	0.008	-	0.4	<0.01	-
Z7152	37.4	32.4	74.6	160	0.109	0.052	3.4	0.53	<0.05

- = no data